UNIVERSITAT POLITÈCNICA DE VALÈNCIA

DEPARTAMENTO DE TECNOLOGÍA DE ALIMENTOS

Programa de Doctorado en Ciencia, Tecnología y Gestión Alimentaria

DOCTORAL THESIS

Innovations in non-destructive techniques for fruit quality control applied to manipulation and inspection lines

Submitted by

Victoria Cortés López

Supervisors:

Full Prof. Pau Talens Oliag

Dr. Sergio Cubero García

Valencia, September 2018

PAU TALENS OLIAG, PhD in Food Technology and Full Professor at the *Universitat Politècnica de València*, and SERGIO CUBERO GARCÍA, PhD in Design, Manufacturing and Industrial Project Management at the *Universitat Politècnica de València*

Certify:

That the work **'*Innovations in non-destructive techniques for fruit quality control applied to manipulation and inspection lines*'** has been developed by Victoria Cortés López under their supervision in the Department of Food Technology of the *Universitat Politècnica de València*, as a Thesis Project in order to obtain the degree of PhD in Food Technology at the *Universitat Politècnica de València*.

Valencia, September 2018.

Full Prof. Pau Talens

Dr. Sergio Cubero

Esta Tesis Doctoral ha sido realizada gracias a una beca predoctoral (FPU) concedida por el Ministerio de Educación, Ciencia y Deporte de España.

"En mi mundo azul

donde yo canto, donde bailo

donde me iluminas tú

todos mis sueños te los mando

y espero tu luz,

y no me sueltes de tu mano

que no fallaré".

(Rosario Flores, Gloria a ti)

Acknowledgements

Agradecimientos

Me gustaría expresar mis más sinceros agradecimientos a mi director **Pau Talens** por ofrecerme esta gran oportunidad, por despertar en mí esta pasión hasta entonces desconocida, y sobre todo, por el gran esfuerzo y dedicación durante estos cuatro años para que este trabajo pudiera salir adelante.

Agradecer enormemente a todos y cada uno de los miembros del **IVIA** por cada consejo dado en el momento oportuno, por el buen ambiente de trabajo que me habéis ofrecido cada vez que iba, por vuestra colaboración desinteresada en cada experimental, por ese interés en el avance de mi investigación, y por infinidad de cosas más, sé que sin vosotros este camino no hubiera sido tan fructífero. Muy especialmente quiero darle las gracias a **Jose Blasco**, porque te has comportado como un auténtico director de tesis, y así lo he sentido en todo momento, porque cada corrección tuya he sabido siempre que sería productiva y porque me has intentado darme los mejores consejos, muchísimas gracias. Gracias a mi co-director **Sergio Cubero** por su entrega en cada experimental, por sus enseñanzas y su apoyo. No quiero olvidarme de "mis chicas", **Nuria Aleixos** y **Sandra Munera**, porque han sido unas excelentes compañeras, y gracias a esos ratitos de "chicas" he podido recargar mis pilas en los momentos más difíciles, gracias.

Dar las gracias también a **Coral Ortiz** por su energía tan positiva y productiva. Gracias también a **Martín Mellado** y **Carlos Blanes** por su entrega, dedicación y esfuerzo en esos experimentales tan claves para mi tesis.

Gracias, como no, a mis compañeros y compañeras de planta de la CPI, porque esos ratitos del "primer turno de comidas" han sido geniales. En especial gracias a **M. Jesús Lerma**, porque desde el primer día que te conocí sentí un gran apoyo por tu parte y me has ayudado muchísimo especialmente en esta recta final, muchísimas gracias. También muchas gracias a **Ana Fuentes** por su ayuda y consejos siempre que los necesitaba y por enseñarme tanto durante las prácticas.

Agradezco también al grupo de investigación MeBioS de la Universidad de Lovaina por acogerme durante mi estancia, y muy especialmente a **Els Bobelyn** y **Wouter Saeys** por dejarme trabajar en su grupo de investigación y hacerme sentir como en casa.

Por último gracias a toda **mi familia** y **amigos**, por vuestro interés en mi trabajo y vuestras caras de asombro cada vez que os contaba algo. Gracias a **mis padres**, porque me siento súper orgullosa de vosotros, porque gracias a vosotros hoy soy la persona que soy, os quiero con toda mi alma. Gracias a **mi hermana**, por ser mi máxima protectora y por darme la máxima lección de la vida que es saber hacer lo correcto. Gracias a **mi cuñado** por su interés y cariño, y gracias a **mis pequeñas** por ser mi alegría cada segundo de mi vida. Muy especialmente quiero agradecer todo el inmenso tiempo dedicado a **mi marido**, Javi, porque ha sido él mi mayor apoyo, quien me ha sabido dar las mejores notas en esta etapa, por calmar mi furia y agobios, por motivarme a luchar y a cruzar cualquier meta que se me presente en esta vida sin tener miedo, GRACIAS.

RESUMEN

La industria alimentaria, concretamente el sector poscosecha, necesita innovar en sus procesos productivos, optimizando los mismos para rentabilizar sus actividades, garantizando productos de calidad capaces de satisfacer las necesidades de los consumidores. En la actualidad, la mejora de los procesos de inspección poscosecha se centra principalmente en su optimización, aplicando nuevas técnicas alternativas que permitan reducir los tiempos de procesado, minimizar la generación de residuos y conseguir una mayor estandarización de sus productos.

La presente tesis doctoral se centra en evaluar el potencial de la espectroscopia visible e infrarrojo cercano (VIS-NIR) para la caracterización e inspección de la calidad de la fruta tanto fuera de línea como a tiempo real en procesos automatizados.

En un primer lugar, la viabilidad de la técnica se estudió a nivel de laboratorio en estado estático (off-line), con el fin de conocer y optimizar las condiciones de medición en función de las características de la materia prima. Posteriormente, se evaluó la calidad interna y externa de diferentes tipos de frutas como son caqui, nectarina y mango. En una segunda etapa, se llevó a cabo una automatización de los procesos de inspección mediante el desarrollo de nuevos prototipos in-line. Para este propósito, y con el objetivo de completar y corroborar los resultados obtenidos de manera estática, se estudió la integración de dos sondas VIS-NIR en una garra robótica capaz de manipular mangos fusionando mediciones no destructivas de la firmeza y de los espectros en el rango VIS-NIR obtenidos de forma simultánea. Finalmente, se estudió la integración de una sonda VIS-NIR a una cinta transportadora como herramienta de monitorización in-line del proceso de inspección de distintas variedades de manzana.

Los resultados obtenidos a nivel estático han demostrado que la espectroscopia VIS-NIR es un método no destructivo muy prometedor para predecir la astringencia en caqui alcanzando un rendimiento de un R^2_P de 0.904 utilizando el espectro completo y un R^2_P de 0.915 seleccionando tan sólo las 41 bandas más importantes. Así mismo, ha demostrado ser una adecuada herramienta para clasificar al 100% entre variedades de nectarinas como “Big Top” y “Diamond Ray” con una apariencia externa e interna muy similar, pero con diferentes propiedades organolépticas. De manera similar, fue posible clasificar al 100% variedades como

"Big Top" y "Magique" de apariencia externa y composición similar pero distinto color de pulpa. Se desarrolló un índice de calidad interna (IQI) para evaluar la calidad de las nectarinas, el cuál puede predecirse a través de espectroscopia VIS-NIR. En el caso de la variedad "Big Top", se obtuvieron valores de R^2_P de 0.909 y para la variedad "Magique" valores de R^2_P de 0.927. Por lo que respecta a los trabajos off-line realizados con mangos de la variedad "Osteen", fue posible predecir su calidad interna mediante los índices de madurez (RPI) y de calidad (IQI) con un gran rendimiento utilizando todo el rango espectral (R^2_P = 0.833-0.879) así como las longitudes de onda más importantes (R^2_P = 0.815-0.896). A su vez, los ensayos experimentales efectuados con estos mismos mangos bajo la manipulación no destructiva de una garra robótica, demostraron que los mejores modelos eran capaces de predecir tanto la firmeza mecánica (r_p = 0.925), el contenido en sólidos solubles (r_p = 0.892), la luminosidad de la pulpa (r_p = 0.893) así como el índice RPI (r_p = 0.937) de las muestras en base a la información obtenida por los acelerómetros instalados en los dedos de la garra robótica.

En cuanto a los ensayos realizados de manera in-line, el primer prototipo desarrollado se basó en la integración de dos sondas VIS-NIR en una garra robótica dispuesta con dos acelerómetros. El sistema desarrollado permitió alcanzar una buena estimación de la calidad del mango a través del índice RPI logrando un R^2_P de 0.832 fusionando la información tanto de los espectros VIS-NIR como del impacto no destructivo de los acelerómetros. De este modo quedó demostrado que era posible obtener una predicción similar trabajando de forma in-line como trabajando de manera off-line para la predicción del mismo índice de calidad en mangos. El segundo prototipo in-line desarrollado se basa en la integración de una sonda VIS-NIR en una cinta transportadora para la identificación de distintas variedades y orígenes de manzanas, alcanzándose con el sistema un éxito de clasificación del 98 %. El prototipo desarrollado permitió registrar resultados de clasificación tan buenos como los efectuados de manera off-line con, por ejemplo, nectarina.

De este modo, se puede concluir que la espectroscopia VIS-NIR permite monitorear la calidad y clasificar fruta poscosecha tanto en modo off-line como in-line, siendo una herramienta que permite mejorar y garantizar la correcta calidad y seguridad alimentaria. Los nuevos prototipos desarrollados aportan claras ventajas respecto a los procesos tradicionales realizados a mano, como son la reducción del tiempo de inspección, la disminución de la cantidad de residuos generados por los

análisis destructivos de calidad y la posibilidad de inspeccionar toda la producción, obteniendo así un análisis más estandarizado de la calidad de los productos.

RESUM

La indústria alimentària, concretament el sector postcollita, necessita innovar en els seus processos productius, optimitzant els mateixos per a rendibilitzar les seues activitats, garantint productes de qualitat capaços de satisfer les necessitats dels consumidors. En l'actualitat, la millora dels processos d'inspecció postcollita es centra principalment en la seua optimització, aplicant noves tècniques alternatives que permeten reduir el temps de processat, minimitzar la generació de residus i aconseguir una major estandardització dels seus productes.

La present tesi doctoral es centra en avaluar el potencial de l'espectroscòpia visible i infraroig pròxim (VIS-NIR) per a la caracterització i la inspecció de la qualitat de la fruita tant fora de línia com a temps real en processos automatitzats.

En un primer lloc, la viabilitat de la tècnica es va estudiar a nivell de laboratori en estat estàtic (off-line), a fi de conéixer i optimitzar les condicions de mesurament en funció de les característiques de la matèria primera. Posteriorment, es va avaluar la qualitat interna i externa de diferents tipus de fruites com són caqui, nectarina i mango. En una segona etapa, es va dur a terme una automatització dels processos d'inspecció per mitjà del desenvolupament de nous prototips in-line. Per aquest propòsit, i amb l'objectiu de completar i corroborar els resultats obtinguts de manera estàtica, es va estudiar la integració de dos sondes VIS-NIR en una garra robòtica capaç de manipular mangos fusionant mesuraments no destructives de la fermesa i dels espectres en el rang VIS-NIR obtinguts de forma simultània. Finalment, es va estudiar la integració d'una sonda VIS-NIR a una cinta transportadora com a ferramenta de monitorització in-line del procés d'inspecció de distintes varietats de poma.

Els resultats obtinguts a nivell estàtic han demostrat que l'espectroscòpia VIS-NIR és un mètode no destructiu molt prometedor per a predir l'astringència en caqui aconseguint un rendiment d'un R^2_P de 0.904 utilitzant l'espectre complet i un R^2_P de 0.915 seleccionant tan sols les 41 bandes més importants. Així mateix, ha demostrat ser una adequada ferramenta per a classificar al 100% entre varietats de nectarines com “Big Top” i “Diamond Ray” amb una aparença externa i interna molt semblant, però amb diferents propietats organolèptiques. De manera semblant, va ser possible classificar al 100% varietats com “Big Top” i “Magique” d'aparença externa i

composició semblant però distint color de polpa. Es va desenvolupar un índex de qualitat interna (IQI) per avaluar la qualitat de les nectarines, que pot predir-se mitjançant l'espectroscòpia VIS-NIR. En el cas de la varietat "Big Top", es van obtindre valors de R^2_P de 0.909 i per a la varietat "Magique" valors de R^2_P de 0.927. Pel que fa als treballs off-line realitzats amb mangos de la varietat "Osteen" va ser possible predir la seua qualitat interna mitjançant els índexs de maduresa (RPI) i de qualitat (IQI) amb un gran rendiment utilitzant tot el rang espectral (R^2_P = 0.833-0.879) així com les longituds d'onda més importants (R^2_P = 0.815-0.896). Al mateix temps, els assajos experimentals efectuats amb estos mateixos mangos baix la manipulació no destructiva d'una garra robòtica, van demostrar que els millors models eren capaços de predir tant la fermesa mecànica (r_p = 0.925), el contingut en sòlids solubles (r_p = 0.892), la lluminositat de la polpa (r_p = 0.893) així com l'índex RPI (r_p = 0.937) de les mostres basant-se en l'informació obtinguda pels acceleròmetres instal·lats en els dits de la garra robòtica.

En quant als assajos realitzats de manera in-line, el primer prototip desenvolupat es va basar en la integració de dos sondes VIS-NIR en una garra robòtica disposada amb dos acceleròmetres. El sistema desenvolupat va permetre aconseguir una bona estimació de la qualitat del mango a través de l'índex RPI aconseguint un R^2_P de 0.832 fusionant l'informació tant dels espectres VIS-NIR com de l'impacte no destructiu dels acceleròmetres. D'esta manera va quedar demostrat que era possible obtindre una predicció semblant treballant de forma in-line com off-line per a la predicció del mateix índex de qualitat en mangos. El segon prototip in-line desenvolupat es va basar en la integració d'una sonda VIS-NIR en una cinta transportadora per a l'identificació de distintes varietats i orígens de pomes, aconseguint-se amb el sistema un èxit de classificació del 98%. El prototip desenvolupat va permetre registrar resultats de classificació tan bons com els efectuats de manera off-line.

D'aquesta manera, es pot concloure que l'espectroscòpia VIS-NIR permet monitorar la qualitat i classificar fruita postcollita tant en mode off-line com in-line, sent una ferramenta que permet millorar i garantir la correcta qualitat i seguretat alimentària. Els nous prototips desenvolupats aporten clars avantatges respecte als processos tradicionals realitzats a mà, com són la reducció del temps d'inspecció, la disminució de la quantitat de residus generats pels anàlisis destructives de qualitat i

la possibilitat d'inspeccionar tota la producció, obtenint així un anàlisi més estandarditzat de la qualitat dels productes.

ABSTRACT

The food industry, concretely the post-harvest sector, needs to innovate in their production processes, optimizing them to make their activities profitable, guaranteeing quality products capable of satisfying the needs of consumers. Nowadays, the improvement of post-harvest inspection processes is mainly focused on their optimization, applying new alternative techniques, which reduce processing times, minimize waste generation and achieve greater standardization of their products.

The present doctoral thesis focuses on evaluating the potential of visible and near infrared spectroscopy (VIS-NIR) for the characterization and inspection of fruit quality both off-line and in real time in automated processes.

Firstly, the viability of the technique was studied at the laboratory level in a static mode (off-line), in order to know and optimise the measurement conditions according to the characteristics of the raw material. Subsequently, the internal and external quality of different types of fruits such as persimmon, nectarine and mango were evaluated. Secondly, an automation of the inspection processes was carried out through the development of new in-line prototypes. For this purpose, and with the aim of completing and corroborating the results obtained in a static mode, the integration of two VIS-NIR probes in a robotic gripper capable of manipulating mangoes was studied, fusionating non-destructive measurements of the firmness and the spectra in the VIS-NIR range obtained simultaneously. Finally, the integration of a VIS-NIR probe to a conveyor belt was studied as an in-line monitoring tool on the inspection process of different apple varieties.

The results obtained in static mode have shown that VIS-NIR spectroscopy is a very promising non-destructive method to predict the astringency in persimmon reaching a performance of R^2_P of 0.904 using the full spectrum and a R^2_P of 0.915 selecting only the 41 bands more important. Likewise, it has demonstrated to be an adequate tool to classify 100% between nectarine varieties such as 'Big Top' and 'Diamond Ray' with very similar external and internal appearance, but with different organoleptic properties. Similarly, it was possible to classify 100% varieties such as 'Big Top' and 'Magique' with external appearance and similar composition but different pulp colour. An internal quality index (IQI) was developed to evaluate the

quality of nectarines, which can be predicted through VIS-NIR spectroscopy. In case of the 'Big Top' variety, R^2_P values of 0.909 were obtained and for the variety 'Magique', R^2_P values of 0.927 were obtained. Regarding the off-line work carried out with mangoes of 'Osteen' variety, it was possible to predict its internal quality through the indexes of maturity (RPI) and quality (IQI) with a high performance using the whole spectral range (R^2_P = 0.833-0.879) as well as the most important wavelengths (R^2_P = 0.815-0.896). Moreover, the experimental tests carried out with these same mangoes under the non-destructive manipulation of a robotic gripper, showed that the best models were able to predict both the mechanical firmness (r_p = 0.925), the soluble solids content (r_p = 0.892), the brightness of the pulp (r_p = 0.893) as well as the RPI index (r_p = 0.937) of the samples based on the information obtained by the accelerometers installed on the fingers of the robotic gripper.

Regarding the tests carried out in an in-line mode, the first developed prototype was based on the integration of two VIS-NIR probes in a robotic gripper fitted with two accelerometers. The developed system allowed reaching a good estimation of mango quality through the RPI index, achieving an R^2_P of 0.832 combining the information of both the VIS-NIR spectra and the non-destructive impact of the accelerometers. In this way, it was demonstrated that it was possible to obtain a similar prediction working in-line as off-line mode for the prediction of the same quality index in mangoes. The second developed in-line prototype is based on the integration of a VIS-NIR probe in a conveyor belt for the identification of different varieties and origins of apples, achieving a success rate of 98% with the system. The developed prototype allowed to register classification results as good as those carried out off-line with, for example, nectarine.

In this way, it can be concluded that VIS-NIR spectroscopy allows monitoring the quality and classifying post-harvest fruit in both off-line and in-line mode, being a tool that allows improving and guaranteeing the correct quality and food safety. The new developed prototypes provide clear advantages over the traditional processes performed by hand, such as the reduction of inspection time, the reduction of the amount of waste generated by destructive quality analysis and the possibility of inspecting full production, obtaining a more standardised analysis of the quality of the products.

PREFACE

This thesis forms part of the project '*Nuevas técnicas de inspección basadas en visión por computador multiespectral para la estimación de propiedades y determinación automática de la calidad y sanidad de la producción agroalimentaria en líneas de inspección y manipulación* (**VIS-DACSA,** RTA2012-00062-C04-03)', funded by the 2013-2016 European Regional Development Fund (FEDER) of the European Commission, and is focused on the evaluation of the potential of visible (VIS) and near-infrared (NIR) spectroscopy for the characterization and inspection of fruit quality both off-line as in real time in automation processes.

The thesis is structured in six sections: Introduction, objectives, scientific contribution, general discussion, conclusions and future perspectives.

The **INTRODUCTION** section focuses on the possibilities of monitoring for fruit quality control by non-destructive techniques. Electromagnetic spectral techniques have proved to have a great potential for the assessment of quality parameters for different fruits. Concretely, visible and near-infrared spectroscopy has showed to be a promising tool to assess of attributes related to quality, which will influence on the acceptance of these fruits by final consumers. Hence, this technique is relatively rapid, simple, cost-effective, non-destructive, environmentally friendly, and moreover, its application in combination with chemometrics allows to obtain successful and robust results.

The **OBJETIVES** section presents the general and specific objectives of the thesis.

The **SCIENTIFIC CONTRIBUTION** section is divided in two sections: section 1, off-line inspection and section 2, processes automation.

In ***section I*** the optimal quality of different fruits with a certain commercial interest based on non-destructive analysis were evaluated under laboratory conditions applying visible and near-infrared spectroscopy device. This section was divided in 4 chapters.

The ***first chapter*** evaluate the feasibility of VIS and NIR spectroscopy combined with chemometrics as a non-destructive tool to determine the level of astringency in persimmons cv. 'Rojo Brillante'.

The ***second chapter*** evaluate the ability of VIS and NIR spectroscopy to discriminate between two varieties of nectarine (cv. 'Big Top' and cv. 'Diamond

Ray'), which, because there are similar in colour and appearance, are very difficult to differentiate visually on the production line but show important differences in taste, thereby affecting the acceptance by the final consumers. Two supervised methods such as linear discriminate analysis (LDA) and partial least squares discriminate analysis (PLS-DA) were used for this purpose.

The ***chapter three*** evaluate the performance of VIS-NIR reflectance spectroscopy as a tool to predict the internal quality of nectarines, and the potential of the information obtained to differentiate among varieties with different commercial interest. To this end, two varieties with a similar composition, grown in the same period, but with different development, cv. 'Big Top' and cv. 'Magique', have been analysed.

In ***chapter four*** a non-destructive method based on external visible and near-infrared reflection spectroscopy for determining the internal quality of intact mango cv. 'Osteen' was investigated. First an internal quality index for the mangoes, based on their main biochemical (total soluble solids) and physical properties (firmness and flesh colour), avoiding the titratable acidity analysis, because it is a laborious and slow analysis that generates waste, were determined. The internal quality index was applied to the mango cv. 'Osteen', and statistical models based on Partial Least Squares (PLS) to predict the internal quality of the samples through the analysis of external VIS-NIR spectral data were developed.

In ***section II***, new strategies based on visible and near-infrared spectroscopy, and its adaption for the automatic inspection and manipulation of fruits were studied with the purpose of developing new fusion non-destructive systems for the automatic quality control of fruits. This section was divided in 3 chapters.

In ***chapter five***, the use of a robot gripper in the assessment of firmness of mango fruit, cv. 'Osteen' was evaluated and relationships between the non-destructive robot gripper measurements with embedded accelerometers in the fingers and the mechanical properties, internal quality (soluble solids, pH and tritatable acidity), flesh colour and the ripening index of mango fruit were established.

Chapter six, is focused on the development of a novel robotic gripper that incorporates accelerometers and fibre-optic probes coupled to a spectrometer to analyse the mango ripening state by simultaneously measuring firmness and visible

and near-infrared reflectance when the fruit is handled in the packing house during postharvest operations.

Chapter seven, is focused in three objectives: a) the development of a prototype system, using VIS-NIR reflectance spectroscopy, to be used for the in-line non-destructive measurement of apples; b) the use of an automated system that ensures that the distance between the probe and the fruit is the same regardless of the size of the fruit; and c) the use of the data obtained by the in-line system to differentiate apple varieties using chemometric methods.

The **GENERAL DISCUSSION**, **CONCLUSIONS** and **FUTURE PERSPECTIVES** sections presents a short general discussion and the main conclusions of the results obtained in this thesis and different proposals for further possible studies.

Dissemination of results

International Journals of JCR

✓ Published

Cortés, V., Rodríguez, A., Blasco, J., Rey, B., Besada, C., Cubero, S., Salvador, A., Talens, P. & Aleixos, N. (2017). Prediction of the level of astringency in persimmon using visible and near-infrared spectroscopy. Journal of Food Engineering, 27-37.

Cortés, V., Blasco, J., Aleixos, N., Cubero, S. & Talens, P. (2017). Visible and near-infrared diffuse reflectance spectroscopy for fast qualitative and quantitative assessment of nectarine quality. Food and Bioprocess Technology, 10, 1755-1766.

Cortés, V., Cubero, S., Aleixos, N., Blasco, J. & Talens, P. (2017). Sweet and nonsweet taste discrimination of nectarines using visible and near-infrared spectroscopy. Postharvest Biology and Technology, 133, 113-120.

Cortés, V., Ortiz, C., Aleixos, N., Blasco, J., Cubero, S. & Talens, P. (2016). A new internal quality index for mango and its prediction by external visible and near-infrared reflection spectroscopy. Postharvest Biology and Technology, 118, 148-158.

Blanes, C., **Cortés, V.**, Ortiz, C., Mellado, M. & Talens, P. (2015). Non-destructive assessment of mango firmness and ripeness using a robotic gripper. Food and Bioprocess Technology, 8, 1914-1924.

Cortés, V., Blanes, C., Blasco, J., Ortíz, C., Aleixos, N., Mellado, M., Cubero, S. & Talens, P. (2017). Integration of simultaneous tactile sensing and visible and near-infrared reflectance spectroscopy in a robot gripper for mango quality assessment. Biosystems Engineering, 162, 112-123.

✓ Under review

Cortés, V., Blasco, J., Aleixos, N., Cubero, S. & Talens, P. (2018). Monitoring strategies for quality control of agricultural products using visible and near-infrared spectroscopy: A review.

Other Journals

Blasco, J., Lorente, D., **Cortés, V.**, Talens, P., Cubero, S., Munera, S. & Aleixos, N. (2016). Application of near infrared spectroscopy to the quality control of citrus fruits and mango. NIR News, 27(7), 4-7.

Requested Patent

Cortés, V., Cubero, S., Blasco, J., Aleixos, N. & Talens, P. (2018). In-line application of visible and near-infrared diffuse reflectance spectroscopy to identify apple varieties.

National and International Conferences

✓ Oral communications

Cortés, V., Aleixos, N., Blasco, J., Cubero, S. & Talens, P. (2016). Rapid prediction of internal quality in intact nectarines using visible and near infrared spectroscopy. 6th International Workshop Applications of Computer Image Analysis and Spectroscopy in Agriculture, June, 26-29 th. Aarhus, Denmark.

Cortés, V., Ortiz, C., Aleixos, N., Blasco, J., Cubero, S. & Talens, P. (2015). Medición no destructiva del índice de madurez en mango 'Osteen' usando técnicas de espectroscopía de infrarrojo cercano. VIII Congreso Ibérico de Agroingeniería, June, 1-3 th. Orihuela, Spain.

✓ Poster

Cortés, V., Blanes, C., Blasco, J., Ortíz, C., Aleixos, N., Mellado, M., Cubero, S. & Talens, P. (2018). Mango quality assessment by optical and mechanical parameters integrated in a robot gripper. 4th International & 5th National Student Congress of Food Science and Technology, February, 22-23 th. Valencia, Spain.

Cortés, V., Blanes, C., Munera-Picazo, S., Talens, P., Mellado, M., Blasco, J. & Ortiz, C. (2016). Clasificación de nectarinas según su firmeza mediante la manipulación con una garra robot. Simposio Nacional de Ingeniería Hortícola, Automatización y TICs en la Agricultura, February, 10-12th. Almería, Spain.

Talens, P. & **Cortés, V.** (2016). A rapid and non-destructive technique for the detection of added water to full fat milk using visible spectroscopy measurements. 4th International ISEKI_Food Conference, July, 6-8 th. Vienna, Austria.

Cortés, V., Aleixos, N., Blasco, J., Cubero, S. & Talens, P. (2016). Non-destructive determination of internal quality in nectarines using Visible and Near Infrared Spectroscopy. 2st International & 3rd National Students Congress of Food Science and Technology, March, 4-5 th. Valencia, Spain.

Cortés, V., Blanes, C., Navarro, M., Mellado, M., Talens, P. & Ortiz, C. (2015). Determinación de la firmeza de mango 'Osteen' mediante una garra robótica sensorizada. VIII Congreso Ibérico de Agroingeniería, June, 1-3 th. Orihuela, Spain.

Lorente, D., **Cortés, V.**, Munera-Picazo, S., Escandell-Montero, P., Cubero, S., Aleixos, N., Talens, P. & Blasco, J. (2015). Detección de podredumbres en cítricos mediante espectroscopía VIS/NIR y métodos de aprendizaje automático. VIII Congreso Ibérico de Agroingeniería, June, 1-3 th. Orihuela, Spain.

Cortés, V., Aleixos, N., Blasco, J., Cubero, S. & Talens, P. (2015). Assesment of Mango Ripeness using Near Infrared Spectroscopy. 1st International Congress of students of Food Science and Technology, March, 5-6 th. Valencia, Spain.

Blanes, C., Ortiz, C., **Cortés, V.**, Mellado, M. & Talens, P. (2015). Robot gripper sensor operation in fresh mango postharvest handling for non-destructive firmness assessment. 1st International Congress of students of Food Science and Technology, March, 5-6 th. Valencia, Spain.

Scholarship recipient

- Ayuda contrato pre-doctoral 2013 FPU (AP2013-04202), Ministerio de Educación. From 16-09-2014 to 16-09-2018.

Participation in Financed Research Projects

- Nuevas técnicas de inspección basadas en visión por computador multiespectral para la estimación de propiedades y determinación automática de la calidad y sanidad de la producción agroalimentaria en

líneas de inspección y manipulación (VIS-DACSA, RTA2012-00062-C04-03), Instituto Nacional de Investigación y Tecnología Agraria y Alimentaria. From 16-09-2014 to 13-12-2016.

- Incorporación de nuevas tecnologías ópticas no destructivas para evaluar la calidad y seguridad alimentaria de frutas (AICO/2015/122), Generalitat Valenciana. From 11-09-2015 to 01-01-2017.

Pre-doctoral Stage at a Foreign Institution

KU Leuven, Department of Biosystems, MeBioS Division. Leuven, Belgium. From 1st May 2016 to 31st July 2016, under the supervision of Wouter Saeys.

Abbreviations

1-Der	First Derivative
2-Der	Second Derivative
ANN	Artificial Neural Network
ANOVA	Analysis of Variance
BC	Background Colour
BOC	Baseline Offset Correction
C*	Chromaticity
CA	Cluster Analysis
CCD	Charge Coupled Device
CDA	Canonical Discriminant Analysis
CR^2	Squared Canonical Correlation
DOSC	Direct Orthogonal Signal Correction
EWs	Effective Wavelengths
h*	Hue angle
InGaAs	Indium Gallium Arsenide
IQI	Internal Quality Index
ITB	Internal Tissue Browning
KNN	K-Nearest Neighbors
L*	Luminosity
LDA	Linear Discriminant Analysis
LS-SVM	Least Squares Support Vector Machine
LVs	Latent Variables
MC-UVE	Monte-Carlo Uninformative Variable Elimination

MLR	Multiple Linear Regression
MSC	Multiplicative Scatter Correction
NIR	Near-Infrared
OSC	Orthogonal Signal Correction
PCA	Principal Component Analysis
PCR	Principal Component Regression
PLS	Partial Least Square
PLS-DA	Partial Least Square -Discriminant Analysis
QDA	Quadratic Discriminant Analysis
QS	Quantitative Starch
$\mathbf{R_{CV}^2}$	Coefficient of determination for Cross-Validation
$\mathbf{R_C^2}$	Coefficient of determination for Calibration
RH	Relative Humidity
RMSEC	Root Mean Square Error of Calibration
RMSECV	Root Mean Square Error of Cross-Validation
RMSEP	Root Mean Square Error of Prediction
$\mathbf{r_p}$	Correlation Coefficient for Prediction
$\mathbf{R_P^2}$	Determination Coefficient for Prediction
RPD	Ratio of Performance to Deviation
RPI	Ripening Index
SEC	Standard Error of Calibration
SECV	Standard Error of Cross-Validation
SEP	Square Error of Prediction
SG	Savitzky-Golay
SIMCA	Soft Independent Modeling of Class Analogy
SMLR	Stepwise Multiple Linear Regressions

SNV	Standard Normal Variate
SPA	Successive Projection Algorithm
SPI	Starch Pattern Index
SSC	Soluble Solids Content
SVM	Support Vector Machine
SWIR	Short-Wavelength Near-Infrared
SWS	Standardized Weighted Sum
TA	Titratable Acidity
TPC	Content of Total Phenolic Compounds
TSS	Total Soluble Solids
VIS	Visible

INDEX

1. INTRODUCTION.

Monitoring strategies for quality control of agricultural products using visible and near-infrared spectroscopy: A review.

Cortés, V.[1], Blasco, J.[2], Aleixos, N.[3], Cubero, S.[2] & Talens, P.[1]

[1]Departamento de Tecnología de Alimentos. Universitat Politècnica de València. Camino de Vera s/n, 46022, Valencia (Spain).

[2]Centro de Agroingeniería. Instituto Valenciano de Investigaciones Agrarias (IVIA). Ctra. CV-315, km. 10,7, 46113, Moncada, Valencia (Spain).

[3]Departamento de Ingeniería Gráfica, Universitat Politècnica de València. Camino de Vera s/n, 46022, Valencia (Spain).

Submitted to Trends in Food Science & Technology.

Under review

ABSTRACT

This review addresses the applicability of visible and near-infrared (VIS-NIR) spectroscopy for the off/in-line monitoring of quality in fruit and vegetables postharvest. VIS-NIR spectroscopy represents an analytical technique widely used in the agriculture and food industry due to its low running cost, not require sample preparation, non-destructive, environmental friendly and rapid technique capable for in-line application. Quantitative analyses for prediction of physico-chemical constituents or different quality and maturity indexes of postharvest fruit and vegetable using this methodology are widespread. Moreover, a wide range of qualitative determinations, e.g. for authenticity control, varietal discrimination or identification of damages or infestations in the products have been reported. Sophisticated conditions for the in-line application comprise among others measurements on moving conveyor belts and cups on conveyor belts. For such purposes, different construction designs of VIS-NIR spectrometers, portable devices and fibre-optic have been developed. The different strategies of application of VIS-NIR spectroscopy reported in the present review highlight its enormous versatility.

Keywords: VIS-NIR spectroscopy, in-line, off-line, chemometrics, quantification, qualification

1. INTRODUCTION

Increasing demand for quality assurance in agro-food production requires sophisticated analytical methods for objective quality control (Porep *et al.*, 2015). Traditional analytical methods are, however, labor-intensive, time-consuming, and expensive (Tümsavas *et al.*, 2013). Vibrational techniques, such as VIS-NIR spectroscopy, offer a straightforward, rapid, convenient, simple, accurate, non-destructive, and cost-effective alternative. Moreover, VIS-NIR techniques allow measurements without prior sample preparation, and the potential exists to develop instruments for in-line measurements. However, since it is based on indirect measurements, thus yielding highly convoluted and broad spectra that are virtually impossible to interpret with the unaided eye, VIS-NIR spectroscopy requires calibration with mathematical and statistical tools (chemometrics) to extract analytical information from the corresponding spectra (Porep *et al.*, 2015; Huang *et al.*, 2008; Siesler, 2008).

The versatile applications of VIS-NIR spectroscopy for fruit quality evaluation have been reviewed by Cen and He (2007) and Kumaravelu and Gopal (2015), while, despite the amount of research conducted, there are few reports that carry out a detailed examination of the VIS-NIR in-line technique in the agro-food sector. Related to the off-line evaluation of the quality in fruits and vegetables using spectroscopy technology, Wang *et al.* (2015) and Nicolaï *et al.* (2007) reviewed a broad spectrum of applications of VIS-NIR analysis to measure the quality properties of fruits and vegetables and its chemometric possibilities.

Specifically, Cozzolino *et al.* (2011) surveyed the different steps, methods and issues to be considered when calibrations based on NIR spectra are developed for the measurement of chemical parameters in fruits. Additionally, the specific applications of VIS-NIR spectroscopy for certain agro-food products, such as citrus fruit or mango, have been reviewed by Magwaza *et al.* (2012) and Jha *et al.* (2010), respectively. However, very limited research work has been conducted on VIS-NIR in-line applications to assess, monitor, and predict quality in fruits and vegetables. Some previous research such as that carried out by Huang *et al.* (2008) was focused on NIR on/in-line applications for monitoring quality in food and beverages, but without going deeper into the agro-food sector and without making any comparisons between off/in-line applications for the same product. In particular, the comparison between off-line and in-line experiences with VIS-NIR spectroscopy of the same agro-food product has been performed in this review. However, in numerous cases, a closer look reveals that on-line application has not been performed at all in the corresponding studies, hence the scarcity of real in-line applications. Therefore, this review compares the main advantages and disadvantages, problems, solutions, and differences between the implementation of VIS-NIR spectroscopy for agro-food products under both laboratory and semi-industrial conditions.

2. VIS-NIR TECHNOLOGY

Infrared spectroscopy relies on the absorbance of radiation at molecular vibrational frequencies. These frequencies can occur for relatively light vibrating C-H, N-H, and O-H groups containing hydrogen as well as groups of "heavier" atoms C-O, C-N, N-O, C-C in organic materials (Soriano-Disla *et al.*, 2014). Overtone and combination vibrations of the relatively light atoms involving hydrogen dominate the NIR (700–2,500 nm; 4,000–14,286 cm^{-1}), while these, plus bonds from the heavier atomic groups, absorb in the mid-infrared (MIR) (2,500–25,000 nm; 400–4,000 cm^{-1}). Electronic transitions absorb in the ultraviolet (250–400 nm; 25,000–40,000 cm^{-1}) and visible (400–700 nm; 14,286–25,000 cm^{-1}) regions (Rossel *et al.*, 2006; Coates, 2000). Figure 1 shows the electromagnetic spectrum, with the location of the different spectral regions.

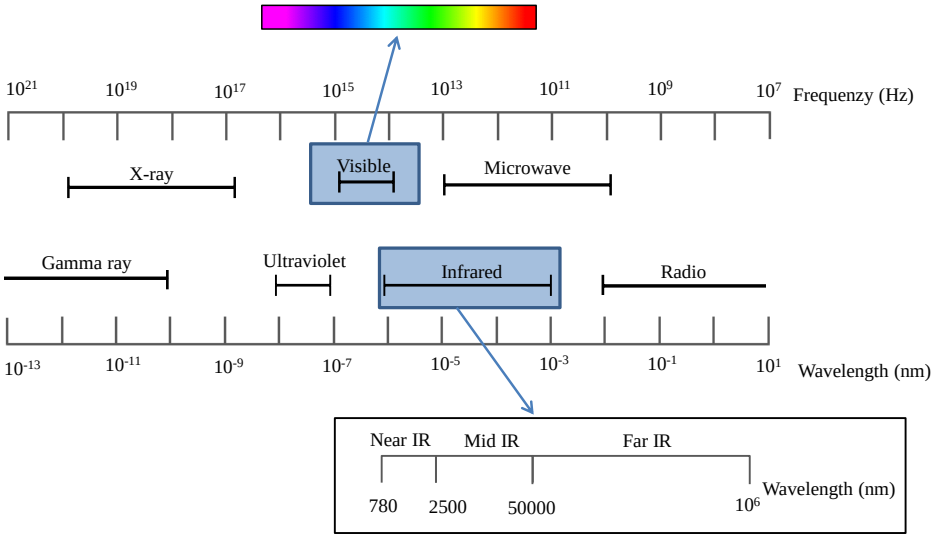

Figure 1. The electromagnetic spectrum with the location of the visible and infrared spectral regions.

Visible and near-infrared technology, as an instrumental analytical technique, has to be calibrated first using chemical reference methods, and it also requires reliable hardware systems and complicated mathematical techniques to interpret chemical information encoded in the spectral data (Cogdill *et al.*, 2005). A wide selection of spectroscopic devices is available and there are around sixty NIR spectrometer manufacturers around the world (McClure & Tsuchikawa, 2007). A typical VIS-NIR spectrometer consists of a light source, a wavelength selection device (e.g., a monochromator), a sample holder, a detector for the measurement of the intensity of the detected light and conversion into electrical signals, and a computer system for spectral data acquisition and processing (Siesler *et al.*, 2008). Figure 2 shows the schematic diagram of a VIS-NIR spectroscopy system based on diffused reflectance. The use of fibre-optic probes is often desirable, as many modern applications are based on their intensive use in order to facilitate data acquisition routines due to their capacity for multiplexing, allowing them to monitor many points (Pasquini, 2003).

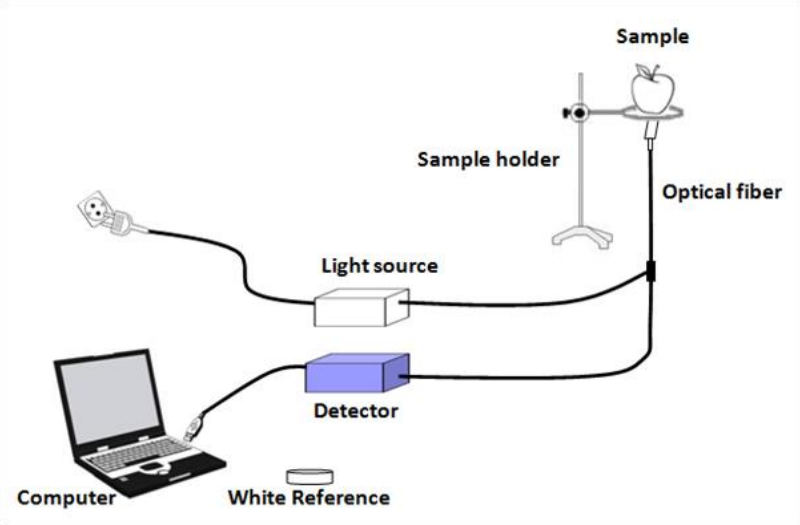

Figure 2. Schematic of spectra detecting system.

Different optical geometries are available for VIS-NIR spectroscopy. The predominant sample presentation modes that can be distinguished are 'transmission', 'reflection', 'transflection' and 'interaction' (Herold *et al.*, 2009; Tsuchikawa, 2007; Alander *et al.*, 2013). Illustrations of these different optical geometries are shown in Figure 3. The location of the detectors with respect to the sample determines the mode of operation. These modes must be provided by the instrument after minimal and easy changes in its configuration. According to the reflection and transmission optical geometry used, light attenuation by the sample, relative to the reference, is referred to as reflectance (R) and transmittance (T), respectively. Most studies use log 1/T or log 1/R values to perform chemometric analyses (Herold *et al.* 2009).

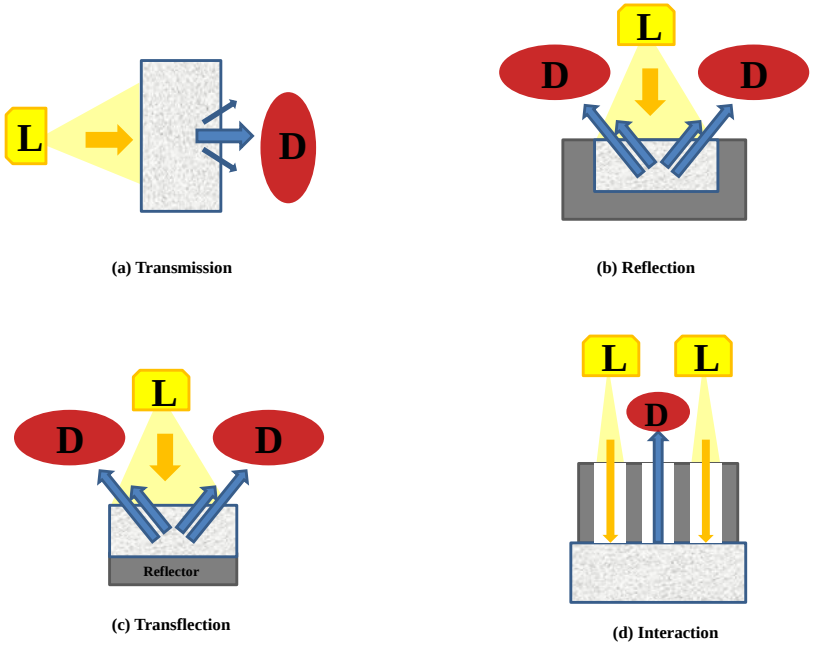

Figure 3. Modes for the acquisition of spectra. L: light source, D: detector.

3. CHEMOMETRICS

The powerful VIS-NIR instruments currently available quickly provide vast amounts of data that require efficient pre-processing and useful evaluation. Chemometrics is a discipline developed for this purpose. It includes all kinds of processes that transform the spectral signals into relevant analytical information. Generally, it involves three steps, as follows: (1) spectral data pre-processing; (2) construction of calibration models for quantitative and qualitative analysis; and (3) model transfer.

A comprehensive description of chemometric techniques used in VIS-NIR spectroscopy would require an extensive treatise on chemometrics, so only the more frequently used chemometric methods are discussed in this article.

3.1. Spectral data pre-processing

In general, pre-processing methods are needed prior to the application of multivariate data analysis techniques. The main aim of spectra pre-treatment is to transform the data into more useful information capable of facilitating its subsequent multivariate analysis.

Frequently, the VIS-NIR spectra are characterized by suffering variations, for instance, by the components of the instrumentation used to record the spectrum (instrumental noise), variations in temperature, humidity or other environmental conditions during registration (background noise), or the signal variations due to the nature of the sample. These variations can be corrected by various pre-processing methods. Some of the more frequent pre-treatments for VIS-NIR spectra include: (i) smoothing methods (for example, moving average, Gaussian filter, median filter, and Savitzky-Golay smoothing) are used to reduce instrumental noise or background information; (ii) derivation methods (usually first and second derivative) are used to remove background noise and increase spectral resolution (Savitzky and Golay, 1964); (iii) MSC (Lorente *et al.*, 2015), (iv) OSC, and (v) SNV to increase resolution and baseline correction by eliminating the multiplicative interferences of scatter in spectra, particle size, and the change of

light distance (Martens *et al.*, 1983; Geladi *et al.*, 1985; Barnes *et al.*, 1989; Wold *et al.*, 1998); (vi) wavelet transformation is often used for smoothing, filtering, and data compression (Liu *et al.*, 2011); (vii) normalization and/or scaling to adjust the individual contributions of the characteristics measured and obtain a result on an equal basis (Berrueta *et al.*, 2007); and (viii) de-trending to eliminate the baseline drift in the spectrum (Wang *et al.*, 2015). Moreover, different combinations thereof applied simultaneously can also be used for signal processing (Brereton, 2003).

3.2. Multivariate analysis methods

After the spectral pre-processing, the calibration model can be built for qualitative and/or quantitative analysis of the samples. In order to do so, many multivariate methods are available. Figure 4 shows a schematic diagram of possible experimental approaches using VIS-NIR spectroscopy techniques.

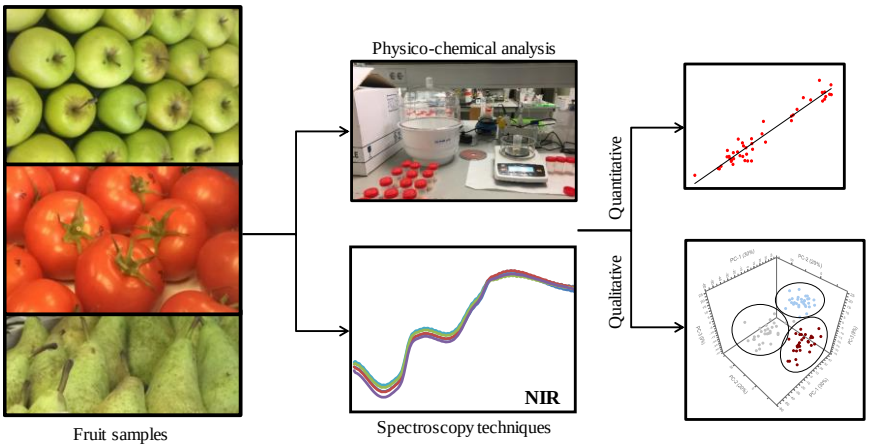

Figure 4. Schematic overview of the different chemometric approches using VIS-NIR spectra.

The first step of the data analysis is often principal component analysis (PCA), in order to detect patterns and outliers (Cozzolino *et al.*, 2011) in the measured data. Other unsupervised pattern recognition techniques can be CA (Næs *et al.*, 2002). In CA, samples are grouped on the basis of similarities (which can be distances, correlations or some combination of the two) without taking into account the information about class membership.

Subsequently, a qualitative or quantitative approach to the data will be decided on according to the objectives of the study. Qualitative analysis is about classifying the samples according to their VIS-NIR spectra based on pattern recognition methods (Roggo *et al.*, 2007). The classification model is developed with a training set of samples with known categories, and subsequently this model is evaluated by a test set of unknown samples. In order to do this, many qualitative methods are used, such as LDA (Coomans *et al.*, 1983; Baranowski *et al.*, 2012), QDA, KNN (Cover & Hart, 1967; Derde *et al.*, 1987), PLS-DA (Liu *et al.*, 2011), SIMCA (Pontes *et al.*, 2006), ANN (Mariey *et al.*, 2001), and SVM (Chen *et al.*, 2007), among others. Of all the different qualitative methods that exist, PLS-DA is a method that is often commonly selected for optimal classification. An example of application of this method is the study by Amodio *et al.* (2017), in which the potential of NIR spectroscopy to discriminate between the three different classes of strawberries produced by different fertility management systems was assessed, a sensitivity and specificity higher than 0.97 being obtained for external samples. A similar result (an accuracy of around 96%) was obtained by Mosceti *et al.* (2016),

who applied NIR spectroscopy to discriminate hailstorm-damaged and undamaged olive fruit, but in this case by LDA and QDA methods. Hu *et al.* (2017) also used different chemometric methods (PCA-DA, SIMCA and LDA) to classify normal and mildewed chestnuts measured using an NIR diffuse reflectance spectroscopy device, accuracy rates of up to 100% being obtained.

The other use of chemometrics is for quantitative analysis, which focuses on predicting some of the properties that, for example, can greatly influence fruit quality. Methods such as PLS, MLR, PCR, and ANN are extensively used for VIS-NIR quantitative analysis. Among them, PLS is recommended as the best modeling method for most VIS-NIR spectra (Lin & Ying, 2009). As mentioned above, with a quantitative approach the calibration and evaluation sets must also contain representative samples of the total set. The accuracy of VIS-NIR models for fruit quality prediction is usually evaluated by means of the R^2 or r, the RMSE, and the RPD (Bobelyn *et al.*, 2010). Generally, a good model should achieve a low RMSE and a high R^2 or r. In addition, an acceptable model should have an RPD value of more than 2.5, a value above 3.0 being very good (Kamruzzaman *et al.*, 2016; Cortés *et al.*, 2016). Other statistical parameters reflecting a good model are low average difference between predicted and measured values (Bias) and a small difference between RMSEC and RMSEP. Moreover, a good model should have as few LV as possible. In the literature, most of the applications of VIS-NIR in the food field follow a quantitative approach. For example, Escribano *et al.* (2017) tested the ability of a handheld NIR device to predict soluble solids content (R^2_p

values ranged from 0.726 to 0.891; RPD from 1.64 to 2.75, and Bias from 0.130 to 1.029) and dry matter content (R^2 values ranged from 0.670 to 0.725; RPD from 1.45 to 1.96, and Bias from 0.005 to 0.345) in sweet cherry variety 'Chelan' and 'Bing' at two different temperatures (0 ºC and 23 ºC). Khodabakhshian *et al.* (2017) investigated the potential of VIS-NIR spectroscopy in transmittance mode to predict quality attributes such as SSC (r_p = 0.92; RPD = 6.38 ºBrix and RMSEP = 0.23 ºBrix), pH (r_p = 0.85; RPD = 4.94 and RMSEP = 0.064), and TA (r_p = 0.93; RPD = 5.31 and RMSEP = 0.26), of pomegranate variety 'Ashraf' during four distinct stages of maturity.

4. MONITORING STRATEGIES IN THE POSTHARVEST FIELD

According to the implementation process used, off-line, at-line, on-line, and in-line measurements can be distinguished. The most commonly used definitions of these terms are as follows (Callis *et al.*, 1987; Dickens, 2010; Koch, 1999):

- off-line: analyzes the sample away from the production line, typically in a laboratory.

- at-line: random samples are manually removed from the production line and analyzed by an instrument installed very close to the process line.

- on-line: the samples are diverted from the production line to be analyzed directly in the recirculation loop (by-pass) and are returned to the production line after analysis.

- in-line: analyzes the sample within the running production line (in situ).

In practice, the terms in-line and on-line are apparently used interchangeably and so, for the publications cited in this review, the term employed in the original article is used. A thorough review of the literature reveals that the VIS-NIR technique has been applied to a wide array of agro-food related applications. One of the major areas that have been impacted by this implementation is the postharvest handling of fruit and vegetables. This section summarizes the current status of research in the aforementioned area by highlighting recent investigative and exploratory studies about off-line and in-line applications.

4.1. Overview of the off-line application

During the off-line application, samples are taken from reaction mixtures or finished products and analyzed on a laboratory scale. The main disadvantages are that this type of analysis requires some time, and in the meanwhile the production of a product of unknown quality continues. Additionally, most commercially available VIS-NIR spectroscopy devices are limited to single point analysis, and therefore, if the sample is heterogeneous, such as fruit, a single value might not be able to characterize the bulk sample (Wold *et al.*, 2011).

Some solutions to these disadvantages are, on the one hand, to bring the spectrometer to the production line and to do the analysis at-line immediately after sampling. This is possible thanks to research innovations that are creating more compact and portable VIS-NIR devices (McClure *et al.*, 2007). On the other hand, another solution is to use a multipoint NIR system capable of monitoring different

points simultaneously. Additionally, the system could use different standoff distances adapting to the shape and size of the product, or even different light sources for individual probes depending on the objectives. Other advantages that these multipoint probes offer are their flexibility and the fact that they can be coupled to different scenarios.

4.2. Overview of the in-line application

The off-line measurement methods are still time-consuming, therefore justifying the recent development of methods for in-line process control (Roggo *et al.*, 2007). Furthermore, nowadays, processing lines increase the demand for strict quality controls and optimization of the product. A critical requirement is to acquire data from the intact product in real time.

In-line monitoring of the food production process has been considered by using specific analytical methods and in situ sensors or probes, such as NIR spectroscopy (Zude, 2008), acoustics and vibration (Patist & Bates, 2008), microwave resonance technology (Kim *et al.*, 1999), visible imaging (Cubero *et al.*, 2011; Cubero *et al.*, 2016), and hyperspectral imaging (Balasundaram *et al.*, 2009; Lorente *et al.*, 2012). In particular, NIR spectroscopy has proven to be a rapid, non-invasive and effective tool in fruit quality analysis, and its in-line application may be used to replace slow and laborious conventional methods (Ait Kaddour & Cuq, 2009; Alcalà *et al.*, 2010; Dowell & Maghirang, 2002). Therefore, the ability to routinely collect data about fruit quality using NIR on-line systems in

the line production could be valuable for companies. For example, its in-line application would allow the product to be labeled with nutritional/quality information, differentiating it from competitors, and thus such products could be sold at a premium price, thereby adding commercial value.

The determination of the quality traits of intact fruit in motion with the use of VIS-NIR technology would be a great advantage for production lines such as conveyor belts, sample cups on a conveyor belt or hopper systems, and studies have been conducted in this regard.

4.3. Comparison between in-line and off-line applications

Although several reviews of VIS-NIR applications on intact harvest fruits and vegetables have been published (Blanco & Villarroya, 2002; Huang *et al.*, 2008; Cen & He, 2007; Su *et al.*, 2017; Wang *et al.*, 2017; López *et al.*, 2013; Lin & Ying, 2009; Magwaza *et al.*, 2012; Opara & Pathare, 2014; Wang *et al.*, 2015; Wiesner *et al.*, 2014; Porep *et al.*, 2015; Wang *et al.*, 2007; Jha *et al.*, 2010; Nicolaï *et al.*, 2007; Cozzolino *et al.*, 2011; Ruiz-Altisent *et al.*, 2010), only one of them (Porep *et al.*, 2015) delves into the possible applications of NIR technology at a semi-industrial and industrial scale. Porep *et al.* (2015) based their review on NIR applications that follow an on-line strategy. In contrast, this paper makes the first comparative study between off- and in-line strategies followed by different authors for the same type of product. The implementations of VIS-NIR spectroscopy that have been reviewed are summarized in Table 1.

The bibliographic analysis that was performed showed that in-line application of NIR for the analysis of intact fruits has been mainly restricted to five types of samples, namely apples, watermelons, nectarines, olives, and pears. In most off-line applications with fruits, the acquisition mode used is reflectance, except for the study conducted by Khatiwada *et al.* (2016) and the two studies by McGlone *et al.* (2002 and 2003) carried out in transmittance mode with apples, as well as the studies by Abebe (2006) and Jie *et al.* (2013) with watermelons or Xu *et al.* (2014) with pears. In the case of in-line applications the situation is similar: the predominant acquisition modes are reflectance, used in all in-line applications with olives (Salguero-Chaparro *et al.*, 2012, 2013 and 2014), and the transmittance mode in the case of pears (Xu *et al.*, 2012; Sun *et al.*, 2016). Examples of both acquisition modes were found in in-line applications with watermelon (Jie *et al.*, 2014; Tamburini *et al.*, 2017) and apple (McGlone *et al.*, 2005; Shenderey *et al.*, 2010; Ignat *et al.*, 2014), but nectarines were the only example found that employed the interactance mode (Golic & Walsh, 2006).

The application of VIS-NIR spectroscopy to the in-line analysis of intact apples has been analyzed by different researchers such as Shenderey *et al.* (2010), McGlone *et al.* (2005) and Ignat *et al.* (2014). In the study by Shenderey *et al.* (2010) moldy core in apples was detected by VIS-NIR mini-spectrometer (400–1,000 nm) installed in-line. The system was fitted with four cells, and in each cell rubber rings at the top and bottom hold the fruit and the fiber-optic probe was installed below the fruit-cell positions. The fruits were scanned in transmittance

mode, with a whole scan time of 1 second per fruit. The accuracy of the classification results was high: 92% detection of healthy apples and 100% detection of decay at levels of damage above 30%. Similarly, and also in transmittance mode, but in this case with a higher analysis speed (approximately 5 fruits per second), McGlone *et al.* (2005) developed two prototype on-line NIR systems to measure the percentage of internal tissue browning in apples in the wavelength range 650–950 nm. Both systems employed the same motor-driven fruit conveyor with 21 fruit cups. The best correlations for the measurement of the ITB in apples, comparing the two transmission systems that were designed, indicated that a conventional large aperture approach to the spectrometry (LAS) was more accurate as well as simpler and less prone to data losses than an alternative based on the recently developed TDIS. In reflectance mode but with the same speed as that employed by Shenderey *et al.* (2010) (1 sample per second), Ignat *et al.* (2014) assessed the feasibility of rapidly measuring the apple quality of three cultivars using two commercial spectrophotometers (VIS-NIR with a spectral region between 340–1014 nm and SWIR between 850–1888 nm). The advantage of this study is that they evaluated both instruments to measure the same product in a static mode (off-line) and on a moving conveyer (in-line). In this case, the conveyer had 24 cells of fruit and the light source illuminated the sample vertically with an optical fiber at an inclination of 45º. The results demonstrated that in-motion measurement modes gave higher SWS than static measurements in some cases. During in-motion measurement modes, the scanned area of the samples is

greater and, therefore, it reflects the individual apples more accurately compared with the static mode, where the optical fiber observes a relatively smaller area.

Additionally, comparing certain quality parameters, such as SSC, in both static and in-motion studies resulted in similar prediction models as regards the in-motion and the static measurements. Moreover, a comparison of certain quality parameters in both off-line and in-line studies resulted in similar and, in some cases, even better models for in-line than for static measurements. For example, observing the prediction of the SSC in studies with similar spectral ranges and the same measurement mode, an R^2=0.86 was obtained for the in-motion study by Ignat *et al.* (2014), which is a very similar result to that found in static studies by Nicolaï *et al.* (2007) with an R^2=0.87, Xiaobo *et al.* (2007) with an R^2=0.93, and the studies by Pissard *et al.* (2013) and Guo *et al.* (2016) with an R^2=0.94.

Watermelons were analyzed by Jie *et al.* (2014) using a prototype in-line detection system based on the VIS-NIR technique for predicting their soluble solids contents in a spectral range of 687–920 nm in transmittance mode. The on-line measurements were conducted by trays moving on a conveyor belt at a speed of 0.3 m/s. According to the authors, a calibration model based on Monte-Carlo uninformative variable elimination (MC-UVE) combined with stepwise multiple linear regressions (SMLR) and baseline offset correction (BOC) spectra pre-processing yielded optimal results (r_p=0.66). Recently, Tamburini *et al.* (2017) developed an NIR in-line system to determine lycopene, β-carotene, and total soluble solids content in red-flesh watermelons in the selected wavelength range

from 900 to 1700 nm in reflectance mode. Watermelons were transported along a conveyor belt system at different speeds (2100, 2400 and 2700 rpm). Models were performed using partial least squares (PLS) on pre-treated spectra (derivate and standard normal variation) and the results confirmed a good predictive ability with R^2_p higher than 0.70.

On comparing the off- and in-line studies by Jie *et al.* (2013 and 2014) in transmittance mode, it is observed that off-line results are slightly better (R^2_p=0.845 for off-line and r_p=0.66 for in-line) but with higher RMSEP (RMSEP=0.574 ºBrix for off-line and RMSEP=0.39 ºBrix for in-line). If this is compared with the other off-line study (Abebe *et al.*, 2006) conducted in transmittance mode found for this type of product, a higher R^2_p (0.81) is also obtained but with higher RMSEP (0.42 %) than for the in-line system.

In the case of nectarines, only one study has been found dealing with an in-line application. In this case, Golic and Walsh (2006) employed an NIR spectrometer (735–930 nm). In contrast to the rest of the in-line systems, this prototype was designed to acquire the fruit spectra in interactance mode (or partial transmittance configuration). The SSC of nectarines were determined above the cup in the conveyor belt by passing each cup at approximately 0.7 m/s, or 6 cups per second. The prediction performance of the model was good in terms of R^2>0.8. Comparing the prediction results of SSC of the in-line system (Golic and Walsh, 2006) with the off-line studies, although the mode of data acquisition was different, it was shown how the in-line system achieved, with a smaller spectral range, results

as good as, or even better than, those developed by Pérez-Marín *et al.* (2009) with an R^2=0.89 and Sánchez *et al.* (2011) with an r^2=0.47–0.68.

Intact olives were also assessed by VIS-NIR reflectance spectroscopy in both off-line and in-line applications by a research group of the University of Córdoba (Salguero-Chaparro *et al.*, 2012, 2013 and 2014). Salguero-Chaparro *et al.* (2012) studied and optimized some parameters such as focal distance and integration time prior to implementation of the system at factory level. The spectrometer was installed on a structure designed specifically to support it and to perform on-line measurements on a conveyor belt in the spectral range of 380–1690 nm. With the same semi-industrial scale process line on a conveyor belt, Salguero-Chaparro *et al.* (2013) determined the acidity, moisture, and fat content in intact olives. Depending on spectra pre-processing and validation strategies, the predictive performance achieved varied. However, the authors concluded that the in-line NIR prediction results were acceptable with R^2>0.74 for the three parameters measured in samples in movement. Additionally, Salguero-Chaparro *et al.* (2014) compared on-line versus off-line NIR systems to analyze the same properties as in the previous study. The parameters used were described in Salguero-Chaparro *et al.* (2012) and were as follows: focal distance of 13 mm, speed of conveyor belt of 0.1 m/s and integration time of 5 s. The results obtained indicated that the accuracy of the on-line analysis in comparison to the traditional off-line approach for the determination of physicochemical composition in intact olives was similar.

More specifically, on comparing the prediction by the PLS method of certain quality parameters such as fat content, free acidity and moisture content for the same mode of acquisition (reflectance), it is observed how the predictions achieved in the in-line studies (Salguero-Chaparro *et al.*, 2013 and 2014) were as good ($R^2_{\text{fat content}}$ = 0.79 and 0.86; $R^2_{\text{free acidity}}$ = 0.74 and 0.77; and $R^2_{\text{moisture content}}$ = 0.87 and 0.89) as those analyzed off-line ($R^2_{\text{fat content}}$ = 0.87; $R^2_{\text{free acidity}}$ = 0.76 ; and $R^2_{\text{moisture content}}$ = 0.89).

In the same way as in two studies dealing with apple and one with watermelon, the in-line systems developed for pears have been used in transmission mode. Xu *et al.* (2012) investigated an application for the on-line determination of sugar content in pears between 533–930 nm. The on-line measuring system included a tray conveyor device with a round hole at the bottom of the tray to install a collimating lens and an optical fiber used to connect the collimating lens and spectrometer. The halogen lamps were installed on two sides of the tray. The speed of the conveyor belt was 0.5 m/s and the integration time 100 ms. Similarly, Sun *et al.* (2016) developed on-line VIS-NIR transmittance system to measure soluble solids content and also brown core in pears. Like Xu *et al.* (2012), VIS-NIR spectra were recorded at a moving speed of 5 samples per second and using a very similar wavelength range from 600 to 904 nm. Furthermore, the system also consisted of a transmission chain, light source, detector, sorting mechanism, and fruit cup.

A comparison of both systems in-line allowed very good results to be obtained for SSC predictions, with R^2 between 0.82 and 0.99. In comparison with the SSC analysis off-line and also in transmission mode (Xu *et al.*, 2014), the in-line results are better than those performed off-line (r_p=0.96). With respect to off-line analyses but in reflectance mode (Li *et al.*, 2013 and Nicolaï *et al.*, 2008), in-line results were still better than those developed off-line (r_p=0.91 and R^2=0.60, respectively).

Table 1. Off-line and in-line applications of VIS-NIR spectroscopy in assessment of quality in agricultural products.

Sample	Application	Acquisition mode	Statistic method	Spectral range (range used)	Attributes analyzed	Performance	Ref.
Apples	**Off-line**	Reflectance	MLR	350-850 nm; 810-999 nm	SSC	R_p^2=0.49; SEP=1.14ºBrix	Ventura *et al.* (1998)
		Transmittance	PLS	500-750 nm	BC	$R^2_{(on\ the\ harvest)}$=0.78; $R^2_{(on\ the\ storage)}$=0.71	McGlone *et al.* (2002)
				500-750 nm	Firmness	$R^2_{(on\ the\ harvest)}$=0.63; $R^2_{(on\ the\ storage)}$=0.59	
				500-750 nm	QS	$R^2_{(on\ the\ harvest)}$=0.66	
				500-750 nm	SPI	$R^2_{(on\ the\ harvest)}$=0.78	
				600-1000 nm; 800-1000 nm	SSC	$R^2_{(on\ the\ harvest)}$=0.63; $R^2_{(on\ the\ storage)}$=0.70	
				500-1100 nm	TA	$R^2_{(on\ the\ harvest)}$=0.38	
		Transmittance	PLS	800-1000 nm	Dry matter	$R^2_{(at\ harvest\ time)}$=0.95 and RMSEP=0.29; $R^2_{(post\text{-}storage)}$=0.97 and RMSEP=0.24;	McGlone *et al.* (2003)
					SSC	$R^2_{(at\ harvest\ time)}$=0.79 and RMSEP=0.52%brix; $R^2_{(post\text{-}storage)}$=0.94 and RMSEP=0.30%brix;	
		Reflectance	PLS	300-1100 nm	SSC	$RMSEP_{con}$=0.65 ºBrix	Roger *et al.* (2003)
						Bias=−0.35 – 0.39 ºBrix	
		Reflectance	CDA	400-1700 nm	Impact bruises and non-bruised tissue	CR^2=0.68	Xing *et al.* (2003)
					Compression bruises and sound tissue	CR^2=0.68	

Table 1. Continuation.

Sample	Application	Acquisition mode	Statistic method	Spectral range (range used)	Attributes analyzed	Performance	Ref.
Apples	Off-line	Reflectance	PLS	380-2000 nm	Streif index	RMSEP=0.14-0.20 log kg cm^{-2} %$brix^{-1}$	Peirs *et al.* (2005)
					Respiratory maturity	RMSEP=4.4-7.9 days	
					Physiological maturity	RMSEP=5.7-8.8 days	
		Reflectance	Conceptual model	400–800 nm	Flavonol content	r^2=0.92; RMSEP=20 nmol/cm^2	Merzlyak *et al.* (2005)
		Reflectance	PLS-DA	400-1700 nm	Bruise detection	Classification accuracy >90%	Xing *et al.* (2005)
		Reflectance	Kernel PLS regression	800-1690 nm	SSC	R^2=0.87; RMSEP=0.44 °Brix	Nicolaï *et al.* (2007)
		Reflectance	PLS	11000–3800 cm^{-1}	SSC	$r_{p\,(full\ spectrum)}$=0.811; RMSEP$_{(full\ spectrum)}$=1.1522; $R_{p\,(optimal\ selected\ intervals)}$=0.93; RMSEP$_{(optimal\ selected\ intervals)}$=0.4424	Xiaobo *et al.* (2007)
		Reflectance	PLS-DA	500-1600 nm	Softening index	Classification accuracy >95%	Xing *et al.* (2007)
			PLS	804-1294 nm	E-modulus	r_p=0.77-0.80	
		Reflectance	LS-SVM	400-2500 nm	Vitamin C	R^2=0.80; SEP=4.9	Pissard *et al.* (2013)
					Total polyphenol	R^2=0.94; SEP=140	
					SSC	R^2=0.94; SEP=0.37	
		Reflectance	ICA-SVM	500-1100 nm	SSC	r_p=0.94; RMSEP=0.39 %	Guo *et al.* (2016)
		Reflectance	PLS-DA	400-1000nm; 1100-2100 nm	Influence of packaging on apple slices	86.7 % – 100 %	Beghi *et al.* (2016)

Table 1. Continuation.

Sample	Application	Acquisition mode	Statistic method	Spectral range (range used)	Attributes analyzed	Performance	Ref.
Apples	**Off-line**	Transmittance	PLS	302-1150 nm and 600-973 nm	Defect level (visual score)	R^2=0.83, RMSEP=0.63	Khatiwada *et al.* (2016)
			PLS-DA, LDA and SVM		Internal flesh browning	Classification accuracy>95%	
		Reflectance	QDA, SVM	800-2500 nm	Bitter pit detection	Average accuracy in the range of 78-87 %,	Kafle *et al.* (2016)
		Reflectance	PLS	6267-4173 cm^{-1}	Total antioxidant capacity	R^2=0.85, SEP=0.13% gallic acid equivalents, RPD=2.8	Schmutzler *et al.* (2016)
					SSC	R^2=0.76, SEP=0.55ºBrix, RPD=2.5	
		Reflectance	PLS	408-2498 nm	Dry matter	$R^2_{(peel)}$=0.94; $RPD^{(peel)}$=4.8; $R^2_{(flesh)}$=0.94; $RPD^{(flesh)}$=4.9	Pissard *et al* (2018)
					TPC	$R^2_{(peel)}$=0.91; $R^2_{(flesh)}$=0.84	
	In-line (sample cups on conveyor)	Transmittance	PLS	650-950 nm	ITB	R^2=0.9; RMSECV=4.1 %	McGlone *et al.* (2005)
	(simulated conveyer)	Transmittance	PLS	400-1000 nm	Moldy core	r^2=0.71; SEP=0.036; RPD=1.71	Shenderey *et al.* (2010)
	(cell conveyer)	Reflectance	PLS	340-1014 nm and 850-1888 nm	SSC	R^2=0.86, RMSEP=0.80	Ignat *et al.* (2014)
					TA	R^2=0.66, RMSEP=0.04	
					Firmness	R^2=0.76, RMSEP=6.60	
					Starch	R^2=0.91, RMSEP=0.86	

Table 1. Continuation.

Sample	Application	Acquisition mode	Statistic method	Spectral range (range used)	Attributes analyzed	Performance	Ref.
Watermelons	Off-line	Transmittance	PLS	700-1100 nm	SSC	R^2=0.81; RMSEP=0.42 %	Abebe (2006)
		Transmittance	MC-UVE-GA-PLS	220-102 nm (680-950 nm)	SSC	R^2=0.845; RMSEP=0.574 ºBrix	Jie *et al.* (2013)
	In-line (conveyor belt)	Transmittance	MC-UVE-SMLR	687-920 nm (200-1100 nm)	SSC	r_p=0.66; RMSEP=0.39 ºBrix	Jie *et al.* (2014)
		Reflectance	PLS	900-1700 nm	Lycopene	R^2=0.805; SECV=16.19 mg/kg	Tamburini *et al.* (2017)
					B-Carotene	R^2=0.737; SECV=0.96 mg/kg	
					SSC	R^2=0.707; SECV=1.4 %	
Nectarines	Off-line	Reflectance	PLS	360-1760 nm	IQI	R^2= 0.909-0.927; RMSEP=0.235-0.238	Cortés *et al.* (2017a)
			PLS-DA and LDA	360-1760 nm	Varietal discrimination	Classification accuracy of 100% and 97.44%	
		Reflectance	PLS-DA and LDA	600-1100 nm	Varietal discrimination	Classification accuracy of 100%	Cortés *et al.* (2017b)
		Reflectance	MPLS	1600-2400 nm; 400-1700 nm	SSC	r^2=0.89;SEP=0.75-0.81%	Pérez-Marín *et al.* (2009)
					Flesh firmness	r^2=0.84-0.86; SP=11.6-12.7 N	
					Weight	r^2=0.98; SEP=5.40 g	
					Diameter	r^2=0.75; SEP= 0.46 cm	
		Reflectance	PLS2-DA	1600-2400 nm	Shelf-life discrimination	86-96%	Pérez-Marín *et al.* (2011)
				400-1700 nm		66-89%	
		Reflectance	MPLS;LOCAL algorithm	1600-2400 nm	Weight	r^2=0.53;0.59	Sánchez *et al.* (2011)
					Diameter	r^2=0.53;0.56	
					Flesh firmness	r^2=0.85;0.87	
					SSC	r^2=0.47;0.68	

Table 1. Continuation.

Sample	Application	Acquisition mode	Statstic method	Spectral range (range used)	Attributes analyzed	Performance	Ref.
Nectarines	**In-line** (the cup conveyor belt)	Interactance	PLS	735-930 nm	SSC	$R^2 > 0.88$; RMSECV=0.53–0.88 %SSC	Golic & Walsh (2006)
Olives	**Off-line**	Reflectance	PLS	400-2500 nm	Fat content	R^2=0.87 ; RMSEP=2.50	Salguero-Chaparro *et al.* (2014)
					Free acidity	R^2=0.76 ; RMSEP=3.07	
					Moisture content	R^2=0.89 ; RMSEP=3.48	
			LS-SVM		Fat content	R^2=0.82 ; RMSEP=2.28	
					Free acidity	R^2=0.69 ; RMSEP=2.95	
					Moisture content	R^2=0.88 ; RMSEP=3.30	
	In-line (conveyor belt)	Reflectance	ANOVA and LSD	380-1690 nm	Focal distance and integration time	RMS (5s)=28.753 - 66.028	Salguero-Chaparro *et al.* (2012)
		Reflectance	PLS	380-1690 nm	Free acidity	R^2=0.74 ; RMSEP=2.53	Salguero-Chaparro *et al.* (2013)
					Moisture content	R^2=0.87 ; RMSEP=2.98	
					Fat content	R^2=0.79 ; RMSEP=2.15	
		Reflectance	PLS	380-1690 nm	Fat content	R^2=0.86 ; RMSEP=2.02	Salguero-Chaparro *et al.* (2014)
					Free acidity	R^2=0.77 ; RMSEP=2.64	
					Moisture content	R^2=0.89 ; RMSEP=3.33	
			LS-SVM		Fat content	R^2=0.83 ; RMSEP=2.19	

Table 1. Continuation.

Sample	Application	Acquisition mode	Statistic method	Spectral range (range used)	Attributes analyzed	Performance	Ref.
Pears	**Off-line**	Reflectance	MLR	1100-2500 nm	Pectin constituents	R=0.93, SEP=0.62 for alcohol insoluble solids in the fresh weight (for AIS in the FW) R=0.95, SEP=8.48 for oxalate soluble pectin content in the alcohol insoluble solids (OSP in the AIS)	Sirisomboon *et al.* (2007)
		Reflectance	PLS	780-1700 nm; 875-1030 nm	SSC	RMSEP=0.44ºBrix; R^2=0.60	Nicolaï *et al.* (2008)
					Firmness	-	
		Reflectance	EW-LS-SVM	380-1800 nm (400-1800 nm)	SSC	r_p=0.9164; RMSEP=0.2506	Li *et al.* (2013)
					pH	r_p=0.8809; RMSEP=0.0579	
					Firmness	r_p=0.8912; RMSEP=0.6247	
		Reflectance	PLS	300-1100 nm and 1000-2500 nm (680-1000 nm and 1100-2350 nm)	Dry matter	R^2=0.78; RMSECV=0.78	Travers *et al.* (2014)
					SSC	R^2=0.84; RMSECV=0.44	
		Transmittance	PLS	465 - 1150 nm	SSC	r_p=0.96; RMSEP=0.29	Xu *et al.* (2014)
	In-line	Transmittance	SMLR	200-1100 nm (533-930 nm)	SSC	R^2=0.8296	Xu *et al.* (2012)
			GA-PLS			R^2=0.8781	
			iPLS			R^2=0.8396	
			GA-SPA-MLR			R^2=0.880	
		Transmittance	PLS	200-1100 nm (600-904 nm)	Brown core	98.30 %	Sun *et al.* (2016)
					SSC	97.8 % – 99 %	

5. CONCLUSIONS AND FUTURE DIRECTIONS

Visible and near-infrared spectroscopy techniques have become powerful tools for the non-destructive sensing of multiple quality and safety attributes of agricultural products. These techniques combined with chemometric methods have revealed great potential due to their fast detection speed, no need for sample disposal, and likelihood of simultaneous prediction of multiple quality parameters or discrimination of the products according to the objectives.

Recent evidence of the relevance of off-line and in-line applications of VIS-NIR spectroscopy may be found in the aforementioned reviews and the original papers cited therein. The possibility of automating processes by the in-line application of VIS-NIR spectroscopic methods is a great advantage compared to routine analyses that are performed off-line, mainly due to the savings achieved in time, material, and personnel. Nevertheless, prior studies on a laboratory scale are necessary in order to later extend the objective and transfer this technology to a semi-industrial scale and finally industrial scale. In this way, the advances of VIS-NIR technology in the agriculture and food industries are promoting the creation of hardware systems that are smaller, faster and more robust, while spectral analysis software is becoming more intelligent.

However, in-line application under industrial prototypes requires extensive research to overcome challenges such as the in-line moving of the products, moving due to speed, coupling the probe to the shape of the product, and inhomogeneity of the samples, among other factors.

Most of the studies published to date do not focus on in-line applications on the prototype scale (not a commercial or industrial level) but on laboratory research. However, recent demands from industries and consumers, together with the advances being made in the technology, more powerful processing units, and a reduction in the price of equipment makes VIS-NIR technology an analytical tool for routine and real-time food safety and quality controls that will become predominant in the next few years. To achieve this, it is necessary to continue to study in greater depth methods to: i) offset the negative influence of movement; ii) homogenize the measurement process regardless of the size or shape of the fruit; iii) measure on different points of the fruit; iv) reduce analysis time; v) speed up the process by measuring several fruits at the same time; and vi) combine manipulation and quality inspection of the fruit simultaneously.

Abbreviations used

ANN, artificial neural network; BC, background colour; CA, cluster analysis; CDA, canonical discriminant analysis; CR^2, squared canonical correlation; IQI, internal quality index; ITB, internal tissue browning; KNN, K-nearest neighbors; LDA, linear discriminant analysis; LV, latent variables; MIR, med-infrared; MLR, multiple linear regression; MSC, multiplicative scatter correction; OSC, orthogonal signal correction; PCR, principal component regression; PLS, partial least square; PLS-DA, partial least squares-discriminant analysis; QDA, quadratic discriminant analysis; QS, quantitative starch; r, correlation coefficient; r_p, correlation

coefficient for prediction; R^2, coefficient of determination; RMSE, root mean square error; RMSECV, root mean square error of cross-validation; RMSEP, root mean square error of prediction; R^2_P, determination coefficient for prediction; RPD, ratio of performance to deviation; SEP, square error of prediction; SIMCA, soft independent modeling of class analogy; SNV, standard normal variate; SPI, starch pattern index; SSC, soluble solids content; SVM, support vector machine; SWIR, short-wavelength near-infrared; SWS, standardized weighted sum; TA, titratable acidity; TDIS, time-delayed integration method; TPC, content of total phenolic compounds; VIS-NIR, visible and near-infrared.

Acknowledgements

This work was partially funded by INIA and FEDER funds through research project RTA2015-00078-00-00. Victoria Cortés López thanks the Spanish Ministry of Education, Culture and Sports for the FPU grant (FPU13/04202).

6. REFERENCES

Abebe, A.T. (2006). Total sugar and maturity evaluation of intact watermelon using near infrared spectroscopy. Journal of Near Infrared Spectroscopy, 14(1), 67-70.

Ait Kaddour, A. & Cuq, B. (2009). In line monitoring of wet agglomeration of wheat flour using near infrared spectroscopy. Powder Technology, 190(1-2), 10-18.

Alander, J.T., Bochko, V., Martinkauppi, B., Saranwong, S. & Mantere, T. (2013). A review of optical nondestructive visual and near-infrared methods for food quality and safety. International Journal of Spectroscopy, 2013.

Alcalà, M., Blanco, M., Bautista, M. & González, J.M. (2010). On-line monitoring of a granulation process by NIR spectroscopy. Journal of Pharmaceutical Sciences, 99(1), 336-345.

Amodio, M.L., Ceglie, F., Chaudhry, M.M.A., Piazzolla, F. & Colelli, G. (2017). Potential of NIR spectroscopy for predicting internal quality and discriminating among strawberry fruits from different production systems. Postharvest Biology and Technology, 125, 112-121.

Balasundaram, D., Burks, T.F., Bulanon, D.M., Schubert, T. & Lee, W.S. (2009). Spectral reflectance characteristics of citrus canker and other peel conditions of grapefruit. Postharvest Biology and Technology, 51(2), 220-226.

Baranowski, P., Mazurek, W., Wozniak, J., Majewska, U. (2012) Detection of early bruises in apples using hyperspectral data and thermal imaging. Journal of Food Engineering, 110, 345–355.

Barnes, R.J., Dhanoa, M.S. & Lister, S.J. (1989). Standard normal variate transformation and de-trending of near-infrared diffuse reflectance spectra. Applied spectroscopy, 43(5), 772-777.

Beghi, R., Giovenzana, V., Civelli, R. & Guidetti, R. (2016). Influence of packaging in the analysis of fresh-cut Valerianella locusta L. and Golden

Delicious apple slices by visible-near infrared and near infrared spectroscopy. Journal of Food Engineering, 171, 145-152.

Berrueta, L.A., Alonso-Salces, R.M. & Héberger, K. (2007). Supervised pattern recognition in food analysis. Journal of chromatography A, 1158(1-2), 196-214.

Blanco, M. & Villarroya, I.N.I.R. (2002). NIR spectroscopy: a rapid-response analytical tool. Trends in Analytical Chemistry, 21(4), 240-250.

Bobelyn, E., Serban, A., Nicu, M., Lammertyn, J., Nicolaï, B. M. & Saeys, W. (2010). Postharvest quality of apple predicted by NIR spectroscopy: study of the effect of biological variability on spectra and model performance. Postharvest Biology and Technology, 55, 133–143.

Brereton, R.G. (2003). Chemometrics: data analysis for the laboratory and chemical plant. John Wiley & Sons.

Callis, J.B., Illman, D.L. & Kowalski, B.R. (1987). Process analytical chemistry. Analytical Chemistry, 59(9), 624A-637A.

Cen, H. & He, Y. (2007). Theory and application of near infrared reflectance spectroscopy in determination of food quality. Trends in Food Science & Technology, 18(2), 72-83.

Chen, Q., Zhao, J., Fang, C.H. & Wang, D. (2007). Feasibility study on identification of green, black and Oolong teas using near-infrared reflectance spectroscopy based on support vector machine (SVM). Spectrochimica Acta Part A: Molecular and Biomolecular Spectroscopy, 66(3), 568-574.

Coates, J. (2000). Interpretation of infrared spectra, a practical approach. Encyclopedia of Analytical Chemistry.

Cogdill, R.P. & Anderson, C.A. (2005). Efficient spectroscopic calibration using net analyte signal and pure component projection methods. Journal of Near Infrared Spectroscopy, 13(3), 119-131.

Coomans, D., Broeckaert, I., Jonckheer, M. & Massart, D.L. (1983). Comparison of multivariate discrimination techniques for clinical data—application to the thyroid functional state. Methods of Information in Medicine, 22(02), 93-101.

Cortés, V., Blasco, J., Aleixos, N., Cubero, S. & Talens, P. (2017a). Visible and Near-Infrared Diffuse Reflectance Spectroscopy for Fast Qualitative and Quantitative Assessment of Nectarine Quality. Food and Bioprocess Technology, 10(10), 1755-1766.

Cortés, V., Cubero, S., Aleixos, N., Blasco, J. & Talens, P. (2017b). Sweet and nonsweet taste discrimination of nectarines using visible and near-infrared spectroscopy. Postharvest Biology and Technology, 133, 113-120.

Cortés, V., Ortiz, C., Aleixos, N., Blasco, J., Cubero, S. & Talens, P. (2016). A new internal quality index for mango and its prediction by external visible and near-infrared reflection spectroscopy. Postharvest Biology and Technology, 118, 148-158.

Cover, T. & Hart, P. (1967). Nearest neighbor pattern classification. IEEE transactions on information theory, 13(1), 21-27.

Cozzolino, D., Cynkar, W.U., Shah, N. & Smith, P. (2011). Multivariate data analysis applied to spectroscopy: Potential application to juice and fruit quality. Food Research International, 44(7), 1888-1896.

Cubero, S., Aleixos, N., Moltó, E., Gómez-Sanchis, J. & Blasco, J. (2011). Advances in machine vision applications for automatic inspection and quality evaluation of fruits and vegetables. Food and Bioprocess Technology, 4(4), 487-504.

Cubero, S., Lee, W.S., Aleixos, N., Albert, F. & Blasco, J. (2016). Automated systems based on machine vision for inspecting citrus fruits from the field to postharvest—a review. Food and Bioprocess Technology, 9(10), 1623-1639.

Derde, M.P., Buydens, L., Guns, C., Massart, D.L. & Hopke, P.K. (1987). Comparison of rule-building expert systems with pattern recognition for the classification of analytical data. Analytical Chemistry, 59(14), 1868-1871.

Dickens, J.E. (2010). Overview of process analysis and PAT. Process analytical technology: Spectroscopic tools and implementation strategies for the chemical and pharmaceutical industries, 1-15.

Dowell, F.E. & Maghirang, E. (2002). Accuracy and feasibility of measuring characteristics of single kernels using near-infrared spectroscopy. Proceedings of the ICC Conference (pp. 313-320).

Escribano, S., Biasi, W.V., Lerud, R., Slaughter, D.C. & Mitcham, E.J. (2017). Non-destructive prediction of soluble solids and dry matter content using NIR spectroscopy and its relationship with sensory quality in sweet cherries. Postharvest Biology and Technology, 128, 112-120.

Geladi, P., MacDougall, D. & Martens, H. (1985). Linearization and scatter-correction for near-infrared reflectance spectra of meat. Applied spectroscopy, 39(3), 491-500.

Golic, M. & Walsh, K.B. (2006). Robustness of calibration models based on near infrared spectroscopy for the in-line grading of stonefruit for total soluble solids content. Analytica Chimica Acta, 555(2), 286-291.

Guo, Z., Huang, W., Peng, Y., Chen, Q., Ouyang, Q. & Zhao, J. (2016). Color compensation and comparison of shortwave near infrared and long wave near infrared spectroscopy for determination of soluble solids content of 'Fuji'apple. Postharvest Biology and Technology, 115, 81-90.

Herold, B., Kawano, S., Sumpf, B., Tillmann, P. & Walsh, K.B. (2009). VIS/NIR spectroscopy. Optical monitoring of fresh and processed agricultural crops, 141-249.

Hu, J., Ma, X., Liu, L., Wu, Y. & Ouyang, J. (2017). Rapid evaluation of the quality of chestnuts using near-infrared reflectance spectroscopy. Food Chemistry, 231, 141-147.

Huang, H., Yu, H., Xu, H. & Ying, Y. (2008). Near infrared spectroscopy for on/in-line monitoring of quality in foods and beverages: A review. Journal of Food Engineering, 87(3), 303-313.

Ignat, T., Lurie, S., Nyasordzi, J., Ostrovsky, V., Egozi, H., Hoffman, A., Friedman, H., Weksler, A. & Schmilovitch, Z. E. (2014). Forecast of apple internal quality indices at harvest and during storage by VIS-NIR spectroscopy. Food and Bioprocess Technology, 7(10), 2951-2961.

Jha, S.N., Narsaiah, K., Sharma, A.D., Singh, M., Bansal, S. & Kumar, R. (2010). Quality parameters of mango and potential of non-destructive techniques for their measurement--a review. Journal of Food Science and Technology, 47(1), 1-14.

Jie, D., Xie, L., Fu, X., Rao, X. & Ying, Y. (2013). Variable selection for partial least squares analysis of soluble solids content in watermelon using near-infrared diffuse transmission technique. Journal of Food Engineering, 118(4), 387-392.

Jie, D., Xie, L., Rao, X. & Ying, Y. (2014). Using visible and near infrared diffuse transmittance technique to predict soluble solids content of watermelon in an on-line detection system. Postharvest Biology and Technology, 90, 1-6.

Kafle, G.K., Khot, L.R., Jarolmasjed, S., Yongsheng, S. & Lewis, K. (2016). Robustness of near infrared spectroscopy based spectral features for non-destructive bitter pit detection in honeycrisp apples. Postharvest Biology and Technology, 120, 188-192.

Kamruzzaman, M., Makino, Y. & Oshita, S. (2016). Rapid and non-destructive detection of chicken adulteration in minced beef using visible near-infrared hyperspectral imaging and machine learning. Journal of Food Engineering, 170, 8-15.

Khatiwada, B.P., Subedi, P.P., Hayes, C., Jnr, L.C.C. & Walsh, K.B. (2016). Assessment of internal flesh browning in intact apple using visible-short wave near infrared spectroscopy. Postharvest Biology and Technology, 120, 103-111.

Khodabakhshian, R., Emadi, B., Khojastehpour, M., Golzarian, M.R. & Sazgarnia, A. (2017). Non-destructive evaluation of maturity and quality parameters of pomegranate fruit by visible/near infrared spectroscopy. International journal of food properties, 20(1), 41-52.

Kim, S.M., Chen, P., McCarthy, M.J. & Zion, B. (1999). Fruit internal quality evaluation using on-line nuclear magnetic resonance sensors. Journal of agricultural engineering research, 74(3), 293-301.

Koch, K.H. (1999). Process analytical chemistry: control, optimization, quality, economy. Springer, Beling, New York.

Kumaravelu, C. & Gopal, A. (2015). A review on the applications of Near-Infrared spectrometer and Chemometrics for the agro-food processing industries. In Technological Innovation in ICT for Agriculture and Rural Development (TIAR), IEEE (pp. 8-12).

Li, J., Huang, W., Zhao, C. & Zhang, B. (2013). A comparative study for the quantitative determination of soluble solids content, pH and firmness of pears by Vis/NIR spectroscopy. Journal of Food Engineering, 116(2), 324-332.

Lin, H. & Ying, Y. (2009). Theory and application of near infrared spectroscopy in assessment of fruit quality: a review. Sensing and instrumentation for food quality and safety, 3(2), 130-141.

Liu, F.; Yusuf, B.L.; Zhong, J.L.; Feng, L.; He, Y. & Wang, L. (2011). Variety identification of rice vinegars using visible and near infrared spectroscopy and multivariate calibrations. International Journal of Food Properties, 14, 1264–1276.

López, A., Arazuri, S., García, I., Mangado, J. & Jarén, C. (2013). A review of the application of near-infrared spectroscopy for the analysis of potatoes. Journal of Agricultural and Food Chemistry, 61(23), 5413-5424.

Lorente, D., Aleixos, N., Gómez-Sanchis, J., Cubero, S., García-Navarrete, O. L. & Blasco, J. (2012). Recent advances and applications of hyperspectral imaging for fruit and vegetable quality assessment. Food Bioprocess Technology, 5, 1121–1142.

Lorente, D., Escandell-Montero, P., Cubero, S., Gómez-Sanchis, J. & Blasco, J. (2015). Visible-NIR reflectance spectroscopy and manifold learning methods applied to the detection of fungal infections on citrus fruit. Journal of Food Engineering, 163, 17-24.

Magwaza, L.S., Opara, U.L., Nieuwoudt, H., Cronje, P.J., Saeys, W. & Nicolaï, B. (2012). NIR spectroscopy applications for internal and external quality analysis of citrus fruit-a review. Food and Bioprocess Technology, 5(2), 425-444.

Mariey, L., Signolle, J.P., Amiel, C. & Travert, J. (2001). Discrimination, classification, identification of microorganisms using FTIR spectroscopy and chemometrics. Vibrational spectroscopy, 26(2), 151-159.

Martens, R., Van Audekercke, R., Delport, P., DeMeester, P. & Mulier, J.C. (1983). The mechanical characteristics of cancellous bone at the upper femoral region. Journal of Biomechanics 16, 971.

McClure, W.F. & Tsuchikawa, S. (2007). Instruments. Near-infrared Spectroscopy in Food Science and Technology; Yukihiro Ozaki, W., Fred McClure, AAC, Eds, 75-107.

McClure, W.F. (2007). In Near-infrared Spectroscopy in Food Science and Technology, Chapter 1, ed. by Y. Ozaki, W. Fred McClure, A.A. Christy (Wiley-Interscience, Hoboken, NJ, 1–10.

McGlone, V.A., Jordan, R.B. & Martinsen, P.J. (2002). Vis/NIR estimation at harvest of pre-and post-storage quality indices for 'Royal Gala'apple. Postharvest Biology and Technology, 25(2), 135-144.

McGlone, V.A., Jordan, R.B., Seelye, R. & Clark, C.J. (2003). Dry-matter-a better predictor of the post-storage soluble solids in apples?. Postharvest Biology and Technology, 28(3), 431-435.

McGlone, V.A., Martinsen, P.J., Clark, C.J. & Jordan, R.B. (2005). On-line detection of brown heart in Braeburn apples using near infrared transmission measurements. Postharvest Biology and Technology, 37(2), 142-151.

Merzlyak, M.N., Solovchenko, A.E., Smagin, A.I. & Gitelson, A.A. (2005). Apple flavonols during fruit adaptation to solar radiation: spectral features and technique for non-destructive assessment. Journal of Plant Physiology, 162(2), 151-160.

Moscetti, R., Haff, R.P., Monarca, D., Cecchini, M. & Massantini, R. (2016). Near-infrared spectroscopy for detection of hailstorm damage on olive fruit. Postharvest Biology and Technology, 120, 204-212.

Næs, T., Isaksson, T., Fearn, T. & Davies, T. (2002). A user friendly guide to multivariate calibration and classification. NIR publications.

Nicolaï, B.M., Theron, K.I. & Lammertyn, J. (2007). Kernel PLS regression on wavelet transformed NIR spectra for prediction of sugar content of apple. Chemometrics and intelligent laboratory systems, 85(2), 243-252.

Nicolaï, B.M., Verlinden, B.E., Desmet, M., Saevels, S., Saeys, W., Theron, K., Cubeddu, R., Pifferi, A. & Torricelli, A. (2008). Time-resolved and continuous wave NIR reflectance spectroscopy to predict soluble solids content and firmness of pear. Postharvest Biology and Technology, 47(1), 68-74.

Opara, U.L. & Pathare, P.B. (2014). Bruise damage measurement and analysis of fresh horticultural produce-a review. Postharvest Biology and Technology, 91, 9-24.

Pasquini, C. (2003). Near infrared spectroscopy: fundamentals, practical aspects and analytical applications. Journal of the Brazilian chemical society, 14(2), 198-219.

Patist, A. & Bates, D. (2008). Ultrasonic innovations in the food industry: from the laboratory to commercial production. Innovative food science & emerging technologies, 9(2), 147-154.

Peirs, A., Schenk, A. & Nicolaï, B.M. (2005). Effect of natural variability among apples on the accuracy of VIS-NIR calibration models for optimal harvest date predictions. Postharvest Biology and Technology, 35(1), 1-13.

Pérez-Marín, D., Sánchez, M.T., Paz, P., González-Dugo, V. & Soriano, M.A. (2011). Postharvest shelf-life discrimination of nectarines produced under different irrigation strategies using NIR-spectroscopy. Food Science and Technology, 44(6), 1405-1414.

Pérez-Marín, D., Sánchez, M.T., Paz, P., Soriano, M.A., Guerrero, J.E. & Garrido-Varo, A. (2009). Non-destructive determination of quality parameters in nectarines during on-tree ripening and postharvest storage. Postharvest Biology and Technology, 52(2), 180-188.

Pissard, A., Baeten, V., Dardenne, P., Dupont, P. & Lateur, M. (2018). Use of NIR spectroscopy on fresh apples to determine the phenolic compounds and dry matter content in peel and flesh. Biotechnology, Agronomy, Society and Environment, 22 (1), 3-12.

Pissard, A., Fernández Pierna, J.A., Baeten, V., Sinnaeve, G., Lognay, G., Mouteau, A., Dupont, P., Rondia, A. & Lateur, M. (2013). Non-destructive measurement of vitamin C, total polyphenol and sugar content in apples using near-infrared spectroscopy. Journal of the Science of Food and Agriculture, 93(2), 238-244.

Pontes, M.J.C., Santos, S.R.B., Araujo, M.C.U., Almeida, L.F., Lima, R.A.C., Gaiao, E.N. & Souto, U.T.C.P. (2006). Classification of distilled alcoholic beverages and verification of adulteration by near infrared spectrometry. Food Research International, 39(2), 182-189.

Porep, J.U., Kammerer, D.R., & Carle, R. (2015). On-line application of near infrared (NIR) spectroscopy in food production. Trends in Food Science & Technology, 46(2), 211-230.

Roger, J.M., Chauchard, F. & Bellon-Maurel, V. (2003). EPO–PLS external parameter orthogonalisation of PLS application to temperature-independent measurement of sugar content of intact fruits. Chemometrics and Intelligent Laboratory Systems, 66(2), 191-204.

Roggo, Y., Chalus, P., Maurer, L., Lema-Martinez, C., Edmond, A. & Jent, N. (2007). A review of near infrared spectroscopy and chemometrics in pharmaceutical technologies. Journal of pharmaceutical and biomedical analysis, 44(3), 683-700.

Rossel, R.V., Walvoort, D.J.J., McBratney, A.B., Janik, L.J. & Skjemstad, J.O. (2006). Visible, near infrared, mid infrared or combined diffuse reflectance

spectroscopy for simultaneous assessment of various soil properties. Geoderma, 131(1-2), 59-75.

Ruiz-Altisent, M., Ruiz-Garcia, L., Moreda, G.P., Lu, R., Hernandez-Sanchez, N., Correa, E.C., Diezma, B., Nicolaï, B. & García-Ramos, J. (2010). Sensors for product characterization and quality of specialty crops-A review. Computers and Electronics in Agriculture, 74(2), 176-194.

Salguero-Chaparro, L. & Peña-Rodríguez, F. (2014). On-line versus off-line NIRS analysis of intact olives. Food Science and Technology, 56(2), 363-369.

Salguero-Chaparro, L., Baeten, V., Abbas, O. & Peña-Rodríguez, F. (2012). On-line analysis of intact olive fruits by vis–NIR spectroscopy: Optimisation of the acquisition parameters. Journal of Food Engineering, 112(3), 152-157.

Salguero-Chaparro, L., Baeten, V., Fernández-Pierna, J.A. & Peña-Rodríguez, F. (2013). Near infrared spectroscopy (NIRS) for on-line determination of quality parameters in intact olives. Food Chemistry, 139(1-4), 1121-1126.

Sánchez, M.T., De la Haba, M.J., Guerrero, J.E., Garrido-Varo, A. & Pérez-Marín, D. (2011). Testing of a local approach for the prediction of quality parameters in intact nectarines using a portable NIRS instrument. Postharvest Biology and Technology, 60(2), 130-135.

Savitzky, A. & Golay, M.J. (1964). Smoothing and differentiation of data by simplified least squares procedures. Analytical Chemistry, 36(8), 1627-1639.

Schmutzler, M. & Huck, C.W. (2016). Simultaneous detection of total antioxidant capacity and total soluble solids content by Fourier transform near-infrared (FT-NIR) spectroscopy: a quick and sensitive method for on-site analyses of apples. Food Control, 66, 27-37.

Shenderey, C., Shmulevich, I., Alchanatis, V., Egozi, H., Hoffman, A., Ostrovsky, V., Lurie, S., Arie, R.B. & Schmilovitch, Z. E. (2010). NIRS detection of moldy core in apples. Food and Bioprocess Technology, 3(1), 79.

Siesler, H.W., Ozaki, Y., Kawata, S. & Heise, H.M. (2008). Near-infrared spectroscopy: principles, instruments, applications. John Wiley & Sons.

Sirisomboon, P., Tanaka, M., Fujita, S. & Kojima, T. (2007). Evaluation of pectin constituents of Japanese pear by near infrared spectroscopy. Journal of Food Engineering, 78(2), 701-707.

Soriano-Disla, J.M., Janik, L.J., Viscarra Rossel, R.A., Macdonald, L.M. & McLaughlin, M.J. (2014). The performance of visible, near-, and mid-infrared reflectance spectroscopy for prediction of soil physical, chemical, and biological properties. Applied Spectroscopy Reviews, 49(2), 139-186.

Su, W.H., He, H.J., & Sun, D.W. (2017). Non-destructive and rapid evaluation of staple foods quality by using spectroscopic techniques: a review. Critical reviews in food science and nutrition, 57(5), 1039-1051.

Sun, X., Liu, Y., Li, Y., Wu, M. & Zhu, D. (2016). Simultaneous measurement of brown core and soluble solids content in pear by on-line visible and near infrared spectroscopy. Postharvest Biology and Technology, 116, 80-87.

Tamburini, E., Costa, S., Rugiero, I., Pedrini, P. & Marchetti, M.G. (2017). Quantification of lycopene, β-carotene, and total soluble solids in intact red-flesh watermelon (Citrullus lanatus) using on-line near-infrared spectroscopy. Sensors, 17(4), 746.

Travers, S., Bertelsen, M.G., Petersen, K.K. & Kucheryavskiy, S.V. (2014). Predicting pear (cv. Clara Frijs) dry matter and soluble solids content with near infrared spectroscopy. Food Science and Technology, 59(2), 1107-1113.

Tsuchikawa, S. (2007). A review of recent near infrared research for wood and paper. Applied Spectroscopy Reviews, 42(1), 43-71.

Tümsavas, Z., Tekin, Y. & Mouazen, A.M. (2013). Effect of moisture content on the prediction of cation exchange capacity using visible and near infrared spectroscopy. Journal of Food, Agriculture & Environment, 11(1), 760-764.

Ventura, M., de Jager, A., de Putter, H. & Roelofs, F.P. (1998). Non-destructive determination of soluble solids in apple fruit by near infrared spectroscopy (NIRS). Postharvest Biology and Technology, 14(1), 21-27.

Wang, H., Peng, J., Xie, C., Bao, Y. & He, Y. (2015). Fruit quality evaluation using spectroscopy technology: a review. Sensors, 15(5), 11889-11927.

Wang, L., Sun, D.W., Pu, H. & Cheng, J.H. (2017). Quality analysis, classification, and authentication of liquid foods by near-infrared spectroscopy: A review of recent research developments. Critical reviews in food science and nutrition, 57(7), 1524-1538.

Wang, W. & Paliwal, J. (2007). Near-infrared spectroscopy and imaging in food quality and safety. Sensing and Instrumentation for Food Quality and Safety, 1(4), 193-207.

Wiesner, K., Fuchs, K., Gigler, A.M. & Pastusiak, R. (2014). Trends in near infrared spectroscopy and multivariate data analysis from an industrial perspective. Procedia Engineering, 87, 867-870.

Wold, J.P., O'Farrell, M., Høy, M. & Tschudi, J. (2011). On-line determination and control of fat content in batches of beef trimmings by NIR imaging spectroscopy. Meat Science, 89(3), 317-324.

Wold, S., Antti, H., Lindgren, F. & Öhman, J. (1998). Orthogonal signal correction of near-infrared spectra. Chemometrics and Intelligent laboratory systems, 44(1-2), 175-185.

Xiaobo, Z., Jiewen, Z., Xingyi, H. & Yanxiao, L. (2007). Use of FT-NIR spectrometry in non-invasive measurements of soluble solid contents (SSC) of 'Fuji'apple based on different PLS models. Chemometrics and Intelligent Laboratory Systems, 87(1), 43-51.

Xing, J. & De Baerdemaeker, J. (2007). Fresh bruise detection by predicting softening index of apple tissue using VIS/NIR spectroscopy. Postharvest Biology and Technology, 45(2), 176-183.

Xing, J., Landahl, S., Lammertyn, J., Vrindts, E. & De Baerdemaeker, J. (2003). Effects of bruise type on discrimination of bruised and non-bruised 'Golden Delicious' apples by VIS/NIR spectroscopy. Postharvest Biology and technology, 30(3), 249-258.

Xing, J., Van Linden, V., Vanzeebroeck, M. & De Baerdemaeker, J. (2005). Bruise detection on Jonagold apples by visible and near-infrared spectroscopy. Food Control, 16(4), 357-361.

Xu, H., Qi, B., Sun, T., Fu, X. & Ying, Y. (2012). Variable selection in visible and near-infrared spectra: Application to on-line determination of sugar content in pears. Journal of Food Engineering, 109(1), 142-147.

Xu, W., Sun, T., Wu, W., Hu, T., Hu, T. & Liu, M. (2014). Determination of soluble solids content in Cuiguan pear by Vis/NIR diffuse transmission spectroscopy and variable selection methods. Knowledge Engineering and Management, 269-276.

2. OBJECTIVES

2.1 General objective

The main objective of this thesis was to contribute to the development of non-destructive inspection and handling systems for the estimation of the quality of some fruits according to their external and internal characteristics and for their correct classification according these properties, based on advanced automatic inspection and intelligent robotic manipulation systems.

2.2. Specific objectives

- Develop visible and near infrared predictive models for determining astringency in persimmon fruits.
- Evaluate visible and near-infrared spectroscopy as classification tool for nectarine varieties with a very similar external appearance.
- Find a suitable predictive method based on VIS-NIR spectroscopy for determining the internal quality of intact nectarines and mangoes.
- Evaluate the possibility of predicting the firmness and ripeness of mango fruits using a non-destructive technique during robot handling operation with a robot gripper.
- To design and integrate sensors with different nature in a robot gripper to determine the mechanical and optical quality properties of mango fruits.
- To design and construct a novel prototype for the in-line identification of apple varieties based on VIS-NIR spectroscopy.

3. SCIENTIFIC CONTRIBUTION

The thesis was divided into two different sections:

a. ***Off-line inspection.*** It was addressed to evaluate the optimal quality of fruits with a certain commercial interest based on non-destructive analysis under laboratory conditions applying visible and near-infrared spectroscopy device.

This section is divided in 4 chapters:

- CHAPTER I. Prediction of the level of astringency in persimmon using visible and near-infrared spectroscopy
- CHAPTER II. Sweet and nonsweet taste discrimination of nectarines using visible and near- infrared spectroscopy
- CHAPTER III. Visible and near-Infrared diffuse reflectance spectroscopy for fast qualitative and quantitative assessment of nectarine quality
- CHAPTER IV. A new internal quality index for mango and its prediction by external visible and near-infrared reflection spectroscopy

b. ***Processes automation.*** It was addressed to study and to develop new strategies based on visible and near-infrared spectroscopy, and its adaption for the automatic inspection and manipulation of fruits with the purpose of create new non-destructive systems based on fusion of sensors for the automatic quality estimation of fruits.

This section is divided in 3 chapters:

- CHAPTER V. Non-destructive assessment of mango firmness and ripeness using a robotic gripper
- CHAPTER VI. Integration of simultaneous tactile sensing and visible and near-infrared reflectance spectroscopy in a robot gripper for mango quality assessment
- CHAPTER VII. In-line application of visible and near infrared diffuse reflectance spectroscopy to identify apple varieties

3.1. SECTION I. OFF-LINE INSPECTION

3.1.1. Chapter I.

Prediction of the level of astringency in persimmon using visible and near-infrared spectroscopy

Cortés, V.[1], Rodríguez, A.[2], Blasco, J.[3], Rey, B.[2], Besada, C.[4], Cubero, S.[3], Salvador, A.[4], Talens, P.[1]& Aleixos, N.[2]

[1]Departamento de Tecnología de Alimentos. Universitat Politècnica de València. Camino de Vera s/n, 46022, Valencia (Spain).

[2]Departamento de Ingeniería Gráfica, Universitat Politècnica de València. Camino de Vera s/n, 46022, Valencia (Spain).

[3]Centro de Agroingeniería. Instituto Valenciano de Investigaciones Agrarias (IVIA). Ctra. CV-315, km. 10,7, 46113, Moncada, Valencia (Spain).

[4]Centro de Tecnología Postcosecha, Instituto Valenciano de Investigaciones Agrarias (IVIA), Ctra. CV-315, km. 10,7, 46113, Moncada, Valencia (Spain).

Journal of Food Engineering, 204 (2017), 27-37

ABSTRACT

Early control of fruit quality requires reliable and rapid determination techniques. Therefore, the food industry has a growing interest in non-destructive methods such as spectroscopy. The aim of this study was to evaluate the feasibility of visible and near-infrared (NIR) spectroscopy, in combination with multivariate analysis techniques, to predict the level and changes of astringency in intact and in the flesh of half cut persimmon fruits. The fruits were harvested and exposed to different treatments with 95 % CO_2 at 20 ºC for 0, 6, 12, 18 and 24 h to obtain samples with different levels of astringency. A set of 98 fruits was used to develop the predictive models based on their spectral data and another external set of 42 fruit samples was used to validate the models. The models were created using the partial least squares regression (PLSR), support vector machine (SVM) and least squares support vector machine (LS-SVM). In general, the models with the best performance were those which included standard normal variate (SNV) in the pre-processing. The best model was the PLSR developed with SNV along with the first derivative (1-Der) pre-processing, created using the data obtained at six measurement points of the intact fruits and all wavelengths (R^2=0.904 and RPD=3.26). Later, a successive projection algorithm (SPA) was applied to select the most effective wavelengths (EWs). Using the six points of measurement of the intact fruit and SNV together with the direct orthogonal signal correction (DOSC) pre-processing in the NIR spectra, 41 EWs were selected, achieving a R^2 of 0.915 and a RPD of 3.46 for the PLSR model. These results suggest that this technology has potential for use as a feasible and cost-effective method for the non-destructive determination of astringency in persimmon fruits.

Keywords: *Diospyros kaki*, fruit internal quality, soluble tannins, near-infrared spectroscopy, chemometrics

1. INTRODUCTION

Persimmon (*Diospyros kaki* L.) is a fruit originally from China, but is now cultivated in warm regions around the world (Ashtiani *et al.*, 2016). The climatic characteristics of the production are important factors that influence the quality and properties of the fruits. The main areas where this fruit is cultivated in Spain are Alicante, Andalucía, Castellón, Extremadura and Valencia, especially in Ribera del Xúquer, which was granted Protected Designation of Origin (PDO) status by the Spanish government in 1998 (Khanmohammadi *et al.*, 2014). Several cultivars of persimmon are grown in Spain, such as the astringent type 'Rojo Brillante'. Persimmon develops an astringent taste due to the presence of soluble tannins. Tannins are polyphenol compounds with a high molecular weight and their large hydroxyl phenolic groups cause astringency. As the fruit ripens, the soluble tannins gradually turn into insoluble tannins, making the fruit less astringent (Noypitak *et al.*, 2015). However, several postharvest treatments can be applied to achieve the fast removal of the astringency of the fruits without affecting the firmness of the pulp (Khademi *et al.*, 2010). Among them, the most widely used commercial technique is based on exposing the fruits to a high concentration of CO_2 (95%–98%). This method promotes anaerobic respiration in the fruit, resulting in an accumulation of acetaldehyde, which reacts with the soluble tannins. The tannins become insoluble with the treatment and the astringency is thus eliminated (Matsuo *et al.*, 1991). If the treatment is too short, it can result in fruits with residual astringency (Besada *et al.*, 2010), whereas if it is too long, it may lead to loss of fruit quality (Novillo *et al.*, 2014). Therefore, it is important to investigate non-destructive techniques to ensure the success of the treatments.

Techniques based on the spectrum analysis, like hyperspectral imaging, have been widely used for the qualitative and quantitative determination of different properties in fruit (Lorente *et al.*, 2012). Munera *et al.* (2017b & 2017a) analysed the astringency and the internal quality of persimmon using hyperspectral imaging, which has the advantage of obtaining both spectral and spatial information. However, one of the most common techniques currently used in food chemistry is near-infrared (NIR) spectroscopy, as it is non-destructive, inexpensive, rapid and reliable (Nicolaï *et al.*, 2007; Vitale *et al.*, 2013; López *et al.*, 2013). This technique has been used for the quantitative determination of several internal

properties or compounds (Schmilovitch *et al.*, 2000; Nagle *et al.*, 2010; Theanjumpol *et al.*, 2013), to determine maturity (Jha *et al.*, 2012) and also to measure quality indices (Attila & János, 2011; Cortés *et al.*, 2016).

The combination of chemometrics and spectroscopy has been applied in the food industry, agriculture and horticulture to obtain information from spectra. Support vector machine (SVM) are learning algorithms used for classification and regression tasks widely used in the analysis of spectroscopic data (Devos *et al.*, 2009; Fernadez-Pierna *et al.*, 2012). Chauchard *et al.* (2004) compared classical linear regression techniques with least square-support vector machine (LS-SVM) regression to predict the total acidity in fresh grapes using NIR spectroscopy. LS-SVM in combination with Standard normal variate (SNV) pre-processing and partial least square regression (PLSR) latent variables increased the rate of prediction. Nicolaï *et al.* (2007) predicted sugar content using PLSR. The covariance, Gaussian and cubic polynomial kernel functions obtained similar results of about R^2=0.87 and Q^2=0.84 for all methods, concluding that kernel PLSR offered no advantages compared to ordinary PLSR. The identification of the spectral variables (wavelengths) can lead to better classification results and simplify the chemical interpretation of the results. Calvini *et al.* (2015) tested sparse principal component analysis (PCA) together with k-Nearest-Neighbours (k-NN) and sparse PLS discriminant analysis (PLS-DA) to discriminate between Arabica and Robusta coffee, and compared the results with the classical approaches based on PCA+kNN and PLS-DA.

Lorente *et al.* (2015) used NIR spectroscopy (650 to 1700 nm) to detect early invisible decay lesions in citrus fruit using MSC and SNV pre-processing, different methods to select the important bands, and linear discriminant analysis (LDA) to classify the fruit as being either sound or rotten with a rate of correct classification above 90 %. Folch-Fortuny *et al.* (2016) used N-way-PLS-DA to detect early invisible decay lesions in citrus fruit, achieving a prediction rate higher than 90 %. Mowat and Poole (1997) found this technology useful in determining persimmon quality. Ito *et al.* (1997) and Noypitak *et al.* (2015) investigated astringency in the persimmons 'Nisimura-wase' and in 'Xichu', respectively. The most common mode used in NIRS is diffuse reflectance, which acquires the

reflected light in the vicinity of the illuminating point and is preferable for the measurement of intact fruit (Shao *et al.*, 2009; He *et al.*, 2007).

The aim of this study was to evaluate the feasibility of visible and NIR spectroscopy combined with chemometrics as a non-destructive tool to determine the level of astringency in persimmons cv. 'Rojo Brillante'.

2. PLANT MATERIAL AND EXPERIMENTAL DESIGN

Persimmon cv. 'Rojo Brillante' fruits were harvested in L'Alcudia (Valencia, Spain) at two stages of commercial maturity (M1 and M2) corresponding to late November and mid-December. The maturity index used to select the fruits was a visual observation of the external colour of the fruit (Salvador *et al.*, 2007). After each harvest, 70 fruits without external damage and of homogenous colour were selected (a total of 140 fruits). In order to characterise the fruit at harvest, the average colour index (CI=100*a*/*Lb*, Hunter parameters) was measured using a colorimeter (CR-300, Konica Minolta Inc, Tokyo, Japan) and the firmness of the flesh was measured by a universal testing machine (4301, Instron Engineering Corp., MA, USA) equipped with an 8 mm puncture probe. The crosshead speed during the firmness test was 10 mm/min. During the test, the force increased slowly until it decreased abruptly when the flesh broke, and then the maximum required force (in Newton) was recorded.

The average CI resulted in 18.20 ± 3.32 for M1 and 21.6 ± 4.05 for M2, while firmness decreased along with maturity at harvest, with mean values being 30.8 N ± 3.5 and 24.4 N ± 4.9 for M1 and M2, respectively.

In order to obtain different levels of astringency, the fruits in each maturity stage were divided into five homogeneous lots. The fruit was then exposed to CO_2 treatments in closed containers (95 % CO_2 at 20 ºC and 90 % RH) for 0, 6, 12, 18 and 24 h. Spectroscopic measurements of the intact fruits and the flesh of half cut fruits were acquired in the 8 h after each treatment with CO_2. Figure 1 shows the location of the selected points for the measurements.

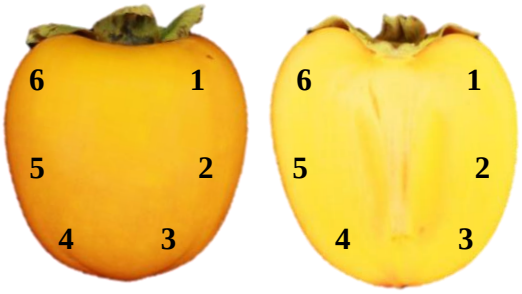

Figure 1. Selected points for the spectroscopic measurements in: a) intact fruit; and b) the flesh of half cut fruit.

The degree of astringency of each fruit was determined as follows. A flesh sample of each fruit was frozen at 20 ºC and the soluble tannin content was analysed using the Folin-Denis method (Taira, 1995). The results were expressed as relative soluble tannins by fresh weight. Prior to this process, each fruit was cut in half and pressed onto 10x10 cm filter paper soaked in a solution of 5 % $FeCl_3$, which resulted in an impression whose quantity and intensity gave information about the content of soluble tannins and their distribution (Matsuo & Ito, 1982). This method of tannin printing is an alternative technique to the Folin-Denis method used in industry in random fruits to determine the level of astringency in fruit lots.

3. VISIBLE AND NEAR-INFRARED SPECTRA COLLECTION

The spectra were alternately collected in reflectance mode using a multi-channel spectrometer platform (AVS-DESKTOP-USB2, Avantes BV, The Netherlands) equipped with two detectors (Fig. 2). The first detector (AvaSpec-ULS2048 StarLine, Avantes BV, The Netherlands) included a 50 mm entrance slit and a 600 lines/mm diffraction grating covering the working visible and near-infrared (VNIR) range from 650 nm to 1050 nm with a spectral FWHM (full width at half maximum) resolution of 1.15 nm. The spectral sampling interval was 0.255 nm. The second detector (AvaSpec-NIR256-1.7 NIRLine, Avantes BV, The Netherlands) was equipped with a 256-pixel non-cooled InGaAs (Indium Gallium Arsenide) sensor (Hamamatsu 92xx, Hamamatsu Photonics K.K., Japan), a 100

mm entrance slit and a 200 lines/mm diffraction grating covering the working NIR range from 1000 nm to 1700 nm with a spectral FWHM resolution of 12 nm. The spectral sampling interval was 3.535 nm. A stabilised 10 W tungsten halogen light source (AvaLight-HAL-S, Avantes BV, The Netherlands) was used. The probe tip was designed to provide reflectance measurements at a 45º angle so as to minimise the specular reflectance of the fruit surface.

Calibration was performed using a 99 % white reflective reference tile (WS-2, Avantes BV, The Netherlands) so that the maximum reflectance of the reference measured over the entire spectral range was 90 % of the value of saturation. Before taking the spectral measurements, the temperature of the persimmons was stabilised at 24 ºC. Measurements were performed at the six different points on the surface of the intact persimmon and the flesh of half cut fruit (Fig. 1), and mean values of the spectra for both types of measurements were used for the analysis. A personal computer equipped with commercial software (AvaSoft version 7.2, Avantes, Inc.) was used to control both detectors and to acquire and pre-process the spectra. The integration time was set at 90 ms for the detector sensitive in the VNIR and 700 ms for the detector sensitive in the NIR region. For both detectors, each spectrum was obtained as the average of five scans in order to reduce the detector's thermal noise (Nicolaï *et al.*, 2007). The mean reflectance measurements of each sample (S) were then converted to relative reflectance (R) values with respect to the white reference using dark reflectance (D) values and the reflectance values of the white reference (W), as shown in (1):

$$R = \frac{S-D}{W-D} \quad (1)$$

The dark spectrum was obtained by switching off the light source and covering the whole tip of the reflectance probe.

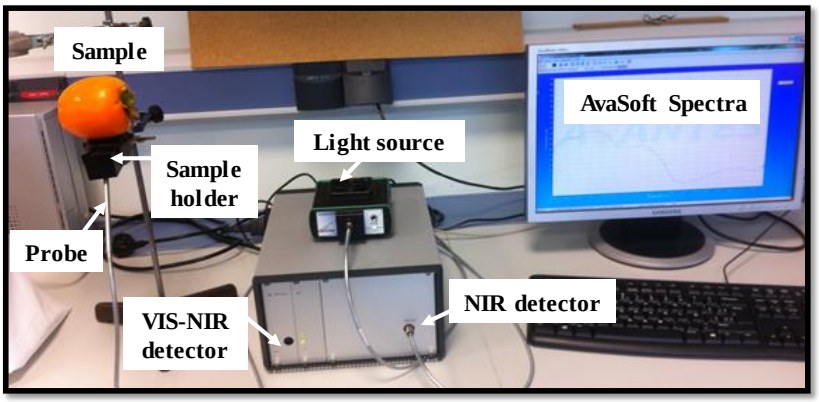

Figure 2. A labelled picture of the spectrometer.

4. STATISTICAL ANALYSIS

Spectral data and the tannin reference values were organised into matrices, where the rows represented the samples (the total of 140 persimmons) and the columns represented the variables. The X-variables, or predictors, were the wavelengths of the VNIR and NIR spectra for each persimmon. The Y-variable, or response, in the last column, represented the measured tannin value associated with each sample.

A total of 28 matrices were generated corresponding to different combinations of the measurement points of the intact fruit and the flesh of the half cut fruit. The first two matrices corresponded to the mean values of reflectance of the measurements at the six points of the intact fruit shown in Figure 1. The third and fourth matrices contained mean values of the measurements at four points (2-5-3-4), which corresponded to the lowest part of the intact persimmon in the VNIR and NIR detectors, respectively. The fifth to fourteenth matrices contained mean values for measurements of other combinations of points (1-6-2-5, 1-6-3-4, 1-6, 2-5 and 3-4) in both VNIR and NIR. Other combinations of measured points have not been taken into account since the deastringency process normally progresses from the top to the bottom of the fruit (Fig. 5) and would not make sense. The remaining 14 matrices corresponded to the mean values of the measurements of the same combinations of points, but from the flesh of the half cut fruit.

4.1. Spectral pre-processing

To remove the influence of unwanted effects such as high-frequency noise, baseline shifts, light scattering, random noise and any other external effects due to instrumental or environmental factors, six methods of spectral pre-processing and their combinations were applied before the development of the prediction models. These methods included standard normal variate (SNV), multiplicative scatter correction (MSC), Savitzky-Golay smoothing (SG), first (1-Der) and second (2-Der) derivatives, and direct orthogonal signal correction (DOSC). All spectral pre-processing methods and the prediction models were carried out using MATLAB R2015b (The Mathworks Inc., Natick, MA, USA).

SNV is commonly used to eliminate the multiplicative noise due to the influence of particle size or scatter interference (Rinnan *et al.*, 2009). SNV subtracts the mean from an individual spectrum and divides it by its standard deviation (Feng & Sun, 2013). Similarly, MSC is used to compensate for the non-uniform scattering effect induced by diverse particle sizes and other physical effects in the spectrum (Fearn *et al.*, 2009; Vidal & Amigo, 2012). It linearises each spectrum to an average spectrum (derived from the calibration set) and adjusts it using the least squares method.

Moreover, smoothing is an effective way to reduce high-frequency noise. There are several smoothing methods in the literature, but one of the most commonly applied is SG smoothing (Savitzky & Golay, 1964). This method has the advantage of preserving signal characteristics such as the maximum and minimum relative values or the width of the peaks, which usually disappear with other smoothing methods. In the present work, SG smoothing was calculated with two-degree polynomials and a window size of seven points.

1-Der and 2-Der are well-accepted pre-processing methods to eliminate the shifting, the scattering and the background noise, as well as to distinguish overlapping peaks and to improve the spectral resolution (Sinija & Mishra, 2011). They were calculated using the SG algorithm with three-point smoothing filters and a two-degree polynomial (Liu *et al.*, 2010).

Finally, DOSC are novel methods used to remove information that has a poor correlation (orthogonal) with the response matrix (Zhu *et al.*, 2008). DOSC

obtains components that are orthogonal to the response matrix and eliminates those that are considered irrelevant, thus improving the predictability.

4.2. Modelling by different calibration methods

Estimation of prediction error is required to evaluate the performance of fitted models. Cross-validation is widely used to estimate the prediction error (Fusiki, 2011). In this work, 70 % of the fruits in each maturity stage were randomly selected to build the models that were internally validated using a 10-fold cross-validation. The remaining 30 % of the samples were never used to build or train the model with the purpose of externally evaluating the performance of the regression techniques used to predict the tannin content. The regression techniques used in this work were PLSR, SVM and the LS-SVM regression.

The PLSR multivariate method is widely used to evaluate the linear relationship between inputs (spectral data or X-variables) and the response variable (tannin content in this case or Y-variable) in spectroscopic analysis (Geladi & Kowalski, 1986). The procedure is based on the use of latent variables (LVs), instead of real variables (spectral data), depending on the covariance between the predictors, or X-variables, and the response, or Y-variable, leading to a parsimonious model with reliable predictive power (Lorber *et al.*, 1987). SVM is a popular machine learning tool for regression (Vapnik, 2013) based on the Vapnik-Chervonenkis (VC) dimension and on the principle of structural risk minimisation (Gunn, 1998). It is considered a non-parametric technique because the SVM models are based on a non-linear kernel function. In short, SVM assigns the calibration dataset to a high-dimensional feature space by means of a non-linear mapping, and then performs a linear regression. This technique has the advantage of being very efficient and robust during the training of the model. In this study, the Matlab statistical and machine learning toolbox was used to train the model with the spectral and tannin information, using a linear kernel and a 10-fold cross-validation.

Finally, LS-SVM is a learning algorithm which improves the generalisation ability of the machine learning procedure based on the principle of structural risk minimisation (Liu *et al.*, 2008; Suykens & Vandewalle, 1999). It handles both linear and non-linear multivariate problems with less computational cost and with a

small sample database. This is achieved using linear equations instead of quadratic problems to reduce the complexity of the optimisation process (Liu & Sun, 2009). The LS-SVM has the advantage of limited over-fitting, high predictive reliability and a strong generalisation capability. The LS-SVMlab v1.8 toolbox (Suykens, Leuven, Belgium) was used to develop the calibration models. During the development of the model, the linear kernel and a 10-fold cross-validation were used to avoid problems of over-fitting. The linear kernel included a regularisation parameter that determined the trade-off between minimising the training error and minimising the model complexity. A large γ implies little regularisation, and therefore a more non-linear model (Sun *et al.*, 2009).

4.3. Variable selection

Since the number of variables used as inputs (wavelengths) in the models is high (1570 variables for the VNIR and 198 for the NIR spectra), they may contain excessive collinearity and redundancy. Therefore, it was considered appropriate to find the most important wavelengths as effective wavelengths (EWs) for each model. This was performed with the purpose of reducing the high dimensionality of the spectral data and the computational cost, thus achieving an optimal model.

The algorithm that was applied to select the EWs was a successive projection algorithm (SPA). SPA is a variable selection algorithm applied to solve collinearity problems and to select the wavelengths with fewer redundancies by means of a simple procedure of projection in a vectorial space, thereby allowing for the selection of the best subsets of wavelengths that conform to the minimum collinearity (Araújo *et al.*, 2001; Galvao *et al.*, 2008; Zhang *et al.*, 2013). SPA was applied for each calibration set and the EWs obtained were used again as inputs of the PLSR, SVM and LS-SVM models.

4.4. Model evaluation

The accuracy and the predictive capability of the three different models were evaluated by means of the coefficient of determination (R^2), the root mean square error (RMSE) and the ratio of performance to deviation (RPD) obtained on the external validation set. Generally, a good model must have high R^2 with low RMSE. In addition, an acceptable model should have an RPD value of more than

2.5, a value above 3.0 being very good (Williams & Sobering, 1993; Viscarra Rossel *et al.*, 2007; Kamruzzaman *et al.*, 2016; Cortés *et al.*, 2016). These parameters can be defined by equations 2 to 4.

$$R^2 = 1 - \frac{\sum_{i=1}^{N}(\hat{y}_i - y_i)^2}{\sum_{i=1}^{N}(\hat{y}_i - \bar{y}_i)^2} \quad (2)$$

$$RMSE = \sqrt{\frac{\sum_{i=1}^{N}(\hat{y}_i - y_i)^2}{N}} \quad (3)$$

$$RPD = \frac{SD(y)}{RMSEP} \quad (4)$$

where:

$\hat{y}_i$ is the estimated value of the i^{th} persimmon.

y_i is the measured value of the i^{th} persimmon.

N: is the number of observations.

SD: is the standard deviation of the measured values.

5. RESULTS AND DISCUSSION

The total number of persimmon samples was 140, with a mean tannin content of 0.250 % (STD=0.221). The statistical values of the persimmon tannin content in the calibration and external validation sets are shown in Table 1.

Before applying the models, the raw reflectance spectra (Figure 3) of the samples were pre-processed using the described methods.

Table 1. Statistical values of tannin content (%) of the studied persimmons.

DATA SET	Sample Nº	Min	Max	Mean	STD
Calibration	98	0.023	0.735	0.243	0.210
Prediction	42	0.023	0.752	0.266	0.245

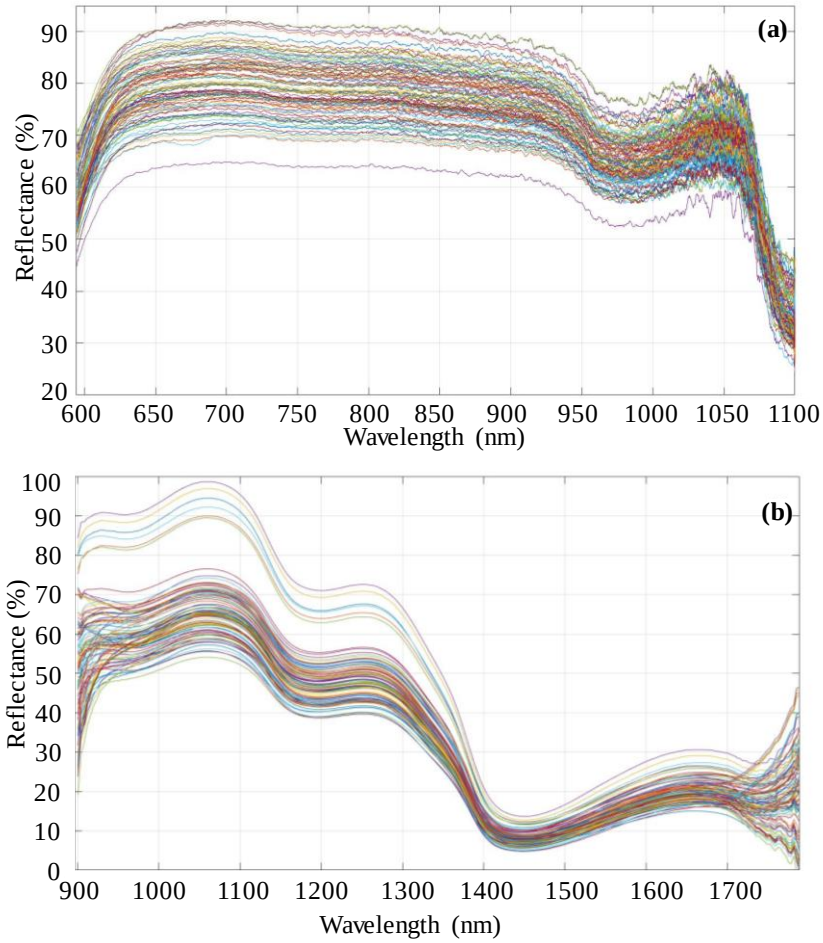

Figure 3. Raw reflectance spectra (%) of the persimmons in the calibration set for: (a) the VNIR region; and (b) the NIR region.

Thus, the PLSR, SVM and LS-SVM models were developed using both raw and pre-processed spectra. Samples in the external validation set were later used to evaluate the performance of the models. The results (R^2, RMSE and RPD) of the models for the external validation set are shown in Table 2 and Table 3. Table 2 shows the results using the average of the six measurement points for the intact fruit set, and Table 3 for the half cut fruit set.

Tables 2 and 3 show that, on average, the models with the best performance are those which included SNV in the pre-processing that was applied (SNV+1-Der, SNV+2-Der, SNV+DOSC). Figure 4 shows the results for the best PLSR model, which was obtained with the spectra measured at the six measurement points of the intact fruits and pre-processed using SNV+1-Der.

Tables 4 and 5 show the results for the three selected methods and the above mentioned pre-processing combinations after applying SPA for wavelength selection.

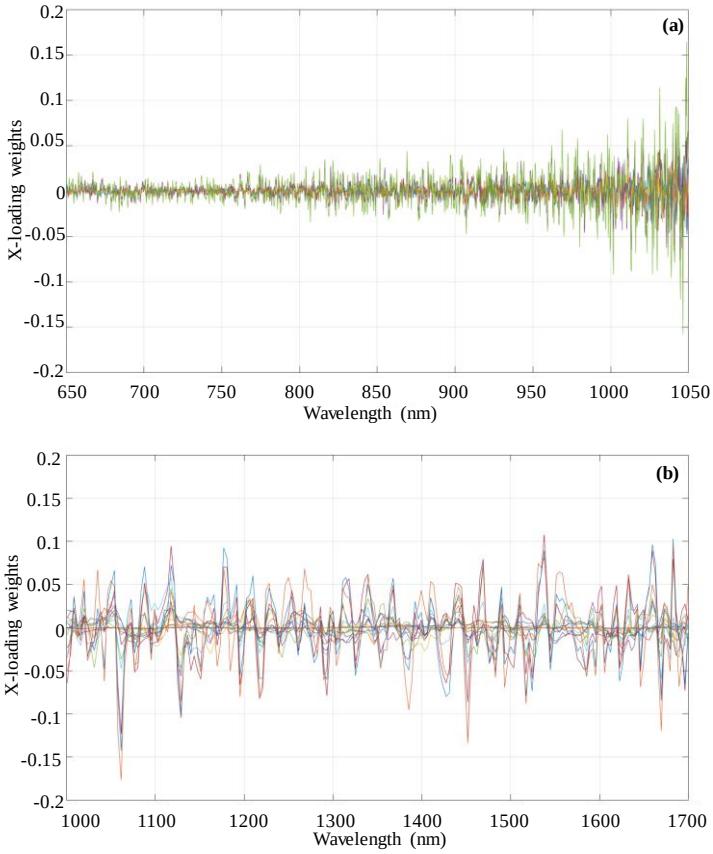

Figure 4. Normalised X-loading weights of the best PLSR model for the six measurement points (with SNV+1-Der pre-processing for the intact fruit set) for the (a) VNIR and (b) NIR detectors, respectively. Only the weights corresponding to the latent variables that explain 95 % of the Y-variable variance are shown (5 for VNIR and 16 for NIR detectors).

Table 2. Results of tannin content using the average of the six measurement points with all wavelengths by PLSR, SVM and LS-SVM models for the intact fruit set.

Model	Pre-treatment	*LV*, *γ*	VNIR			*LV*, *γ*	NIR		
			R^2	RMSE	RPD		R^2	RMSE	RPD
PLSR	**RAW**	18	0.829	0.100	2.45	36	0.813	0.105	2.34
	SNV	17	0.828	0.101	2.44	35	0.810	0.106	2.32
	SG	19	0.802	0.108	2.28	46	0.758	0.119	2.06
	1-Der	9	0.898	0.077	3.17	28	0.850	0.094	2.61
	2-Der	9	0.885	0.082	2.98	24	0.755	0.120	2.05
	MSC	17	0.828	0.101	2.44	34	0.821	0.103	2.39
	DOSC	1	0.817	0.104	2.37	1	0.704	0.132	1.86
	SNV + 1-Der	10	0.904	0.075	3.26	27	0.861	0.090	2.72
	SNV+ 2-Der	10	0.883	0.083	2.96	22	0.795	0.110	2.23
	SNV+DOSC	1	0.814	0.104	2.35	18	0.814	0.105	2.34
SVM	**RAW**		0.813	0.105	2.34		0.117	0.256	0.96
	SNV		0.863	0.090	2.74		0.010	0.241	1.02
	SG		0.813	0.105	2.34		0.107	0.255	0.96
	1-Der		0.893	0.079	3.09		0.728	0.126	1.94
	2-Der		0.896	0.078	3.14		0.811	0.105	2.33
	MSC		0.861	0.090	2.71		0.016	0.244	1.00
	DOSC		0.835	0.099	2.49		0.731	0.126	1.95
	SNV + 1-Der		0.894	0.079	3.11		0.852	0.093	2.63
	SNV+ 2-Der		0.897	0.078	3.15		0.861	0.090	2.72
	SNV+DOSC		0.834	0.099	2.48		0.899	0.077	3.19

Table 2. Continuation.

Model	Pre-treatment	*LV*, γ	VNIR			*LV*, γ	NIR		
			R^2	RMSE	RPD		R^2	RMSE	RPD
LS-SVM	**RAW**	1.828	0.805	0.107	2.29	4126.52	0.814	0.105	2.35
	SNV	4278.28	0.821	0.102	2.39	59.782	0.870	0.087	2.81
	SG	111.231	0.789	0.111	2.20	4035.02	0.760	0.119	2.07
	1-Der	82.282	0.868	0.088	2.79	1.275	0.805	0.107	2.29
	2-Der	13.288	0.860	0.091	2.71	0.215	0.738	0.124	1.98
	MSC	0.014	0.829	0.100	2.44	80.185	0.862	0.090	2.72
	DOSC	1.35×10^{10}	0.817	0.104	2.37	4.61×10^{13}	0.704	0.132	1.86
	SNV + 1-Der	358.236	0.877	0.085	2.88	89.781	0.866	0.089	2.77
	SNV+ 2-Der	184.810	0.885	0.082	2.99	0.109	0.805	0.107	2.29
	SNV+DOSC	2.10×10^{6}	0.815	0.104	2.35	0.002	0.897	0.078	3.15

Table 3. Results of tannin content using the average of the six measurement points with all wavelengths by PLSR, SVM and LS-SVM models for the half cut fruit set.

Model	Pre-treatment	*LV*, *γ*	VNIR			*LV*, *γ*	NIR		
			R^2	RMSE	RPD		R^2	RMSE	RPD
PLSR	**RAW**	15	0.761	0.118	2.07	38	0.733	0.125	1.96
	SNV	14	0.741	0.123	1.99	37	0.736	0.125	1.97
	SG	17	0.727	0.127	1.94	59	0.329	0.198	1.24
	1-Der	9	0.856	0.092	2.66	31	0.659	0.142	1.73
	2-Der	9	0.864	0.089	2.74	22	0.583	0.156	1.57
	MSC	14	0.741	0.123	1.99	37	0.729	0.126	1.94
	DOSC	1	0.741	0.123	1.99	1	0.604	0.153	1.61
	SNV + 1-Der	8	0.844	0.096	2.57	30	0.678	0.138	1.78
	SNV+ 2-Der	9	0.861	0.090	2.72	22	0.642	0.145	1.69
	SNV+DOSC	1	0.744	0.123	2.00	7	0.712	0.130	1.88
SVM	**RAW**		0.826	0.101	2.43	0	0.174	0.220	1.11
	SNV		0.813	0.105	2.34	0	0.557	0.161	1.52
	SG		0.792	0.110	2.22	0	0.098	0.230	1.07
	1-Der		0.872	0.087	2.83	0	0.822	0.102	2.40
	2-Der		0.877	0.085	2.88	0	0.841	0.097	2.54
	MSC		0.800	0.108	2.26	0	0.526	0.167	1.47
	DOSC		0.754	0.120	2.04	0	0.629	0.148	1.66
	SNV + 1-Der		0.858	0.091	2.68	0	0.812	0.105	2.33
	SNV+ 2-Der		0.871	0.087	2.82	0	0.853	0.093	2.64
	SNV+DOSC		0.760	0.119	2.06	0	0.826	0.101	2.42

Table 3. Continuation.

Model	Pre-treatment	*LV*, γ	VNIR			*LV*, γ	NIR		
			R^2	RMSE	RPD		R^2	RMSE	RPD
LS-SVM	**RAW**	1.946	0.796	0.109	2.24	1458.98	0.736	0.125	1.97
	SNV	0.004	0.795	0.110	2.23	32.265	0.794	0.110	2.23
	SG	190.193	0.760	0.119	2.07	1334.51	0.655	0.142	1.72
	1-Der	0.011	0.858	0.091	2.69	0.378	0.819	0.103	2.38
	2-Der	32.619	0.870	0.087	2.80	0.049	0.794	0.110	2.23
	MSC	0.003	0.796	0.110	2.24	24.415	0.783	0.113	2.17
	DOSC	3.26×10^{10}	0.741	0.123	1.99	3.58×10^{9}	0.604	0.153	1.61
	SNV + 1-Der	9577.86	0.849	0.094	2.61	0.163	0.795	0.110	2.23
	SNV+ 2-Der	1.15×10^{4}	0.866	0.089	2.76	0.051	0.817	0.104	2.37
	SNV+DOSC	89.830	0.744	0.123	2.00	0.405	0.819	0.103	2.38

Table 4. Results of tannin content using the average of the six measurement points with EWs for the models created by PLSR, SVM and LS-SVM for the intact fruits set.

Model	Pre-treatment	*EW/LV, EW, EW/γ*	VNIR			*EW/LV, EW, EW/γ*	NIR		
			R^2	RMSE	RPD		R^2	RMSE	RPD
PLSR	**SNV + 1-Der**	22/22	0.861	0.090	2.72	48/48	0.893	0.079	3.10
	SNV+ 2-Der	26/26	0.891	0.080	3.06	54/54	0.822	0.102	2.40
	SNV+DOSC	1/1	0.871	0.087	2.81	41/41	0.915	0.071	3.46
SVM	**SNV + 1-Der**	22	0.849	0.094	2.61	48	0.761	0.118	2.07
	SNV+ 2-Der	26	0.884	0.082	2.98	54	0.768	0.117	2.10
	SNV+DOSC	1	0.878	0.085	2.89	41	0.895	0.079	3.12
LS-SVM	**SNV + 1-Der**	22/9.06 x 10^4	0.821	0.103	2.39	48/10.309	0.833	0.099	2.48
	SNV+ 2-Der	26/0.982	0.889	0.081	3.04	54/50.492	0.836	0.098	2.50
	SNV+DOSC	1/122.96	0.874	0.086	2.85	41/3.818	0.893	0.079	3.09

* Only the best prediction results for each model are shown, indicating the associated pre-processing

Table 5. Results of tannin content using the average of the six measurement points with EWs for the models created by PLSR, SVM and LS-SVM for the half cut fruit set.

Model	Pre-treatment	*EW/LV, EW, EW/γ*	VNIR			*EW/LV, EW, EW/γ*	NIR		
			R^2	RMSE	RPD		R^2	RMSE	RPD
PLSR	**SNV + 1-Der**	30/30	0.880	0.084	2.92	28/28	0.834	0.099	2.48
	SNV+ 2-Der	25/25	0.880	0.084	2.92	38/38	0.790	0.111	2.21
	SNV+DOSC	1/1	0.856	0.092	2.67	51/51	0.850	0.094	2.62
SVM	**SNV + 1-Der**	30	0.879	0.084	2.91	28	0.837	0.098	2.51
	SNV+ 2-Der	25	0.894	0.079	3.12	38	0.743	0.123	2.00
	SNV+DOSC	1	0.862	0.090	2.72	51	0.828	0.101	2.44
LS-SVM	**SNV + 1-Der**	30/0.288	0.865	0.089	2.76	28/8.152	0.774	0.115	2.13
	SNV+ 2-Der	25/2.468	0.885	0.082	2.98	38/6.694	0.743	0.123	2.00
	SNV+DOSC	1/97.163	0.857	0.092	2.68	51/0.030	0.825	0.101	2.42

* Only the best prediction results for each model are shown, indicating the associated pre-processing

This analysis was performed for the different combinations of the six measurement points, obtaining the results in Table 6, which shows the best results for each combination of points and each model. Tables 7 and 8 show the results for the combination of measurement points 2-5-3-4 (average of the equator and bottom of the fruit) for the intact and half cut fruit sets, respectively, for the three models (PLSR, SVM, LS-SVM), and the best pre-processing combinations for the six measurement points (SNV+1-Der, SNV+2-Der and SNV+DOSC). The highest RPD achieved was always equal to or better than the highest RPD obtained with any other combination of points. This is reasonable, since from the tannin prints observed in Figure 5, which were obtained using the technique based on $FeCl_3$, the highest differences are in the lower part of the fruit, the upper part being more similar in fruits with different CO_2 treatments (Fig. 5b-e).

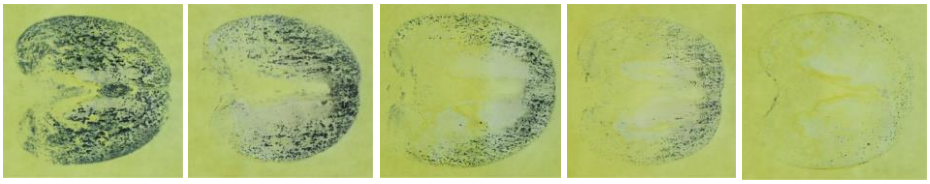

a b c d e

Figure 5. Impressions of tannin content representing the evolution of the astringency distribution and intensity for persimmons after different CO_2 treatments: a) untreated; and b-e) treated with CO_2 for 6, 12, 18 and 24h, respectively.

As in the previous case, SPA was applied for wavelength selection. Tables 9 and 10 show the results of these analyses for the three models and pre-processing combinations.

Table 6. Results of tannin content achieved using different combinations of measurement points and pre-processing methods with all wavelengths by PLSR, SVM and LS-SVM models.

Points	Model	Pre-treatment	Entire				BEST	Half cut			
			REG.	R^2	RMSE	RPD	PRE-TREAT.	REG.	R^2	RMSE	RPD
1-6-2-5	**PLSR**	**1-Der**	VNIR	0.885	0.082	2.98	**SNV+1-Der**	VNIR	0.829	0.100	2.45
	SVM	**SNV+ 1-Der**	VNIR	0.894	0.079	3.11	**2-Der**	VNIR	0.860	0.091	2.70
	LS-SVM	**SNV+1-Der**	VNIR	0.885	0.082	2.99	**2-Der**	VNIR	0.851	0.094	2.62
1-6-3-4	**PLSR**	**SNV+1-Der**	VNIR	0.884	0.083	2.97	**SNV+2-Der**	VNIR	0.863	0.090	2.73
	SVM	**SNV+ 1-Der**	VNIR	0.885	0.082	2.99	**2-Der**	VNIR	0.883	0.083	2.96
	LS-SVM	**SNV+ 2-Der**	VNIR	0.874	0.086	2.85	**2-Der**	VNIR	0.871	0.087	2.82
1-6	**PLSR**	**SNV+ 1-Der**	VNIR	0.815	0.104	2.35	**SNV+1-Der**	VNIR	0.803	0.108	2.28
	SVM	**SNV+ 1-Der**	VNIR	0.857	0.092	2.67	**2-Der**	VNIR	0.848	0.094	2.60
	LS-SVM	**SNV+ 1-Der**	VNIR	0.843	0.096	2.56	**SNV+2-Der**	VNIR	0.842	0.096	2.54
2-5	**PLSR**	**2-Der**	VNIR	0.869	0.088	2.80	**SNV+1-Der**	VNIR	0.786	0.112	2.19
	SVM	**SNV+ 1-Der**	VNIR	0.882	0.083	2.94	**SNV+2-Der**	NIR	0.837	0.098	2.51
	LS-SVM	**1-Der**	VNIR	0.866	0.089	2.77	**1-Der**	NIR	0.814	0.104	2.35
3-4	**PLSR**	**SNV+ 1-Der**	VNIR	0.837	0.098	2.51	**2-Der**	VNIR	0.852	0.093	2.63
	SVM	**SNV+ 2-Der**	VNIR	0.872	0.087	2.82	**SNV+2-Der**	NIR	0.853	0.093	2.64
	LS-SVM	**SNV+ 2-Der**	VNIR	0.863	0.090	2.73	**1-Der**	VNIR	0.843	0.096	2.55

* Only the best prediction results for each model are shown, indicating the associated pre-processing

Table 7. Results of tannin content achieved using the average of the four measurement points (2-5-3-4) with all wavelengths by PLSR, SVM and LS-SVM models for the intact fruit set.

Model	Pre-treatment	*LV*, γ	VNIR			*LV*, γ	NIR		
			R^2	RMSE	RPD		R^2	RMSE	RPD
PLSR	**SNV + 1-Der**	9	0.874	0.086	2.86	27	0.830	0.100	2.46
	SNV+ 2-Der	9	0.889	0.081	3.04	21	0.760	0.119	2.07
	SNV+DOSC	1	0.808	0.106	2.31	15	0.810	0.106	2.32
SVM	**SNV + 1-Der**		0.895	0.079	3.12		0.862	0.090	2.72
	SNV+ 2-Der		0.890	0.080	3.06		0.813	0.105	2.34
	SNV+DOSC		0.824	0.102	2.41		0.857	0.092	2.68
LS-SVM	**SNV + 1-Der**	4.880	0.872	0.087	2.83	0.230	0.851	0.093	2.62
	SNV+ 2-Der	547.70	0.872	0.087	2.83	0.073	0.760	0.119	2.07
	SNV+DOSC	1.04×10^7	0.808	0.106	2.31	0.001	0.858	0.091	2.68

* Only the best prediction results for each model are shown, indicating the associated pre-processing

Table 8. Results of tannin content achieved using the average of the four measurement points (2-5-3-4) with all wavelengths by PLSR, SVM and LS-SVM models for the half cut fruit set.

Model	Pre-treatment	*LV*, γ	VNIR			*LV*, γ	NIR		
			R^2	RMSE	RPD		R^2	RMSE	RPD
PLSR	**SNV + 1-Der**	8	0.843	0.096	2.55	30	0.627	0.148	1.66
	SNV+ 2-Der	8	0.827	0.101	2.43	19	0.765	0.117	2.09
	SNV+DOSC	1	0.712	0.130	1.89	7	0.630	0.147	1.66
SVM	**SNV + 1-Der**		0.856	0.092	2.66		0.827	0.101	2.43
	SNV+ 2-Der		0.834	0.099	2.49		0.877	0.085	2.88
	SNV+DOSC		0.725	0.127	1.93		0.783	0.113	2.17
LS-SVM	**SNV + 1-Der**	2952	0.861	0.091	2.71	1.876	0.812	0.105	2.33
	SNV+ 2-Der	54.177	0.834	0.099	2.48	0.067	0.839	0.097	2.52
	SNV+DOSC	2.62×10^6	0.713	0.130	1.89	12.150	0.761	0.119	2.07

* Only the best prediction results for each model are shown, indicating the associated pre-processing

Table 9. Results of tannin content achieved using the average of the four measurement points (2-5-3-4) by PLSR, SVM and LS-SVM models with EWs selected by SPA for the intact fruit set.

Model	Pre-treatment	*EW/LV, EW, EW/γ*	VNIR			*EW/LV, EW, EW/γ*	NIR		
			R^2	RMSE	RPD		R^2	RMSE	RPD
PLSR	**SNV + 1-Der**	16/16	0.838	0.098	2.51	28/28	0.856	0.092	2.67
	SNV+ 2-Der	30/30	0.854	0.093	2.65	28/28	0.779	0.114	2.15
	SNV+DOSC	1/1	0.860	0.091	2.70	30/30	0.865	0.089	2.76
SVM	**SNV + 1-Der**	16	0.851	0.094	2.62	28	0.759	0.119	2.06
	SNV+ 2-Der	30	0.864	0.089	2.74	28	0.806	0.107	2.30
	SNV+DOSC	1	0.862	0.090	2.73	30	0.857	0.092	2.68
LS-									
SVM	**SNV + 1-Der**	16/0.317	0.834	0.099	2.49	28/4.435	0.813	0.105	2.34
	SNV+ 2-Der	30/0.144	0.843	0.096	2.56	28/0.823	0.749	0.122	2.02
	SNV+DOSC	1/5.785	0.861	0.090	2.71	30/0.009	0.855	0.092	2.65

* Only the best prediction results for each model are shown, indicating the associated pre-processing

Table 10. Results of tannin content achieved using the average of the four measurement points (2-5-3-4) by PLSR, SVM and LS-SVM models with EWs selected by SPA for the half cut fruit set.

Model	Pre-treatment	*EW/LV, EW, EW/γ*	VNIR			*EW/LV, EW, EW/γ*	NIR		
			R^2	RMSE	RPD		R^2	RMSE	RPD
PLSR	**SNV + 1-Der**	23/23	0.865	0.089	2.75	28/28	0.823	0.102	2.41
	SNV+ 2-Der	18/18	0.835	0.098	2.49	17/17	0.798	0.109	2.25
	SNV+DOSC	1/1	0.814	0.104	2.35	57/57	0.805	0.107	2.29
SVM	**SNV + 1-Der**	23	0.859	0.091	2.70	28	0.826	0.101	2.43
	SNV+ 2-Der	18	0.811	0.105	2.33	17	0.818	0.103	2.37
	SNV+DOSC	1	0.823	0.102	2.41	57	0.770	0.116	2.11
LS-									
SVM	**SNV + 1-Der**	23/0.249	0.860	0.091	2.70	28/1.30 x 105	0.805	0.107	2.29
	SNV+ 2-Der	18/44.110	0.835	0.098	2.49	17/39.054	0.775	0.115	2.13
	SNV+DOSC	1/18.698	0.815	0.104	2.36	57/0.051	0.756	0.120	2.05

* Only the best prediction results for each model are shown, indicating the associated pre-processing

In this work, different models were obtained to estimate the content of tannins in persimmon from their original and pre-processed reflectance spectra. The models were created for measurements of the skin (intact fruit) and the flesh (half cut fruit). For the intact fruit, good results were obtained for the three methods analysed (PLSR, SVM and LS-SVM), achieving a RPD>3 in the best cases, using the average of the six measurement points. The best results using the prediction set were obtained using PLSR and SNV+1-Der pre-processing, in the VNIR region (RPD=3.26, R^2=0.904, RMSE=0.075). Using SVM, the best results were for the NIR spectra and the SNV+DOSC pre-processing. However, the analysis of the VNIR spectra using SVM gave similar results with some pre-processing such as SNV+2-Der. Finally, the best results with the LS-SVM method were obtained with the SNV+DOCS pre-processing in the NIR region. Regarding half cut fruit and the average of six measurement points, the results were poorer than in the case of intact fruit.

The selection of the most important wavelengths using SPA generally improves the results, especially in the case of half cut fruit. A model with an RPD greater than 3 was obtained for the VNIR spectra with the SNV+2-Der pre-processing and SVM method. In the case of the intact fruit, although the results did not always improve, the best result of the study was obtained using PLSR with SNV+DOSC in the NIR region, with a RPD of 3.46 (R^2=0.915, RMSE=0.071). As shown in Figure 4a, the values of the loading weights were higher around the 1000 nm band for the VNIR range, which corresponds to the information presented by Noypitak *et al.* (2015) in relation with the spectrum for the tannic acid powder. These loadings explained the better results obtained with the VNIR probe over those obtained in the NIR, and also the reduced number of EWs obtained in the VNIR range.

For both the intact and the half cut fruit cases, the three methods analysed achieved poorer predictions using the average of the four measurement points (combination 2-5-3-4) than those obtained with the six measurement points. Regarding the selection of EWs with SPA (with this combination of points), this method also improved the results obtained for the half cut fruit, similarly to the results obtained with six measurement points. However, the SPA analysis showed no significant improvement in intact fruit (RPD<3).

6. CONCLUSIONS

This study points to visible and NIR spectroscopy as a non-destructive method suitable for determining astringency in persimmon fruits in an easy and rapid way without expensive and tedious chemical analysis or the subjective evaluation of the tannin print method. Reflectance spectra at selected points in intact and half cut persimmons were acquired in the VIS and NIR regions. A total of seven signal pre-processing methods including SNV, SG, 1-Der, 2-Der, MSC, DOSC and combinations of them have been used in the measurements of the single point and the combination of selected points. The combinations considered were SNV+1-Der, SNV+2-Der and SNV+DOSC, since they showed the best performance from all the combinations evaluated. Astringency in persimmon fruits was predicted using three regression techniques, such as PLSR, SVM, and LS-SVM.

In addition, EWs were obtained using SPA. Depending on the method, the EWs varied from 1 to 30 when the VNIR spectra were used and from 17 to 57 when using the NIR spectra.

The best performance for intact fruits was obtained using PLSR on the full spectra of the six measurement points after pre-processing with SNV+1-Der, an R^2=0.904 and RPD=3.26 being achieved. Moreover, the best prediction results obtained with the EWs (41 bands) were obtained for the PLSR model using the six measurement points of the intact fruit in the NIR spectra and SNV+DOSC pre-processing (R^2=0.915; RPD=3.46).

Hence, this technology has proved itself to be a feasible non-destructive method to determine the astringency in persimmon fruits, since the best results were achieved in intact fruits.

Acknowledgements

This work has been partially funded by the Instituto Nacional de Investigación y Tecnología Agraria y Alimentaria de España (INIA) through research projects RTA2012-00062-C04-01/03, RTA2015-00078-00-00 and RTA2013-00043-C02 with the support of European FEDER funds, and by the Conselleria d' Educació, Investigació, Cultura i Esport, Generalitat Valenciana,

through the project AICO/2015/122. V. Cortés thanks the Spanish MEC for the FPU grant (FPU13/04202).

7. REFERENCES

Araújo, M.C.U., Saldanha, T.C.B., Galvão, R.K.H., Yoneyama, T., Chame, H.C. & Visani, V. (2001). The successive projections algorithm for variable selection in spectroscopic multicomponent analysis. Chemometrics and Intelligent Laboratory Systems, 57(2), 65-73.

Ashtiani, S.M., Salarikia, A., Golzarian, M.R. & Emadi, B. (2016). Non-Destructive Estimation of Mechanical and Chemical Properties of Persimmons by Ultrasonic Spectroscopy, International Journal of Food Properties, 19:7, 1522-1534.

Attila, N. & János, T. (2011). Sweet cherry fruit analysis with reflectance measurements. Journal Analele Universităţii din Oradea, Fascicula: Protecţia Mediului, 17, 263-270.

Beghi, R., Giovanelli, G., Malegori, C., Giovenzana, V. & Guidetti, R. (2014). Testing of a VIS-NIR System for the Monitoring of Long-Term Apple Storage. Food and Bioprocess Technology, 7, 2134-2143.

Besada, C., Salvador, A., Arnal, L. & Martínez-Jávega, J.M. (2010). Optimization of the duration of deastringency treatment depending on persimmon maturity. Acta Horticulturae 858, 69-74.

Calvini, R., Ulrici, A. & Amigo, J.M. (2015). Practical comparison of sparse methods for classification of Arabica and Robusta coffee species using near infrared hyperspectral imaging. Chemometrics and Intelligent Laboratory Systems, 146, 503-511.

Chauchard, F., Cogdill, R., Roussel, S., Roger, J.M. & Bellon-Maurel, V. (2004). Application of LS-SVM to non-linear phenomena in NIR spectroscopy: development of a robust and portable sensor for acidity prediction in grapes. Chemometrics and Intelligent Laboratory Systems, 71, 141-150.

Cortés, V., Ortiz, C., Aleixos, N., Blasco, J., Cubero, S. & Talens, P. (2016). A new internal quality index for mango and its prediction by external visible and near-infrared reflection spectroscopy. Postharvest Biology and Technology, 118, 148-158.

Devos, O., Ruckebusch, C., Durand, A., Duponchel, L. & Huvenne, J.P. (2009). Support vector machines (SVM) in near infrared (NIR) spectroscopy: Focus on parameters optimization and model interpretation. Chemometrics and Intelligent Laboratory Systems, 96, 27-33.

Fearn T., Riccioli C., Garrido-Varo, A. & Guerrero-Ginel, J.E. (2009). On the geometry of SNV and MSC. Chemometrics and Intelligent Laboratory Systems, 96, 22-26.

Feng, Y.Z. & Sun, D.W. (2013). Near-infrared hyperspectral imaging in tandem with partial least squares regression and genetic algorithm for non-destructive determination and visualization of Pseudomonas loads in chicken fillets. Talanta, 109, 74-83.

Fernández Pierna, J.A., Vermeulen, P., Amand, O., Tossens, A., Dardenne, P. & Baeten, V. (2012). NIR hyperspectral imaging spectroscopy and chemometrics for the detection of undesirable substances in food and feed. Chemometrics and Intelligent Laboratory Systems, 117, 233-239.

Folch-Fortuny, A., Prats-Montalbán, J.M., Cubero, S., Blasco, J. & Ferrer, A. (2016). NIR hyperspectral imaging and N-way PLS-DA models for detection of decay lesions in citrus fruits. Chemometrics and Intelligent Laboratory Systems, 156, 241-248.

Fushiki, T. (2011). Estimation of prediction error by using K-fold cross-validation. Statistics and Computing, 21, 137-146

Galvao, R.K.H., Araujo, M.C.U., Fragoso, W.D., Silva, E.C., Jose, G.E., Soares, S.F.C. & Paiva, H.M. (2008). A variable elimination method to improve the parsimony of MLR models using the successive projections algorithm. Chemometrics and Intelligent Laboratory Systems, 92(1), 83-91.

Geladi, P. & Kowalski, B.R. (1986). Partial least-squares regression: a tutorial. Analytica chimica acta, 185, 1-17.

Gunn, S.R. (1998). Support vector machines for classification and regression. ISIS technical report, 14.

He, Y., Li, X. & Shao, Y. (2007). Fast discrimination of apple varieties using vis/nir spectroscopy. International Journal of Food Properties, 10 (1), 9-18.

Ito, S., Ootake, Y. & Kito, I. (1997). Classification of astringency in pollination variant non-astringent persimmon fruits cv. "Nisimura-wase" by near infrared spectroscopy. Research Bulletin of the Aichi-ken Agricultural Research Center, 29, 213-218.

Jha, S.N., Jaiswal, P., Narsaiah, K., Sharma, R., Bhardwaj, R., Gupta, M. & Kumar, R. (2013). Authentication of mango varieties using near infrared spectroscopy. Agricultural Research, 2(3), 229-235.

Kamruzzaman, M., Makino, Y. & Oshita, S. (2016). Rapid and non-destructive detection of chicken adulteration in minced beef using visible near-infrared hyperspectral imaging and machine learning. Journal of Food Engineering, 170, 8-15.

Khademi, O., Mostofi, Y., Zamani, Z. & Fatahi, R. (2010). The effect of deastringency treatments on increasing the marketability of persimmon fruit. Acta Horticulturae, 877, 687-691.

Khanmohammadi, M., Karami, F., Mir-Marqués, A., Bagheri Garmarudi, A., Garrigues, S. & de la Guardia, M. (2014). Classification of persimmon fruit origin by near infrared spectrometry and least squares-support vector machines. Journal of Food Engineering, 142, 17-22.

Liu, F., He, Y. & Sun, G. (2009). Determination of protein content of Auricularia auricula using near infrared spectroscopy combined with linear and nonlinear calibrations. Journal of Agricultural and Food Chemistry, 57(11), 4520-4527.

Liu, F., He, Y. & Wang, L. (2008). Comparison of calibrations for the determination of soluble solids content and pH of rice vinegars using visible and short-wave near infrared spectroscopy. Analytica chimica acta, 610(2), 196-204.

Liu, Y., Sun, X., Zhou, J., Zhang, H. & Yang, C. (2010). Linear and nonlinear multivariate regressions for determination sugar content of intact Gannan navel orange by Vis–NIR diffuse reflectance spectroscopy. Mathematical and Computer Modelling, 51(11), 1438-1443.

Lopez, A., Arazuri, S., Garcia, I., Mangado, J. & Jaren, C. (2013). A review of the application of near-infrared spectroscopy for the analysis of potatoes. Journal of Agricultural and Food Chemistry, 61, 5413-5424.

Lorber, A., Wangen, L. & Kowalski, B. (1987). A theoretical foundation for the PLS algorithm. Journal of Chemometrics, 1, 19-31.

Lorente, D., Escandell-Montero, P., Cubero, S., Gómez-Sanchis, J. & Blasco, J. (2015). Visible-NIR reflectance spectroscopy and manifold learning methods applied to the detection of fungal infections on citrus fruit. Journal of Food Engineering, 163, 17-21.

Matsuo, T. & Ito, S. (1982). A model experiment for de-astringency of persimmon fruit with high carbon dioxide: in vitro gelation of kaki-tannin by reacting with acetaldehyde. Journal of Agricultural Food Chemistry 46, 683-689.

Matsuo, T., Ito, S. & Ben-Arie, R. (1991). A model experiment for elucidating the mechanism of astringency removal in persimmon fruit using respiration inhibitors. Journal of the Japanese Society for Horticultural Science 60, 437-442.

Mowat, A.D. & Poole, P.R. (1997). Non-destructive discrimination of persimmon fruit quality using visible-near infrared reflectance spectrophotometry. Acta Hort. (ISHS) 436, 159–164, http://www.actahort.org/books/436/436_17.htm (accessed January 2017).

Munera, S., Besada, C., Aleixos, A., Talens, P., Salvador, A., Sun, D.W., Cubero, C. & Blasco, J. (2017b). Non-destructive assessment of the internal quality of intact persimmon using colour and VIS/NIR hyperspectral imaging. LWT - Food Science and Technology, 77C, 241-248.

Munera, S., Besada, C., Blasco, J., Cubero, S., Salvador, A., Talens, P. & Aleixos, N. (2017a). Astringency assessment of persimmon by hyperspectral imaging. Postharvest Biology and Technology, 125, 35-41.

Nagle, M., Mahayothee, B., Rungpichayapichet, P., Janjai, S. & Müller, J. (2010). Effect of irrigation on near-infrared (NIR) based prediction of mango maturity. Scientia Horticulturae, 125(4), 771-774.

Nicolaï, B.M., Beullens, K., Bobelyn, E., Peirs, A., Saeys, W., Theron, K.I. & Lammertyn, J. (2007). Non-destructive measurement of fruit and vegetable quality by means of NIR spectroscopy: A review. Postharvest Biology and Technology, 46(2), 99-118.

Nicolaï, B.M., Theron, K.I. & Lammertyn, J. (2007). Kernel PLS regression on wavelet transformed NIR spectra for prediction of sugar content of apple. Chemometrics and Intelligent Laboratory Systems, 86, 243-252.

Novillo, P., Salvador, A., Llorca, E., Hernando, I. & Besada, C. (2014). Effect of CO_2 deastringency treatment on flesh disorders induced by mechanical damage in persimmon. Biochemical and microstructural studies. Food Chemistry 145, 453-463.

Noypitak, S., Terdwongworakul, A., Krisanapook, K. & Kasemsumran, S. (2015). Evaluation of astringency and tannin content in 'Xichu' persimmons using near infrared spectroscopy. International Journal of Food Properties, 18(5), 1014-1028.

Rinnan, Å., van den Berg, F. & Engelsen, S.B. (2009). Review of the most common pre-processing techniques for near-infrared spectra. TrAC Trends in Analytical Chemistry, 28(10), 1201-1222.

Savitzky, A. & Golay, M.J. (1964). Smoothing and differentiation of data by simplified least squares procedures. Analytical chemistry, 36(8), 1627-1639.

Shao, Y., He, Y., Bao, Y. & Mao, J. (2009). Near-infrared spectroscopy for classification of oranges and prediction of the sugar content. International Journal of Food Properties, 12(3), 644-658.

Schmilovitch, Z., Mizrach, A., Hoffman, A., Egozi, H. & Fuchs, Y. (2000). Determination of mango physiological indices by near-infrared spectrometry. Postharvest Biology and Technology, 19(3), 245-252.

Sinija, V.R. & Mishra, H.N. (2011). FTNIR spectroscopic method for determination of moisture content in green tea granules. Food and Bioprocess Technology, 4(1), 136-141.

Sun, T., Lin, H., Xu, H. & Ying, Y. (2009). Effect of fruit moving speed on predicting soluble solids content of 'Cuiguan' pears (*Pomaceae pyrifolia Nakai* cv. Cuiguan) using PLS and LS-SVM regression. Postharvest biology and technology, 51(1), 86-90.

Suykens, J.A. & Vandewalle, J. (1999). Least squares support vector machine classifiers. Neural processing letters, 9(3), 293-300.

Taira, S. (1995). Astringency in persimmon. In: Linskens, H.F., Jackson, J.F. Fruit Analysis. Springer, Hannover, Germany, 97-110.

Theanjumpol, P., Self, G., Rittiron, R., Pankasemsu, T. & Sardsud, V. (2013). Selecting Variables for Near Infrared Spectroscopy (NIRS) Evaluation of Mango Fruit Quality. Journal of Agricultural Science, 5(7), 146-159.

Vapnik, V. (2013). The nature of statistical learning theory. Springer Science & Business Media.

Vidal, M. & Amigo, J.M. (2012). Pre-processing of hyperspectral images. Essential steps before image analysis. Chemometrics and Intelligent Laboratory Systems, 117, 138-148.

Viscarra Rossel, R.A., Taylor, H.J. & McBratney, A.B. (2007). Multivariate calibration of hyperspectral γ-ray energy spectra for proximal soil sensing. European Journal of Soil Science, 58(1), 343-353.

Vitale, R., Bevilacqua, M., Bucci, R., Magrì, A.D., Magrì, A.L. & Marini, F. (2013). A rapid and non-invasive method for authenticating the origin of pistachio samples by NIR spectroscopy and chemometrics. Chemometrics and Intelligent Laboratory Systems, 121, 90-99.

Williams, P. & Sobering, D. (1993). Comparison of commercial near infrared transmittance and reflectance instruments for analysis of whole grains and seeds. Journal of Near Infrared Spectroscopy, 1, 25-32.

Zhang, S., Zhang, H., Zhao, Y., Guo, W. & Zhao, H. (2013). A simple identification model for subtle bruises on the fresh jujube based on NIR spectroscopy. Mathematical and Computer Modelling, 58(3), 545-550.

Zhu, D., Ji, B., Meng, C., Shi, B., Tu, Z. & Qing, Z. (2008). The application of direct orthogonal signal correction for linear and non-linear multivariate calibration. Chemometrics and Intelligent Laboratory Systems, 90(2), 108-115.

3.1.2. Chapter II.

Sweet and nonsweet taste discrimination of nectarines using visible and near-infrared spectroscopy

Cortés, V.[1], Cubero, S.[2], Aleixos, N.[3], Blasco, J.[2] & Talens, P.[1]

[1]Departamento de Tecnología de Alimentos. Universitat Politècnica de València. Camino de Vera s/n, 46022, Valencia (Spain).

[2]Centro de Agroingeniería. Instituto Valenciano de Investigaciones Agrarias (IVIA). Ctra. CV-315, km. 10,7, 46113, Moncada, Valencia (Spain).

[3]Departamento de Ingeniería Gráfica, Universitat Politècnica de València. Camino de Vera s/n, 46022, Valencia (Spain).

Postharvest Biology and Technology, 133 (2017), 113-120

ABSTRACT

The feasibility of using visible and near-infrared spectroscopy technology combined with multivariate analysis to discriminate cv. 'Big Top' and cv. 'Diamond Ray' nectarines has been studied. These varieties are very difficult to differentiate visually on the production line but show important differences in taste that affects the acceptance by final consumers. The relationship between the diffuse reflectance spectra and the two nectarine varieties was established. Five hundred nectarine samples (250 of each variety) were used for the study. Tests were performed by using a spectrometer capable of measuring in two different spectral ranges (600–1100 nm and 900–1700 nm). These spectral ranges were used to develop two accurate classification models based on linear discriminate analysis (LDA) and partial least squares discriminate analysis (PLS-DA). Later, selection techniques were applied to select the most effective wavelengths. The results showed that the PLS-DA model achieved better accuracy and less latent variables than LDA model, and specifically, good results with 100% classification accuracy were obtained using only the 600– 1100 nm spectral range for the two models and eight selected wavelengths. These results places visible and near-infrared spectroscopy as an accurate classification tool for nectarine varieties with a very similar appearance but different tastes that could be potentially used in an automated inspection system.

Keywords: nectarine, sweet taste, nonsweet taste, visible and near-infrared spectroscopy, discrimination, chemometrics

1. INTRODUCTION

Nectarine and peach fruit [*Prunus persica* (L.) Batch] are the second most important fruit crop in the European Union (EU) after apple (Iglesias and Echeverría, 2009). Recently, significant innovations have been made in the field of fruit varieties that seek improvements in colour and size, consistency of pulp, texture, taste and flavour (Jha *et al.*, 2012, 2006, 2005; Picha, 2006; Jha & Matsuoka, 2004). New varieties obtained show an attractive range of colours, tastes and forms as well as having an extended maturity schedule, which have given rise to excellent acceptance by consumers in both national and international markets (Iglesias, 2013; Iglesias & Casals, 2014). The most appreciated attributes among fruit consumers have been described as being taste, food safety (absence of pesticides), ease of consumption and cost (Wandel & Bugge, 1997; Radman, 2005; Dragsted, 2008). Regarding taste consumers generally prefer sweet and balanced tastes, except in some countries like Germany or England, where there is preference for nonsweet tastes (Cembalo *et al.*, 2009). In fact, the introduction of 'Big Top' nectarine variety intro the market represented a remarkable innovation for its sweet taste (< 6 g L-1 of malic acid) and excellent consistency, and has been widely accepted by national and international markets. Recently, new varieties of nectarines completing the collection period from late May to late September have been introduced into the market. This varietal range is complemented by new or existing varieties showing a similar appearance, but a balanced or nonsweet taste (> 6 g L-1 of malic acid), as occurs in the case of the 'Diamond Ray' variety. In nectarine fruit, it is essential to differentiate the varieties from in processing line, which would allow the consumer to choose the ones that best adapt to their preferences. The application of visible and near-infrared spectroscopy for the analysis of fruit has allowed the prediction of chemical composition, notably sugar content (Li *et al.*, 2013; Reita *et al.*, 2008), and textural parameters (Lee *et al.*, 2012; Sánchez *et al.*, 2011), as well as the identification of varieties (Li *et al.*, 2016; Guo *et al.*, 2016) and the measurement of quality-related parameters (Pérez-Marín *et al.*, 2011). This technique is relatively rapid, simple, cost-effective, non-destructive, and environmentally friendly. Its application in combination with chemometrics has been successfully used in non-destructive discrimination between varieties of agricultural products such as peach (Guo *et al.*, 2016),

bayberry (Li *et al.*, 2007), orange (Suphamitmongkol *et al.*, 2013), and pummelos (Li *et al.*, 2016).

This study aimed to evaluate the ability of visible and near-infrared spectroscopy to discriminate between two varieties of nectarine (cv. 'Big Top' and cv. 'Diamond Ray'), which, because there are similar in colour and appearance, are very difficult to differentiate visually on the production line but show important differences in taste, thereby affecting the acceptance by the final consumers. Two supervised methods such as linear discriminate analysis (LDA) and partial least squares discriminate analysis (PLS-DA) were used for this purpose.

2. MATERIALS AND METHODS

2.1. Experimental procedure

A total of 500 nectarines with commercial maturity and uniform size and the absence of any external damage were harvested in a commercial orchard in Lérida, Spain. They were then stored at 0.1 °C with 87 % relative humidity to prevent the evolution of maturity during the experiment and to extend their shelf-life (Gorny *et al.*, 1998). Half of the total samples belonged to the variety ‘Big Top’ and the other half to the variety ‘Diamond Ray’. These varieties were selected because they are grown in the same period and have a similar evolution and physical appearance, although they differ critically in some of their organoleptic properties.

On arrival at the laboratory, fruits were cleaned, individually numbered and each variety was randomly divided into five sets of 50 fruits. The visible and near-infrared spectra of the fruits in each set were collected and their physicochemical properties (soluble solids, firmness and flesh and external colour) were analysed by standard destructive methods (Cortés *et al.*, 2016; Martins *et al.*, 2016; Li *et al.*, 2013; Hernández *et al.*, 2006).

2.2. Visible and near-infrared spectra acquisition

Diffuse visible and near-infrared reflectance spectra of intact nectarines were collected using a multichannel spectrometer platform (AvaSpecAS-5216 USB2-DT, Avantes BV, The Netherlands) equipped with two detectors. The first detector (AvaSpec-ULS2048 StarLine, Avantes BV, The Netherlands) included a 2048-pixel charge-coupled device (CCD) sensor (SONY ILX554, SONY Corp., Japan),

50 μm entrance slit and a 600 line mm-1 diffraction grating covering the visible and near-infrared range from 600 nm to 1100 nm (VNIR) with a spectral FWHM (full width at half maximum) resolution of 1.15 nm and a spectral sampling interval of 0.255 nm. The second detector (AvaSpec-NIR256-1.7 NIRLine, Avantes BV, The Netherlands) was equipped with a 256 pixel non-cooled InGaAs (Indium Gallium Arsenide) sensor (Hamamatsu 92xx, Hamamatsu Photonics K.K., Japan), with a 100 μm entrance slit and a 200 line mm-1 diffraction grating covering the near-infrared range from 900 nm to 1700 nm (NIR) with a spectral FWHM resolution of 12 nm and a spectral sampling interval of 3.535 nm.

The measurements were performed using a bi-directional fibre-optic reflectance probe (FCR-7IR200-2-45-ME, Avantes BV, The Netherlands). The probe was configured fitted with an illumination leg which connects to a stabilised 10 W tungsten halogen light source (AvaLight-HAL-S, Avantes B0V, The Netherlands) and the other leg of the fibre-optic probe was connected to both detectors for simultaneous measurement. A personal computer equipped with software (AvaSoft version 7.2, Avantes, Inc.) was used to control both detectors and to acquire the spectra. The integration times were adjusted for each spectrophotometer using a 99 % reflective white reference tile (WS-2, Avantes BV, The Netherlands), so that the maximum reflectance value over each wavelength range was around 90 % of saturation (Lorente *et al.*, 2015). The white reference tile for reflectance measurements was a 32 mm diameter and 10 mm thick block of white polytetrafluoroethylene (PTFE). The white reference tile was placed at a distance of 5 mm from the probe to make a reference measurement. The dark spectrum was obtained by turning off the light source and completely covering the tip of the reflectance probe. The integration time was set to 120 ms for the VNIR detector and 550 ms for the NIR detector due to the different features of the two detectors. For both detectors, each spectrum was obtained as the average of five scans to reduce the thermal noise of the detector (Nicolaï *et al.*, 2007). The average reflectance measurements of each sample (S) were then converted into relative reflectance values (R) with respect to the white reference using dark reflectance values (D) and the reflectance values of the white reference (W), as shown in equation 1:

$$R = \frac{S-D}{W-D} \quad (1)$$

Prior to the spectral measurements, the temperature of the nectarines was stabilised at a room temperature of 22 ± 1 ºC. All the measurements were taken at two points on each side of the fruit and mean values of the spectra were used for the analysis.

2.3. Determination of the quality attributes

Destructive methods were performed immediately after the spectral acquisition to determine the quality attributes for use as reference values. Both the external and the flesh colours were measured using a spectrocolorimeter (CM-700d, Minolta Co., Tokyo, Japan) every 10 nm between 400 and 700 nm. The colour was evaluated using the L*, a* and b* space proposed by the International Commission on Illumination (CIE). L*a*b* were determined from the reflectance spectra, considering standard illuminant D65 and standard observer 10˚. L* refers to the luminosity or lightness component, a* (intensity of red (+) and green (-)) and b* (intensity of yellow (+) and blue (-)) are the chromaticity coordinates. The total colour difference (ΔE) between the 'Big Top' samples and the 'Diamond Ray' samples was calculated by equation 2.

$$\Delta E = \sqrt{(L^*_{BT} - L^*_{DR})^2 + (a^*_{BT} - a^*_{DR})^2 + (b^*_{BT} - b^*_{DR})^2} \quad (2)$$

where subscript '*BT*' refers to the colour reading of the 'Big Top' samples and '*DR*' refers to the colour reading of the 'Diamond Ray' samples.

Nectarine firmness was measured using a Universal Testing Machine (TextureAnalyser-XT2, Stable MicroSystems, Haslemere, England) to perform puncture tests using a 6 mm diameter cylindrical probe (P/15ANAMEsignature) to a relative deformation of 30 % at a speed of 1 mm s^{-1}. Two measurements were performed for each fruit on opposite sides along the equator. The fracture strength (F_{max}) was analysed for all samples as the maximum force applied to break up the sample, being expressed in Newtons.

Immediately after firmness measurements, juice samples were extracted to estimate the total soluble solids content (TSS) and titratable acidity (TA). The TSS

was determined by refractometry (%) with a digital refractometer (set RFM330+, VWR International Eurolab S.L Barcelona, Spain) at 20 ºC with a sensitivity of ± 0.1 %. Samples were analysed in triplicate and average values were calculated. The analysis of the TA was performed with an automatic titrator (CRISON, pH-burette 24, Barcelona, Spain) with 0.5 N NaOH until a pH of 8.1 (UNE34211:1981), using 15 g of crushed nectarine, which was diluted in 60 mL of distilled water. The TA was determined based on the percentage of citric acid, which was calculated using equation 3.

$$TA\ [g\ citric\ acid/100\ g\ of sample] = (((A \times B \times C)/D) \times 100)/E \quad (3)$$

where *A* is the volume of NaOH consumed in the titration (in L), *B* is the normality of NaOH (0.5 N), *C* is the molecular weight of citric acid (192.1 g mol-1), *D* is the weight of the sample (15 g) and *E* is the valence of citric acid (E = 3).

2.4. Spectral pre-processing

The spectral data were organised in a matrix, where the rows represent the number of samples (#N = 500 samples) and the columns represent the variables (X-variables and Y-variables). The X-variables, or predictors, were the spectral signals from the two detectors. The Y-variables, or responses, were the artificial (dummy) variables created by assigning different values or letters to the different classes to be discriminated. In the case of PLS-DA, assuming a discrete numerical value (zero for the cv. 'Diamond Ray' or one for the cv. 'Big Top'), was used as Y-variable. However, for LDA the Y-variable was a categorical value created by assigning different letter to the different cultivar (A for the cv. 'Diamond Ray' and B for the cv. 'Big Top'). In addition, for LDA the number of samples in the training set must be larger than the number of variables included in the model (Kozak & Scaman, 2008; Sádecká *et al.*, 2016), thus requiring a variable selection or variable reduction. This was performed using the principal component analysis (PCA) scores as input data, since the linear combinations of the original variables, called principal components, are uncorrelated (Rodríguez-Campos *et al.*, 2011).

The raw spectra were transformed to apparent absorbance (log (1/R)) values so as to be able to linearise the correlation with the concentration of the

constituents (Hernández *et al.*, 2006; Shao *et al.*, 2007; Liu *et al.*, 2009) using The Unscrambler X software package (CAMO, Norway). Then, the raw spectra belonging to the two detectors were normalised (Bakeev, 2010) by dividing each variable by its standard deviation (Bouveresse *et al.*, 1996). By so doing, the spectral intensities are rescaled to a common range, thus allowing the comparison of spectra acquired using two detectors with different resolutions.

In addition, different pre-processing techniques were applied. Savitzky-Golay smoothing with a gap of three data points (Carr *et al.*, 2005) was applied to improve the signal-to-noise ratio in order to reduce the effects caused by the physiological variability of samples (Carr *et al.*, 2005; Beghi *et al.*, 2017). Due to the fresh light scattering in samples (Gelbukh *et al.*, 2006), the light does not always travel the same distance in the sample before it is detected. A longer light traveling path corresponds to a lower relative reflectance value, since more light is absorbed. This causes a parallel translation of the spectra. This kind of variation interferes in the calibration models and need to be eliminated by the extend multiplicative scatter correction (EMSC) technique (He *et al.*, 2007; Martens *et al.*, 2003; Bruun *et al.*, 2007). In addition to those two pre-processing, the second derivate with Gap-Segment (2.3) were applied for the NIR spectra because it allowed the extraction of useful information (Cortés *et al.*, 2016; Rodriguez-Saona *et al.*, 2001).

2.5. Multivariate data analysis of spectral data

PCA (Naes *et al.*, 2004), PLS-DA and LDA were used in this work by means of The Unscrambler X software package. PCA was selected as the method for outlier detection (through the analysis of Hotelling's T^2 and squared residual statistics) and to explore the data structure and the relationship between objects (Beghi *et al.*, 2017; Beebe *et al.*, 1998), in order to pinpoint the most relevant varietal groups and spectral features. So, the use of suitable projection, e.g., PCA or partial least square regression (PLS) (Balabin *et al.*, 2007; Xiabo *et al.*, 2010) may help to minimize the large number of spectral variables in the data sets and identify variables that contribute useful information (effective wavelengths, EWs). In this study, wavelengths with large loading weight values were selected as important for the varietal discrimination. EWs were selected as only those located

at the peaks or valleys of x-loading weights plots, and with an absolute x-loading weight higher than 0.1 (Liu *et al.*, 2008).

PLS-DA and LDA were used to classify the nectarines in terms of variety. These discriminant analyses seek to correlate spectral variations (X) with defined classes (Y), attempting to maximise the covariance between the two types of variables.

A training set was used and consisted in randomly selecting 80 % of the samples that were studied to develop a calibration model. Each calibration model was internally validated using the leave-one-out cross-validation technique (Huang *et al.*, 2008). In order to correct the relative influences of the different instrumental responses on a model, a standardization technique was used, where the weight of each X-variable was the standard deviation of the variable (Bouveresse *et al.*, 1996). An independent test set composed of the remaining 20 % of the samples was used for the evaluation and comparison of the classification models (Soares *et al.*, 2013).

2.6. Model performance evaluation

The PLS-DA cut-off value for nectarine samples discrimination was fixed at 0.5. If the predicted value of a sample was less than 0.5, the sample was assigned to the group of the 'Diamond Ray' samples, while if the predicted value was more than 0.5, the sample was assigned to the group of the 'Big Top' samples. The determination coefficient (R^2), root mean square error (RMSE) and the number of latent variables (LVs) were used to evaluate the accuracy of the PLS-DA calibration model to predict new samples. In the case of LDA, the criterion for the selection of LVs is maximum differentiation between the categories and minimal variance within categories (Cardoso & Silva, 2016; Naes *et al.*, 2002; Adams, 1995). The method produces a number of orthogonal linear discriminant functions, equal to the number of categories minus one, that allow the samples to be classified in one category or another (Naes *et al.*, 2002; Otto, 1999).

3. RESULTS AND DISCUSSION

3.1. Analysis of the quality attributes

Table 1 shows the minimum, maximum, mean and standard deviation of the physicochemical characteristics (fracture strength, total soluble solids, tritatable acidity, and flesh and external colour) analysed in the samples of both varieties of nectarines (#N = 250 samples for each variety).

Table 1. Descriptive statistics for the physicochemical characteristics of nectarines during the storage period.

					Flesh colour					External colour				
		TSS (%)	TA (g 100g^{-1})	F_{max} (N)	L^*_{flesh}	a^*_{flesh}	b^*_{flesh}	C^*_{flesh}	h^*_{flesh}	L^*_{ext}	a^*_{ext}	b^*_{ext}	C^*_{ext}	h^*_{ext}
cv. 'Diamond Ray'	Max	17	1.07	57	76	23	35	36	100	59	38	28	42	60
	Min	8	0.36	5	52	-6	23	28	46	25	15	4	18	10
	Mean	12	0.65	33	67	2	31	32	86	37	28	14	32	26
	Sdev	2	0.12	10	4	4	2	1	8	7	4	5	4	10
cv. 'Big Top'	Max	22	0.57	53	75	4	36	36	103	63	34	31	39	75
	Min	7	0.20	6	60	-8	30	30	83	26	8	4	21	12
	Mean	13	0.37	35	68	-2	33	33	93	37	27	14	31	26
	Sdev	2	0.07	7	3	2	1	1	3	6	4	5	4	10

No differences were observed between the two varieties, and among the different sets, in terms of soluble solids, firmness, and flesh and external colour.

The TSS ranged from 8 to 17 % with an average value of 12 ± 2 % for cv. 'Diamond Ray' and from 7 to 22 % with an average value of 13 ± 2 % for cv. ‘Big Top’. In all cases, the values of TSS were greater than 8 %, which is the minimum established by the European Union to market peaches and nectarines (R-CE No. 1861/2004). Several authors have reported a linear relationship between TSS and

consumer acceptance (Crisosto & Crisosto, 2005), a TSS below 10 % generally being unacceptable to consumers (Clareton, 2000).

The firmness of 'Diamond Ray' samples ranged from 5 to 57 N with an average value of 33 ± 10 N, and 'Big Top' samples ranged from 6 to 53 N with an average value of 35 ± 7 N. According to Crisosto (2002) and Valero *et al.* (2007), these firmness values are in the commercial range considered 'ready to buy'.

For flesh colour, L*, a*, b*, C* and h* ranged from 52 to 76, -6 to 23, 23 to 35, 28 to 36 and 46 to 100 for cv. 'Diamond Ray' and from 60 to 75, -8 to 4, 30 to 36, 30 to 36 and 83 to 105 for cv. 'Big Top', with average values of 67 ± 4, 2 ± 4, 31 ± 2, 32 ± 1, 86 ± 8 and 68 ± 3, -2 ± 2, 33 ± 1, 33 ± 1, 93 ± 3 respectively. These values indicated that the flesh of both varieties has a high luminosity, low chroma and yellow hue. No differences were observed in luminosity and chroma between sets and between varieties, whereas slight differences in hue were observed between varieties. Despite these differences, the overall perception of flesh colour would make it very difficult to discriminate both varieties, especially during any industrial process where fruits must be inspected quickly, as shown in the images in Figure 1 with examples of each of the sets analysed. According to ISO 12647-2, colour differences (ΔE) lower than ± 5 units make the human eye unable to discriminate two samples. In this case, the ΔE between both varieties measured with the colorimeter was ± 4.5. Furthermore, differentiating nectarine varieties by the flesh colour requires the destruction of the sample, and therefore this destructive analysis results in high costs and does not allow the whole production to be analysed (Torres *et al.*, 2013).

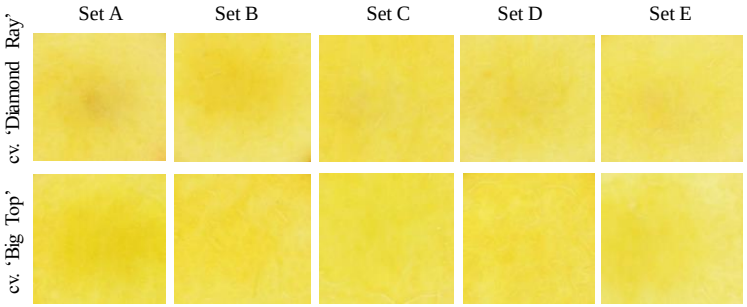

Figure 1. Example of the internal appearance of both cultivars on each day of analysis.

Regarding the external colour of the nectarines, no significant differences were found in the values of luminosity, chroma and hue for the sets and the varieties studied. The L*, a*, b*, C* and h* ranged from 25 to 59, 15 to 38, 4 to 28, 18 to 42 and 10 to 60 for cv. 'Diamond Ray' and from 26 to 63, 8 to 34, 4 to 31, 21 to 39 and 12 to 75 for cv. 'Big Top', with average values of 37 for luminosity, 31.3 for chroma and 25.9º for hue, for both varieties. These values indicated that, externally, both varieties had low luminosity, low chroma and red-orange hue. The ΔE of external colour between varieties was 1.5, and therefore barely perceptible. Hence, this non-destructive analysis was not valid for varietal discrimination.

The main difference between the two varieties of nectarine was TA, the 'Diamond Ray' variety being more acid than the 'Big Top' variety or, according to the definition of Reig *et al.* (2013), the are a nonsweet and sweet variety, respectively. All sets of the cv. 'Diamond Ray' had an average value of 0.65 ± 0.1 g 100g-1, unlike the average value of the sets of the cv. 'Big Top' which was 0.37 ± 0.1 g 100g-1. These results are in accordance with the sensorial profile performed by Iglesias (2012). The study concluded that the only difference between these two varieties is in the perception of acidity. Similarly, Reig *et al.* (2013) and Liverani *et al.* (2002) compared sweet cultivars (such as 'Big Top', 'Gardeta' and 'Luciana') with nonsweet cultivars (such as 'Diamond Ray', 'Amiga' and 'Rose Diamond'), and determined that they differed mainly in their TA value and the perception of acidity, the rest of their physicochemical characteristics being similar among the cultivars.

3.2. Visible and Near-infrared spectra of the two nectarine varieties

Figure 2 represents the mean raw VNIR and NIR spectra for the 'Diamond Ray' and 'Big Top' samples at different sets of analysis. The trend and absorbance bands of the spectral curves were similar. Previous studies have documented similar values (Pérez-Marín *et al.*, 2009; Pérez-Marín *et al.*, 2011; Martins *et al.*, 2016). The varieties analysed showed the same absorbance bands around 670 nm, 970 nm, 1160 nm and 1450 nm. Authors such as Tijskens *et al.* (2007) confirmed that the absorption at 670 nm allowed the maturity of nectarine to be evaluated because it is indicative of the presence of chlorophyll, with its characteristic green colour (Merzlyak *et al.*, 2003; Hernández *et al.*, 2006). The peak centred at 970 nm

is present in the signal recorded by the two detectors. This peak and the one present at 1450 nm are related to pure water (Williams & Norris, 1987; McGlone & Kawano, 1998). A characteristic absorption band at around 1160 nm related to second overtone C-H stretching (Osborne *et al.*, 1993; Walsh *et al.*, 2004).

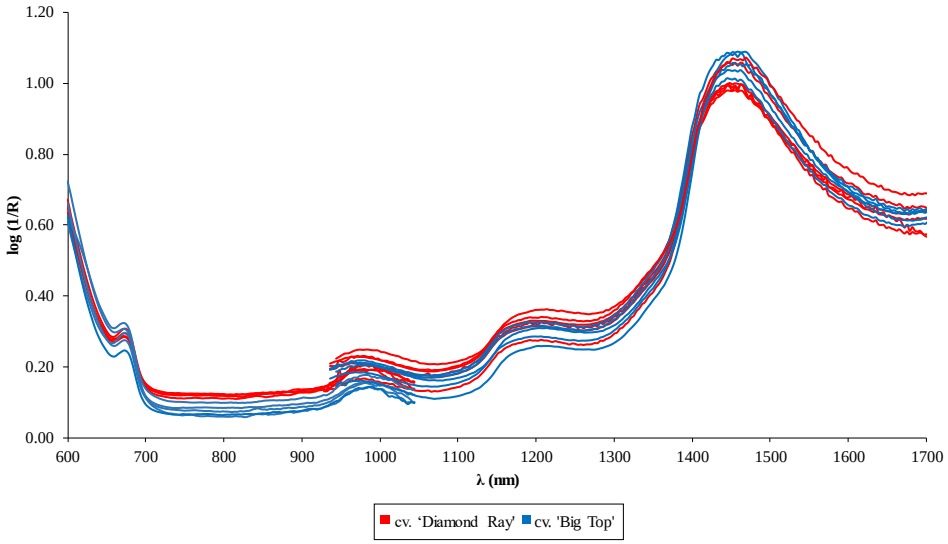

Figure 2. Averaged raw VNIR and NIR spectra for the two varieties of nectarines at different sets of analysis.

3.3. Varietal classification

Classification models were built based on supervised PLS-DA and LDA with the full spectral range, with only the VNIR and NIR spectral ranges separately, and with the effective wavelengths selected (EWs) from the original ranges. Table 2 shows the predictive ability for each validation set for the twelve models developed. Similar results were obtained to PLS-DA models for each spectral ranges and with the most important EWs. However, the LDA models were less accurate with higher number of LV and EWs than PLS-DA models. The optimal number of LVs was chosen according to the lowest RMSE cross-validation (RMSECV) by internal validation using the leave-one-out cross validation technique, in combined analysis with the cumulative variance in the X and Y

blocks (Bachion de Santana *et al.*, 2016). The x-loading weights obtained for the different spectral ranges with only the EWs selected are shown in Figure 3.

Table 2. Varietal classification results for each methods, presented both as a percentage and an absolute number of correctly classified samples in the validation sets.

Methods				**Classification accuracy**		
		EWs	LVs	cv. 'Diamond Ray'	cv. 'Big Top'	Total samples
PLS-DA	Full	2189	5	100 % (50/50)	100 % (50/50)	100 %
		12	4	94 % (47/50)	86 % (43/50)	90 %
	VNIR	1838	6	100 % (50/50)	100 % (50/50)	100 %
		8	5	100 % (50/50)	100 % (50/50)	100 %
	NIR	213	8	100 % (50/50)	100 % (50/50)	100 %
		7	4	92 % (46/50)	98 % (49/50)	95 %
LDA	Full	2189	14	100 % (50/50)	100 % (50/50)	100 %
		12	10	94 % (47/50)	86 % (43/50)	90 %
	VNIR	1838	12	98 % (49/50)	100 % (50/50)	99 %
		8	7	100 % (50/50)	100 % (50/50)	100 %
	NIR	213	5	84 % (42/50)	76 % (38/50)	80 %
		7	6	98 % (49/50)	96 % (48/50)	97 %

Using all 2189 spectrum features, PLS-DA and LDA achieved external validation accuracies of 100 %. Selecting 12 wavelengths, PLS-DA and LDA achieved classification accuracy of 90% with four and ten LVs, respectively. PLS-DA was able to correctly classify all samples in the validation set by using the 213 wavelengths of NIR detector and with only seven EWs and four LVs attained 95 %, although LDA achieved better results with only seven EWs and six LVs (97 % of accuracy) than with all wavelengths of the NIR detector (80 % of accuracy). However, selecting only eight EWs out 1838 available features of VNIR detector, PLS-DA and LDA model attained 100 % validation accuracies with five and seven LVs, respectively. These eight EWs were selected including 648, 883, 949, 1006,

1025, 1026, 1037, and 1054 nm. So, with only these eight EWs obtained by VNIR detector was possible achieved better accuracy classification results (100 %) than the other models developed with the other spectral ranges. An explanation for this result would be that visible spectroscopy is more suitable for the characterization of nectarine colours, which are very similar in both varieties, while near infrared spectra provides complementary information (Liu *et al.*, 2003) related to the macronutrients and the interactions that they can develop with other constituents (Lucas *et al.*, 2008).

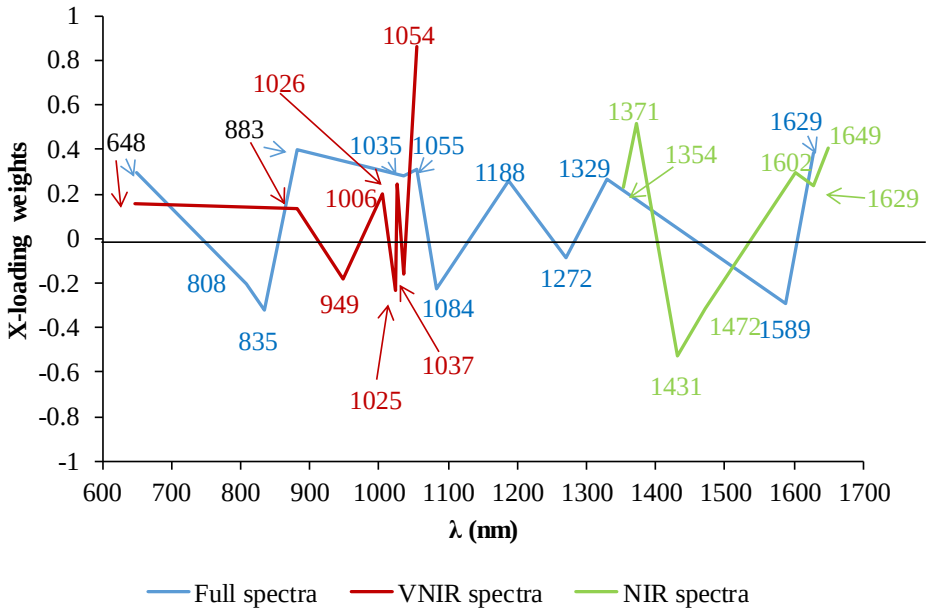

Figure 3. The X-loading weights for the EWs selected at different spectral ranges.

Figure 4 shows that all the training set and validation samples were correctly classified by the best PLS-DA model obtained with eight EWs. In this situation, all 'Big Top' samples have predictive values close to 1, thus classifying these as belonging to class ‘1’, and 'Diamond Ray' samples have predictive values close to 0, thereby classifying these as belonging to class ‘0’. The values of the RMSE were 0.179 and 0.183 for calibration and validation respectively, which exhibit good agreement, thus indicating that the calibration error is a good estimation of the standard error of prediction observed in samples of the test set. Moreover, the test

set yielded similar results to those of the calibration set, with R^2 of 0.872 and 0.866 respectively, which indicates a good performance of the model for varietal classification.

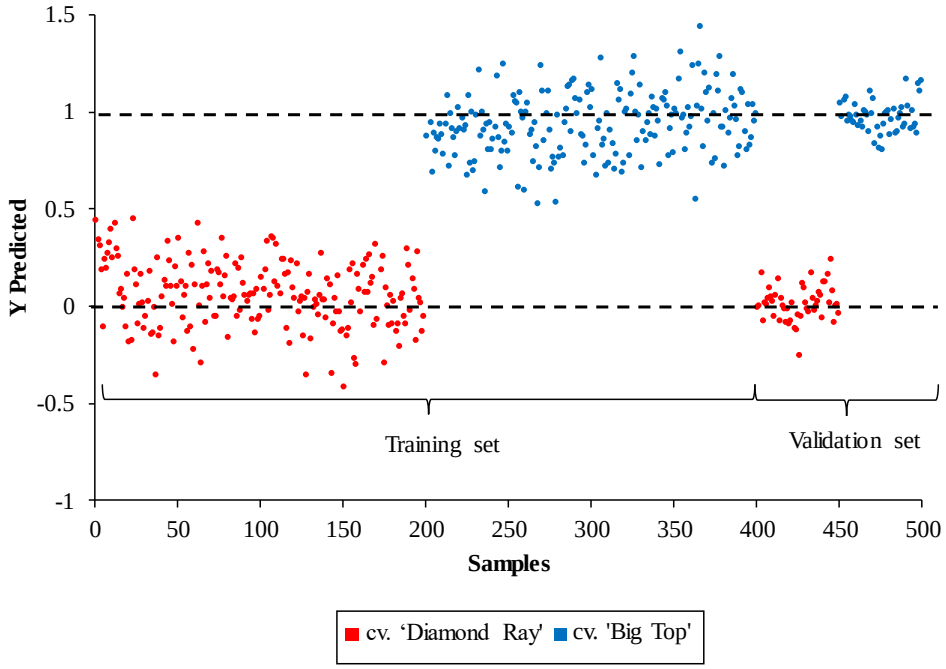

Figure 4. Estimated class values for training and validation sets for varietal discrimination by the best PLS-DA model.

Regarding LDA, Figure 5 shows the results of the external validation by test set (20 %) of each variety. Validation samples of the cv. 'Big Top' are displayed in blue while samples of the cv. 'Diamond Ray' are in red. There were not misclassified samples, so the classification accuracy was 100 % using only eight wavelengths of the VNIR spectral region.

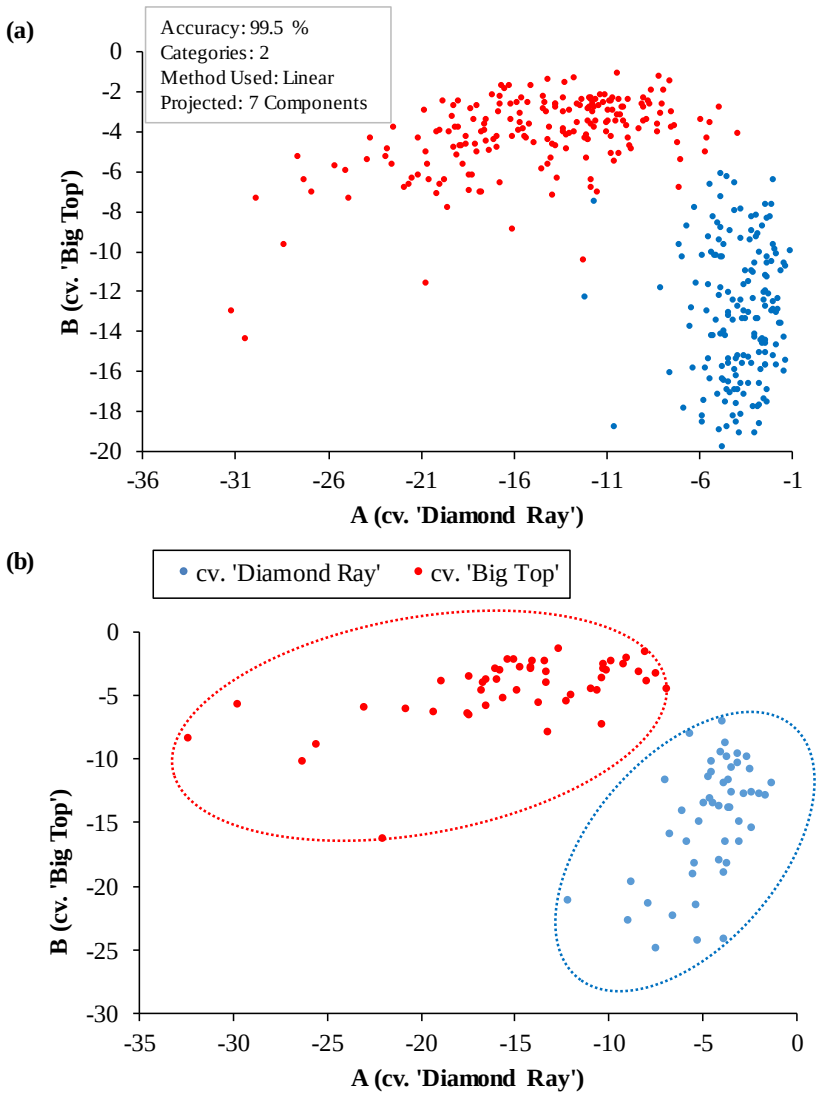

Figure 5. Discrimination plot of the best LDA model for (a) the training samples and (b) the validation samples.

Several authors (Balabin *et al.*, 2010; Liu *et al.*, 2006; Sinelli *et al.*, 2007) have reported that the PLS-DA method is more effective than LDA. Indeed the LDA method suffers from several limitations, for example, the number of variables cannot exceed the number of samples (Roggo *et al.*, 2003) and it is not able to cope with highly collinear data, which are quite common. To overcome some

limitations, over the years other techniques, in particular PLS-DA, have been devised (Marini, 2010). Similarly, to us, Long *et al.* (2015) combined near-infrared spectroscopy with PLS-DA for the discrimination of transgenic rice and they achieved a classification rate of 100 % in the validation test. Additionally, a considerable effort has been made in this work towards the development of models that objectively identify variables that provide useful information and eliminate those that contain unnecessary data.

4. CONCLUSIONS

Classification models were developed in order to discriminate two nectarine varieties (cv. 'Big Top' and cv. 'Diamond Ray') in different spectral ranges (VNIR, NIR, and the whole spectra combined). Two classification methods including PLS-DA and LDA were evaluated based on all wavelengths or the EWs selected for the spectral regions considered. The best models were obtained using only eight EWs out of the 1838 available features of the VNIR detector, identified from the x-loading weights as the most important ones. PLS-DA and LDA models attained an accuracy of 100 % for the validation set with five and seven LVs, respectively. Therefore, PLS-DA and LDA resulted as robust models for discriminating varieties of nectarine with a satisfactory level of accuracy. The comparison of the different analysis performed indicated that both detectors were able to achieve a good varietal classification, being the detector sensible in the VNIR range the one that achieved better results identifying the studied varieties of nectarines, almost identical in external and internal appearance but very different in taste and organoleptic properties.

Acknowledgements

This work was partially funded by the Generalitat Valenciana through the project AICO/2015/122 and by the INIA and FEDER funds through projects RTA2012-00062-C04-01 and 03. Victoria Cortés López thanks the Spanish Ministry of Education, Culture and Sports for the FPU grant (FPU13/04202). The authors wish to thank the cooperative 'Fruits de Ponent' for providing the fruit.

5. REFERENCES

Adams, M.J. (1995). Chemometrics in Analytical Spectroscopy. Analytical Spectroscopy Monographs, 216.

Bachion de Santana, F., Caixeta Gontijo, L., Mitsutake, H., Júnior Mazivila, S., de Souza, L.M. & Borges Neto, W. (2016). Non-destructive fraud detection in rosehip oil by MIR spectroscopy and chemometrics. Food Chemistry, 209, 228-233.

Bakeev, K.A. (2010). Process Analytical Technology. United Kingdom: Wiley.

Balabin, R.M., Safieva, R.Z. & Lomakina, E.I. (2010). Gasoline classification using near infrared (NIR) spectroscopy data: Comparison of multivariate techniques. Analytica Chimica Acta, 671, 27-35.

Balabin, R.M., Safieva, R.Z. & Lomakina, E.I. (2007). Comparison of linear and nonlinear calibration models based on near infrared (NIR) spectroscopy data for gasoline properties prediction. Chemometrics and Intelligent Laboratory Systems 88, 183-187.

Beebe, K.R., Pell, R.J. & Seasholtz, M.B. (1998). Chemometrics: a Practical Guide. Wiley-Interscience, 4.

Beghi, R., Giovenzana, V., Brancadoro, L. & Guidetti, R. (2017). Rapid evaluation of grape phytosanitary status directly at the check point station entering the winery by using visible/near infrared spectroscopy. Journal of Food Engineering, 204, 46-54.

Bouveresse, E., Hartmann, C., Last, I. R., Prebble, K.A. & Massart, L. (1996). Standardization of Near-Infrared Spectrometric Instruments. Analytical Chemistry, 68, 982-990.

Bruun, S.W., Sondergaard, I. & Jacobsen, S. (2007). Analysis of protein structures and interactions in complex food by Near-Infrared spectroscopy. 1. Gluten Powder. Journal of Agricultural and Food Chemistry, 55, 7234-7243.

Cardoso, S.M & Silva, A.M.S. (2016). Chemistry, Biology and Potential Applications of Honeybee Plant-Derived Products. Bentham Science Publishers, Sharjah, UAE.

Carr, G.L., Chubar, O. & Dumas, P. (2005). Spectrochemical Analysis Using Infrared Multichannel Detectors 1st edn. (eds., Bhargava, R. & Levin, I.W.) 56–84. Oxford: Wiley-Blackwell.

Cembalo, L., Cicia, G. & Giudice, T.D. (2009). The influence of country of origin on German consumer preference for peaches: A latent class choice model. Proc. 113th Eur. Assoc. of Agricultural Economists Seminar, Chania (Greece), September 3-6, 1-9.

Clareton, M. (2000). Peach and nectarine production in France: trends, consumption and perspectives. Summaries Prunus breeders meeting, EMBRAPA, clima temperado Pelotas (RS), 83-91.

Commission Regulation EC, No.1861/2004 of 28 October 2004.

Cortés, V., Ortiz, C., Aleixos, N., Blasco, J., Cubero, S. & Talens, P. (2016). A new internal quality index for mango and its prediction by external visible and near infrared reflection spectroscopy. Postharvest Biology and Technology, 118, 148-158.

Crisosto, C. & Crisosto, G. (2005). Relationship between ripe soluble solids concentration (RSSC) and consumer acceptance of high and low acid meeting flesh peach and nectarine (*Prunus persica* (L.) Batsch) cultivars. Postharvest Biology & Technology, 38, 239-246.

Crisosto, C.H. (2002). How do we increase peach consumption? Proceedings of 5th International Symposium on Peach, ISHS, Acta Horticulturae, 592, 601-605.

Dragsted, L. (2008). How we can improve the consumers health through fruit consumption?. ISAFRUIT Project (www.isafruit.org).

Gelbukh, A. & Reyes-Garcia, C.A. (November 2006). MICAI 2006: Advances in Artificial Intelligence. 5th Mexican Internacional Conference on Artificial Intelligence Apizaco, Mexico.

Gorny, J.R., Hess-Pierce, B. & Kader, A.A. (1998). Effects of fruit ripeness and storage temperature on the deterioration rate of fresh-cut peach and nectarine slices. Postharvest Biology & Technology, 33 (1), 110-113.

Guo, W., Gu, J., Liu, D. & Shang, L. (2016). Peach variety identification using near-infrared diffuse reflectance spectroscopy. Computers and Electronics in Agriculture 123, 297-303.

He, Y., Li, X. & Deng, X. (2007). Discrimination of varieties of tea using near infrared spectroscopy by principal component analysis and BP model. Journal of Food Engineering, 79, 1238-1242.

Hernández, A., He, Y. & García, A. (2006). Non-destructive measurement of acidity, soluble solids and firmness of Satsuma mandarin using Vis/NIR-spectroscopy techniques. Journal of Food Engineering 77, 313-319.

Huang, H., Yu, H., Xu, H. & Ying, Y. (2008). Near infrared spectroscopy for on/in-line monitoring of quality in foods and beverages: A review. Journal of Food Engineering, 87 (3), 303-313.

Iglesias, I. (2012). ¿Hacia dónde va el consumo de fruta? Análisis de los vectores que rigen su compra. Revista de Fruticultura, 28.

Iglesias, I. (2013). Peach production in Spain: Current situation and trends, from production to consumption. Proceedings of the 4th Conference, Innovation in fruit growing, Blegrade, 75-89.

Iglesias, I. & Casals, E. (2014). Producción, exportación y consumo de melocotón en España. Vida Rural 373, 21-30.

Iglesias, I. & Echeverría, G. (2009). Differential effect of cultivar and harvest date on nectarine colour, quality and consumer acceptance. Scientia Horticulturae, 120, 41-50.

Jha S.N., Jaiswal P., Narsaiah K., Gupta M., Bhardwaj R. & Singh A.K. (2012). Nondestructive prediction of sweetness of intact mango using near infrared spectroscopy. Scientia Horticulturae, 138, 171-175.

Jha S.N., Kingsly A.R.P. & Chopra S. (2006). Nondestructive determination of firmness and yellowness of mango during growth and storage using visual spectroscopy. Biosystems Engineering, 94(3), 397-402.

Jha, S.N. & Matsuoka, T. (2004). Nondestructive determination of acid brix ratio (ABR) of tomato juice using near infrared (NIR) spectroscopy. International Journal of Food Science and Technology, 39(4), 425-430.

Jha, S.N., Chopra, S. & Kingsly, A.R.P. (2005). Determination of sweetness of intact mango using visual spectral analysis. Biosystems Engineering, 91(2), 157-161.

Kozak, M. & Scaman, C.H. (2008). Unsupervised classification methods in food sciences: discussion and outlook. Journal of the Science of Food and Agriculture, 88, 1115-1127.

Lee, J.S., Kim, S.C., Seong, K.C., Kim, C.H., Um, Y.C. & Lee, S.K. (2012). Quality prediction of kiwifruit based on near infrared spectroscopy. Kor. Journal of Horticultural Science & Technology, 30 (6), 709-717.

Li, J.B., Huang, W.Q., Zhao, C.J. & Zhang, B.H. (2013). A comparative study for the quantitative determination of soluble solids content, pH and firmness of pears by Vis/NIR spectroscopy. Jorunal of Food Engineering, 116 (2), 324-332.

Li, S., Zhang, X., Shan, Y., Su, D., Ma, Q., Wen, R. & Li, J. (2017). Qualitative and quantitative detection of honey adulterated with high-fructose corn syrup and maltose syrup by using near-infrared spectroscopy. Food Chemistry, 218, 231-236.

Li, X., He, Y. & Fang, H. (2007). Non-destructive discrimination of Chinese bayberry varieties using Vis/NIR spectroscopy. Journal of Food Engineering, 81, 357-363.

Li, X., Yi, S., He, S., Lu, Q., Xie, R., Zheng, Y. & Deng, L. (2016). Identification of pummelo cultivars by using Vis/NIR spectra and pattern recognition methods. Precision Agriculture, 17, 365-374.

Liu, F., He, Y. & Wang, L. (2008). Determination of effective wavelengths for discrimination of fruit vinegars using near infrared spectroscopy and multivariate analysis. Analytica Chimica Acta, 615, 10-17.

Liu, F., Jiang, Y. & He, Y. (2009). Variable selection in visible/near infrared spectra for linear and nonlinear calibrations: A case study to determine soluble solids content of beer. Analytica Chimica Acta, 635, 45-52.

Liu, L., Cozzolino, D., Cynkar, W.U., Gishen, M. & Colby, C.B. (2006). Geographic classification of Spanish and Australian Tempranillo Red Wines by Visible and Near-Infrared Spectroscopy combined with Multivariate Analysis. Journal of Agricultural and. Food Chemistry, 54, 6754-6759.

Liu, Y., Lyon, B.G., Windham, W.R., Realini, C.E., Pringle, T.D. & Duckett, S. (2003). Prediction of color, texture, and sensory characteristics of beef steaks by visible and near infrared reflectance spectroscopy. A feasibility study. Meat Science 65, 1107-1115.

Liverani, A., Giovannini, D. & Brandi, F. (2002). Increasing fruit quality of peaches and nectarines: the main goals of ISF-FO (Italy). Acta Horticulturae 592, 507-514.

Long, Z., Shan-shan, W., Yan-fei, D., Jia-rong, P. & Cheng, Z. (2015). Discrimination of Transgenic Rice Based on Near Infrared Reflectance Spectroscopy and Partial Least Squares Regression Discriminant Analysis. Rice Science, 22 (5), 245-249.

Lorente, D., Escandell-Montero, P., Cubero, S., Gómez-Sanchis, J. & Blasco, J. (2015). Visible-NIR reflectance spectroscopy and manifold learning methods applied to the detection of fungal infections on citrus fruit. Journal of Food Engineering, 163, 17-21.

Lucas, A., Andueza, D., Rock, E. & Martin, B. (2008). Prediction of Dry Matter, Fat, pH, Vitamins, Minerals, Carotenoids, Total Antioxidant Capacity, and Color in Fresh and Freee-Dried Cheeses by Visible-Near-Infrared Reflectance Spectroscopy. Journal of Agricultural and Food Chemistry, 56, 6801-6808.

Marini, F. (2010). Classification Methods in Chemometrics. Current Analytical Chemistry, 6, 72-79.

Martens, H., Nielsen, J.P. & Engelsen, S.B. (2003). Light scattering and light absorbance separated by extended multiplicative signal correction. Application to near-infrared transmission analysis of powder mixtures. Analytical Chemistry, 75, 394-404.

Martins, P.A., Cirino de Carvalho, L., Cunha, L.C., Manhas, F. & Teixeira, G.H. (2016). Robust PLS models for soluble solids content and firmness determination in low chilling peach using near infrared spectroscopy (NIR). Postharvest Biology and Technology, 111, 345-351.

McGlone, V.A. & Kawano, S. (1998). Firmness, dry-matter and soluble-solids assessment of post-harvest kiwifruit by NIR spectroscopy. Postharvest Biology and Technology, 13, 131-141.

Merzlyak, M.N., Solo, A.E. & Gitelson, A.A. (2003). Reflectance spectral features and non-destructive estimation of chlorophyll, carotenoid and anthocyanin content in apple fruit. Postharvest Biology and Technology, 27, 197-211.

Naes, T., Isaksson, T., Fearn, T. & Davies, T. (2002). A User-friendly guide to multivariate calibration and classification. NIR Publications: Chichester, U.K.; 420.

Naes, T., Isaksson, T., Fearn, T. & Davies, T. (2004). Interpreting PCR and PLS solutions. In: A User-Friendly Guide to Multivariate Calibration and Classification. Chichester, UK.

Nicolaï, B.M., Beullens, K., Bobelyn, E., Peirs, A., Saeys, W., Theron, I.K. & Lammertyn, J. (2007). Non-destructive measurement of fruit and vegetable quality by means of NIR spectroscopy: a review. Postharvest Biology and Technology, 46, 99-118.

Osborne, B.G., Fearn, T. & Hindle, P.H. (1993). Practical NIR Spectroscopy with Applications in Food and Beverage Analysis, 2nd ed. Longman Group, Burnt Mill, Harlow, Essex, England, UK, 123-132.

Otto, M. (1999). Chemometrics; Wiley-VCH: Hemsbach, Germany, 314.

Ouyang, Q., Liu, Y., Chen, Q., Zhang, Z., Zhao, J., Guo, Z. & Gu, H. (2017). Intelligent evaluation of color sensory quality of black tea by visible-near infrared spectroscopy technology: A comparison of spectra and color data information. Sepectrochimica Acta Part A: Molecular and Biomolecular Spectroscopy, 180, 91-96.

Pérez-Marín, D., Sánchez, M.T., Paz, P., González-Dugo, V. & Soriano, M.A. (2011). Postharvest shelf-life discrimination of nectarines produced under different irrigation strategies using NIR-spectroscopy. Food Science and Technology, 44, 1405-1414.

Pérez-Marín, D., Sánchez, M.T., Paz, P., Soriano, M.A., Guerrero, J.E. & Garrido-Varo, A. (2009). Non-destructive determination of quality parameters in nectarines during on-tree ripening and postharvest storage. Postharvest Biology and Technology, 52, 180-188.

Picha, D. (2006, August). Horticultural crop quality characteristics important in international trade. In IV International Conference on Managing Quality in Chains-The Integrated View on Fruits and Vegetables Quality 712, 423-426.

Radman, M. (2005). Consumer consumption and perception of organic products in Croatia. British Food Journal, 107 (4), 263-273.

Reig, G., Iglesias, I., Gatius, F. & Alegre, S. (2013). Antioxidant Capacity, Quality, and Nutrient Contents of Several Peach Cultivars [*Prunus persica* (L.) Batsch] grown in Spain. Journal of Agricultural and Food Chemistry, 61 (26), 6344-6357.

Reita, G., Peano, C., Saranwong, S. & Kawano, S. (2008). An evaluating technique for variety compatibility of fruit applied to a near infrared Brix calibration system: a case study using Brix calibration for nectarines. Journal of Near Infrared Spectroscopy, 16 (2), 83-89.

Rodriguez-Campos, J., Escalona-Buendía, H.B., Orozco-Avila, I., Lugo-Cervantes, E. & Jaramillo-Flores, M.E. (2011). Dynamics of volatile and non-volatile compounds in cocoa (Theobroma cacao L.) during fermentation and drying processes using principal components analysis. Food Research International, 44, 250-258.

Rodriguez-Saona, L.E., Fry, F.S., McLaughlin, A. & Calvey, E.M. (2001). Rapid analysis of sugars in fruit juices by FT-NIR spectroscopy. Carbohydrate Research, 336, 63-74.

Roggo, Y., Duuponchel, L., Ruckebusch, C. & Huvenne, J.P. (2003). Statistical tests for comparison of quantitative and qualitative models developed with near infrared spectral data. Journal of Molecular Structure, 654, 253-262.

Sádecká, J., Jakubíková, M., Májek, P. & Kleinová, A. (2016). Classification of plum spirit drinks by synchronous fluorescence spectroscopy. Food Chemistry, 196, 783-790.

Sánchez, M.T., De la Haba, M.J., Guerrero, J.E., Garrido-Varo, A. & Pérez-Marín, D. (2011). Testing of a local approach for the prediction of quality parameters in intact nectarines using a portable NIRS instrument. Postharvest Biology and Technology, 60 (2), 130-135.

Shao, Y., He, Y., Gómez, A.H., Pereir, A.G., Qiu, Z. & Zhang, Y. (2007). Visible/near infrared spectrometric technique for nondestructive assessment of tomato 'Heatwave' (Lycopersicumesculentum) quality characteristics. Journal of Food Engineering, 81 (4), 672-678.

Sinelli, N., Stella Cosio, M., Gigliotty, C. & Casiraghi, E. (2007). Preliminary study on application of mid infrared spectroscopy for the evaluation of the virgin olive oil "freshness". Analytica Chimica Acta, 598, 128-134.

Soares, S.F.C., Gomes, A.A., Galvão Filho, A.R., Araújo, M.C.U. & Galvão, R.K.H. (2013). The successive projections algorithm. Trends in Analytical Chemistry, 42, 84-98.

Suphamitmongkol, W., Nie, G.L., Liu, R., Kasemsumran, S. & Shi, Y. (2013). An alternative approach for the classification of orange varieties based on near infrared spectroscopy. Computer and Electronical Agriculture, 91, 87-93.

Tijskens, L.M.M., Zerbini, P.E., Schouten, R.E., Vanoli, M., Jacob, S., Grassi, M. & Torricelli, A. (2007). Assessing harvest maturity in nectarines. Postharvest Biology and Technology, 45, 204-213.

Torres, R., Montes, E.J., Perez, O.A. & Andrade, R.D. (2013). Relación del color y dele estado de madurez con las propiedades fisicoquímicas de frutas tropicales. Información Tecnológica, 24 (4), 51.

UNE-ISO 12647-2:2010. Tecnología gráfica. Control del proceso para la elaboración de separaciones de color, pruebas e impresos de mediotono. Parte 2: Procesos litográficos offset.

Valero, A., Marín, S., Ramos, A. J. & Sanchis, V. (2007). Effect of preharvest fungicides and interacting fungi on Aspergillus carbonarius growth and ochratoxin. A synthesis in dehydrating grapes. Letters in Applied Microbiology, 45, 194-199.

Walsh, K.B., Golic, M. & Greensill, C.V. (2004). Sorting of fruit and vegetables using near infrared spectroscopy: application to soluble solids and dry matter content. Journal of Near Infrared Spectroscopy, 12, 141-148.

Wandel, M. & Bugge, A. (1997). Environmental concern in consumer evaluation of food quality. Food Quality and Preference, 8 (10), 19-26.

Williams, P.C. & Norris, K.H. (1987). Qualitative applications of near infrared reflectance spectroscopy. In P. C. Williams & K. H. Norris (Eds.), Near infrared technology in the agricultural and food industries, 241-246.

Xiaobo, Z., Jiewen, Z., Povey, M.J.W., Holmes, M. & Hanpin, M. (2010). Variables selection methods in near-infrared spectroscopy. Analytica Chimica Acta, 667, 14-32.

3.1.3. Chapter III.

Visible and near-infrared diffuse reflectance spectroscopy for fast qualitative and quantitative assessment of nectarine quality

Cortés, V.[1], Blasco, J.[2], Aleixos, N.[3], Cubero, S.[2] & Talens, P.[1]

[1]Departamento de Tecnología de Alimentos. Universitat Politècnica de València. Camino de Vera s/n, 46022, Valencia (Spain).

[2]Centro de Agroingeniería. Instituto Valenciano de Investigaciones Agrarias (IVIA). Ctra. CV-315, km. 10,7, 46113, Moncada, Valencia (Spain).

[3]Departamento de Ingeniería Gráfica, Universitat Politècnica de València. Camino de Vera s/n, 46022, Valencia (Spain).

Food Bioprocess Technology, 10 (2017), 1755-1766

ABSTRACT

Visible and near-infrared spectroscopy has been widely used as a non-invasive and rapid assessment technique for the quality control of agricultural products. In this study, 325 samples of nectarines representing two commercial varieties, cv. 'Big Top' and cv. 'Magique', were analysed by visible and near-infrared diffuse reflectance spectroscopy (VIS-NIR). The spectral data were pre-treated and analysed to predict the internal quality of the samples and to discriminate between the two varieties. Good prediction of the internal quality of the samples, using partial least squares regressions, was observed for both (R^2_P of 0.909 and 0.927 and RMSEP of 0.235 and 0.238 for cv. 'Big Top' and 'Magique', respectively). Discriminant models, using linear discriminant and partial least squares discriminant analyses were built to classify the nectarines. Both methods provided good results with rates of 97.44 % and 100 % of correctly classified samples. The results indicated that visible and near infrared techniques can be useful and simple methods for quality control and for the correct identification of nectarines in commercial lines as an alternative to the slower and less accurate manual classification.

Keywords: fruit quality, spectroscopy, nectarine, chemometrics, prediction, discrimination

1. INTRODUCTION

Nectarine (*Prunus persica* var. *nucipersica*), is one of the most dynamic species of fruit in terms of the emergence of new varieties on the market. This dynamism has contributed to the development of improved varieties that are better adapted to the growing conditions and market requirements. In terms of evolution and according to the type of fruit, nectarine is the most important fruit group with 41 % of total production, followed by peaches (35 %) and clingstone peaches (24 %) (Iglesias, 2013). The total estimated production of European nectarine was over 1,508,288 tonnes in 2012, shared among Italy (53 %), Spain (32 %), France (10 %), and Greece (5 %) (GenCat, 2013). This high productivity has triggered the necessity to verify nectarine varieties in the industrial fruit packing-line. For example, in Spain, in the region of Lérida the optimal harvesting time is in the summer season (between 1st June and 30th September). At the end of July more than 20 nectarine varieties are being picked simultaneously across the entire region. In the specific case of the village of Aitona (south of Lérida), in practice, the largest number of nectarine varieties that may be harvested simultaneously is six, all of which could reach the post-harvesting industry concurrently in average amounts of 500 tonnes/day, thus generating huge problems in the classification of varieties. In addition, it must be taken into account that nowadays, growers can choose between a large range of nectarine varieties adapted to the climate, different harvest periods and the agronomic characteristics of each particular area. The combination of a large number of small orchards and a wide range of varieties with different demand (Bonany *et al.*, 2013) and market value, can become a source of potential problems for the local post-harvesting industry because of the involuntary or fraudulent mixing of different fruit varieties (Font *et al.*, 2014).

Additionally, the commercial-scale introduction of yellow flesh colour varieties with a strong colour and sweet flavour, as is the variety ‘Big Top’, represented a remarkable innovation for its sweet taste (<6 g/L of malic acid) and the excellent consistency of the fruit, being widely accepted by consumers. Satisfying consumers demands a key aspect, which is the selection of good indicators of quality. Previous works have shown the relationship between consumer acceptance and a high concentration of total soluble solids (TSS) or other

factors like the acidity, TSS/acidity relationship or phenolics and volatile substances (Crisosto *et al.*, 1997; Crisosto *et al.*, 2002; Crisosto *et al.*, 2003).

Nectarine is a climacteric fruit and therefore the physicochemical changes produced during postharvest will determine the final status of the product quality. Only the accurate control of these changes can ensure the customer enjoys good organoleptic and sensorial quality. Traditionally, the internal quality monitoring of the fruit has been performed using destructive methods, so that only a small number of pieces can be measured per set, but the observations may differ greatly from the real status of the whole of production (Valero *et al.*, 2007). One of the aims of the postharvest sensing technologies, such as computer vision (Cubero *et al.*, 2011) hyperspectral imaging (Lorente *et al.*, 2012) or near-infrared (NIR) spectroscopy (Nicolaï *et al.*, 2007), is to allow the analysis of the whole production in terms of quality and commercial organoleptic, nutritional and health characteristics, and varietal verification, while losses and process cost are minimised (Ferrer *et al.*, 2001). The use of sensors based on NIR technology, along with chemometric data models, is one of the fastest and cleanest techniques to achieve this aim. The literature contains different studies on the applicability of NIR technology to the analysis and classification of nectarine varieties (Carlomagno *et al.*, 2004; Pérez-Marín *et al.*, 2011; Reita *et al.*, 2008). For example, Pérez-Marín *et al.* (2011) evaluated the ability of different NIR instruments, to classify intact nectarines cv. 'Sweet Lady' according to internal quality in postharvest storage as a function of pre-harvest irrigation strategies. Sánchez *et al.* (2011) predicted of some quality parameters (weight, diameter, soluble solid content and flesh firmness), both on-side and in-line, in nectarines cv. 'Sweet Lady' with different harvests and crop practices. Reita *et al.* (2008) developed different methods for ºBrix determination of nectarine cv. ‘Big Bang Maillar’, cv. ‘Sweet Red’ and cv. ‘Nectaross’. Peiris *et al.* (1998), Golic & Walsh (2006) and Ma *et al.* (2007), determined the sugar content of peaches, while Fang *et al.* (2013) determined sugar content, acidity and water content in yellow peach between 350 - 2500 nm and achieved $R2 > 0.61$ for all properties except acidity determination, which still needs to be improved. These previous works have conducted studies on the use of VIS-NIR technology to assess the internal quality of stone fruits but they focus only on certain properties. The use of quality indexes

can correlate these properties. For instance, the IQI index (Cortés *et al.*, 2016) includes different analytical parameters, specifically three parameters typically employed in postharvest handling to evaluate the quality of this fruit. The study by Carlomagno *et al.* (2004) already assessed ripeness of peaches according to the combination of firmness and sugar content. The IQI, however, has the advantage of including the visual component (internal colour), which is a property of great importance to the consumer, in addition to the compositional aspects (firmness and soluble solids content), but avoiding the titratable acidity analysis because it is a laborious and slow process that generates waste. Indeed, one of the main benefits of the IQI is that all the required analyses are less time-consuming, with less pre-treatment of the sample and lower costs, and can be assessed using VIS-NIR diffuse reflectance spectroscopy.

This study aims to evaluate the performance of VIS-NIR reflectance spectroscopy as a tool to predict the internal quality of nectarines, and the potential of the information obtained to differentiate among varieties with different commercial interest. To this end, two varieties with a similar composition, grown in the same period, but with different development, cv. 'Big Top' and cv. 'Magique', have been analysed.

2. MATERIALS AND METHODS

2.1. Experimental procedure

The experimental part of this paper was carried out using 325 fruits of two commercial varieties of nectarines, cv. 'Big Top' and cv. 'Magique', harvested in a commercial orchard in Lérida, Spain. These varieties were chosen because they represent 36 % of the overall Spanish nectarine production (Font *et al.*, 2014), are grown at the same time and have a similar composition and organoleptic properties. Both are classified as a melting (slow-melting) phenotype, but present a large degree of variability in terms of development and maturation speed, and must therefore be handled differently in postharvest.

The samples were free from visual damage and with had a uniform size and colour. On arrival at the laboratory, fruits were cleaned, individually numbered and randomly divided into sets of 25 fruits each. All sets were stored at 15 °C to simulate the room conditions allowing the gradual maturation of the product. As

the 'Magique' variety ripens more slowly than 'Big Top', a total of six sets were analysed for the 'Big Top' variety on the 1st, 2nd, 3rd, 4th, 5th and 9th days, while a total of seven sets were analysed for the 'Magique' variety on the 1st, 3rd, 5th, 8th, 11th, 15th and 17th days. The VIS and NIR spectra of the fruits in each set were collected and their physicochemical properties were analysed by standard destructive methods.

2.2. Visible and near-infrared spectra acquisition

The visible spectra of the fruits were collected using a conventional spectrocolorimeter (CM-700d, Minolta Co., Tokyo, Japan) every 10 nm between 360 nm and 700 nm. The VNIR and NIR spectra were collected using a multichannel VIS-NIR spectrometer platform (AvaSpecAS-5216 USB2-DT, Avantes BV, The Netherlands) equipped with two detectors (Figure 1), one sensitive in the range from 595 nm to 1100 nm with a spectral FWHM (full width at half maximum) resolution of 1.15 nm and a spectral sampling interval of 0.255 nm (AvaSpec-ULS2048 StarLine, Avantes BV, The Netherlands) and the other sensitive in the NIR range from 888 nm to 1795 nm with a spectral FWHM resolution of 12 nm and a spectral sampling interval of 3.535 nm (AvaSpec-NIR256-1.7 NIRLine, Avantes BV, The Netherlands). The measurements were performed using a bi-directional fibre-optic reflectance probe (FCR-7IR200-2-45-ME, Avantes BV, The Netherlands). The probe is configured with an illumination leg with six 200 μm fibre cables which connects to a fibre-coupled light source and a single 200 μm read fibre cable to measure the diffuse reflectance via connection to a spectrometer. A 10 W tungsten halogen light source (AvaLight-HAL-S, Avantes BV, The Netherlands) was used to ensure a constant light intensity over the whole measurement range. The probe tip is designed to enable diffuse reflectance measurements under an angle of 45 ° to prevent direct back reflection from the surface of the fruit. A personal computer equipped with commercial software (AvaSoft version 7.2, Avantes, Inc.) was used to control both the detectors and to acquire the spectra. The integration times were adjusted for each spectrophotometer using a 99 % reflective white reference (WS-2, Avantes BV, The Netherlands), so that the maximum reflectance value over each wavelength range was around 90 % of saturation (Lorente *et al.*, 2015). They were set to 120

ms for the first detector and 500 ms for the second one. To reduce the thermal noise of the detector, each spectrum was obtained as the average of five scans (Nicolaï *et al.*, 2007). The average reflectance measurements of each sample (S) were then converted into relative reflectance values (R) with respect to the white reference using dark reflectance values (D) and the reflectance values of the white reference (W), as shown in equation 1:

$$R = \frac{S-D}{W-D} \quad (1)$$

The dark spectrum was obtained by turning off the light source and covering the tip of the reflectance probe.

Prior to spectral measurements, the temperature of the nectarines was stabilised at a room temperature of 22 ± 1 ºC. All the measurements were performed by placing the skin of the fruit on the equipment. Measurements were taken at two points on each side of fruit and mean values of the spectra were used for the analysis.

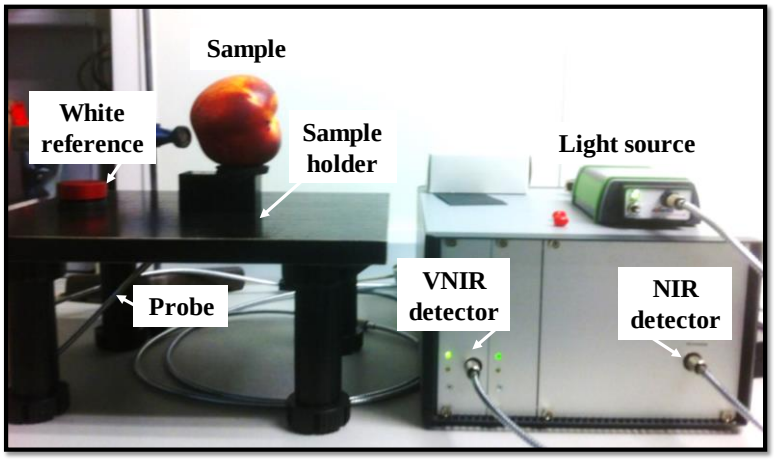

Figure 1. A labelled photograph of the VIS-NIR equipment.

2.3. Determination of quality attributes

Standard destructive quality testing methods were performed immediately after the acquisition of the spectral measurements to determine quality attributes for use as reference values. Flesh colour was determined with the

spectrocolorimeter using the standard illuminant D65 and the 10˚observer for all colour measurements. Colour attributes such as luminosity (L*), chromaticity (C^*) and hue angle (h^*) were obtained from the CIELab colour space. L* was obtained directly by the spectrocolorimeter whereas C^* and h^* were estimated by equations 2 and 3, respectively.

$$h^* = arctg\frac{b^*}{a^*} \quad (2)$$

$$C^* = \sqrt{a^{*2} + b^{*2}} \quad (3)$$

a^* and b^* being the CIELab attributes.

Firmness of the nectarines was measured using a Universal Testing Machine (XT2 Texture Analyser, Stable MicroSystems, Haslemere, England) to perform puncture tests using a 6 mm diameter cylindrical probe (P/15ANAMEsignature) to a relative deformation of 30 % at a speed of 1 mm/s. Two measurements were performed for each fruit on opposite sides along the equator. The fracture strength (F_{max}) was analysed for all samples, expressed the maximum force, in Newtons, applied to break the sample.

Immediately after firmness measurements, samples of nectarine juice were extracted to estimate the TSS by refractometry (°Brix) with a digital refractometer (RFM330+ set, VWR International Eurolab S.L. Barcelona, Spain) at 20 ºC with a sensitivity of ± 0.1 ºBrix. Samples were analysed in triplicate and average values were calculated.

Subsequently, the multi-parameter internal quality index (IQI, Cortés *et al.* (2016) was calculated by equation 4.

$$IQI = \ln(100 \cdot F \cdot L^* \cdot h^*_{ab} \cdot TSS^{-1} \cdot C^{*-1}_{ab}) \quad (4)$$

where F is the fracture strength (Newton), TSS is the total soluble solids (°Brix) and L^*, h^*_{ab}, C^*_{ab} are the colour attributes of the colour of the flesh.

2.4. Spectral pre-processing

The raw spectra from each of the three measuring devices were normalised (Bakeev, 2005) by dividing each variable by its standard deviation. In this way, the spectral intensities are rescaled to a common range, thus making it possible to compare the spectra acquired using different pieces of equipment with different resolutions. Then, the spectra were transformed to apparent absorbance (log (1/R)) values to linearise the correlation with the concentration of the constituents (Hernández *et al.*, 2006) using The Unscrambler V10.3 software package (CAMO, Norway). In addition, two pre-processing techniques were applied: Savitzky-Golay smoothing with a gap of three data points (Carr *et al.*, 2005) combined with extended multiplicative scatter correction (EMSC) (Martens *et al.*, 2003; Bruun *et al.*, 2007). Smoothing, which includes moving smoothing and Savitzky-Golay smoothing, is one of the methods that are most often used to eliminate noise (Gorry, 1990; Savitzky & Golay, 1964), and EMSC is a method that is well suited to the removal of physical effects from chemical information, i.e. it is particularly useful for minimising wavelength-dependent light scattering variation (Santos *et al.*, 2013). Figure 2 shows raw VIS-NIR spectra and their correction after the application of the pre-processing methods.

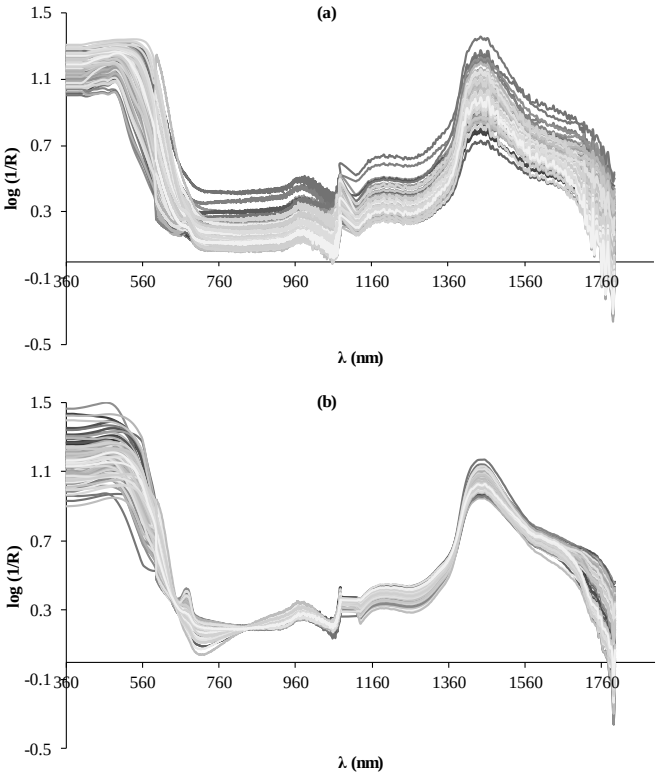

Figure 2. VIS-NIR spectra of the 150 cv. 'Big Top' samples; a) Raw and b) Smoothing Savitzky-Golay + EMSC transformed.

2.5. Chemometric data treatment

A one-way analysis of variance (ANOVA) was conducted to determine significant differences in the physicochemical properties (F_{max}, TSS, L*, h*, C* and IQI) during the postharvest evolution of the fruit using the software Statgraphics Plus for Windows 5.1 (Manugistics Corp., Rockville, MD, USA). The multivariate analysis was performed through partial least squares discriminant analysis (PLS-DA) and linear discriminant analyses (LDA) were performed using the Unscrambler X software package.

2.5.1 Prediction analysis of internal quality

Two matrices were created for each variety of nectarines, where the rows represented the samples (#N = 150 for cv. 'Big Top' and #N = 175 for cv.

'Magique') and the columns represented the variables (X-variables and Y-variables). The X-variables, or predictors, were the different VIS-NIR spectra while the Y-variable, or response, was the IQI estimated for each sample. Before calibration, principal component analysis (PCA) was performed to extract the most important information about spectral data and to exclude samples considered outliers.

Two regression models for each variety of nectarines were developed by partial least squares (PLS) to predict the IQI based on the spectral measurements. This method is often used in spectroscopy analysis to evaluate the quality characteristics of intact fruits, for example, mandarin (Hernández *et al.*, 2006), tomato (Shao *et al.*, 2007), orange (Cayuela & Weiland, 2010), mulberry (Huang *et al.*, 2011) and banana (Jaiswal *et al.*, 2012). Samples were randomly separated into two groups: 75 % of the samples were used for development and evaluation by a cross-validation model using the leave-one-out cross technique (Huang *et al.*, 2008), while the remaining samples (25 %) were used as the prediction set (Kamruzzaman *et al.*, 2012). The root mean square error of calibration (RMSEC), root mean squared error of cross validation (RMSECV), root mean square error of prediction (RMSEP), coefficient of determination for calibration (R^2_C), coefficient of determination for cross-validation (R^2_{CV}) and for prediction (R^2_P), and the required number of latent variables (LV) were used to judge the accuracy of the PLS model.

2.5.2. Discriminant analysis for varietal differentiation

Discriminant models, using LDA and PLS-DA were built to classify nectarines in terms of variety. A training set consisting of a random selection of 75 % of the studied samples was used to develop a qualitative calibration model. Each model was validated using the leave-one-out cross-validation technique (Huang *et al.*, 2008) and the weight of the spectral variables selected was 1/Sdev. A test set (25 % of remaining samples) was used for the evaluation and comparison of the classification models (Soares *et al.*, 2013). These discriminant analyses seek to correlate spectral variations (X) with defined classes (Y), with attempts being made to maximise the covariance between the two types of variables. In this type of approach, the Y variables used are not continuous, as they are in quantitative

analysis, but rather categorical "dummy" variables created by assigning different values to the different classes to be discriminated. In the case of PLS-DA, the Y-variable was a vector with zeroes (for the cv. 'Big Top') and ones (for the cv. 'Magique'). However, for LDA the number of samples in the training set must be larger than the number of variables included in the model (Kozak & Scaman, 2008; Sádecká *et al.*, 2016), thus requiring a variable reduction. This was performed using the PCA scores as input data, since linear combinations of the original variables called principal components (PCs) are uncorrelated (Rodríguez-Campos *et al.*, 2011). In this study, the first seven principal components were used to replace the original one data (He *et al.*, 2006). The RMSEC, RMSECV, R^2_C, R^2_{CV}, LV and percentage of correctly classified samples were used to evaluate the discriminating capacity of the models.

3. RESULTS AND DISCUSSION

3.1. Analysis of the quality attributes

The changes observed in the firmness and TSS of the two varieties of nectarines during postharvest storage are shown in Figure 3.

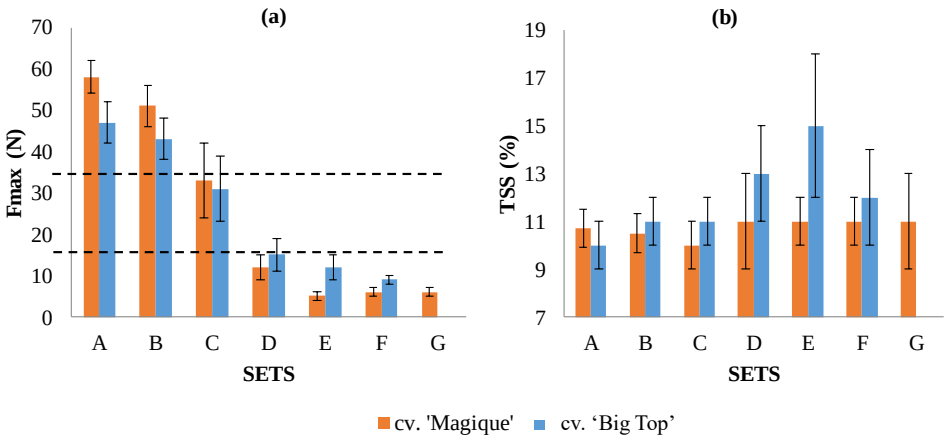

Figure 3. Mean and standard deviation of a) firmness and b) TSS of nectarines at different sets of analysis. Discontinuous lines in the mechanical plot (left) indicate firmness thresholds.

As expected, the changes in both parameters during ripening are indicative of the physiological development of the fruit (Valero *et al.*, 2007). In both cultivars a steady decrease was observed in fruit firmness over time from around 47 N to 9 N for cv. 'Magique', and from 58 N to 6 N for cv. 'Big Top'. These values coincide with those reported by Ghiani *et al.* (2011) for nectarine cv. 'Big Top'. The textural changes that took place in the fruit during the postharvest period can be attributed to different factors, such as significant changes in the composition and structure of cell walls and, particularly, the degradation of the polysaccharides. As a result, the decrease in firmness during the process is due to a loss of neutral sugars, solubilisation and de-polymerisation of the polysaccharides of the cell wall, and the reorganisation of their interconnections (Singh *et al.*, 2013). The firmness values cover all the commercial ranges proposed by Crisosto (2002) and Valero *et al.* (2007), which are less than 18 N (ready to eat), between 18 and 35 N (ready to buy) and over 35 N (immature).

On the other hand, TSS increased continuously, from 10 ± 1 to 15 ± 3 during postharvest storage for cv. 'Big Top', which is nowadays the reference cultivar, known for quickly reaching its typical mature colour, sweet taste and optimum fruit size (Iglesias & Echeverría, 2009). This increment is due to the conversion of starch to glucose and fructose, which are used as substrates during fruit respiration (Eskin *et al.*, 2013). However, the increase in TSS observed for cv. 'Magique' remained around 10-11 % probably because this variety has a different pattern of ripening. However, in all cases, the values were greater than 8 ºBrix, which is the minimum established by the European Union to market peaches and nectarines (R-CE No. 1861/2004). Several authors have reported a linear relationship between TSS and consumer acceptance (Crisosto & Crisosto, 2005), a TSS of below 10 % generally being unacceptable to consumers (Clareton, 2000).

Figure 4 shows the evolution of the flesh colour of the two varieties of nectarines during the postharvest storage. Flesh colour was taken as the evaluation parameter rather than external colour because for some nectarine varieties with early development of the external colour, such as cv. 'Big Top', their external colour should not be used as a maturity index (Ravaglia *et al.*, 1996) because they reach the appearance of being mature before they are ready to eat (Della Cara, 2005; Iglesias & Echeverría, 2009). In this sense, other authors such as Tijskens *et*

al. (2007) suggest that flesh colour is a good index to determine the development of the fruit. It can be observed that L* and h* decrease and C* increases during the storage for both varieties. Cv. 'Big Top' changes from L* = 72, h* = 79 and C* = 42 in the unripe stage until L* = 62, h* = 74 and C* = 60 at the states of further development, and cv. 'Magique' changes from L* = 72, h* = 102 and C* = 24 to L* = 70, h* = 86 and C* = 29. Figure 4b shows an example of the internal appearance of both cultivars on each day of analysis. The flesh colour changed from whitish-yellow to orange-red for the cv. 'Big Top' and from whitish-green to yellow-orange during postharvest storage especially for the cv. 'Magique', similar to the findings of Padilla-Zakour (2009), who reported that the colour of peaches changed from yellow-greenish to yellow-orange or orange-reddish when fruits matured.

Figure 5 shows the evolution of the IQI, which is represented by a sigmoidal curve for both varieties. The values of the indices clearly decreased during the storage period for cv. 'Big Top' (Figure 5a) and for cv. 'Magique' (Figure 5b), but three trends can be differentiated in the graph. Initially, the two IQI decline slowly until 17.5 because the maturation of the product has not yet been produced at the beginning of the IQI curve, and then drops sharply when the fruits ripen to achieve their optimum organoleptic properties, which are related to adequate firmness, content in TSS and flesh colour. Finally, fruit reach the stage of over-ripeness, where the curve follows a constant trend because the product reaches a maximum TSS content and a minimum firmness. It should be noted that, even though they have the same trends, the two varieties have different maturation speeds. Thus, while cv. 'Big Top' nectarines reach over-ripeness at day 5 (E in Figure 5a), cv. 'Magique' nectarines do so at day 15 (F in Figure 5b).

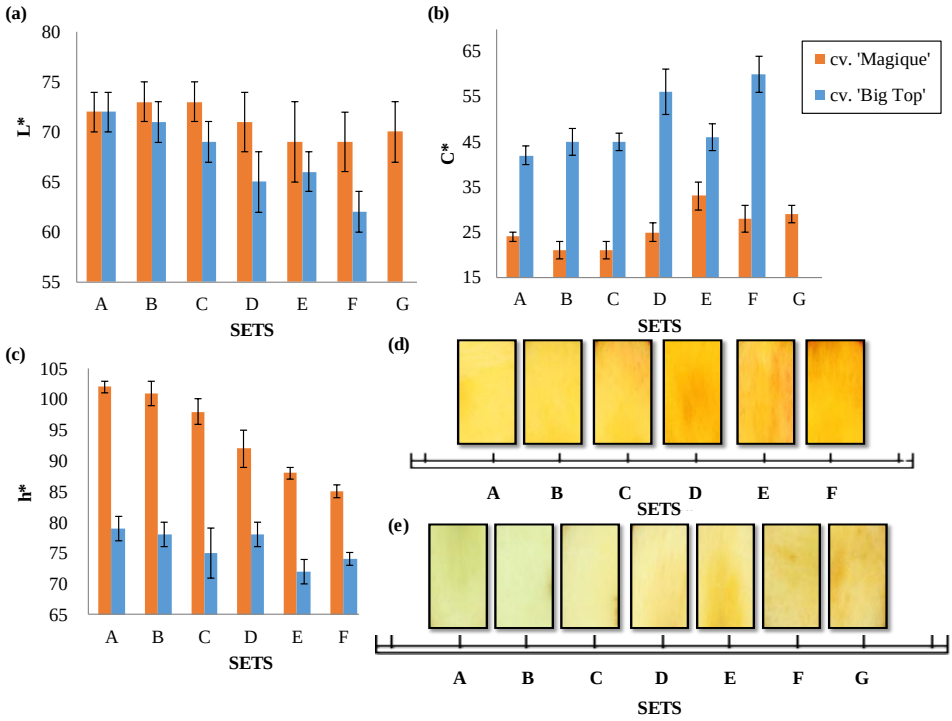

Figure 4. a) b) and c) Flesh colour atributes (L*, h* and C*); and d) an example of internal colour appearance of nectarines cv. 'Big Top'; and e) cv. 'Magique' during the storage period.

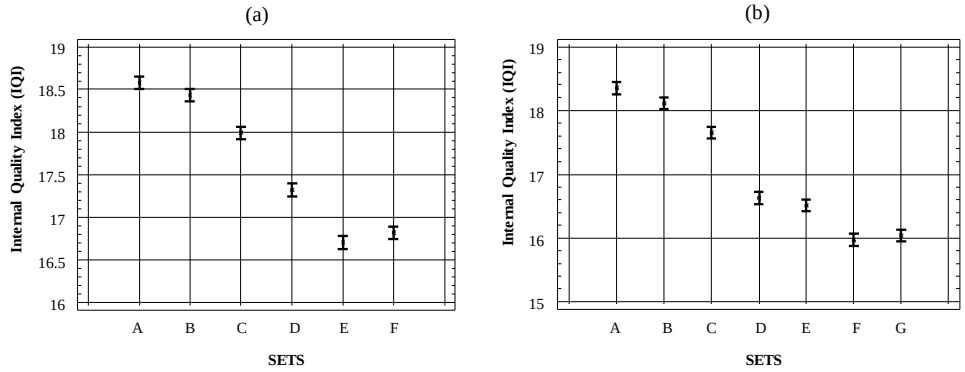

Figure 5. Evolution of the IQI during the storage period of the a) nectarines cv. 'Big Top' and b) nectarines cv. 'Magique'.

3.2. Spectral analysis

Figure 6 presents the VIS-NIR absorbance spectra of each day of storage for both varieties. Each spectrum represents an average of the measurements done. As can be seen, there was considerable spectral similarity between the varieties analysed, due to the existing features being very similar in their chemical structures. Even, the pattern of the absorption curves is similar to other fruits such as pear (Liu *et al.*, 2008), açaí and juçara fruits (Cunha *et al.*, 2016), peach (Martins *et al.*, 2016) and mandarin (Magwaza *et al.*, 2012), although the position and magnitude of the peaks are specific for each fruit.

From the visible region (360 - 770 nm), a continuous decrease in absorbance, with the minimum at 680 nm, is observed. The spectra show a broad absorbance band around 450 nm associated with carotenes and xanthophylls (Lichtenthaler & Buschamann, 2001). The high absorbance observed around 670 nm is indicative of the presence of chlorophyll, which gives the fruit its characteristic green colour (Merzlyak *et al.*, 2003; Gómez *et al.*, 2006). Furthermore, Tijskens *et al.* (2007) concluded that absorption at 670 nm allowed the evaluation of the variation in maturity of individual nectarines. The peaks centred at 970 nm and 1400 nm that appear are probably due to the presence of water (Williams & Norris, 1987; McGlone & Kawano, 1998). A characteristic absorption band at around 1160 nm was sugar-related (Osborne *et al.*, 1993; Walsh *et al.*, 2004). Lu (2004) stated that the absorption of radiation increases as fruit firmness decreases, i.e. firmer fruit reflect more radiation than softer fruit. Fu *et al.* (2007) stated that this is also linked to water and pectin content.

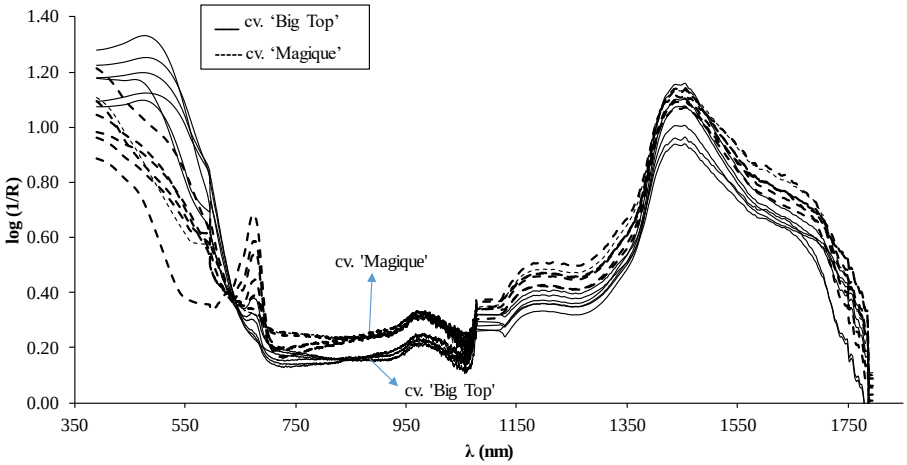

Figure 6. Fruit samples absorbance spectra between 360 and 1795 nm for the two varieties of nectarines at different storage times.

3.3. Analysis of internal quality

Table 1 displays the results for the calibration and prediction models of the internal quality of intact nectarines.

Table 1. Results of the PLS models for the prediction of the IQI in nectarines samples with different flesh colour.

Parameter	#LV	Calibration		Cross Validation		Prediction	
		R^2_c	RMSEC	R^2_{cv}	RMSECV	R^2_P	RMSEP
IQI , cv. 'Big Top'	7	0.948	0.179	0.910	0.237	0.909	0.235
IQI, cv. 'Magique'	7	0.965	0.183	0.942	0.238	0.927	0.238

PLS models built for both varieties showed similar prediction coefficients and performance. The best method is usually the one that minimises the prediction error (RMSEP) and number of LV for an independent test set (Faber, 1999) while maximising the R^2_P. In this case, when applied to an independent prediction set, the PLS models were capable of predicting IQI with R^2_P of 0.909 and 0.927 and RMSEP of 0.235 and 0.238 for cv. 'Big Top' and 'Magique', respectively. Figure 7

shows a good prediction performance of the PLS models for IQI. These results suggest that the calibration models optimised with leave-one-out cross-validation are representative and the models can accurately predict unknown sample data.

These results are similar to those obtained by Cortés *et al.* (2016), who have recently developed models to predict the internal quality of mangoes cv. 'Osteen' using the IQI (R^2_p = 0.833). Thus, it is confirmed that the IQI can be applied to various types of fruits to ensure an adequate quality of the final product for the consumer.

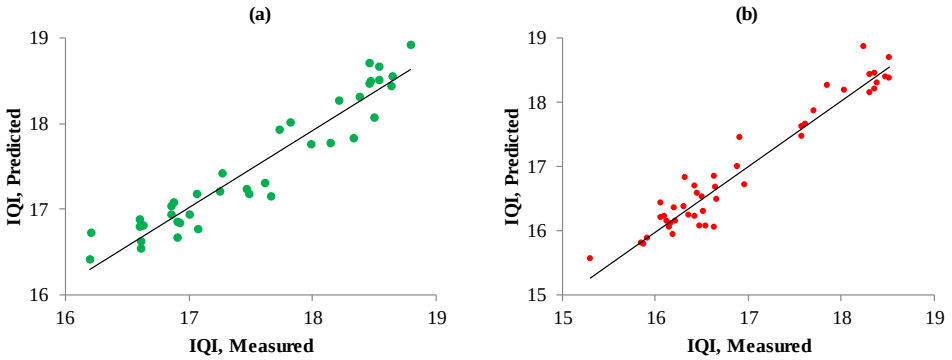

Figure 7. Predicted vs measured values of IQI in the examined samples of variety a) 'Big Top' and b) 'Magique'.

3.4. Varietal classification

Before performing discriminant analysis, PCA decomposition was conducted to recognise any possible pattern of classification. The spectrum of each sample was represented as a point, with respect to these new axes (Downey, 1997). The samples of cv. 'Magique' were used to develop the PCA model used later and to project the samples of cv. 'Big Top'. Figure 8 shows the two-dimensional scatter plot of scores for two principal components (PCs) from projection results. The two PCs explain over 70 % (53 % for the first PC and 18 % for the second PC) of the variation. This justifies the possibility of differentiating between varieties using the spectra measured in intact nectarines.

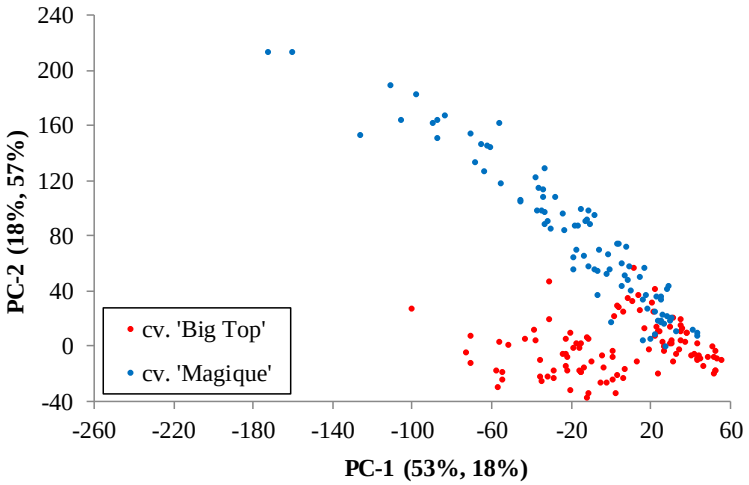

Figure 8. Projection of nectarines samples in the space defined by the two first PCs.

After proving the performance of an unsupervised method such as PCA to classify samples belonging to different varieties, the next step consisted in building classification models based on supervised LDA and PLS-DA. The best models were chosen with seven LV for both cases. The optimal number of latent variables was chosen according to the lowest RMSECV by internal validation, i.e. 'leave-one-out', in combined analysis with the cumulative variance in the X and Y blocks (Bachion de Santana *et al.*, 2016).

All the training set and validation samples were correctly classified by the PLS-DA model, as shown in Figure 9. In this situation, all cv. 'Big Top' samples have predictive values close to, 1 thus classifying these as belonging to class '1', and cv. 'Magique' samples have predictive values close to 0, therefore classifying these as belonging to class '0'. The values of the RMSEC and RMSEP were 0.112 and 0.133, respectively, which exhibit a good agreement, indicating that the calibration error is a good estimation of the standard error of prediction observed in samples in the test set. Moreover, the validation set gave a similar result to the calibration set, with R^2 of 0.949 and 0.926 respectively, thereby indicating good performance of the model for varietal classification.

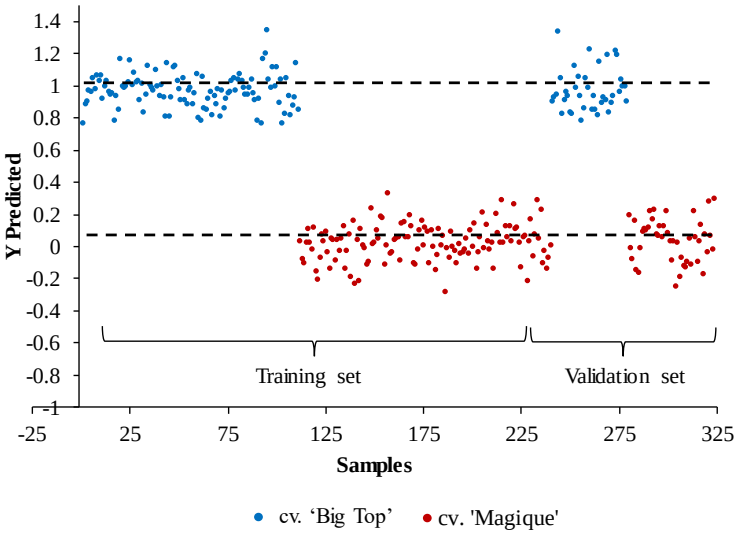

Figure 9. Estimated class values for training and validation sets for varietal discrimination by PLS-DA model.

Regarding LDA, Figure 10 shows the results of the external validation by test set (25 %) of each variety. Validation samples of the cv. 'Big Top' are displayed in blue, while samples of the cv. 'Magique' are in red. The classification accuracy was 97.44 %, all cv. 'Magique' samples being classified correctly and only two cv. 'Big Top' samples misclassified.

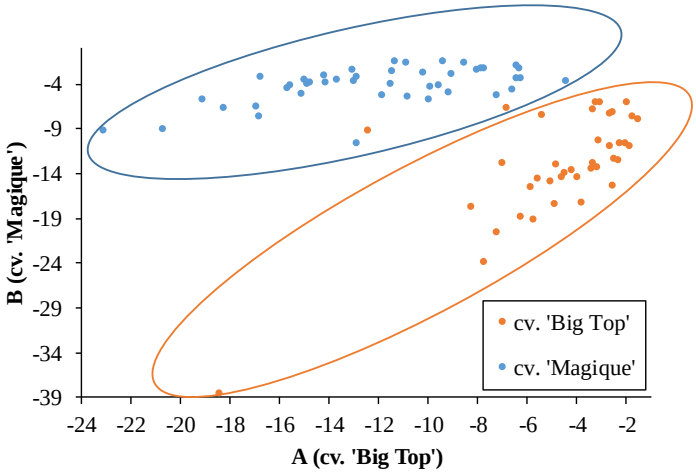

Figure 10. Discrimination plot of the LDA results for the validation samples.

Table 2 shows the summary of the classification accuracy for each analysis, presented as both as percentage and absolute number of correctly classified samples.

As both varieties have a similar composition, to develop a tool capable of differentiating them is challenging and could be possible to be applied to differentiate other varieties with greater difference. Based on these results, the ability of these VIS-NIR instruments to classify fruit as depending on its variety for compositionally similar samples has been demonstrated satisfactorily for nectarine. So, it is possible to explain the postharvest shelf-storage time using these techniques for varieties with different speeds of evolution because they are classified correctly from their origin.

Table 2. Confusion matrix obtained in prediction for the PLS-DA and LDA analysis.

			Reference variety		**Classification accuracy**
			cv. 'Big Top'	cv. 'Magique'	
LDA	**Sample variety**	cv. 'Big Top'	94.87% (37)	5.13% (2)	97.44%
		cv. 'Magique'	0% (0)	100% (45)	
PLS-DA	**Sample variety**	cv. 'Big Top'	100% (39)	0% (0)	100%
		cv. 'Magique'	0% (0)	100% (45)	

4. CONCLUSIONS

The quantitative and qualitative results of this study confirmed that VIS-NIR spectroscopy is a technique capable of determining the internal quality of intact nectarines with significant reliability. The partial least squares regression analysis showed strong performance in predicting the internal quality of the samples, with an R^2_P and RMSEP of 0.909 and 0.235 for cv. 'Big Top', and 0.927 and 0.238 for 'Magique'. It has been possible to differentiate three trends of the IQI curve, where initially the maturation of the product has not yet been produced, followed by the development of the optimum organoleptic properties, and finally the fruit reaches the stage of over-ripeness. Despite being two varieties with a similar composition and grown in the same period, it was possible to separate the two with a perfect

classification rate of 100 % using PLS-DA and 97.44 % using the model developed by LDA models. This represents an advance in the creation of tools for monitoring the fruit quality for the postharvest industry compared to the present situation where the evaluation of the state of the fruit is mostly carried out based on the subjective experience of trained experts. Further studies are needed to improve the calibration specificity, accuracy and robustness, and to extend the discrimination to other nectarine varieties.

Acknowledgements

This work was partially funded by the Generalitat Valenciana through project AICO/ 2015/122 and by INIA and FEDER funds through projects RTA2012-00062-C04-01 and 03, and RTA2015-00078-00-00. Victoria López Cortés thanks the Spanish Ministry of Education, Culture and Sports for the FPU grant (FPU13/04202). The authors are also grateful to Fruits de Ponent (Lérida) for providing the fruit.

5. REFERENCES

Bachion de Santana, F., Caixeta Gontijo, L., Mitsutake, H., Júnior Mazivilla, S., Maria de Souza, L. & Borges Neto, W. (2016). Non-destructive fraud detection in rosehip oil by MIR spectroscopy and chemometrics. Food Chemistry 209, 228-233.

Bakeev, K.A. (2010). Process Analytical Technology. United Kingdom: Wiley.

Bonany, J., Buehler, A., Carbó, J., Codarin, S., Donati, F., Echeverria, G., Egger, S., Guerra, W., Hilaire, C., Höller, I., Iglesias, I., Jesionkowska, K., Konopacka, D., Kruczynska, D., Martinelli, A., Pitiot, C., Sansavini, S., Stehr, R. & Schoorl, F. (2013). Consumer eating quality acceptance of new apple varieties in different European countries. Food Quality and Preference, 30, 250-259.

Bruun, S.W., Sondergaard, I. & Jacobsen, S. (2007). Analysis of protein structures and interactions in complex food by Near-Infrared spectroscopy. 1. Gluten Powder. Journal of Agricultural and Food Chemistry, 55, 7234-7243.

Carlomagno, G., Capozzo, L., Attolico, G. & Distante, A. (2004). Non-destructive grading of peaches by near-infrared spectrometry. Infrared Physics & Technology 46, 23-29.

Carr, G.L., Chubar, O. & Dumas, P. (2005). Spectrochemical Analysis Using Infrared Multichannel Detectors 1st edn. (eds., Bhargava, R. & Levin, I.W.) 56–84. Oxford: Wiley-Blackwell.

Cayuela, J.A. & Weiland, C. (2010). Intact orange quality prediction with two portable NIR spectrometers. Postharvest Biology and Technology 58 (2), 113-120.

Clareton, M. (2000). Peach and nectarine production in France: trends, consumption and perspectives. Summaries Prunus breeders meeting, EMBRAPA, clima temperado Pelotas (RS), 83-91.

Commission Regulation EC, No.1861/2004 of 28 October 2004.

Cortés, V., Ortiz, C., Aleixos, N., Blasco, J., Cubero, S. & Talens, P. (2016). A new internal quality index for mango and its prediction by external visible and near infrared reflection spectroscopy. Postharvest Biology and Technology, 118, 148-158.

Crisosto, C. & Crisosto, G. (2005). Relationship between ripe soluble solids concentration (RSSC) and consumer acceptance of high and low acid meeting flesh peach and nectarine (Prunus persica (L.) Batsch) cultivars. Postharvest Biology and Technology, 38, 239-246.

Crisosto, C.H., Crisosto, G.M. & Metheney, P. (2003). Consumer acceptance of 'Brooks' and 'Bing' cherries is mainly dependent on fruit SSC and visual skin color. Postharvest Biology and Technology, 28, 159-167.

Crisosto, C.H., Crisosto, G.M., Ritenour, M.A. (2002). Testing the reliability of skin color as an indicator of quality for early season 'Brooks' (Prunus aviumL.) cherry. Postharvest Biology and Technology, 24, 147-154.

Crisosto, C.H., Garner, D., Crisosto, G.M., Wiley, P. & Southwick, S. (1997). Evaluation of the minimum maturity index for new cherry cultivars growing in the San Joaquin Valley. Visalia, CA: California Cherry Growers Association.

Crisosto, C.H. (2002). How do we increase peach consumption? Proceedings of 5th International Symposium on Peach, ISHS, Acta Horticulturae, 592, 601-605.

Cubero, S., Aleixos, N., Moltó, E., Gómez-Sanchis, J. & Blasco, J. (2011). Advances in machine vision applications for automatic inspection and quality evaluation of fruits and vegetables. Food and Bioprocess Technology, 4, 487-504.

Cunha, L.C., Teixeira, G.H.A., Nardini, V. & Walsh, K. (2016). Quality evaluation of intact açaí and juçara fruit by means of near infrared spectroscopy. Postharvest Biology and Technology, 112, 64-74.

Della Cara, R. (2005). In calo i consumi e l'export de pesche e nettarine italiane. Rivista di Frutticoltura, 7-8, 19-20.

Downey, G. (1997). Authentication of food and food ingredients by near infrared spectroscopy. Journal of Near Infrared Spectroscopy, 4, 47-61.

Eskin, N.A.M., Hoehn, E., Shahidi, F., (2013). Fruits and vegetables, Eskin, N.A.M., Shahidi, F. (Eds.), Biochemistry of foods, 49-126.

Faber, N.M. (1999). Multivariate Sensitivity for the Interpretation of the Effect of Spectral Pretreatment Methods on Near-Infrared Calibration Model Predictions. Journal of Analytical Chemistry, 71, 557-565.

Fang, L., Li, H., Liu, Z. & Xian, X. (2013) Online evaluation of yellow peach quality by visible and near-infrared Spectroscopy. Advance Journal of Food Science and Technology, 5 (5), 606-612.

Ferrer, P., Montesinos, J.L., Valero, F. & Solá, C. (2001). Production of native and recombinant lipases by Candida rugosa. Applied Biochemistry and Biotechnology, 95(3), 221-255.

Font, D., Tresanchez, M., Pallejà, T., Teixidó, M., Martinez, D., Moreno, J. & Palacín, J. (2014). An image processing method for in-line nectarine variety verification based on the comparison of skin feature histogram vectors. Computers and Electronics in Agriculture, 102, 112-119.

Fu, X., Yibin, Y., Lu, H., Xu, H. & Yu, H. (2007). FT-NIR diffuse reflectance spectroscopy for kiwifruit firmness detection. Sensing and Instrumentation for Food Quality and Safety, 1, 29-35.

GenCat: Generalitat de Cataluña. Technical report 1/2011 and Technical Indicator A2. <http://www20.gencat.cat> (accessed 13.05.13).

Ghiani, A., Negrini, N., Morgutti, S., Baldin, F., Nocito, F.F., Spinardi, A., Mignani, I., Bassi, D. & Cocucci, M. (2011). Melting of 'Big Top' Nectarine Fruit: Some Physiological, Biochemical, and Molecular Aspects. Journal of the American Society for Horticultural Science, 136, 61-68.

Golic, M., Walsh, K.B. (2006). Robustness of calibration models based on near infrared spectroscopy for the in-line grading of stonefruit for total soluble solids content. Analytica Chimica Acta, 555 (2), 286-291.

Gómez, A.H., He, Y. & Pereira, A.G. (2006). Nondestructive measurement of acidity: Soluble solids and firmness of Satsuma mandarin using Vis/NIRspectroscopy techniques. Journal of Food Engineering, 77(2), 313-319.

Gorry, P.A. (1990). General least-squares smoothing and differentiation by the convolution (Savitzky-Golay) method. Analytical Chemistry, 62, 570-573.

He, Y., Li, X.L. & Shao, Y.N. (2006). Discrimination of varieties of apple using near infrared spectra based on principal component analysis and artificial neural network model. Spectroscopy and Spectral Analysis, 26, 850-853.

Hernández, A., He, Y. & García, A. (2006). Non-destructive measurement of acidity, soluble solids and firmness of Satsuma mandarin using Vis/NIR-spectroscopy techniques. Journal of Food Engineering, 77, 313-319.

Huang, H., Yu, H., Xu, H. & Ying, Y. (2008). Near infrared spectroscopy for on/in-line monitoring of quality in foods and beverages: A review. Journal of Food Engineering, 87 (3), 303-313.

Huang, L., Wu, D., Jin, H., Zhang, J., He, Y. & Lou, C. (2011). Internal quality determination of fruit with bumpy surface using visible and near infrared spectroscopy and chemometrics: A case study with mulberry fruit. Biosystems Engineering, 109 (4), 377-384.

Iglesias, I. & Echeverría, G. (2009). Differential effect of cultivar and harvest date on nectarine colour, quality and consumer acceptance. Scientia Horticulturae, 120, 41-50.

Iglesias, I. (2013). Peach production in Spain: Current situation and trends, from production to consumption. Preceedings of the 4th Conference, Innovation in fruit growing, Blegrade, 75-89.

Jaiswal, P., Jha, S.N. & Bharadwaj, R. (2012). Non-destructive prediction of quality of intact banana using spectroscopy. Scientia Horticulturae, 135, 14-22.

Kamruzzaman, M., ElMasry, G., Sun, D. & Allen, P. (2012). Non-destructive prediction and visualization of chemical composition in lamb meat using NIR hyperspectral imaging and multivariate regression. Innovate Food Science and Emerging Technologies, 16, 218-226.

Kozak, M. & Scaman, C.H. (2008). Unsupervised classification methods in food sciences: discussion and outlook. Journal of the Science of Food and Agriculture, 88, 1115-1127.

Lichtenthaler, H.K. & Buschmann, C. (2001). Chlorophylls and carotenoids: measurement and characterization by UV-VIS spectroscopy. Current Protocols in Food Analytical Chemistry, (F:F4:F4.3.).

Liu, Y., Chen, X. & Ouyang, A. (2008). Nondestructive determination of pear internal quality indices by visible and near infrared spectrometry. LWT-Food Science and Technology, 41, 1720-1725.

Lorente, D., Aleixos, N., Gómez-Sanchis, J., Cubero, S., García-Navarrete, O.L. & Blasco, J. (2012). Recent advances and applications of hyperspectral imaging for fruit and vegetable quality assessment. Food Bioprocess Technology, 5, 1121-1142.

Lorente, D., Escandell-Montero, P., Cubero, S., Gómez-Sanchis, J. & Blasco, J. (2015). Visible-NIR reflectance spectroscopy and manifold learning methods applied to the detection of fungal infections on citrus fruit. Journal of Food Engineering, 163, 17-21.

Lu, R. (2004). Multispectral imaging for predicting firmness and soluble solids content of apple fruit. Postharvest Biology and Technology, 31(2), 147-157.

Ma, G., Fu, X.P., Zhou, Y., Ying, Y.B., Xu, H.R., Xie, L.J., Lin, T. (2007). Nondestructive sugar content determination of peaches by using near infrared spectroscopy technique. Spectroscopy and Spectral Analysis, 27(5), 907-910.

Magwaza, L.S., Opara, L.U., Nieuwoudt, H., Cronje, P.J.R., Saeys, W. & Nicolaï, B. (2012). NIR Spectroscopy Applications for Internal and External Quality Analysis of Citrus Fruit- A Review. Food and Bioprocess Technology, 5, 425-444.

Martens, H., Nielsen, J.P. & Engelsen, S.B. (2003). Light scattering and light absorbance separated by extended multiplicative signal correction. Application to near-infrared transmission analysis of powder mixtures. Journal of Analytical Chemistry, 75, 394-404.

Martins, P.A., Cirino de Carvalho, L., Cunha, L.C., Manhas, F. & Teixeira, G.H. (2016). Robust PLS models for soluble solids content and firmness determination in low chilling peach using near infrared spectroscopy (NIR). Postharvest Biology and Technology, 111, 345-351.

McGlone, V.A. & Kawano, S. (1998). Firmness, dry-matter and soluble-solids assessment of post-harvest kiwifruit by NIR spectroscopy. Postharvest Biology and Technology, 13, 131-141.

Merzlyak, M.N., Solo, A.E. & Gitelson, A.A. (2003). Reflectance spectral features and non-destructive estimation of chlorophyll, carotenoid and anthocyanin content in apple fruit. Postharvest Biology and Technology, 27, 197-211.

Nicolaï, B.M., Beullens, K., Bobelyn, E., Peirs, A., Saeys, W., Theron, I.K. & Lammertyn, J. (2007). Non-destructive measurement of fruit and vegetable quality by means of NIR spectroscopy: a review. Postharvest Biology and Technology, 46, 99-118.

Osborne, B.G., Fearn, T. & Hindle, P.H. (1993). Practical NIR Spectroscopy with Applications in Food and Beverage Analysis, 2nd ed. Longman Group, Burnt Mill, Harlow, Essex, England, UK, 123-132.

Padilla-Zakour, O.I. (2009). Good manufacturing practices. In N. Heredia, I. Wesley, & S. Garcia (Eds.), Microbiologically Safe Foods, 395–415. New York: John Wiley and Sons Inc.

Peiris, K.H.S., Dull, G.G., Leffler, R.G. & Kays, S.J. (1998). Near-infrared spectrometric method for nondestructive determination of soluble solids content of peaches. Journal of the American Society for Horticultural Science, 123(5), 898-905.

Pérez-Marín, D., Sánchez, M.T., Paz, P., González-Dugo, V. & Soriano, M.A. (2011). Postharvest shelf-life discrimination of nectarines produced under different irrigation strategies using NIR-spectroscopy. Food Science and Technology, 44, 1405-1414.

Ravaglia, G., Sansavini, S., Ventura, M. & Tabanelli, D. (1996). Indici di maturazione e miglioramento cualitativo delle pesche. Revista di Frutticoltura, 3, 61-66.

Reita, G., Peano, C., Saranwong, S. & Kawano, S. (2008). An evaluating technique for variety compatibility of fruit applied to a near infrared Birx calibration system: a case study using Brix calibration for nectarines. Journal of Near Infrared Spectroscopy, 16(2), 83-89.

Rodriguez-Campos, J., Escalona-Buendía, H.B., Orozco-Avila, I., Lugo-Cervantes, E. & Jaramillo-Flores, M.E. (2011). Dynamics of volatile and non-volatile compounds in cocoa (Theobroma cacao L.) during fermentation and drying processes using principal components analysis. Food Research International, 44, 250-258.

Sádecká, J., Jakubíková, M., Májek, P. & Kleinová, A. (2016). Classification of plum spirit drinks by synchronous fluorescence spectroscopy. Food Chemistry, 196, 783-790.

Sánchez, M.T., De la Haba, M.J., Guerrero, J.E., Garrido-Varo, A. & Pérez-Marín, D. (2011). Testing of a local approach for the prediction of quality parameters in intact nectarines using a portable NIRS instrument. Postharvest Biology and Technology, 60(2), 130-135.

Santos, P., Santos, F., Santos, J. & Bezerra, H. (2013). Application of extended multiplicative signal correction to short-wavelength near infrared spectra of moisture in Marzipan. Journal of Data Analysis and Information Processing, 1, 30-34.

Savitzky, A. & Golay, M.J.E. (1964). Smoothing and differentiation of data by simplified squares procedures. Analytical Chemistry, 36, 1627-1639.

Shao, Y., He, Y., Gómez, A.H., Pereir, A.G., Qiu, Z. & Zhang, Y. (2007). Visible/near infrared spectrometric technique for nondestructive assessment of tomato 'Heatwave' (Lycopersicumesculentum) quality characteristics. Journal of Food Engineering, 81(4), 672-678.

Singh, Z., Singh, R.K., Sane, V.A. & Nath, P. (2013). Mango–Postharvest biology and biotechnology. Critical Reviews in Plant Sciences, 32(4), 217-236.

Soares, S.F.C., Gomes, A.A., Galvão Filho, A.R., Araújo, M.C.U. & Galvão, R.K.H. (2013). The successive projections algorithm. Trends in Analytical Chemistry, 42, 84-98.

Tijskens, L.M.M., Zerbini, P.E., Schouten, R.E., Vanoli, M., Jacob, S., Grassi, M. & Torricelli, A. (2007). Assessing harvest maturity in nectarines. Postharvest Biology and Technology, 45, 204-213.

Valero, A., Marín, S., Ramos, A.J. & Sanchis, V. (2007). Effect of preharvest fungicides and interacting fungi on Aspergillus carbonarius growth and ochratoxin. A synthesis in dehydrating grapes. Letters in Applied Microbiology, 45, 194-199.

Walsh, K.B., Golic, M. & Greensill, C.V. (2004). Sorting of fruit and vegetables using near infrared spectroscopy: application to soluble solids and dry matter content. Journal of Near Infrared Spectroscopy, 12, 141-148.

Williams, P.C. & Norris, K.H. (1987). Qualitative applications of near infrared reflectance spectroscopy. In P. C. Williams & K. H. Norris (Eds.), Near infrared technology in the agricultural and food industries, 241-246.

3.1.4. Chapter IV.

A new internal quality index for mango and its prediction by external visible and near-infrared reflection spectroscopy

Cortés, V.[1], Ortiz, C.[2], Aleixos, N.[3], Blasco, J.[4], Cubero, S.[4] & Talens, P.[1]

[1]Departamento de Tecnología de Alimentos. Universitat Politècnica de València. Camino de Vera s/n, 46022, Valencia (Spain).

[2]Departamento de Ingeniería Rural y Agroalimentaria. Universitat Politècnica de València. Camino de Vera s/n, 46022, Valencia (Spain).

[3]Departamento de Ingeniería Gráfica, Universitat Politècnica de València. Camino de Vera s/n, 46022, Valencia (Spain).

[4]Centro de Agroingeniería. Instituto Valenciano de Investigaciones Agrarias (IVIA). Ctra. CV-315, km. 10,7, 46113, Moncada, Valencia (Spain).

Postharvest Biology and Technology, 118 (2016), 148-158

ABSTRACT

A non-destructive method based on external visible and near-infrared reflection spectroscopy for determining the internal quality of intact mango cv. 'Osteen' was investigated. An internal quality index, well correlated with the ripening index of the samples, was developed based on the combination of a biochemical property (total soluble solids) and physical properties (firmness and flesh colour) of mango samples. The diffuse reflectance spectra of the samples were recorded and used to predict the internal quality and the ripening index. These spectra were obtained using different spectroscopic external measurement sensors involving a spectrometer, capable of measuring in different spectral ranges (600-1100 nm and 900-1750 nm), and also a spectrocolorimeter that measured in the visible range (400-700 nm). Three regression models were developed by partial least squares to establish the relationship between spectra and indices. Good results in the prediction of internal quality of the samples were obtained using the full spectral range (R^2_p = 0.833-0.879, RMSEP = 0.403-0.507 and RPD = 2.341-2.826) and some selected wavelengths (R^2_p = 0.815-0.896, RMSEP = 0.403-0.537 and RPD = 2.060-2.905). The results obtained from this study revealed that external visible and near-infrared reflection spectroscopy can be used as a non-destructive method to determine the internal quality of mango cv. 'Osteen'.

Keywords: reflection spectroscopy, fruit, quality, chemometrics, non-destructive

1. INTRODUCTION

Spain is the main European producer of subtropical fruits, with approximately 1400 ha dedicated to mango (Galán & Farre, 2005). In particular, the south-west region has a large potential for the production of tropical and subtropical fruit, with a favourable year-round climate and infrequent frosts.

Mango fruit is sold in the market in quality categories. In the past, skin colour, fruit size and shape, freedom from defects and the absence of decay were the most common quality determinants, but nowadays other organoleptic characteristics related with internal and nutritional quality play an important role in the consumer's decision, as opposed to just appearance. The quality of mangoes changes almost daily and it is essential to correlate all the major quality parameters with one another in order to reveal the overall quality of the fruit (Jha *et al.*, 2011).

In a climacteric fruit, such as mango, the fruit is not considered to be of desired eating quality at the time it initially becomes mature. It requires a ripening period before it achieves the taste and texture desired at the time of consumption. The ripening process is regulated by genetic and biochemical events that result in biochemical changes such as the biosynthesis of carotenoids (Mercadante & Rodriguez-Amaya, 1998), loss of ascorbic acid (Hernández *et al.*, 2006), increase in total soluble solids (Padda *et al.*, 2011); physical changes such as weight, size, shape, firmness and colour (Ornelas-Paz *et al.*, 2008; Kienzle *et al.*, 2011); and changes in aroma, nutritional content and flavour of the fruit (Giovannoni, 2004). Traditional determination of the internal quality of mango requires a destructive methodology using specialised equipment, procedures and trained personnel, which results in high analysis costs and does not allow the whole production to be analysed (Torres *et al.*, 2013). Nevertheless, new technologies to monitor fruit quality changes during the postharvest handling chain are rapidly being introduced, especially those based on non-destructive assessment methods, recently reviewed by Jha *et al.* (2010) and Nicolaï *et al.* (2014). These fast and non-destructive methods can help to provide decisive parameters with which to obtain better quality mango products and to promote consumption of mangoes with better health benefits (Ibarra-Garza *et al.*, 2015).

Several non-destructive technologies have been widely explored to predict the quality and maturity of mango, such as nuclear magnetic resonance (NMR) (Gil

et al., 2000), impact response (Padda *et al.*, 2011; Wanitchang *et al.*, 2011), electronic nose (Lebrun *et al.*, 2008; Zakaria *et al.*, 2012), hyperspectral analysis (Vélez-Rivera *et al.*, 2014a), and near-infrared spectroscopy (Saranwong *et al.*, 2004). Conversely, some authors, such as Jha *et al.* (2005), have included in their studies the full visible spectrum using spectroscopy in intact mangoes, although studies using colour coordinates are more common, such as Jha *et al.* (2007), Subedi *et al.* (2007) or Rungpichayapichet *et al.* (2015).

Schmilovitch *et al.* (2000) studied the feasibility of near-infrared spectroscopy (NIRS) to determine the total soluble solids, firmness and acidity of mangoes cv. 'Tommy Atkins' in relation to the maturity stage. Nagle *et al.* (2010) developed a method to measure total soluble solids, total acidity and dry matter in mango cv. 'Chok Anan' on the trees using NIRS. Theanjumpol *et al.* (2013) studied the possibility of predicting six main chemical substances found in mango fruit cv. 'Keitt' and cv. 'Nam Dok Mai Si Thong', which are important in Thailand, such as glucose, sucrose, citric acid, malic acid, starch and cellulose. They used VIS/NIR spectrometry but decided not to use the visible information to avoid the influence of colour pigments. Jha *et al.* (2013) studied the properties of different mangoes that are important for the Indian production using NIRS in the 1200–2200 nm range to measure properties that make it possible to predict the maturity stage. They were able to predict the sweetness of the mangoes from measurements of total soluble solids and pH (Jha *et al.*, 2012) or to determine a maturity index based on the estimations of total soluble solids, dry matter and total acidity that was compared with destructive analysis and sensory panels, and corrected using a constant that depended on the cultivar (Jha *et al.*, 2014). Watanawan *et al.* (2014) studied the 700–1100 nm region in an attempt to correlate total soluble solids, total acidity and dry matter of mango cv. 'Namdokmai' with maturity in order to predict the optimum harvesting time. They found good correlations among NIRS values and firmness and dry matter content at harvest, and predicted TSS with very high accuracy, although they consider that their study needs to be revised in order to reduce the heterogeneity in fruit maturity and increase the outturn quality.

The main problem of using NIRS to assess fruit quality is the robustness of the calibration model (Rungpichayapichet *et al.*, 2016). Additionally, fruit cultivar, size, and harvest season also play an important role in the robustness of NIRS

models (Bobelyn *et al.*, 2010). In this study, a non-destructive method based on visible and near-infrared spectroscopy was investigated to determine the internal quality of mango cv. 'Osteen' during ripening because this is the main variety of mango grown in Spain. This variety could be included in the group of late-ripening mangoes, with higher weights and prices than other varieties of the same fruit. For this reason, this variety is considered to be optimal for export owing to its late maturing characteristics and final relatively low weight loss (Siller-Cepeda *et al.*, 2009).

Hence, the aims of this research were (a) to determine an internal quality index for mangoes, based on their main biochemical (total soluble solids) and physical properties (firmness and flesh colour), avoiding the titratable acidity analysis, because it is a laborious and slow analysis that generates waste, (b) to apply it to mango cv. 'Osteen', and (c) to develop statistical models based on Partial Least Squares (PLS) to predict the internal quality of the samples through the analysis of external VIS-NIR spectral data.

2. MATERIALS AND METHODS

2.1. Experimental procedure

A batch of 140 unripe mangoes (*Mangifera indica L.*, cv 'Osteen') were obtained from plantations in Málaga (Spain). The fruit selected were free of external damage or diseases, showing a uniform shape and size. All mangoes were washed and dried to completely remove any water from the surface and then were marked on each side. All sets were ripened in a storage chamber at 18.0 ± 2.1 ºC and 67.6 ± 3.3% RH. Sets of twenty mangoes were randomly collected and analysed every 2-3 days until reaching senescence (16 days).

The visible and near-infrared spectra of the external skin of each mango were measured on the centre of one cheek and two points on the other cheek (Figure 1) on each day of storage. After the measurements, the physical and biochemical properties were analysed.

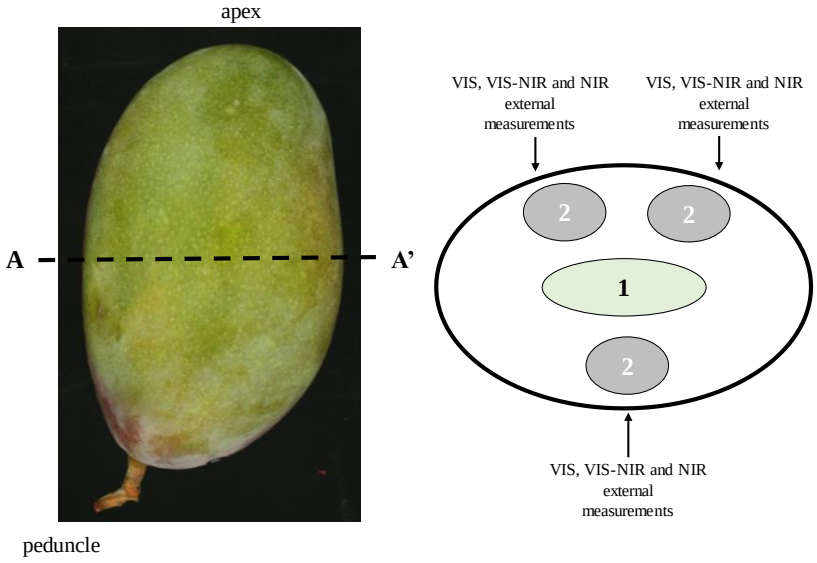

Figure 1. External reflection spectroscopy measurements in fruit slice AA' (1: seed; 2: penetrometer firmness and flesh colour measurement locations).

2.2. Visible and near-infrared spectra collection

The spectral characteristics of the external skin of the intact mangoes were measured in the visible and in the short and medium near-infrared range using a conventional spectrocolorimeter and a VIS-NIR spectrometer.

The external visible spectra of mango samples between 400 and 700 nm, every 10 nm, were measured using a spectrocolorimeter (CM-700d, Minolta Co., Tokyo, Japan). All the measurements were performed by placing the spectrocolorimeter directly onto the skin of the fruit.

The visible-near infrared and near-infrared spectra of mango samples were collected alternately in reflectance mode using a multichannel spectrometer platform (AVS-DESKTOP-USB2, Avantes BV, The Netherlands) equipped with two detectors (Figure 2). The first detector (AvaSpec-ULS2048 StarLine, Avantes BV, The Netherlands) included a 2048-pixel charge-coupled device (CCD) sensor (SONY ILX554, SONY Corp., Japan), 50 µm entrance slit and a 600 lines/mm diffraction grating covering the VIS-NIR range from 600 nm to 1100 nm with a

spectral FWHM (full width at half maximum) resolution of 1.15 nm. The spectral sampling interval was 0.255 nm. The second detector (AvaSpec-NIR256-1.7 NIRLine, Avantes BV, The Netherlands) was equipped with a 256 pixel non-cooled InGaAs (Indium Gallium Arsenide) sensor (Hamamatsu 92xx, Hamamatsu Photonics K.K., Japan), a 100 µm entrance slit and a 200 lines/mm diffraction grating covering the NIR range of 900 nm to 1750 nm and a spectral FWHM resolution of 12 nm. The spectral sampling interval was 3.535 nm. A Y-shaped fibre-optic reflectance probe (FCR-7IR200-2-45-ME, Avantes BV, The Netherlands) was configured with an illumination leg which connects the fibre coupled to a stabilised 10 W tungsten halogen light source (AvaLight-HAL-S, Avantes BV, The Netherlands). The light source ensures a permanent light intensity over the whole measurement range. A holder was used to position the sample properly over the probe and the reflectance probe delivered the light to the sample and collected the reflectance from the sample, which was carried by the fibre cable to the spectrometer in use. The reflectance probe, consisting of seven fibres with a diameter of 200 µm, delivered the light to the sample through a bundle of six fibres. The probe tip was designed to provide reflectance measurements at an angle of 45° so as to minimise specular reflectance from the surface of the fruit. The calibration was performed using a 99% reflective white reference tile (WS-2, Avantes BV, The Netherlands) so that the maximum reflectance value over the range of wavelengths was around 90% of saturation.

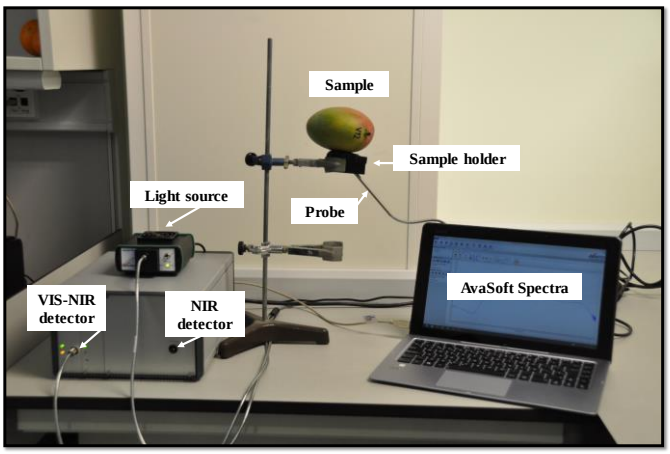

Figure 2. A labelled photograph of the VIS-NIR equipment.

Prior to spectral measurements, the temperature of the mangoes was stabilised at 24 ± 1 ºC. Measurements were taken at three longitudinal points over the surface of the fruit and mean values of the spectra were used for the analysis. A personal computer equipped with commercial software (AvaSoft version 7.2, Avantes, Inc.) was used to control both detectors and to acquire the spectra. The signals were pre-processed using AvaSoft software. The integration time was set to 90 ms for the detector sensitive in the VIS-NIR region and to 700 ms for the detector sensitive in the NIR region. For both detectors, each spectrum was obtained as the average of five scans to reduce the thermal noise of the detector (Nicolaï *et al.*, 2007). The average reflectance measurements of each sample (S) were then converted into relative reflectance values (R) with respect to the white reference using dark reflectance values (D) and the reflectance values of the white reference (W), as shown in equation 1:

$$R = \frac{S-D}{W-D} \quad (1)$$

The dark spectrum was obtained by turning off the light source and completely covering the tip of the reflectance probe.

2.3 Physical and biochemical analysis

The physical properties analysed were firmness, peel colour and flesh colour of the mangoes. The firmness, in Newtons, was analysed through a puncture test by using a universal test machine (TextureAnalyser-XT2, Stable MicroSystems (SMS) Haslemere, England). The tests were performed in triplicate in the axial direction at three locations in the equatorial section (Figure 1 (b)) with a punch with a diameter of 6 mm (P/15ANAMEsignature) until a relative deformation of 30%, at a speed of 1 mm/s.

CIE (Internationale de l'éclairage) colour values of Luminosity (L^*), chromaticity (C_{ab}^*) and hue angle (h_{ab}^*) for each fruit on both peel (external colour) and flesh (internal colour) were determined using the spectrocolorimeter. The standard illuminant D65 and the 10º standard observer were used for all colour measurements in the study. The colour values were averaged from three different measurements taken at three points on the fruit in order to have representative

values. The biochemical properties analysed were the total soluble solids (TSS) and the titratable acidity (TA). TSS content was determined by refractometry (ºBrix) with a digital refractometer (set RFM330+, VWR International Eurolab S.L., Barcelona, Spain) at 20 °C and with a sensitivity of ±0.1 ºBrix. The analysis of TA was performed with an automatic titrator (CRISON, pH-burette 24, Barcelona, Spain) with 0.5 N NaOH until a pH of 8.1 (UNE34211:1981), using 15 g of crushed mango which was diluted in 60 mL of distilled water. The TA was determined based on the percentage of citric acid that was calculated using equation 2.

$$TA\ [g\ citric\ acid/100g\ of\ the\ sample]=((A\times B\times C/D)\times 100))/E \quad (2)$$

where A is the volume of NaOH consumed in the titration (in L), B is the normality of NaOH (0.5 N), C is the molecular weight of citric acid (192.1g/mol), D is the weight of the sample (15 g) and E is the valence of citric acid (E = 3).

Two indices, a ripening index (RPI) and an internal quality index (IQI) were calculated by equations 3 and 4. The RPI was described previously by Vásquez-Caicedo *et al.* (2005) and Vélez-Rivera *et al.* (2014b). However, titratable acidity analysis is complex, laborious, slow and generates waste. Furthermore, the colour has previously been proved to be a quality indicator of mango (Jha *et al.*, 2006a and 2006b). In Jha *et al.* (2007) colour parameters were highly correlated with TSS through the creation of several models based on the CIELAB coordinates. From these studies, the IQI was calculated combining TSS, firmness, and flesh colour. These parameters have been used in packing houses to measure the quality of mangoes. They require less time, less pretreatment of the sample and lower costs.

$$RPI = \ln(100 \cdot F \cdot TA \cdot TSS^{-1}) \quad (3)$$

$$IQI = \ln(100 \cdot F \cdot L^{*} \cdot h_{ab}^{*} \cdot TSS^{-1} \cdot C_{ab}^{*-1}) \quad (4)$$

where F is firmness (Newtons), TA is titratable acidity (g citric acid equivalent/100 g sample), TSS is total soluble solids (°Brix) and L^*, h^*_{ab} and C^*_{ab} are the colour attributes of the flesh colour.

2.4. Statistical analysis

The spectroscopic data and both indices were organised into three different matrices: the first matrix for the visible spectra (400-700 nm), the second matrix for the VIS-NIR spectra (600-1100 nm) and the third matrix for the NIR spectra (900-1750 nm). In all the matrices, the rows represent the number of samples (#N = 140 samples) and the columns represent the number of variables (X-variables and Y-variables). The X-variables, or predictors, were the different spectra and the Y-variables, or responses, were the two variables provided by RPI and IQI. All the matrices were analysed using The Unscrambler Version 9.7 software package (CAMO Software AS, Oslo, Norway). First, all the spectral data were pre-processed. The X-variables were transformed to apparent absorbance (log (1/R)) values to obtain linear correlations of the NIR values with the concentration of the estimated constituents (Shao *et al.*, 2007; Liu *et al.*, 2010) and centred by subtracting their averages in order to ensure that all results will be interpretable in terms of variation around the mean. Due to the high resolution causing an increased occurrence of signal noise by its spectral range measurement, the VIS-NIR spectra were reduced using a reduction factor of 7. In order to reduce the influence of light scattering (Santos *et al.*, 2013) and the baseline drift various pre-processing methods were applied to the spectra. Savitzky-Golay smoothing with a gap of three data points combined with extended multiplicative scatter correction (EMSC) were considered the best results for the VIS-NIR spectra, and those two pretreatments and second derivative with Gap-Segment (2.3) were the best results for the NIR spectra. After the pre-processing steps, the X-variables in the matrices were 31, 285 and 242 for the visible spectrum, VIS-NIR spectrum and NIR spectrum, respectively.

Secondly, each set was divided randomly into two groups, a calibration set (75% of the samples) and a prediction set (25% of the samples). Partial least squares regression (PLS) was applied to the matrix to construct separate calibration models for each ripening index and each spectrum with segments of 20 objects

(Næs *et al.*, 2004) and it was evaluated by means of a cross validation methodology. PLS defines the latent variables (principal components) based on the covariance between the independent and dependent variables, the advantage of PLS regression being its ability to analyse data with many, noisy, collinear, and even incomplete variables in both X and Y (Næs *et al.*, 2004). This technique has usually been used in multivariate calibration in fruit applications (Liu *et al.*, 2010) and allows obtaining the best results when linear relations between spectra and properties of samples exist (Li *et al.*, 2010). Liu *et al.* (2008) used the MLR technique based on the regression of the discrete parts of the spectra and PLS based on the full spectrum; the results of the two techniques in their study appeared to be very similar.

In order to reduce the high dimensionality of the spectral data, to avoid the presence of noise or information that is not related to the quality characteristics of the mango, and to make the PLS models more robust, the most important wavelengths to predict both indices were selected (ElMasry *et al.*, 2007; Talens *et al.*, 2013). For each calibration model, the weighted regression coefficients resulting from the PLS models were used to select the important wavelengths. Regression coefficients show the weight of the contribution of each wavelength to the calibration model and eliminate the spectral regions with less contribution. Standardised spectral data were used to develop the PLS models to obtain the weighted regression coefficients.

The relative performance of the constructed models was assessed by the required number of latent variables (LVs), the coefficient of determination for calibration (R_C^2), the root mean square error of calibration (RMSEC) and the root mean square error of leave-one-out cross-validation (RMSECV). A model can be considered good when a low number of LVs are required and it has a low RMSEC and RMSECV and high R_C^2. The predictive ability of the models was evaluated using the coefficient of determination for prediction (R_P^2), the root mean square error of prediction (RMSEP) and the ratio of prediction to deviation (RPD=SD/RMSEP), where the SD was the standard deviation of the Y-variable in the prediction set. A value below 1.5 for the RPD indicates that the calibration is not usable. A value between 1.5 and 2.0 for the RPD reveals a possibility to distinguish between high and low values, while a value between 2.0 and 2.5 makes

approximate quantitative predictions possible. For values between 2.5 and 3.0, and above 3.0, the prediction is considered to be good and excellent, respectively (Williams & Sobering, 1993; Saeys *et al.*, 2005; Cozzolino *et al.*, 2011). R_C^2 measured the performance of a multivariate calibration model and can be defined as the following equations 5 and 6 (Yahaya *et al.*, 2015):

$$RMSEC = \sqrt{\frac{1}{n_v}\sum_{i=1}^{n_c}(\hat{y}_i - y_i)^2} \quad (5)$$

$$RMSECV, RMSEP = \sqrt{\frac{1}{n_p}\sum_{i=1}^{n_p}(\hat{y}_i - y_i)^2} \quad (6)$$

where:

$\hat{y}_i$ is the predicted value of the ith observation

y_i is the measured value of the ith observation

n_c is the number of observations in the calibration set

n_p is the number of observations in the validated set

3. RESULTS AND DISCUSSION

3.1. Changes in mango quality during ripening

Table 1 shows the range (minimum and maximum values), mean and standard deviation of the quality parameters analysed in the mango samples (#N = 140 samples).

Table 1. Descriptive statistics for the quality parameters analysed in the mango samples.

Mango	Weight (g)	Diameter (mm)	Lenght (mm)	TSS	TA (g/100g)	Firmness (N)	L^*_{ext}	C^*_{ext}	h^*_{ext}	L^*_{int}	C^*_{int}	h^*_{int}
Min	402	78.2	113	5.8	0.07	11.8	32.0	34.5	14.0	56.3	8.6	70.4
Max	506.4	87.4	141	20.7	0.98	124.3	56.5	65.0	94.2	81.8	46.8	86.1
Mean	445.5	82.3	128.8	13.4	0.47	76.1	43.1	53.0	47.2	72.7	25.2	78.7
Sdev	23.5	1.7	5.5	3.5	0.22	35.8	4.7	6.3	18.3	6.4	9.1	4.0

The firmness ranged from 124.3 to 11.8 N. The peel luminosity, peel chroma and peel hue ranged from 32, 34.5, 14 to 56.5, 65, 94.2, respectively, whereas flesh luminosity, flesh chroma and flesh hue ranged from 56.3, 8.6, 70.4 to 81.8, 46.8 and 86.1, respectively. The ºBrix and the titratable acidity ranged from 5.85 to

19.50 ºBrix and 0.97 to 0.07 g citric acid/100 g of sample, respectively. Similar values were observed by other authors during the ripening process of mangoes, working with other mango varieties such as 'Alphonso' (Yashoda *et al.*, 2007), 'Tommy Atkins' (Lucena *et al.*, 2007), 'Nam Dokmai' and 'Irwin' (Fukuda *et al.*, 2014).

Table 2 shows the Pearson correlation coefficients and was calculated to check for significant inter-correlations between the parameters analysed in mango samples. The results indicated that, in general, peel/external colour showed lower correlations with respect to the other physical and biochemical properties, whereas higher correlations were found between firmness, flesh/internal colour and the biochemical properties. Positive correlations were found between firmness and internal L^* (0.93), internal h_{ab}^* (0.88) and TA (0.63), and negative correlations were found between firmness and internal C_{ab}^* (-0.78) and TSS (0.79).

Table 2. Pearson correlation coefficients between quality parameters analysed in mango samples.

	Weight (g)	*Diameter (mm)*	*Lenght (mm)*	*TSS*	*TA (g/100g)*	*Firmness (N)*	*L*ext*	*C* ext*	*h*ext*	*L* Int*	*C*int*	*h* Int*	*RPI*	*IQI*
Weight (g)	1													
Diameter (mm)	0.55	1												
Lenght (mm)	0.41	-0.11	1											
TSS	-0.21	0.01	0.02	1										
TA (g/100g)	0.29	0.08	-0.01	-0.36	1									
Firmness (N)	0.30	0.01	-0.01	-0.79	0.63	1								
L*ext	-0.05	-0.02	-0.02	0.16	-0.10	-0.23	1							
C* ext	-0.33	-0.05	-0.12	0.64	-0.52	-0.78	0.15	1						
h*ext	0.08	0.01	0.11	-0.06	0.20	0.08	0.62	-0.21	1					
L* Int	0.29	-0.04	0.07	-0.83	0.55	0.93	-0.22	-0.77	0.09	1				
C*int	-0.25	0.03	0.08	0.67	-0.59	-0.75	0.46	0.58	0.15	-0.72	1			
h* Int	0.30	0.00	0.09	-0.81	0.54	0.88	-0.16	-0.84	0.22	0.94	-0.67	1		
RPI	0.33	0.04	-0.01	-0.76	0.82	0.92	-0.19	-0.72	0.12	0.89	-0.77	0.83	1	
IQI	0.31	0.01	-0.03	-0.87	0.63	0.95	-0.29	-0.75	0.02	0.94	-0.87	0.89	0.94	1

Figure 3 shows the changes in firmness, peel and flesh colour, TA and TSS of mangoes at different days of storage. As expected, firmness values of 'Osteen' mangoes decrease constantly during ripening. At the beginning of the process, the firmness remained fairly constant, although a pronounced decrease in the firmness values was observed from 11 to 16 days of storage, the loss of firmness on the last day of storage being around 75% of the firmness recorded at the beginning of the study. A similar behaviour has been reported for other mango varieties such as

'Alphonso' (Yashoda *et al.*, 2005), 'Ataulfo' (Palafox-Carlos *et al.*, 2012) or 'Keitt' (Ibarra-Garza *et al.*, 2015). These changes can be attributed to different factors, such as the enzymatic activity (Prasanna *et al.*, 2007; Yashoda *et al.*, 2007) and/or the solubilisation, de-esterification, and de-polymerisation of the middle lamella, accompanied by an extensive loss of neutral sugars and galacturonic acid (Singh *et al.*, 2013), which modify the structural integrity of the cell wall and middle lamella.

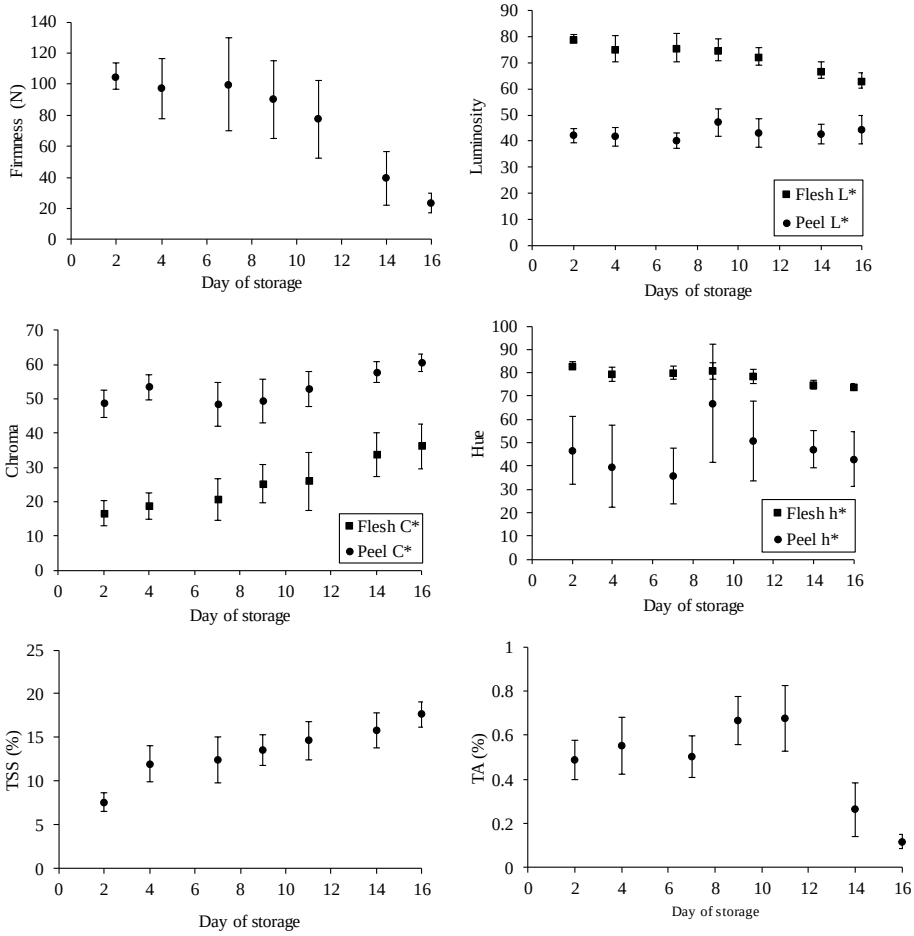

Figure 3. Firmness, peel colour, flesh colour, TSS and TA of mangoes at different days of analysis.

The changes in peel/external and flesh/internal colour observed during the ripening of mangoes cv. 'Osteen' are also shown in Figures 3 and 4. Whereas flesh luminosity and flesh hue values decreased from 79º to 63º and from 83º to 74º, respectively, and flesh chroma values increased from 16 to 36, no clear changes in peel luminosity and peel hue values and small differences in peel chroma values could be observed, which is logical since the colour of the peel is heterogeneous and varies from one sample to another. In general, the peel colour changes were not uniform, indicating that peel colour is not an adequate quality parameter for cv. 'Osteen' mango cultivars.

However, flesh colour changes were uniform when fruit advances in ripening and can serve as an adequate quality parameter (Figures 3 and 4). The increase in the yellow-orange intensity of mango flesh can be associated with an increase in carotenoid content of mango fruit, as has been reported previously by other authors (Ornelas-Paz *et al.*, 2008; Ibarra-Garza *et al.*, 2015). This change is accompanied by a decrease in the L^* value, although, despite the correlation, there is no evidence that the changes in the luminosity of the flesh (L^*) are actually due to the increase in carotenoids.

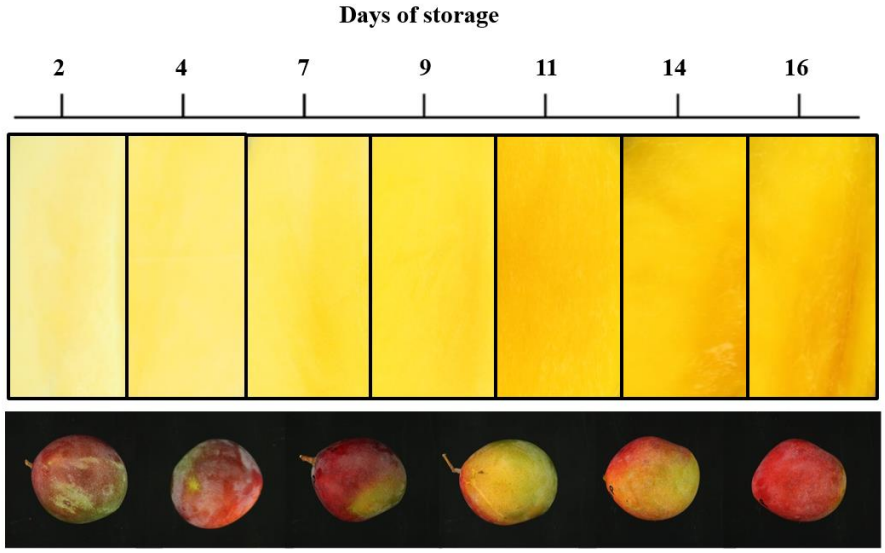

Figure 4. External appearance and flesh colour of mango cv. 'Osteen' at different days of storage.

Loss of firmness and changes in flesh colour correlate with the increase of the TSS ratio and decrease of TA (Figure 3). During ripening the TSS increased due to the conversion of starch into glucose and fructose, which are used as substrates during fruit respiration (Eskin *et al.*, 2013), while the TA tends to decrease due to the cell metabolisation of volatile organic acids and non-volatile constituents (Padda *et al.*, 2011).

Taking into account the strong correlation found between the biochemical properties (TSS and TA) and the firmness and flesh colour (Table 2), two indices were calculated. The ripening index, RPI, involves the most essential physical and biochemical properties of the fruit linked with the sensory perception of the ripeness of the mangoes. The internal quality index, IQI, was calculated because it is a good indicator to assess changes in the mesocarp during the ripening of mangoes. In fact, firmness, total soluble solids and flesh/internal colour are the three parameters used in mango packing-lines to assess mango quality and stage of ripeness (Brecht *et al.*, 2010), whereas the TA is more difficult and laborious to determine. Table 2 shows the Pearson correlation coefficient between the two indices, with higher positive correlations (0.94). Figure 4 shows the changes in the RPI and IQI indices calculated for the mangoes at different days of storage. In both cases, it can be observed that the values of the indices decreased during ripening. Based on previous studies working with RPI in mango cv. 'Manila' (Vélez-Rivera *et al.*, 2014b) and comparing the values of this study, three ripeness phases were identified: unripe mangoes (values higher than 6, day 2), intermediate-ripe mangoes (values between 6 and 4, days 4 to 11) and over-ripe mangoes (values less than 4, days 14 to 16), the intermediate-ripe mangoes being the mangoes with the best quality.

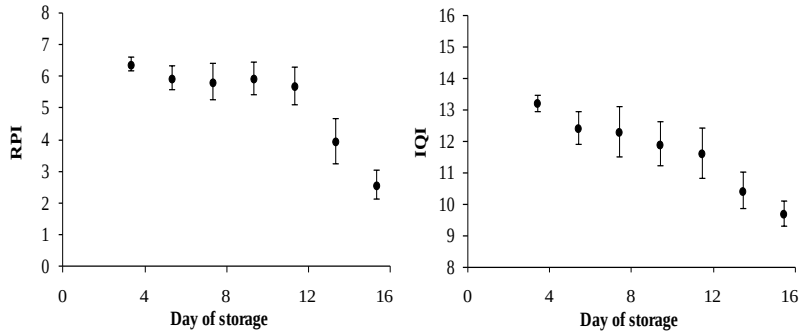

Figure 5. RPI and IQI of mangoes at different days of storage.

3.2. Analysis of visible and near-infrared spectra.

When assessing ripening with a visible and/or near-infrared spectroscope, it is crucial to identify the spectral changes associated with pigment evolution and compositional changes. Typical apparent absorbance spectral of mangoes at different ripening stages for the visible region, the VIS-NIR and the NIR regions are shown in Figure 6.

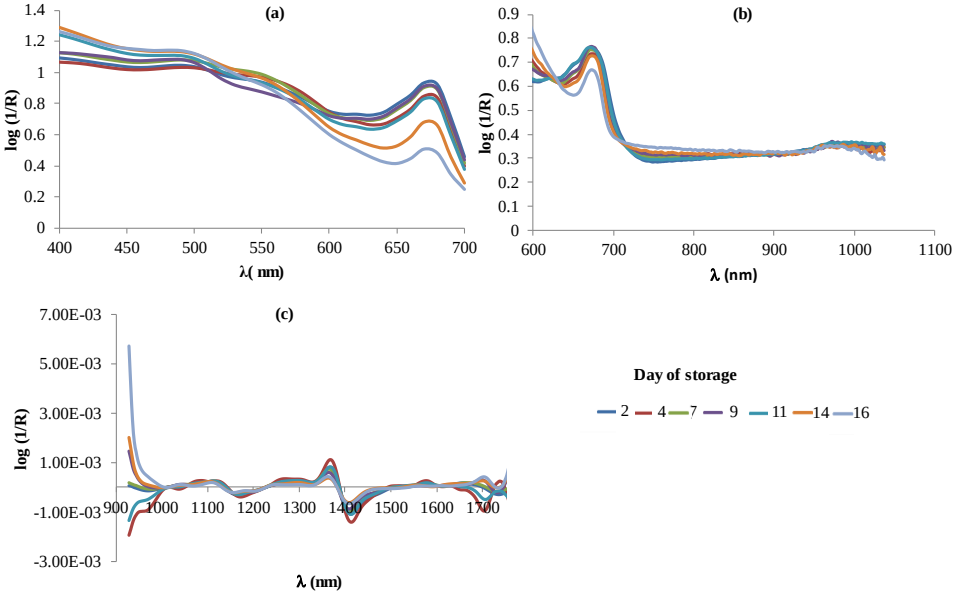

Figure 6. Apparent absorbance spectra of mangoes at different ripening stages for the (a) visible region, (b) the VIS-NIR region and (c) the NIR region after pretreatments.

All the spectra have a similar pattern with the main maxima located in the visible and near-infrared region, which showed the strong absorbance characteristics of the mangoes within the range of study. In the visible range, the light peaks around 400-500 nm are correlated with the carotenoid pigments (Lichtenthaler & Buschmann, 2001) and the peak around 640-700 nm illustrated the colour transition of mangoes correlated with the chlorophyll content that absorbs radiation in this region (Merzlyak *et al.*, 2003). Similarly, Knee (1980) and Bodria *et al.* (2004) analysed apples and claimed that their reflectance minimum in the 670 nm to 680 nm range was strongly related to chlorophyll content. Therefore, the ripening process of the fruit, with changes in chlorophyll, carotenoid and anthocyanin contents, indicated the influence of pigment content and composition on the colouration of the entire spectral visible reflectance of the fruit (Yahaya *et al.*, 2014; Omar, 2013). This view is supported by the study of Magwaza *et al.* (2012), who described the pattern of the absorption curves for Satsuma mandarin, which is similar to that for other fruit like mangoes and kiwis. On the other hand, the water peaks were recorded at around 950-1050 nm and 1350-1550 nm due to the second overtone of the OH stretching band (Büning-Pfaue, 2003), and the variations at 1100-1250 nm are correlated with the sugar content (Osborne *et al.*, 1993; Walsh *et al.*, 2004). Figure 5a and 5b shows an increase in absorbance within the blue region during ripening, mainly linked to an increase in the carotenoids content, and a decreased absorbance in the red region, mainly linked to a decrease in the chlorophyll content. Merzlyak *et al.* (2003) suggested that carotenoid synthesis is induced when chlorophyll degradation occurs during fruit ripening and senescence. Also during ripening, an increase in TSS is produced and could be mainly due to hydrolysis of starch into soluble sugars such as sucrose, glucose and fructose (Agravante *et al.*, 1990; Cordenunsi & Lajolo, 1995).

3.3. Non-destructive prediction of mango quality

Multivariate analysis was performed in order to establish the quantitative relationship between the absorbance spectra and the internal quality of mango. The full range spectra for the three regions studied were used to establish calibration models based on PLS to explain RPI and IQI. The performance of the calibration

models was optimised by internal cross-validation and then validated by external validation in an independent validation set.

Table 3 and Table 4 show the results obtained for the calibration and cross-validation sets for the three models developed. Similar results on the calibration and cross-validation sets were obtained to predict RPI and IQI using the VIS, VIS-NIR or NIR detector. The models were very accurate with high R_C^2 (0.902-0.934) and R_{CV}^2 (0.831-0.903), while RMSEC (0.335-0.509) and RMSECV (0.395-0.546) were low. The models applied to the independent validation set were capable of predicting RPI with R_P^2 of 0.871, 0.902 and 0.845, and RMSEP of 0.520, 0.470 and 0.592, respectively, for the three spectral regions. On the other hand, the results achieved for the IQI were R_P^2 of 0.879, 0.877 and 0.833, and RMSEP of 0.464, 0.435 and 0.507, respectively, for the VIS, VIS-NIR and NIR detector. Although better results were obtained when visible information was used, the models developed using the VIS/NIR and NIR spectra also presented high values of R_P^2 and low values of RMSEP.

Table 3. Results of the PLS models for the calibration and prediction of RPI in mango samples by using the full spectral range and the important wavelengths.

DETECTOR	#W	#LV	CALIBRATION		CROSS VALIDATION		PREDICTION		
			R_C^2	RMSEC	R_{CV}^2	RMSECV	R_P^2	RMSEP	RPD
VIS	31	6	0.907	0.415	0.886	0.463	0.871	0.520	2.916
	5	4	0.893	0.445	0.882	0.471	0.871	0.520	2.827
VIS-NIR	285	8	0.934	0.335	0.902	0.412	0.902	0.470	2.767
	6	6	0.847	0.509	0.827	0.546	0.795	0.548	2.373
NIR	242	10	0.922	0.364	0.868	0.478	0.845	0.592	2.340
	9	5	0.853	0.499	0.830	0.542	0.831	0.613	2.259

Table 4. Results of the PLS models for the calibration and prediction of IQI in mango samples by using the full spectral range and the important wavelengths.

DETECTOR	#W	#LV	CALIBRATION		CROSS VALIDATION		PREDICTION		
			R_C^2	RMSEC	R_{CV}^2	RMSECV	R_P^2	RMSEP	RPD
VIS	31	6	0.916	0.363	0.903	0.395	0.879	0.464	2.826
	5	4	0.881	0.433	0.871	0.455	0.838	0.537	2.522
VIS-NIR	285	4	0.905	0.389	0.891	0.421	0.877	0.435	2.691
	5	5	0.827	0.525	0.796	0.575	0.896	0.403	2.905
NIR	242	10	0.902	0.394	0.831	0.523	0.833	0.507	2.341
	7	5	0.841	0.503	0.820	0.540	0.815	0.531	2.060

The RPD values of the resulting models gave the relative predictive performance of the model more directly in comparison to either R^2 or RMSEP used alone. In this study, the RPD values obtained were 2.916, 2.767 and 2.340 for RPI and 2.826, 2.691 and 2.341 for IQI for the VIS, VIS-NIR and NIR detectors, respectively. In all cases they are high values indicating a greater ability of the models to accurately predict the internal ripeness of the mango in new samples.

Figure 7 shows the regression coefficient plots with the important wavelengths for RPI and IQI for each spectral range. These wavelengths corresponded to -H and -OH functional groups, which are related to carbohydrates (namely sugars and starches), organic acids and water (Rungpichayapichet *et al.*, 2016).

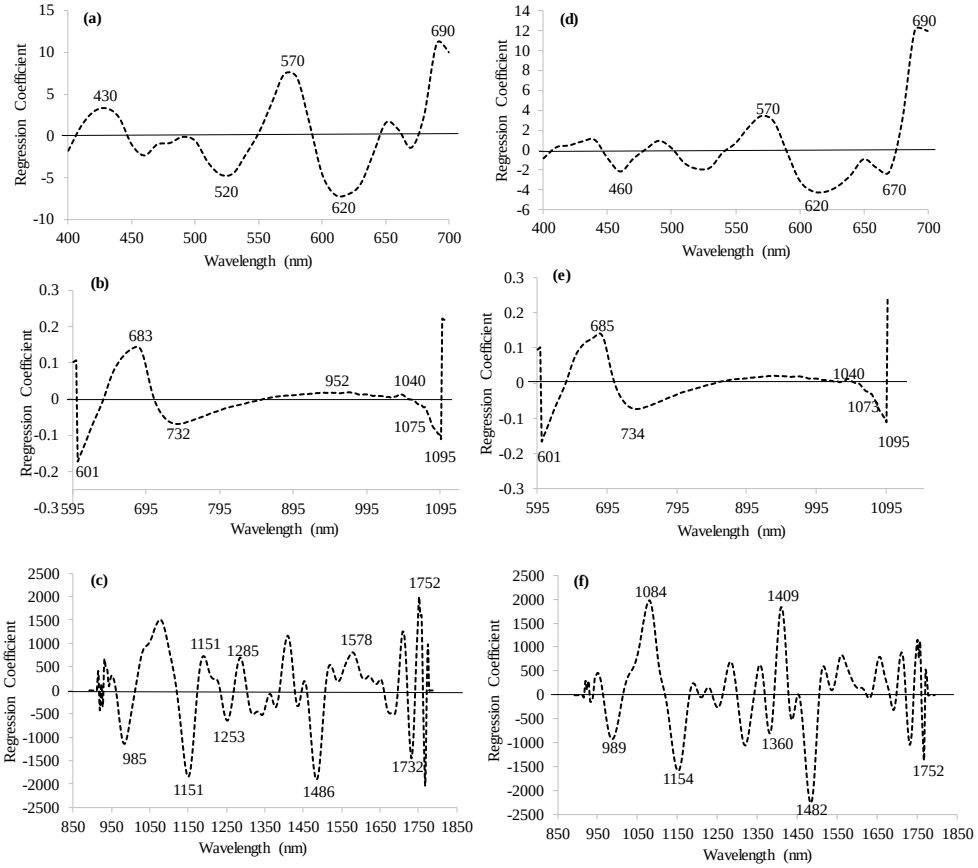

Figure 7. Regression coefficient plot of PLS calibration models developed from overall data for RPI (a, b and c) and IQI (d, e and f) for each spectral range.

After identifying the optimal wavelengths, the reduced sets of bands were used to build new PLS models using the absorbance at these particular wavelengths as independent variables, and the measured values of RPI and IQI as dependent variables. Figure 8 shows the efficiency of PLS models for this prediction, indicating that it is possible to use a reduced number of bands in the visible and near-infrared region to predict the internal quality of mango 'Osteen'.

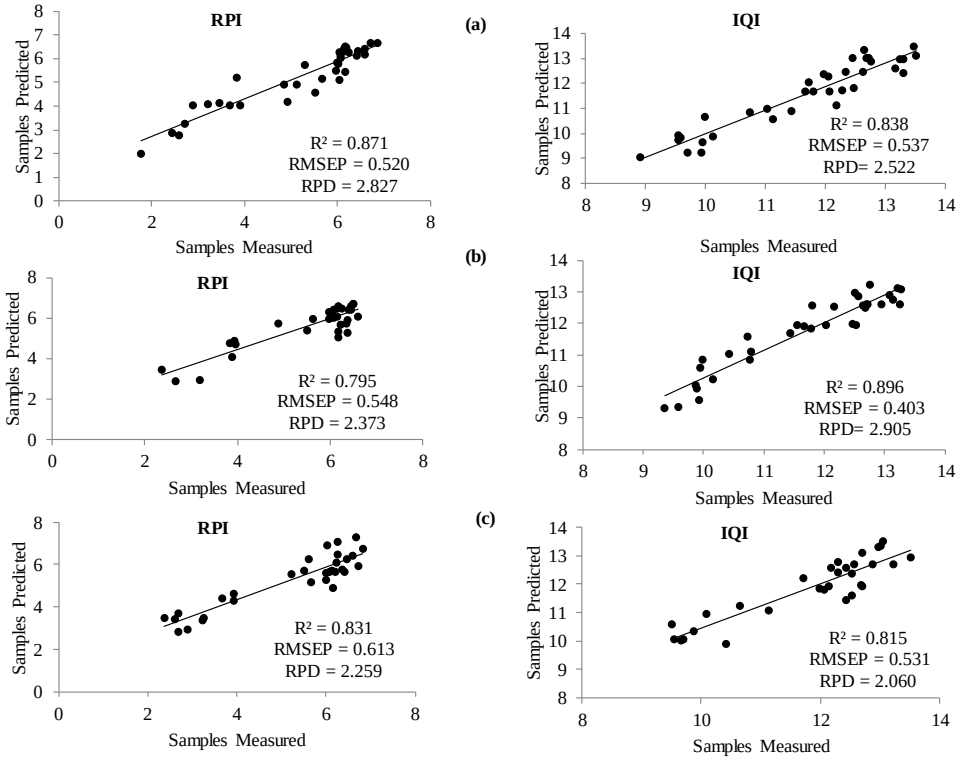

Figure 8. Predicted versus measured values of RPI and IQI for the visible region (a), the visible-near infrared region (b) and near-infrared region (c).

The feasibility of VIS-NIR to predict RPI of mango was indicated by an Rp2 between 0.795-0.871, RMSEP of 0.520-.613 and RPD of 2.259-2.827 (Figure 8). The results corroborated other studies on the use of spectroscopy techniques to predict RPI, such as Mahayothee (2005), with R^2 of 0.8 and SEP of 0.9, or Rungpichayapichet *et al.* (2016) with $R^2 > 0.8$ and SEP > 0.8 for 'Nam Dokmai' mangoes. Other indices that have been developed, for example, Jha *et al.* (2007), predicted the maturity index (I_m) using colour values with a correlation of 0.92 and SEP of 10.72 for mango cv. 'Dashehari'. Likewise, IQI has been identified as a quality indicator for mango cv. 'Osteen', and in this study R_p^2, RMSEP and RPD values were between 0.815-0.896, 0.403-0.537 and 2.060-2.905 respectively. As shown in Table 3 and Table 4, the PLS models created from the selected wavelengths reduced the number of latent variables while maintaining a similar

performance to PLS models created with the full spectrum. Likewise, their calibration and prediction errors do not worsen and both indices remain the same range in mango samples.

4. CONCLUSIONS

The internal quality of intact mango 'Osteen' fruit has been assessed using external visible and near-infrared reflection spectroscopy. In order to assess the internal quality of the fruit, two indices have been used, the ripening index (RPI) and the internal quality index (IQI). Different spectroscopy systems were used to measure different spectral ranges (VIS, VIS-NIR and NIR) externally in reflectance mode. The partial least squares regression analysis showed a strong performance in predicting RPI and IQI for the VIS, VIS-NIR and NIR detectors using the full spectral range and the most important wavelengths. However, accuracy may be compromised when the measuring is being implemented on samples with different external geometry by two spectroscopy systems that are structured differently in terms of their optical-electronics configuration within the spectrometer or in their interfacing with the sample. Nevertheless, the results obtained from this study clearly reveal that external visible and near-infrared spectroscopy combined with chemometrics can be used for the non-destructive prediction of the internal quality of mango 'Osteen'. This technological development could even be integrated in continuous fruit packing lines as part of the quality assurance system.

Acknowledgements

This work was partially funded by the Conselleria d' Educació, Investigació, Cultura i Esport, Generalitat Valenciana, through the project AICO/2015/122 and by the INIA through the projects RTA2012-00062-C04-01, 02 and 03 with the support of FEDER funds. V. Cortés López thanks the Spanish MEC for the FPU grant (FPU13/04202).

5. REFERENCES

AENOR, 1981. Productos derivados de frutas y verduras, determinación de la acidez valorable. UNE 34211:1981.

Agravante, J.U., Matsui, T. & Kitagawa, H. (1990). Starch breakdown in ethylene and ethanol treated bananas: changes in phosphorylase and invertase activities during ripening. Journal of the Japanese Society for Food Science and Technology, 37(11), 911-915.

Bobelyn, E., Serban, A.S., Nicu, M., Lammertyn, J., Nicolai, B.M. & Saeys, W. (2010). Postharvest quality of apple predicted by NIR-spectroscopy: Study of the effect of biological variability on spectra and model performance. Postharvest Biology and Technology, 55, 133-143.

Bodria, L., Fiala, M., Guidetti, R. & Oberti, R. (2004). Optical techniques to estimates the ripeness of red-pigmented fruits. Transactions of the ASAE, 47, 815.

Brecht, J., Sargent, S., Kader, A., Mitcham, E., Maul, F., Brecht, P., & Menocal, O. (2010). Mango Postharvest Best Management Practices Manual. Gainesville: Univ. of Fla., Horticultural Sciences Department, 78.

Büning-Pfaue, H. (2003). Analysis of water in food by near infrared spectroscopy. Food Chemistry, 82, 107-115.

Cordenunsi, B.R. & Lajolo, F.M. (1995). Starch breakdown during banana ripening: sucrose synthase and sucrose phosphate syntase behavior. Journal Agricultural Food Chemistry, 43, 347-351.

Cozzolino, D., Cynkar, W.U., Shah, N. & Smith, P. (2011). Multivariate data analysis applied to spectroscopy: Potential application to juice and fruit quality. Food Research International, 44(7), 1888-1896.

ElMasry, G., Wang, N., ElSayed, A. & Ngadi, M. (2007). Hyperspectral imaging for nondestructive determination of some quality attributes for strawberry. Journal of Food Engineering, 81(1), 98-107.

Eskin, N.A.M., Hoehn, E. & Shahidi, F. (2013). Fruits and vegetables. Eskin, N.A.M., Shahidi, F. (Eds.), Biochemistry of foods, 49-126.

Fukuda, S., Yasunaga, E., Nagle, M., Yuge, K., Sardsud, V., Spreer, W. & Müller, J. (2014). Modelling the relationship between peel colour and the quality of

fresh mango fruit using Random Forests. Journal of Food Engineering, 131, 7-17.

Galán, S.V. & Farré, M.J.M. (2005). Tropical and Subtropical Fruits in Spain. Acta Horticulturae, 694, 259-264.

Gil, A., Duarte, I., Delgadillo, I., Colquhoun, I., Casuscelli, F., Humpfer, E. & Spraul, M. (2000). Study of the Compositional Changes of Mango during Ripening by Use of Nuclear Magnetic Resonance Spectroscopy. Journal of Agricultural and Food Chemistry, 48(5), 1524-1536.

Giovannoni, J.J. (2004). Genetic regulation of fruit development and ripening. Plant Cell, 16, 170-180.

Hernández, Y., Lobo, M.G. & González, M. (2006). Determination of vitamin C in tropical fruits: A comparative evaluation of methods. Food Chemistry, 96(4), 654-664.

Ibarra-Garza, I.P., Ramos-Parra, P.A., Hernández-Brenes, C. & Jacobo-Velázquez, D.A. (2015). Effects of postharvest ripening on the nutraceutical and physicochemical properties of mango (*Mangifera indica L.* cv. Keitt). Postharvest Biology and Technology, 103, 45-54.

Jha, S.N., Chopra, S. & Kingsly, A.R.P. (2005). Determination of Sweetness of Intact mango using Visual Spectral Analysis. Biosystems Engineering, 91 (2), 157-161.

Jha, S.N., Kingsly, A.R.P. & Chopra, S. (2006a). Physical and mechanical properties of mango during growth and storage for determination of maturity. Journal of Food Engineering, 72(1), 73-76.

Jha, S.N., Kingsly A.R.P. & Chopra S. (2006b). Nondestructive determination of firmness and yellowness of mango during growth and storage using visual spectroscopy. Biosystems Engineering, 94(3), 397-402.

Jha, S.N., Chopra, S. & Kingsly, A.R.P. (2007). Modeling of color values for nondestructive evaluation of maturity of mango. Journal of Food Engineering, 78, 22-26.

Jha, S.N., Narsaiah, K., Sharma, A.D., Manpreet, S., Sunil, B. & Kumar, R. (2010). Quality parameters of mango and potential of non-destructive techniques for their measurement – a Review. Journal of Food Science and Technology, 47(1), 1-14. 4.

Jha, S.N., Jaiswal, P., Narsaiah, K., Singh, A.K., Kaur, P.P., Sharma, R., Kumar, R. & Bhardwaj, R. (2011). Prediction of Sensory Profile of Mango Using Textural Attributes During Ripening. Food and Bioprocess Technology, 6, 734-745.

Jha, S.N., Jaiswal, P., Narsaiah, K., Gupta, M., Bhardwaj, R. & Singh, A.K. (2012). Non-destructive prediction of sweetness of intact mango using near infrared spectroscopy. Scientia Horticulturae, 138, 171-175.

Jha, S.N., Jaiswal, P., Narsaiah, K., Sharma, R., Bhardwaj, R., Gupta, M. & Kumar, R. (2013). Authentication of mango varieties using near infrared spectroscopy. Agricultural Research, 2(3), 229-235.

Jha, S.N., Narsaiah, K., Jaiswal, P., Bhardwaj, R., Gupta, M., Kumar, R. & Sharma, R. (2014). Nondestructive prediction of maturity of mango using near infrared spectroscopy. Journal of Food Engineering, 124, 152-157.

Kienzle, S., Sruamsiri, P., Carle, R., Sirisakulwat, S., Spreer, W. & Neidhart, S. (2011). Harvest maturity specification for mango fruit (Mangiferaindica L. 'Chok Anan') in regard to long supply chains. Postharvest Biology and Technology, 61, 41-55.

Knee, M. (1980). Methods of measuring green colour and chlorophyll content of apple fruit. Journal Food Technology, 15, 493.

Lebrun, M., Plotto, A., Goodner, K., Ducamp, M. & Baldwin, E. (2008). Discrimination of mango fruit maturity by volatiles using the electronic nose and gas chromatography. Postharvest Biology and Technology, 48(1), 122-131.

Lichtenthaler, H.K. & Buschmann, C. (2001). Chlorophylls and Carotenoids: Measurement and Characterization by UV-VIS Spectroscopy. Current Protocols in Food Analytical Chemistry, F:F4:F4.3.

Liu, Y., Chen, X. & Ouyang, A. (2008). Nondestructive determination of per internal quality indices by visible and near-infrared spectrometry. LWT- Food Science and Technology, 41, 1720-1725.

Liu, Y., Sun, X. & Ouyang, A. (2010). Nondestructive measurement of soluble solid content of navel orange fruit by visible–NIR spectrometric technique with PLSR and PCA-BPNN. Food Science and Technology, 43(4), 602-607.

Lucena, E., Simão de Assis, J., Alves, R., Macêdo da Silva, V. & Filho, J. (2007). Alterações físicas e químicas durante o desenvolvimento de mangas 'Tommy Atkins' no vale de São Francisco, Petrolina-PE. Revista Brasileira de Fruticultura [online], 29(1), 96-101.

Magwaza, L.S., Opara, U.L., Nieuwoudt, H., Cronje, P.J.R., Saeys, W. & Nicolaï, B. (2012). NIR Spectroscopy Applications for Internal and External Quality Analysis of Citrus Fruit: a review. Food Bioprocess Technology, 5, 425.

Mahayothee, B. (2005). The influence of raw material on the quality of dried mango slices (Mangifera indica L.) with special reference to postharvest ripening. Ph.D. Thesis, Hohenheim University. In Schriftenreihe des Lehrstuhls Lebensmittel pflanzlicher Herkunft; Carle, R., (Ed.); Shaker Verlag: Aachen, Germany.

Mercadante, A.Z. & Rodriguez-Amaya, D.B. (1998). Effects of Ripening, Cultivar Differences, and Processing on the Carotenoid Composition of Mango. Journal of Agricultural and Food Chemistry, 46(1), 128-130.

Merzlyak, M.N., Solovchenko, A.E. & Gitelson, A.A. (2003). Reflectance spectral features and non-destructive estimation of chlorophyll, carotenoid and anthocyanin content in apple fruit. Postharvest Biology and Technology, 27(2), 197-211.

Næs, T., Isaksson, T., Fearn, T. & Davies, T. (2004). A User-Friendly Guide to Multivariate Calibration and Classification. NIR Publications, Charlton, Chichester, UK.

Nagle, M., Mahayothee, B., Rungpichayapichet, P., Janjai, S. & Müller, J. (2010). Effect of irrigation on near-infrared (NIR) based prediction of mango maturity. Scientia Horticulturae, 125(4), 771-774.

Nicolaï, B.M., Beullens, K., Bobelyn, E., Peirs, A., Saeys, W., Theron, I.K. & Lammertyn, J. (2007). Non-destructive measurement of fruit and vegetable quality by means of NIR spectroscopy: a review. Postharvest Biology and Technology, 46, 99-118.

Nicolaï, B., Defraeye, T., De Ketelaere, B., Herremans, E., Hertog, M.L.A.T.M., Saeys, W., Torricelli, A., Vandendriessche, T. & Verboven, P. (2014). Nondestructive measurements of fruit and vegetable quality. Ann. Rev. Food Sci. Technol., 5, 285-312.

Omar, A.F. (2013). Spectroscopic profiling of soluble solids content and acidity of intact grape, lime and star fruit. Sensor Review, 33, 238.

Ornelas-Paz, J.D.J., Yahia, E.M. & Gardea-Bejar, A.A. (2008). Changes in external and internal color during postharvest ripening of 'Manila' and 'Ataulfo' mango fruit and relationship with carotenoid content determined by liquid chromatography–APcI+-time-of-flight mass spectrometry. Postharvest Biology and Technology, 50(2), 145-152.

Osborne, B.G., Fearn, T. & Hindle, P.H. (1993). Practical NIR Spectroscopy with Applications in Food and Beverage Analysis. 2nd ed., Longman Group, Burnt Mill, Harlow, Essex, England, UK, p. 123-132.

Padda, S.M., do Amarante, C.V.T., Garcia, R.M., Slaughter, D.C. & Mitcham, E.M. (2011). Methods to analyze physicochemical changes during mango ripening: a multivariate approach. Postharvest Biology and Technology, 62, 267-274.

Palafox-Carlos, H., Yahia, E., Islas-Osuna, M.A., Gutierrez-Martinez, P., Robles-Sánchez, M. & González-Aguilar, G.A. (2012). Effect of ripeness stage of mango fruit (Mangiferaindica L., cv. Ataulfo) on physiological parameters and antioxidant activity. Scientia Horticulturae, 135(0), 7-13.

Prasanna, V., Prabha, T.N. & Tharanathan, R.N. (2007). Fruit Ripening Phenomena- An Overview. Critical Reviews in Food Science and Nutrition, 47, 1-19.

Rungpichayapichet, P., Mahayothee, B., Khuwijitjaru, P., Nagle, M. & Müller, J. (2015). Non-destructive determination of β-carotene content in mango by near-infrared spectroscopy compared with colorimetric measurements. Journal of Food Composition and Analysis, 38, 32-41.

Rungpichayapichet, P., Mahayothee, B., Nagle, M., Khuwijitjaru, P. & Müller, J. (2016). Robust NIRS models for non-destructive prediction of postharvest fruit ripeness and quality in mango. Postharvest Biology and Technology, 111, 31-40.

Saeys, W., Mouazen, A.M. & Ramon, H. (2005). Potential for Onsite and Online Analysis of Pig Manure using Visible and Near Infrared Reflectance Spectroscopy. Biosystems Engineering, 91(4), 393-402.

Santos, J., Trujillo, L.A., Calero, N., Alfaro, M.C. & Muñoz, J. (2013). Physical characterization of a commercial suspoemulsion as a reference for the development of suspoemulsions. Chemical Engineering & Technology, 11, 1-9.

Saranwong, S., Sornsrivichai, J. & Kawano, S. (2004). Prediction of ripe-stage eating quality of mango fruit from its harvest quality measured nondestructively by near infrared spectroscopy. Postharvest Biology and Technology, 31, 137-145.

Schmilovitch, Z., Mizrach, A., Hoffman, A., Egozi, H. & Fuchs, Y. (2000). Determination of mango physiological indices by near-infrared spectrometry. Postharvest Biology and Technology, 19(3), 245-252.

Shao, Y., He, Y., Gómez, A.H., Pereir, A.G., Qiu, Z. & Zhang, Y. (2007). Visible/near infrared spectrometric technique for nondestructive assessment of tomato 'Heatwave' (Lycopersicumesculentum) quality characteristics. Journal of Food Engineering, 81(4), 672-678.

Siller-Cepeda, J., Muy-Rangel, D., Báez-Sañudo, M., Araiza-Lizarde, E. & Ireta-Ojeda, A. (2009). Calidad poscosecha de cultivares de mango de maduración temprana, intermedia y tardía. Revista Fitotecnia Mexicana, 32(1), 45.

Singh, Z., Singh, R.K., Sane, V.A., & Nath, P. (2013). Mango – Postharvest Biology and Biotechnology. Critical Reviews in Plant Sciences, 32(4), 217-236.

Subedi, P.P., Walsh, K.B. & Owens, G. (2007). Prediction of mango eating quality at harvest using short-wave near infrared spectrometry. Postharvest Biology and Technology, 43, 326-334.

Talens, P., Mora, L., Morsy, N., Barbin, D.F., ElMasry, G. & Sun, D. (2013). Prediction of water and protein contents and quality classification of Spanish cooked ham using NIR hyperspectral imaging. Journal of Food Engineering, 117(3), 272-280.

Theanjumpol, P., Self, G., Rittiron, R., Pankasemsu, T. & Sardsud, V. (2013). Selecting Variables for Near Infrared Spectroscopy (NIRS) Evaluation of Mango Fruit Quality. Journal of Agricultural Science, 5(7).

Torres, R., Montes, E.J., Perez, O.A. & Andrade, R.D. (2013). Relación del color y del estado de madurez con las propiedades fisicoquimicas de frutas tropicales. Información Tecnológica, 24(4), 51.

Vásquez-Caicedo, A.L., Sruamsiri, P., Carle, R. & Neidhart, S. (2005). Accumulation of all-trans-b-carotene and its 9-cis and 13-cis stereoisomers during postharvest ripening of nine Thai mango cultivars. Journal of Agricultural and Food Chemistry, 53, 4827-4835.

Vélez-Rivera, N., Blasco, J., Chanona-Pérez, J., Calderón-Domínguez, G., Perea-Flores, M.J., Arzate-Vázquez, I., Cubero, S. & Farrera-Rebollo, R. (2014b). Computer vision system applied to classification of 'Manila' mangoes during ripening process. Food and Bioprocess Technology, 7, 1183-1194.

Vélez-Rivera, N., Gómez-Sanchis, J., Chanona-Pérez, J., Carrasco, J.J., Millán-Giraldo, M., Lorente, D., Cubero, S. & Blasco, J. (2014a). Early detection of mechanical damage in mango using NIR hyperspectral images and machine learning. Biosystems Engineering, 122, 91-98.

Walsh, K.B., Golic, M. & Greensill, C.V. (2004). Sorting of fruit and vegetables using near infrared spectroscopy: application to soluble solids and dry matter content. Journal of Near Infrared Spectroscopy, 12, 141-148.

Wanitchang, P., Terdwongworakul, A., Wanitchang, J. & Nakawajana, N. (2011). Non-destructive maturity classification of mango based on physical, mechanical and optical properties. Journal of Food Engineering, 105(3), 477-484.

Watanawan, C., Wasusri, T., Srilaong, V., Wongs-Aree, C. & Kanlayanarat, S. (2014). Near infrared spectroscopic evaluation of fruit maturity and quality of export Thai mango (*Mangiferaindica L.* var. Namdokmai). International Food Research Journal, 21(3), 1073-1078.

Williams, P. & Sobering, D. (1993). Comparison of commercial near infrared transmittance and reflectance instruments for analysis of whole grains and seeds. Journal of Near Infrared Spectroscopy, 1, 25.

Yahaya, O.K.M., Matjafri, M.Z., Aziz, A.A. & Omar, A.F. (2014). Non-destructive quality evaluation of fruit by color based on RGB LEDs system. Proceeding of the 2nd International Conference on Electronic Design (ICED), 19–21, pg. 230.

Yahaya, O.K.M., MatJafri, M.Z., Aziz, A.A. & Omar, A.F. (2015). Visible spectroscopy calibration transfer model in determining pH of Sala mangoes. Journal of Instrumentation, 10, T05002.

Yashoda, H.M., Prabha, T.N. & mTharanathan, R.N. (2007). Mango ripening – Role of carbohydrases in tissue softening. Food Chemistry, 102(3), 691-698.

Yashoda, H.M., Prabha, T.N. & Tharanathan, R.N. (2005). Mango ripening-chemical and structural characterization of pectic and hemicellulosic polysaccharides. Carbohydrate research, 340(7), 1335-1342.

Zakaria, A., Shakaff, A.Y.M., Masnan, M.J., Saad, F.S.A., Adom, A.H., Ahmad, M.N. & Kamarudin, L.M. (2012). Improved Maturity and Ripeness Classifications of Magnifera Indica cv. Harumanis Mangoes through Sensor Fusion of an Electronic Nose and Acoustic Sensor. Sensors, 12(5), 6023-6048.

3.2. SECTION II. PROCESS AUTOMATION

II.A. Robotic Inspection

3.2.1. Chapter V.

Non-destructive assessment of mango firmness and ripeness using a robotic gripper

Blanes, C.[1], **Cortés, V.**[2], Ortiz, C.[3], Mellado, M.[1] & Talens, P.[2]

[1]Instituto de Automática e Informática Industrial. Universitat Politècnica de València. Camino de Vera s/n, 46022, Valencia (Spain).

[2]Departamento de Tecnología de Alimentos. Universitat Politècnica de València. Camino de Vera s/n, 46022, Valencia (Spain).

[3]Departamento de Ingeniería Rural y Agroalimentaria. Universitat Politècnica de València. Camino de Vera s/n, 46022, Valencia (Spain).

Food Bioprocess Technology, 8 (2015), 1914-1924

ABSTRACT

The objective of the study was to evaluate the use of a robot gripper in the assessment of mango (cv. 'Osteen') firmness as well as to establish relationships between the non-destructive robot gripper measurements with embedded accelerometers in the fingers and the ripeness of mango fruit. Intact mango fruit was handled and manipulated by the robot gripper and the major physicochemical properties related with their ripening index were analyzed. Partial least square regression models (PLS) were developed to explain these properties according to the variables extracted from the accelerometer signals. Correlation coefficients of 0.925, 0.892, 0.893 and 0.937 with a root-mean-square error of prediction of 2.524 N/mm, 1.579 ºBrix, 3.187 and 0.517, were obtained for the prediction of fruit mechanical firmness, total soluble solids, flesh luminosity and ripening index, respectively. This research showed that it is possible to assess mango firmness and ripeness during handling with a robot gripper.

Keywords: robot gripper, non-destructive, firmness, ripening index, mango

1. INTRODUCTION

Mango (*Mangifera indica L.*) is a tropical fruit with high added-value and among the most widely cultivated and consumed fruit in tropical regions. It is the fifth fruit in global consumption and third among tropical fruits, immediately behind banana and pineapple. It has been cultivated in India for more than 4000 years, but the increasing demand has stimulated production of mango and nowadays is being grown in more than 80 countries. The major producers of mango in terms of volume are India, China and Thailand (FAOSTAT, 2014). In Spain, cultivation of mango is centered in two regions, Andalucía and the Islas Canarias. Due to its good climatic adaptation, the absence of pests and the increment in inside market, Málaga region (Andalucía) has shown a significant increase during last years. Therefore, all future predictions point to an increase in the expansion of the mango market, thus extending their growing areas, productions and markets.

Mangoes are climacteric fruits, and their ripening process takes place rapidly during post-harvest time after being picked. During the ripening process, several physiological and biochemical pathways are activated simultaneously bringing changes in the fruit (Bouzayen *et al.*, 2010), which are initiated by autocatalytic production of ethylene and increase in respiration. The changes observed generally include textural softening (Yashoda *et al.*, 2007; Jha *et al.*, 2010), changes in color due to the disappearance of chlorophyll and appearance of other pigments as carotenoids (Gouado *et al.*, 2007; Zaharah *et al.*, 2012; Rungpichayapichet *et al.*, 2015), loss of organics acids, increase of soluble solid content, decrease of tritatable acidity and in general changes in taste, aroma and flavor (Singh *et al.*, 2013). Accurate determination of fruit ripening stage is important to determine the packing procedure in the postharvest handling (Hahn, 2004) and to provide a consistent supply of good quality fruit (Saranwong *et al.*, 2004). The measurement of total soluble solids, starch content, acidity, or firmness, are used as maturity index, but not always these parameters are correlated with optimal fruit quality. Among these parameters, firmness has been considered a reliable indicator of mango maturity at harvest and ripeness stages during commercial mango handling, as well as an important tool for growers, importers, retailers and consumers (Padda *et al.*, 2011). Firmness can be measured manually by a trained person with a hand

held penetrometer but this technique shows many disadvantages in terms of poor repeatability, subjectivity and is limited at certain stages of maturity (Peacock *et al.*, 1986). The use of automated penetrometers is another alternative to measure the firmness of mango fruit but shows the disadvantage that is a destructive method which can be applied only to one sample of a fruit batch. The development of a reliable non-destructive method to assess the mango ripeness at the packing site is critical to the success of the mango industry.

Mango fruit primary packaging operations are usually done by hand. Human manipulation is able of handling mangoes with care at high speed and, at the same time, sorting the mangoes by certain quality attributes. This manual operation could spread foodborne diseases and operators can suffer musculoskeletal disorders for repetitive movements. In the automation of primary packaging lines in food industry, robotics has clear opportunities (Wilson, 2010). To achieve the objective, robot grippers need to improve their ability for handling irregular and sensitive products like mango fruit, and incorporate tactile sensing. Different solutions regarding the development of robot grippers for handling fruits and vegetables have been proposed by Blanes *et al.*, 2011. In this study, gripper finger should be adapted to the product for achieving an adequate manipulation by means of the actuation on the gripper mechanisms (Meijneke *et al.*, 2011). Some developments related to the use of this technology can be found in industrial applications (Lacquey, www.lacquey.nl). Jamming grippers have a tremendous potential in robotics (Jaeger *et al.*, 2014). By using the jamming of granular material it is possible to adapt product shapes and, at the same time, manipulate irregular products (Brown *et al.*, 2010). Despite of the developments made in the tactile sensors for robotic applications, the entry in the industrial automation is extremely low especially due to the lack of reliable and simple solutions (Girao *et al.*, 2013). Some developments can be found for vegetable grading using tactile sensing in robot grippers. Naghdy and Esmaili, 1996 use the measurement of the current of the gripper actuator. Bandyopadhyaya *et al.*, 2014 employ piezo resistive force sensors, and Blanes *et al.*, 2015 use accelerometers attached to the gripper fingers.

The aim of this paper was to evaluate the use of a robot gripper in the assessment of firmness of mango fruit, cv. ‘Osteen’ and to establish relationships between the non-destructive robot gripper measurements with embedded

accelerometers in the fingers and the mechanical properties, internal quality (soluble solids, pH and tritatable acidity), flesh color and the ripening index of mango fruit.

2. MATERIALS AND METHODS

2.1. Experimental procedure

A batch of 350 mangoes (*Mangifera indica L.*, cv. 'Osteen') manually harvested in Malaga (Spain) were selected showing uniform size and color and free of external blemishes or infections.

All mangoes were washed with a soap solution prepared with two drops of dishwasher with water and dried with disposable paper to completely remove water from the surface. Mangoes were individually numbered and randomly divided into 7 sets of fifty mangoes (A, B, C, D, E, F and G). All sets were stored during one day in a cold chamber (11.9 ± 0.4 ºC and 84.3 ± 1.7% RH) until gripper tests started. Thus, fruits of set A were analyzed one day after reception and the remaining groups were placed in the storage chamber at 18.0 ± 2.1 ºC and 67.6 ± 3.3% RH. Every 2-3 days, the next set was removed from the storage chamber and fruits were analyzed. From each set, all the mangoes were handled by the robotic gripper. Twenty fruits were used to evaluate the mechanical properties, the internal composition (ºBrix, pH and titratable acidity) and the flesh color. The other thirty fruits were used to evaluate the damage caused by the robotic gripper. These fruits were maintained in the storage chamber during two weeks after handling in order to detect fruit bruises.

2.2. Robotic gripper

Based on the experiences and results of previous tests (Blanes *et al.*, 2014), a specific robot gripper was designed and manufactured for the handling and the assessment of mangoes (figure 1). The gripper has parallel action and is actuated by one pneumatic cylinder. It has three fingers (A, B and C) and one suction cup located between the fingers B and C. To ensure the manipulation of mango fruits without damaging, the fingers of the robotic gripper adapt to the irregular shapes of the mangoes. The adaptability of the fingers B and C was achieved by means of their three free rotations while the adaptability of finger A is based on the use of

jamming transition of its internal granular fluid. The pad of finger A is a latex membrane filled with sesame seeds. This pad is soft when its internal pressure is atmospheric or slightly positive because the sesame seeds are loose and the friction forces between them are low. On the other hand, the pad is hard when its internal pressure is negative and the sesame seeds are in contact and for hence there are friction forces between them. Every finger has at its rear side an analog accelerometer ADXL278 connected to a data acquisition USB NI-6210 device. The gripper is attached to an ABB IRB 340 FlexPicker robot. The gripper open-close operation is controlled by an electro-valve, the suction cup by a vacuum generator electrically piloted and the state soft or hard of the pad of finger A with another vacuum generator electrically piloted with blow action function. A robot program controls the gripper movements and all its devices for the good performance of the gripper.

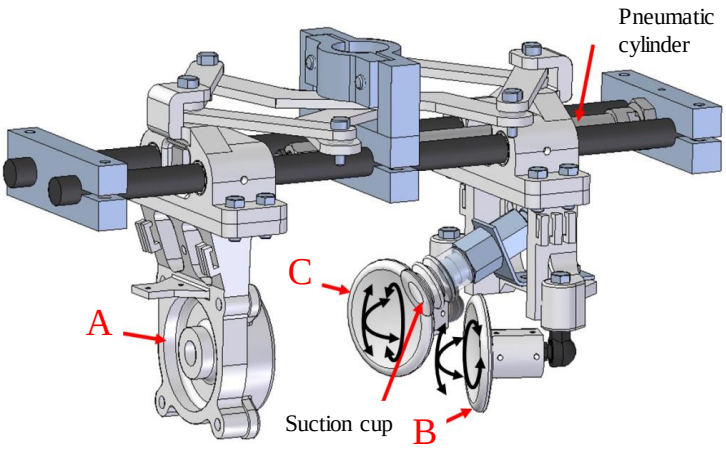

Figure 1. Robot gripper model denomination, the black arrows are the degrees of freedom of fingers B and C

2.3. Physicochemical analysis

In order to assess the firmness and ripeness of mango fruits, mechanical properties, internal composition, and flesh color of mangoes were analyzed. All of these analyzes were performed immediately after robotic gripper measurements. A total of 140 samples were evaluated (20 fruits per set).

The mechanical properties were analyzed through a puncture test by using a universal test machine (TextureAnalyser-XT2, Stable MicroSystems (SMS) Haslemere, England). The test was performed with a punch of 6mm diameter (P/15ANAMEsignature) to a relative deformation of 30%, at a speed of 1 mm/s by triplicate. Sample dimensions were measured with calipers before the analysis and force-true stress data were estimated from the force-distance data (Dobraszczyk & Vincent, 1999). Different parameters were analyzed for all samples. The fracture strength (FS) expressed by the maximum force applied to break up the sample (N), the fruit deformation (DF) expressed by the deformation until the fracture point (mm) and the fruit mechanical firmness (FF) expressed by the slope of the force-true stress curve until the fracture point (N/mm).

The internal composition was analyzed through the total soluble solids (TSS), pH and the titratable acidity (TA) of the samples. TSS content was determined by refractometry (ºBrix) with a digital refractometer (set RFM330+, VWR International Eurolab S.L Barcelona, Spain) at 20°C and with a sensitivity of ±0.1 ºBrix. The analysis of TA were performed with an automatic titrator (CRISON, pH-burette 24, Barcelona, Spain) with 0.5N NaOH until a pH of 8.1 (UNE34211:1981) using 15g of crushed mango and diluting it in 60 mL of distilled water. The pH and TA was determined based on the percentage of citric acid that it was calculated using the equation 1.

$$TA\ [g\ citric\ acid/100g\ of\ the\ sample]=((A\times B\times C/D)\times 100))/E \quad (1)$$

where A is the volume of NaOH consumed in the titration (in L), B is the normality of NaOH (0.5N), C is the molecular weight of citric acid (192,1g/mol), D is the weight of the sample (15g) and E is the valence of citric acid (3).

The flesh color was measured using a MINOLTACM-700d spectrocolorimeter (Minolta CO. Tokyo, Japan). The reflectance spectra between 400-700 nm were measured in different points of the flesh and the color coordinates L*, a* and b* for D65 illuminant and 10° observer in the CIELab space were obtained. Hue (h^*) and chroma (C^*) were estimated by the equations 2 and 3, respectively.

$$h^* = arctg\frac{b^*}{a^*} \quad (2)$$

$$C^* = \sqrt{a^{*^2} + b^{*^2}} \quad (3)$$

a^* and b^* being the CIELab attributes.

A ripening index (RPI) was calculated, as described Vélez-Rivera *et al.*, 2014, by equation 4.

$$RPI = \ln(100 \cdot F_S \cdot TA \cdot TSS^{-1}) \quad (4)$$

where F_S is fracture strength (Newton), TA is titratable acidity (g citric acid equivalent/100 g sample), and TSS is total soluble solids (ºBrix).

2.4. Robot operation

Previously to the physicochemical analysis, mangoes were placed manually over a cradle where the gripper picks them up. Robot moves down till locate the gripper center tool in the mango position. During 0.03 seconds the finger A pad is blown to ensure a soft behavior before the mangoes are grasped. Then the gripper starts to close their fingers. The pad of the finger A is soft and can adapt to the mango shape during the first contact between the mango and the pad. During this first contact the fingers B and C rotate till find the parallel orientation to the shape of the mango and for hence their accelerometers are then oriented perpendicular to the mango surface. After a stabilization period of time, a negative pressure changes the pad state from soft to hard and the vacuum of the suction cup starts. The hard state was used during robot displacements and impacts for sensing the mangoes. Robot moves up the gripper and mango fruit and starts a cycle loop of five quick opening and closing impacts while the mango was maintained attached to B and C fingers due to the action of the suction cup. During the first impact the pad changed again from soft to hard, soft when was open and hard after the closing action when the pad was in contact with the mango fruit. Mangoes were grasped from a cradle and the fingers adapt their orientations and shapes while mangoes are contacting the cradle. When the gripper is in the up position and mango is not contacting the

cradle some relative motion between mango and fingers B and C can occur. This process ensures that finger surfaces were hard and parallel to the surface of the mango. During this cycle loop deceleration signals are collected and recorded in a computer.

Figure 2 shows the flow chart of the operational process of robot gripper and its control.

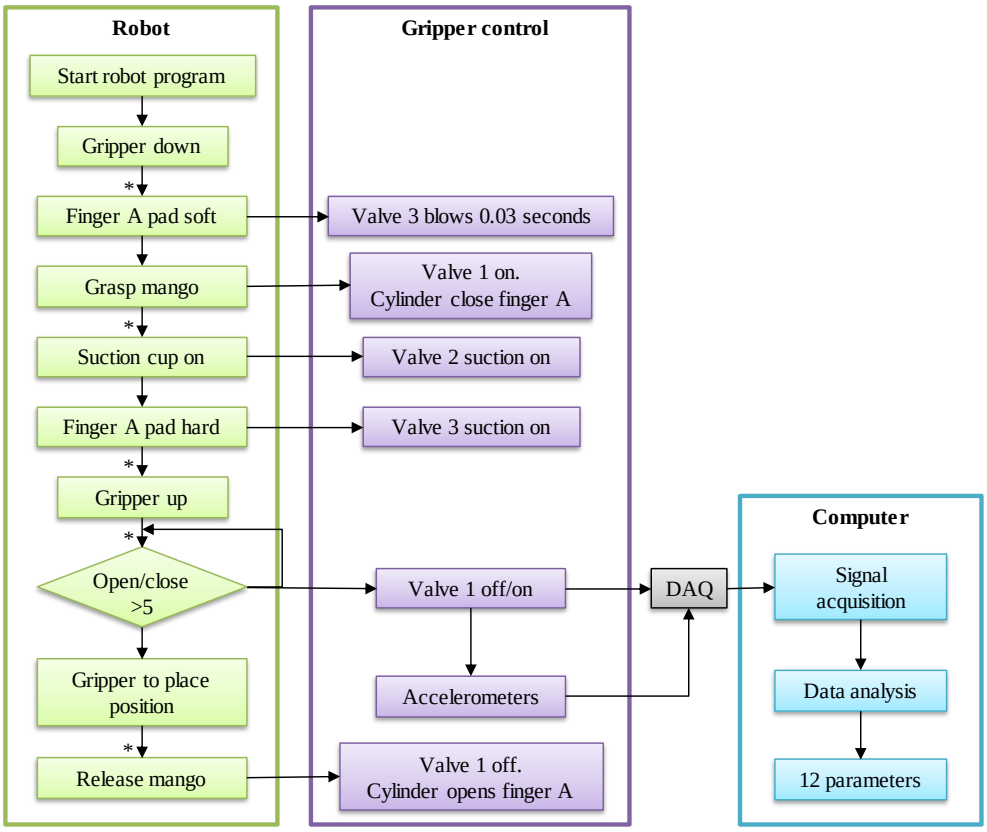

Figure 2. Flow chart of the operational process of robot gripper and its control.

2.5. Robotic gripper damage

A total of 210 samples (7 sets, from A to G, of 30 mangoes fruits) were analyzed in order to evaluate possible damages onto the mango caused by the robotic gripper during handling. The samples were visually evaluated every day

during the two weeks storage period using a lighter magnifying glass. After two week storage period, the inner part of each fruit was also evaluated.

2.6. Processing and data analysis

2.6.1. Robot gripper data analysis

A data acquisition module USB NI-6210 collected the signals of the accelerometers ADXL278 that were attached to every finger of the robot gripper. Signals were sampled at 30 KHz, filtered with a low cut-pass at 1500 Hz and, recorded during 8 Kbs for every finger A, B and C. A LabVIEW program processed every signal to obtain 12 parameters. Signals were cut for analyzing only the period of time where fingers were impacting against the mango (Figure 3).

These signals were used with the equation 5 to extract the independent values VA, VB and VC. Those parameters were extracted from a fixed period of time in which the fingers hit against the mango. Max A, Max B and Max C are the maximum decelerations for each finger during the contact with the mango.

$$VA = \int_{t_0}^{t_1} A^2 dt\ ; \qquad VB = \int_{t_0}^{t_1} B^2 dt\ ; \qquad VC = \int_{t_0}^{t_1} C^2 dt \quad (5)$$

The deceleration severity that happens after the first contact between the finger and the fruit was calculated using the smoothed signals, as the slope of the line from the first contact till the maximum value. In the figure 3 the deceleration signal of the Finger A, in this case and mostly, had two peaks because the finger A rebounded during the impact. This peak created interferences for calculating this slope. To avoid several peaks signals were smoothed and processed to get the slope of every finger. With the derivative function of the signals smoothed is possible to obtained the maximum values of the line slopes; MaxSlp A, MaxSlp B and MaxSlp C, and the slope average; AvgSlp A, AvgSlp B and AvgSlp C.

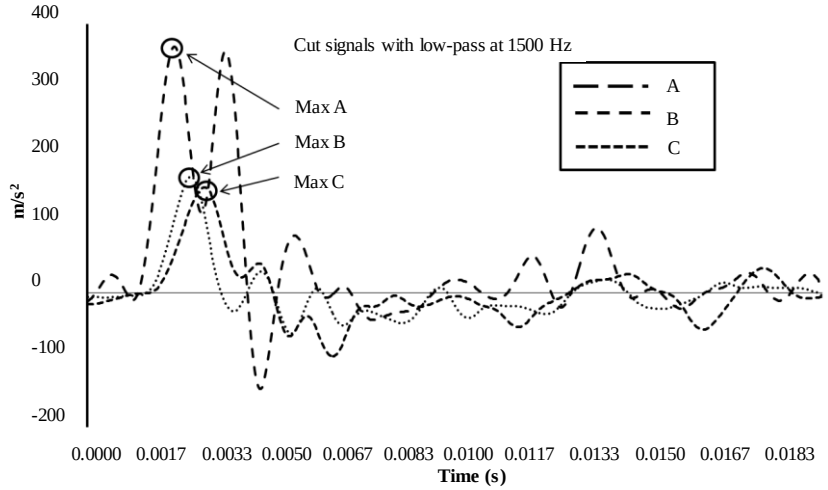

Figure 3. An example of the decelerations of the gripper fingers A, B and C during the contact of the finger against the mango.

2.6.2. Physicochemical data analysis

Ten physicochemical parameters were analyzed (fracture strength, fruit deformation, fruit mechanical firmness, total soluble solids, pH, tritatable acidity, flesh luminosity, flesh hue, flesh chroma and the ripening index).

Analysis of variance (ANOVA) was conducted to determine significant differences in the physicochemical and robot gripper parameters using the software Statgraphics Plus for Windows 5.1 (Manugistics Corp., Rockville, Md.). Fisher´s least significant difference (LSD) procedure was used at the 95% confidence level.

2.6.3. Multivariate data analysis

The extracted parameters provided by the robot gripper (VA, VB, VC, Max A, Max B, Max C, MaxSlp A, MaxSlp B, MaxSlp C, AvgSlp A, AvgSlp B and AvgSlp C) and the data obtained from the physicochemical analysis (FF, DF, FS, TSS, pH, TA, L*, C*, H* and RPI) were then arranged in a matrix where the rows represent the number of samples (#N = 140 samples) and the columns represent the number of variables (#V = 22 variables). The X-variables or predictors were the 12 variables provided by the robot gripper and the Y-variables or responses were the 10 variables provided by the physicochemical analysis. The data set was separated randomly into two groups, one group (105 samples) was used as calibration set and

the other group composed by the remaining samples (35 mangoes) was used to prediction set.

Partial least squares regression (PLS) was applied to the matrix for constructing separate calibration models for each physicochemical property. PLS technique is particularly useful when it is necessary to predict a set of response variables from a set of predictor variables (Abdi, 2010). In PLS, prediction is achieved by transferring the inter-correlated variables to a set of independent factors called latent variables (LVs) which describe the maximum covariance between the robot gripper information and the response variable (i.e. fruit mechanical firmness, total soluble solids, flesh luminosity or ripening index in our case). The LVs of each PLS model are uncorrelated and carry all relevant information to realize more stable predictions. The number of LVs used in each model was determined at the minimum value of predicted residual error sum of squares (PRESS) (Esquerre *et al.*, 2009; Talens *et al.*, 2013). When the number of latent factors in the model increased, the value of PRESS decreased until its lowest value corresponding to the ideal number of latent factors. The calibration models were strictly built using the calibration dataset and optimized by internal cross-validation (leave-one-out). The performances of the developed calibration models were further validated to predict the physicochemical parameters in an independent testing set (prediction dataset).

Before the PLS analysis, the predictors were transformed to make their distributions be fairly symmetrical in order to giving each variable the same prior importance in the analysis. Each variable was centered by subtracting their averages and scaled to unit variance by dividing them by their standard deviation. The centering ensures that all results will be interpretable in terms of variation around the mean and the scaling gives all X-variables the same chance to influence the estimation of the physicochemical property.

Performance of the models was evaluated using the standard error of calibration (SEC), the standard error of cross-validation (SECV), the root-mean-square error of calibration (RMSEC), the root-mean square error of cross-validation (RMSECV) and the correlation coefficient (r).

The software used for the multivariate analysis was The Unscrambler v9.7 (CAMO Software AS, OSLO, Norway).

3. RESULTS AND DISCUSSION

3.1. Physicochemical analysis

The physicochemical characteristics (mechanical properties, total soluble solids, pH, tritatable acidity and flesh color) of mangoes during the storage period are presented in Table 1. As expected, during the ripening process a textural alteration (loss of fracture strength and fruit mechanical firmness and increase of fruit deformation) of mango samples was observed. The fracture strength and the slope of the linear range until the fracture point decreased whereas the deformation in the fracture point increased during the storage period. These changes may be due to an increase in the enzymatic activity on the fruit that provokes changes in the structural integrity of the cell wall and middle lamella as was described previously by Yashoda *et al.*, 2007. During fruit softening, cell walls were modified by solubilisation, de-esterification, and de-polymerization, accompanied by an extensive loss of neutral sugars and galacturonic acid (Singh *et al.*, 2013). Other internal compositional changes were observed during the storage time. Total soluble solids and pH increase, whereas tritatable acidity decreases (table 1). Generally, soluble solid content in mango range from 7.0 to 17.4 ºBrix, depending on the variety, the production place and maturity stage (Lucena *et al.*, 2007). For 'Osteen' variety the mature stage where the fruit attains the stage of maximum consumer acceptability is reached when the mangoes has around 14-15 ºBrix (Vilela *et al.*, 2013). The mango fruit tested in the present experiment range from 5.85 to 19.50 ºBrix. According to these values, A set samples are unripe mangoes, G set samples are over-ripe samples, whereas B, C, D, E and F set samples are intermediate-ripe mangoes.

The pH and the tritatable acidity of the mango tested in the present experiment range from 3.35 to 6.62 and from 0.97 to 0.07, respectively. Similar values were observed by Yashoda *et al.*, 2007 working with Alphonso variety. The increase in pH and the decrease in the tritatable acidity during the ripening process can be explained by the cell metabolization of volatile organic acids and non-volatile constituents.

Regarding color measurements, a clear tendency was observed in the changes of flesh color of the mangoes during the ripening process. Among the

three elements of flesh color evaluated: luminosity, hue and chroma; the luminosity seems to be the best parameter to assess the maturity of mangoes.

Table 1. Physicochemical characteristics of Mangoes during the storage period.

Set name	Set A	Set B	Set C	Set D	Set E	Set F	Set G
Days of storage	2	4	7	9	11	14	16
Fracture strength (N)	105 ± 8^{a}	$97 \pm 19^{a,b}$	$100 \pm 30^{a,b}$	$90 \pm 25^{b,c}$	77 ± 25^{c}	40 ± 17^{d}	24 ± 6^{e}
Fruit deformation (mm)	7 ± 3^{c}	7 ± 1^{c}	$8 \pm 1^{b,c}$	9 ± 1^{b}	10 ± 1^{c}	10 ± 2^{a}	10 ± 2^{a}
Fruit mechanical Firmness (N/mm)	18 ± 2^{a}	15 ± 4^{b}	14 ± 5^{b}	11 ± 4^{c}	8 ± 4^{d}	4 ± 2^{e}	2 ± 1^{e}
Total Soluble Solids (° Brix)	8 ± 1^{f}	12 ± 2^{e}	$12 \pm 3^{e,d}$	$14 \pm 2^{d,c}$	$15 \pm 2^{b,c}$	16 ± 2^{b}	18 ± 1^{a}
pH	4.10 ± 0.13^{d}	4.09 ± 0.23^{d}	4.04 ± 0.17^{d}	3.71 ± 0.21^{c}	3.68 ± 0.15^{c}	4.89 ± 0.60^{b}	5.70 ± 0.40^{a}
Titratable acidity (g/100g)	0.49 ± 0.09^{b}	0.55 ± 0.13^{b}	0.50 ± 0.09^{b}	0.67 ± 0.11^{b}	0.67 ± 0.15^{a}	0.26 ± 0.12^{c}	0.12 ± 0.03^{d}
Flesh Luminosity (L*)	79 ± 1^{a}	76 ± 4^{b}	76 ± 5^{b}	75 ± 4^{b}	73 ± 3^{c}	67 ± 3^{d}	64 ± 3^{e}
Flesh Chroma (C*)	49 ± 4^{c}	53 ± 4^{b}	48 ± 6^{c}	49 ± 6^{c}	53 ± 5^{b}	58 ± 3^{a}	61 ± 3^{a}
Flesh Hue (h*)	83 ± 2^{a}	$79 \pm 3^{b,c}$	80 ± 3^{b}	81 ± 3^{b}	78 ± 3^{c}	75 ± 2^{d}	74 ± 1^{d}
Ripening index (RPI)	6.5 ± 0.2^{a}	6.1 ± 0.4^{b}	5.9 ± 0.6^{b}	5.9 ± 0.5^{b}	5.8 ± 0.6^{b}	4.1 ± 0.7^{c}	2.8 ± 0.4^{d}

Values are mean ± SD

$^{a-f}$ Different superscripts in the same row indicate significant difference among sets ($p < 0.05$).

In general, the physicochemical analysis showed that the best parameters to assess the maturity of 'Osteen' mangoes are the firmness, the soluble solid content and the flesh color. These results agree with the studies done by Padda *et al.*, 2011 where described that the best tools to assess changes in mangoes during ripening process are the penetrometer, followed by flesh color and total soluble solids content. In fact, these parameters are used in the mango packing-lines to assess ripeness stage (Brecht, 2010).

3.2. Robot gripper analysis

The robot gripper was capable of grasping 100% of the mangoes from sets A to F without any damage. In the case of the extremely over-ripe mangoes from the set G, 10% of the fruits were severely damaged during the robot handling.

Table 2 shows the range (minimum and maximum values), mean and standard deviation of the extracted parameters provided by the robot gripper analysis. All parameters were measured along the X axis because no clear correlation was found between the sample hardness and acceleration measured along the Y axis. The same effect was previously observed by Blanes *et al.*, 2015 working with eggplants.

Table 2. Range, mean and standard deviation of the 12 extracted parameters provided by the robot gripper analysis for the mangoes studied.

Parameters	Minimum value	Maximum value	Mean	Sdev
VA (m^2/s^2)	95.76	260.27	173.09	30.52
VB (m^2/s^2)	14.45	45.49	27.69	6.79
VC (m^2/s^2)	10.97	87.61	45.10	11.55
Max A (m/s^2)	205.36	441.58	330.73	41.34
Max B (m/s^2)	74.19	198.41	132.37	26.82
Max C (m/s^2)	64.76	236.35	154.72	29.18
MaxSlp A	2.12	6.98	4.71	1.03
MaxSlp B	1.00	3.38	2.22	0.45
MaxSlp C	-0.24	3.86	2.50	0.76
AvgSlop A	1.15	2.98	2.34	0.31
AvgSlop B	0.30	1.14	0.79	0.17
AvgSlop C	0.42	2.27	1.16	0.28

During the robot gripper analysis it was observed that gripper fingers suffered the most violent deceleration when the ripening stage of mango was low whereas deceleration decreased when the ripening stage of mango was high. The best parameters that showed this behavior were Max A, Max B, Max C and MaxSlp A, MaxSlp B, MaxSlp C. Figure 4 shows median plots with 95% confidence intervals of average of maximum deceleration parameters during the contact between fingers and fruits (figure 4a), and average of deceleration severity parameters after this contact (figure 4b) during the storage period of samples where clearly this behavior was observed.

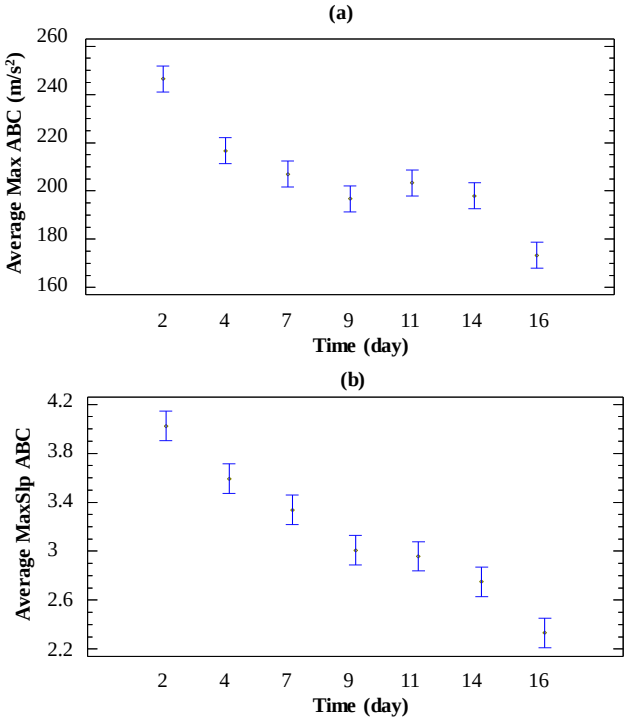

Figure 4. Median plots with 95% confidence intervals of average of maximum deceleration parameters (a) and average of deceleration severity parameters (b) during the storage period of samples.

3.3. Correlation between robot gripper measurements and mango physicochemical characteristics

In order to see if the robot gripper can assess the mango firmness and ripeness partial least square regression models (PLS) were developed to explain the physicochemical characteristics according to the variables extracted from the accelerometer signals. The mango samples (#N = 140) were separated randomly into a calibration set (105 samples) and a validation set (35 mangoes). The critical step for an accurate PLS calibration model is to select the correct number of LVs needed to obtain the best prediction. If fewer latent variables are selected, the model will easily result in under-fitting, while the selection of many latent variables will cause over-fitting. The ideal number of latent factors for predicting fruit mechanical firmness, soluble solid content and flesh luminosity identified from PRESS plot shown in figure 5a was 4, 3 and 3, respectively. At these latent factors, the PRESS had the lowest value and the models had a good predictive power. The performance of the calibration models for each constituent was optimized by internal cross-validation and then validated by external validation in an independent validation set.

Table 3 shows the standard error of calibration (SEC), the standard error of cross-validation (SECV), the standard error of prediction (SEP), the root-mean-square error of calibration (RMSEC), the root-mean-square error of cross-validation (RMSECV), the root-mean-square error of prediction (RMSEP), the correlation coefficient (r), and the numbers of the latent variables required (#LVs) for fruit mechanical firmness (slope of the linear range until the fracture point), soluble solid content, and flesh luminosity for the calibration and prediction sets. The results indicated that the PLS calibration models for these parameters exhibited low values of SEC, SECV, RMSEC and RMSECV, and high values of r, indicating good performance of the models.

When the models were used to predict the new 35 samples of mango, predictions were also high. The best results were obtained for the mango fruit mechanical firmness. The correlation coefficient between robot gripper values and the slope of the linear range until the fracture point was 0.925, with a standard error of prediction of 2.524 N/mm, root-mean-square error of prediction of 2.517 and a

BIAS of -0.380 N/mm. This result indicates that there are good relationships between robot gripper measurements and mango firmness.

In the case of total soluble solids, the correlation coefficient between robot gripper values and TSS was 0.892, with a standard error of prediction of 1.579 ºBrix, the root-mean-square error of prediction of 1.574 ºBrix and the systematic difference between predicted and measured values (BIAS) of -0.228 ºBrix. For flesh luminosity, the correlation coefficient between robot gripper values and flesh luminosity was 0.893, with a standard error of prediction of 3.187, root-mean-square error of prediction of 3.166 and a BIAS of 0.396.

The scatter plots of figure 5 shows the efficiency of the PLS models for predicting fruit mechanical firmness (figure 5b), soluble solid content (figure 5c) and flesh luminosity (figure 5d). In all figures, the ordinate and abscissa axes represent the predicted and measured fitted values of the appropriate parameters, respectively. The correlation between the measured and predicted values for each parameter showed a good prediction performance.

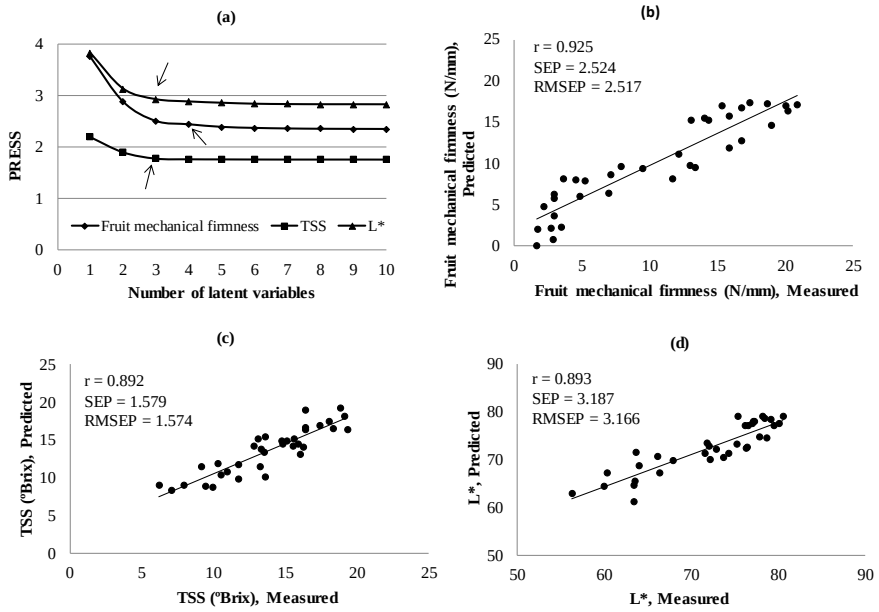

Figure 5. Prediction of fruit mechanical firmness, soluble solids and flesh luminosity using the PLS models. (a) PRESS plot for identifying the optimum number of LVs. Predicted vs measured values of (b) fruit mechanical firmness, (c) soluble solids, and (d) flesh luminosity.

Table 3. Results of the PLS models for the prediction of soluble solid content, fruit mechanical firmness and flesh luminosity in mango samples.

Parameter	#N	#LV	Calibration			Cross Validation			Prediction		
			r	SEC	RMSEC	r	SECV	RMSECV	r	SEP	RMSEP
Fruit mechanical firmness	12	4	0.918	2.457	2.446	0.904	2.656	2.644	0.925	2.524	2.517
Soluble solid content	12	3	0.859	1.795	1.786	0.834	1.936	1.927	0.892	1.579	1.574
Flesh Luminosity	12	3	0.874	2.940	2.930	0.853	3.170	3.156	0.893	3.187	3.166

#N: total number robot gripper parameters, #LV: number of latent variables, SEC: standard error of calibration, SECV: standard error of cross-validation, SEP: standard error of prediction; RMSEC: root-mean-square error of calibration, RMSECV: root-mean-square error of cross-validation, RMSEP: root-mean-square error of prediction, r: correlation coefficient.

The most essential physical and chemical properties of mangoes linked with the sensory perception of the ripeness of the fruits can be described by the ripening index (RPI). This RPI combined the values of fracture strength, titratable acidity and total soluble solids. Table 4 shows the results of the PLS models for the prediction of fracture strength, titratable acidity, total soluble solids and RPI. The RPI model showed the best prediction coefficient and the best performance of the models. This result indicate that the non-destructive information obtained from the robot gripper could be used to predict the combination of parameters related to the ripeness stage and the RPI index more accurately than any of the parameters individually. Figure 6a shows the median plot with 95% confidence intervals of the RPI during the storage of the samples. Similarly, to the results observed by Vélez-Rivera *et al.*, 2014 working with 'Manila' mango the RPI values decrease during the storage. Three ripeness phases were identified based on the RPI parameter: unripe mangoes (A set samples), intermediate-ripe mangoes (B, C, D, E and F set samples) and over-ripe mangoes (G set samples). A PLS calibration model was developed to explain the RPI according to the variables extracted from the robot gripper. The correlation of calibration between the variables extracted from the accelerometer signals and the RPI was 0.887, with SEC and RMSEC of 0.617 and 0.614 respectively. When the model was used to predict the new mango samples, it showed a better correlation coefficient (r = 0.937), with a standard error of prediction of 0.517, root-mean-square error of prediction of 0.518 and a BIAS of -0.089. Figure 6b shows the good prediction performance of the PLS model for RPI.

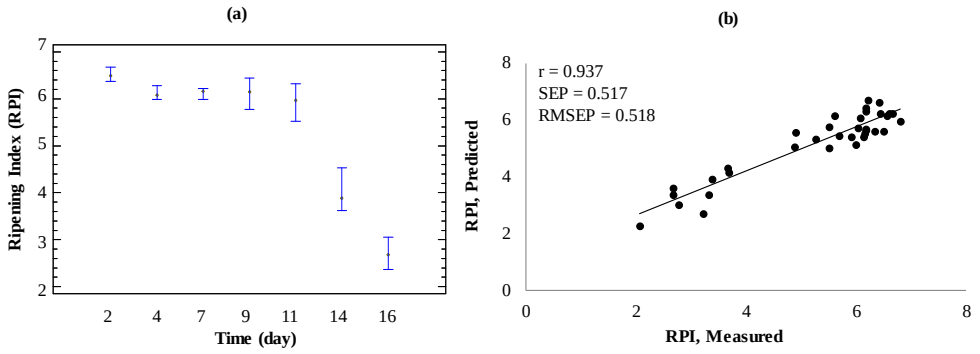

Figure 6. (a) Evolution of the ripening index during the storage period of the samples and (b) predicted vs measured values of RPI.

Table 4. Results of the PLS models for the prediction of fracture strength, titratable acidity, total soluble solids and RPI in mango samples.

	#N	#LV	Calibration			Cross Validation			Prediction		
Parameter			**r**	**SEC**	**RMSEC**	**r**	**SECV**	**RMSECV**	**r**	**SEP**	**RMSEP**
Fracture strength	12	3	0.856	18.410	18.402	0.831	19.948	19.853	0.872	18.211	17.989
Soluble solid content	12	3	0.859	1.795	1.786	0.834	1.936	1.927	0.892	1.579	1.574
Tritatable acidity	12	3	0.798	0.1240	2.930	0.753	0.135	0.135	0.820	0.124	0.127
RPI	12	4	0.887	0.617	0.614	0.862	0.679	0.675	0.937	0.517	0.518

#N: total number robot gripper parameters, #LV: number of latent variables, SEC: standard error of calibration, SECV: standard error of cross-validation, SEP: standard error of prediction; RMSEC: root-mean-square error of calibration, RMSECV: root-mean-square error of cross-validation, RMSEP: root-mean-square error of prediction, r: correlation coefficient.

4. CONCLUSIONS

The physicochemical analysis showed that the best parameters to assess the ripeness of cv. 'Osteen' mangoes are fruit mechanical firmness, soluble solid content, and flesh luminosity. These variables are the parameters used in the mango packaging -lines to assess fruit ripeness and to take decisions according to their values. The prediction models, developed by partial least square regression, have the potential to estimate the described parameters and also the ripening index of the samples based on the information obtained from the robot gripper accelerometers. This research showed that it is possible to assess the firmness and ripeness of mango fruits using a non-destructive technique during robot handling operation with a robot gripper.

Acknowlegments

This research is supported by MANI-DACSA projects (ref. RTA2012-00062-C04-02 and RTA2012-00062-C04-03), partially funded by the Spanish Government (Ministerio de Economía y Competitividad), and by the project PAID-05-11-2745, Vicerectorat d´Investigació, Universitat Politècnica de València. Victoria Cortés thanks Spanish Ministerio de Educación, Cultura y Deporte for a FPU grant (FPU13/04202).

5. REFERENCES

Abdi, H. (2010). Partial least squares regression and projection on latent structure regression (PLS Regression). Wiley Interdisciplinary Reviews: Computational Statistics, 2(1), 97-106.

Bandyopadhyaya, I., Babu, D., Bhattacharjee, S. & Roychowdhury, J. (2014). Vegetable Grading Using Tactile Sensing and Machine Learning. In Anonymous Advanced Computing, Networking and Informatics-Volume 1. Smart Innovation, Systems and Technologies. Springer 27, 77-85.

Blanes, C., Ortiz, C., Mellado, M. & Beltrán, P. (2015). Assessment of eggplant firmness with accelerometers on a pneumatic robot gripper. Computers and Electronics in Agriculture, 113, 44-50.

Blanes, C., Ortiz, C., Talens, P. & Mellado, M. (2014). Mango postharvest handling and firmness assessment with a robotic gripper. In Proceedings International Conference of Agricultural Engineer, Zurich, Switzerland.

Blanes, C., Mellado, M., Ortiz, C. & Valera, A. (2011). Technologies for robot grippers in pick and place operations for fresh fruits and vegetables. Spanish Journal of Agricultural Research, 9(4), 1130-1141.

Bouzayen, M., Latché, A., Nath, P. & Pech, J. (2010). Mechanism of fruit ripening. In Anonymous Plant Developmental Biology-Biotechnological Perspectives, 319-339. Springer. (ISBN 978-3-642-02300-2)

Brecht, J., Sargent, S., Kader, A., Mitcham, E., Maul, F., Brecht, P. & Menocal, O. (2010). Mango Postharvest Best Management Practices Manual. Gainesville: Univ.of Fla.Horticultural Sciences Department, 78. Available at web page accessed 19/1/2015 http://edis.ifas.ufl.edu/pdffiles/HS/HS118500.pdf

Brown, E., Rodenberg, N., Amend, J., Mozeika, A., Steltz, E., Zakin, M.R., Lipson, H. & Jaeger, H.M. (2010). From the Cover: Universal robotic gripper based on the jamming of granular material. Proceedings of the National Academy of Sciences of the United States of America, 107(44), 18809-18814.

Dobraszczyk, B.J. & Vincent, J.F. (1999). Measurement of mechanical properties of food materials in relation to texture: the materials approach. Food texture: Measurement and perception, 99-151.

Esquerre, C., Gowen, A.A., O'Donnell, C.P. & Downey, G. (2009). Initial Studies on the Quantitation of Bruise Damage and Freshness in Mushrooms Using Visible-Near-infrared Spectroscopy. Journal of Agricultural and Food Chemistry, 57(5), 1903-1907.

FAOSTAT, (2014). ProdSTAT. Food and Agriculture Organization of the United Nations. Available at web page accessed 19/1/2015 http://faostat.fao.org/site/339/default.aspx (Retrieved 10.03.14).

Girao, P.S., Ramos, P.M.P., Postolache, O. & Dias J.M. (2013). Tactile sensors for robotic applications. Measurement, 46(3), 1257-1271.

Gouado, I., Schweigert, F.J., Ejoh, R.A., Tchouanguep, M.F. & Camp, J.V. (2007). Systemic levels of carotenoids from mangoes and papaya consumed in three forms (juice, fresh and dry slice). European journal of clinical nutrition, 61(10), 1180-1188.

Hahn, F. (2004). Mango Firmness Sorter. Biosystems engineering, 89(3), 309-319.

Jaeger, H. (2014). Celebrating Soft Matter's 10th Anniversary: Toward jamming by design. Soft matter, 11(1), 12-27.

Jha, S.K., Sethi, S., Srivastav, M., Dubey, A.K., Sharma, R.R., Samuel, D.V.K., & Singh, A.K. (2010). Firmness characteristics of mango hybrids under ambient storage. Journal of Food Engineering, 97(2), 208-212.

Lucena, E.M.P.D., Assis, J.S.D., Alves, R.E.E.A.T., Silva, V.C.M.D. & Enéias Filho, J. (2007). Alterações físicas e químicas durante o desenvolvimento de mangas' Tommy Atkins' no vale de São Francisco, Petrolina-PE. Revista Brasileira de Fruticultura, 29, 96-101.

Meijneke, C., Kragten, G. & Wisse, M. (2011). Design and performance assessment of an under actuated hand for industrial applications. Mechanical Science, 2, 9-15.

Naghdy, F. & Esmaili, M. (1996). Soft Fruit Grading using a Robotics Gripper, International Journal of Robotics & Automation, 11, 93-101.

Padda, M., Padda, M.S., Garcia, R., Slaughter, D. & Mitcham, E. (2011). Methods to analyze physico-chemical changes during mango ripening: A multivariate approach. Postharvest Biology and Technology, 62(3), 267-274.

Peacock, B., Murray, C., Kosiyachinda, S., Kosittrakul, M. & Tansiriyakul, S. (1986). Influence of harvest maturity of mangoes on storage potential and ripe fruit quality. Asean Food Jorunal, 2, 99-101.

Rungpichayapichet, P., Rungpichayapichet, B., Mahayothee, P., Khuwijitjaru, M., Nagle, J. & Müller, J. (2015). Non-destructive determination of ß-carotene content in mango by near-infrared spectroscopy compared with colorimetric measurements. Journal of food composition and analysis, 38, 32-41.

Saranwong, S., Sornsrivichai, J. & Kawano, S. (2004). Prediction of ripe-stage eating quality of mango fruit from its harvest quality measured nondestructively by near infrared spectroscopy. Postharvest Biology and Technology, 31(2), 137-145.

Singh, Z., Singh, R.K., Sane, V.A. & Nath P. (2013). Mango - Postharvest Biology and Biotechnology. Critical Reviews in Plant Sciences, 32(4), 217-236.

Talens, P., Mora, L., Morsy, N., Barbin, D.F., ElMasry, G. & Sun, D. (2013). Prediction of water and protein contents and quality classification of Spanish cooked ham using NIR hyperspectral imaging. Journal of Food Engineering, 117(3), 272-280.

Velez-Rivera, N., Blasco, J., Chanona-Perez, J., Calderon-Dominguez, G., de Jesus Perea-Flores, M., Arzate-Vazquez, I., Cubero, S. & Farrera-Rebollo, R. (2014). Computer Vision System Applied to Classification of "Manila" Mangoes During Ripening Process. Food and Bioprocess Technology, 7(4), 1183-1194.

Vilela, C., Cordeiro, N., Silvestre, A.J.D., Oliveira, L. & Camacho, J. (2013). The ripe pulp of *Mangifera indica L.*: A rich source of phytosterols and other lipophilic phytochemicals. Food Research International, 54(2), 1535-1540.

Wilson, M. (2010). Developments in robot applications for food manufacturing. Industrial Robot, 37(6), 498-502.

Yashoda, H.M., Prabha, T.N. & Tharanathan, R.N. (2007). Mango ripening - Role of carbohydrases in tissue softening. Food Chemistry, 102(3), 691-698.

Zaharah, S.S., Singh, Z., Symons, G.M. & Reid, J.B. (2012). Role of Brassinosteroids, Ethylene, Abscisic Acid, and Indole-3-Acetic Acid in Mango Fruit Ripening. Journal of plant growth regulation, 31(3), 363-372.

http://www.lacquey.nl, available at web page accessed 19/1/2015.

3.2.2. Chapter VI.

Integration of simultaneous tactile sensing and visible and near-infrared reflectance spectroscopy in a robot gripper for mango quality assessment

Cortés, V.[1], Blanes, C.[2], Blasco, J.[3], Ortiz, C.[4], Aleixos, N.[5], Mellado, M.[2], Cubero, S.[3] & Talens, P.[1]

[1]Departamento de Tecnología de Alimentos. Universitat Politècnica de València. Camino de Vera s/n, 46022, Valencia (Spain).

[2]Instituto de Automática e Informática Industrial. Universitat Politècnica de València. Camino de Vera s/n, 46022, Valencia (Spain).

[3]Centro de Agroingeniería. Instituto Valenciano de Investigaciones Agrarias (IVIA). Ctra. CV-315, km. 10,7, 46113, Moncada, Valencia (Spain).

[4]Departamento de Ingeniería Rural y Agroalimentaria. Universitat Politècnica de València. Camino de Vera s/n, 46022, Valencia (Spain).

[5]Departamento de Ingeniería Gráfica, Universitat Politècnica de València. Camino de Vera s/n, 46022, Valencia (Spain).

Biosystems Engineering, 162 (2017), 112-123

ABSTRACT

Development of non-destructive tools for determining mango ripeness would improve the quality of industrial production postharvest processes This study addresses the creation of a new sensor that combines the capability of obtaining mechanical and optical properties of the fruit simultaneously. It has been integrated in a robot gripper that can handle the fruit obtaining non-destructive measurements of firmness, incorporating two spectrometer probes to simultaneously obtain reflectance properties of the visible and near infrared and two accelerometers attached to the rear side of two fingers. Partial least square regression was applied to different combinations of the spectra data obtained from the different sensors to determine the combination that provides the best results. Best prediction of ripening index was achieved using both spectral measurements and two finger accelerometers signals, with R^2_p = 0.832 and RMSEP of 0.520. These results demonstrate that simultaneous measurement and analysis of the data fusion set improves the robot gripper features, allowing assessment the quality of the mangoes during pick and place operations.

Keywords: spectrometry, chemometrics, non-destructive sensor, tactile sensor, accelerometer

1. INTRODUCTION

Mango (*Mangifera indica L.*) is a tropical fruit marketed throughout the world with a very high economic importance (Calatrava, 2014; Luke, 2013) and is generally harvested a little before the fully mature stage to avoid the onset of climacteric respiration during transportation to distant markets (Jha *et al.*, 2007). Therefore, mango requires a ripening period before it achieves the taste and texture desired at the time of consumption (Cortés *et al.*, 2016). The ripening process, and hence the organoleptic quality, is regulated by genetic and biochemical events that result in biochemical changes such as the biosynthesis of carotenoids (Mercadante & Rodriguez-Amaya, 1998), loss of ascorbic acid (Hernández *et al.*, 2006), increase in total soluble solids (Padda *et al.*, 2011); physical changes in mass, size, shape, firmness and colour etc. (Kienzle *et al.*, 2011; Ornelas-Paz *et al.*, 2008), and changes in aroma, nutritional content and flavour of the fruit (Giovannoni, 2004). The evaluation of these changes plays an important role for determining the ripening level at harvest, which will decide the market (i.e. domestic, exportation) and/or price of the product. Traditional determination of these changes has required a destructive methodology using specialised equipment, procedures and trained personnel, which results in high analysis costs (Torres *et al.*, 2013). In addition, destructive methods allow only a small set of samples to be analysed to represent the variability of the whole production, though the ideal situation could be only achieved if all fruits are inspected in automated lines (Kondo, 2010). Traditionally, electronic sorters based on computer vision, used in postharvest to inspect the quality of the fruit, work at a very high speed, analysing the surface of the fruits but not providing any internal inspection. The most advanced and innovative sorters can incorporate NIR technology for testing the internal properties of produce e.g. Vélez-Rivera *et al.* (2014a) and Vélez-Rivera *et al.* (2014b) developed computer vision techniques to determine damages and ripeness of mango 'Manila' through colour measurements. However light is projected on to the fruit from a fixed distance and the reflected or transmitted light is also measured at a certain fixed distance from the fruit. As the fruits have different sizes and shapes, the measurements can be strongly influenced by these features.

Robots have enormous potential to automate production in the food sector (Blasco *et al.*, 2003; Wilson, 2010). Their main current function is to transport and

manipulate objects but they have clear difficulties when handling soft and variable products (Bogue, 2009). Advances in new robot grippers are allowing their introduction in industrial and manufacturing systems for monitoring and controlling production (Tai *et al.*, 2016). Automation with robots, in primary packaging operations, makes possible to incorporate different sensors that can be used to assess fruits quality. Tactile sensors added to gripper fingers provide the capability to evaluate a product through physical contact (Lee, 1999) and have been used for classifying aubergine (Blanes *et al.*, 2015a) and to assess the firmness of mangoes cv. 'Osteen' (Blanes *et al.*, 2015b) with a good prediction performance of the PLS model (R^2_P = 0.760 and RMSEP = 17.989).

Visible and near-infrared spectroscopy combined with multivariate analysis has been widely used for quantitative determination of several internal properties or compounds, to determine ripeness, and to measure quality indices in fruits in general and in mango in particular (Schmilovitch *et al.*, 2000; Theanjumpol *et al.*, 2013; Jha *et al.*, 2013; Cortés *et al.*, 2016). Cortés *et al.* (2016) predicted, in a laboratory, the internal quality index for cv. 'Osteen' mangoes using visible and near-infrared spectrometry (VIS-NIR) obtaining good results with the full spectral range and some selected wavelengths (R^2_P = 0.833 and R^2_P = 0.815, respectively). Thus, incorporating the capability of performing spectral measurements to gripper fingers in combination with other sensors would multiply the possibilities of measuring internal fruit quality when the fruit is handled. However, this would require development of sensor fusion techniques to obtain the maximum value from the combined information of all the sensors, and avoid redundancy (Cimander *et al.*, 2002).

Furthermore, sensor fusion enables rapid and economical in-line implementation for fruit quality assessment (Ignat *et al.*, 2015). Multiple sensors have been widely used in a variety of fields. Steintmetz *et al.*, (1999) developed a robotic quality inspection system for apples that included a colour camera and NIR spectroscopy to predict sugar content using sensor fusion techniques. Since then, significant advances in the field of sensor fusion for food products have been developed, for example in computer vision and near-infrared spectroscopy to assess fish freshness (Huang *et al.*, 2016), fusion of impedance e-tongue and optical spectroscopy to determine the botanical origin of honey (Ulloa *et al.*, 2013),

sensor fusion of electronic nose and acoustic sensor to improve mango ripeness classification (Zakaria *et al.*, 2012) and fusion of electronic nose, near-infrared spectrometer and standard bioreactor probes to monitor yoghurt fermentation (Cimander *et al.*, 2002). Hitherto, examples of combination of visible and near-infrared spectroscopy spectral data and tactile sensors in a robot gripper are non-existent. Therefore, getting a sensor fusion system integrating tactile and spectral properties of the fruit would be a key advance for the post-harvest industry.

Thus, the aim of this study is to develop a novel robotic gripper that incorporates accelerometers and fibre-optic probes coupled to a spectrometer to analyse the mango ripening state by simultaneously measuring firmness and visible and near-infrared reflectance when the fruit is handled in the packing house during postharvest operations.

2. MATERIALS AND METHODS

2.1. Experimental procedure

A batch of 275 unripe mangoes (*M. indica L.*, cv. 'Tommy Atkins') were selected with similar size and colour and free of external damage. During the experiments, fruits were ripened in a storage chamber at 20.0 ± 2.1 ºC and 67.6 ± 3.3% RH and fruits were divided into sets of 45 fruits each (sets marked as M1, M2, M3, M4, M5 and M6). Every 2-3 days one set was analysed, starting with set M1, until the last set M6 reached senescence (18 days). All the mangoes in each set were handled by the robotic gripper to obtain non-destructive measurements and later their physicochemical properties (total soluble solids, titratable acidity and destructive firmness) were evaluated. Prior to the measurements, the temperature of the mangoes was stabilised at 24 ± 1 ºC.

2.2. Reference analysis

Routine methods were used to determine the quality attributes of the mangoes. Mango firmness was measured using a Universal Testing Machine (TextureAnalyser-XT2, Stable MicroSystems (SMS), Haslemere, England) through puncture tests using a 6 mm diameter cylindrical probe (P/15ANAMEsignature) until a relative deformation of 30% of fruit size, at a speed of 1 mm/s. Two

measurements were performed per fruit, on opposite sides of the equator. The fracture strength (F_{max}, N) was also obtained for all samples.

The total soluble solids (TSS) content was determined by refractometry (%) with a digital refractometer (set RFM330+, VWR International Eurolab S.L Barcelona, Spain) at 20 ºC with a sensitivity of ±0.1 ºBrix. Samples were analysed in triplicate.

The analysis of the titratable acidity (TA) was performed with an automatic titrator (CRISON, pH-burette 24, Barcelona, Spain) with 0.5 N NaOH until a pH of 8.1 (UNE34211:1981), using 15 g of crushed mango which was diluted in 60 mL of distilled water. The TA was determined based on the percentage of citric acid that was calculated using equation 1.

$$TA\ [g\ citric\ acid/100g\ of\ the\ sample]=((A\times B\times C/D)\times 100))/E \quad (1)$$

where A is the volume of NaOH consumed in the titration (in L), B is the normality of NaOH (0.5 N), C is the molecular weight of citric acid (192.1g/mol), D is the weight of the sample (15 g) and E is the valence of citric acid (E = 3).

A multi-parameter ripening index (RPI) was calculated using equation 2, described previously by Vásquez-Caicedo, *et al.* (2005) and Vélez-Rivera, *et al.* (2014b):

$$RPI = \ln(100 \cdot F_{max} \cdot TA \cdot TSS^{-1}) \quad (2)$$

where F_{max} is the fracture strength (N), TSS is the total soluble solids (g soluble solids per 100 g of sample) and TA is the titratable acidity (g citric acid equivalent per 100 g of sample).

This index was then used as reference to test the measurements obtained by the robot gripper.

2.3. Robot gripper

A robot gripper has been specifically developed to handle quasi-spherical fruit and was programmed in these experiments to work with mango fruits. The gripper has four fingers: *FA1*, *FA2*, *FB1* and *FB2* (Figure 1). The design of the

gripper fingers and its mechanical configuration can adapt to a wide range of varied shapes during handling, and provides a good performance of the accelerometers as intrinsic tactile sensors (Blanes *et al.*, 2016). The *FA2*, which has a hemispherical concave shape, is attached to the chassis of the gripper and linked by a ball joint. The *FA1* is linked to a pneumatic cylinder (DSN 10-80P, Festo, Germany) with a float joint and has straight motion aligned with *FA2*. The *FB1* and *FB2* are linked to their respective pneumatic cylinders (CD85N10-50B, SMC, Japan) with two float joints and move on parallel paths. *FA1*, *FB1* and *FB2* have pads of a latex membrane filled with sesame seeds. Each pad is soft when its internal pressure is atmospheric or slightly higher and hard when its internal pressure is lower than atmospheric. The design of these fingers allows the gripper to adapt to every mango shape while it is grasped. The gripper was attached to a delta robot (IRB 340, Flexpicker, ABB, Switzerland).

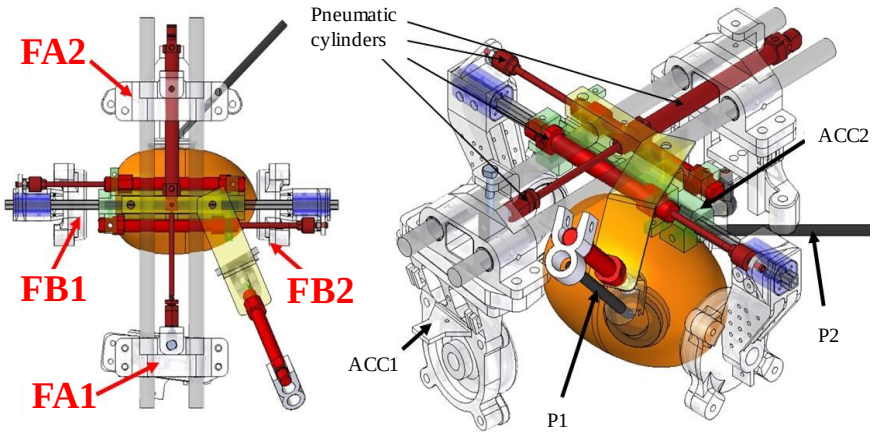

Figure 1. Robot gripper with the accelerometers (*ACC1* and *ACC2*) and the VIS-NIR spectrometer probes (*P1* and *P2*).

In addition, the gripper was equipped with two types of sensors, two accelerometers (*ACC1* and *ACC2*) and two reflectance probes (*P1* and *P2*). The signals captured by the sensors were recorded in a laptop by means of a data acquisition module (USB 6210, National Instruments, USA) in the case of accelerometers, and a multichannel VIS-NIR spectrometer platform (AVS-

DESKTOP-USB2, Avantes BV, The Netherlands) for the reflectance probes (Figure 2).

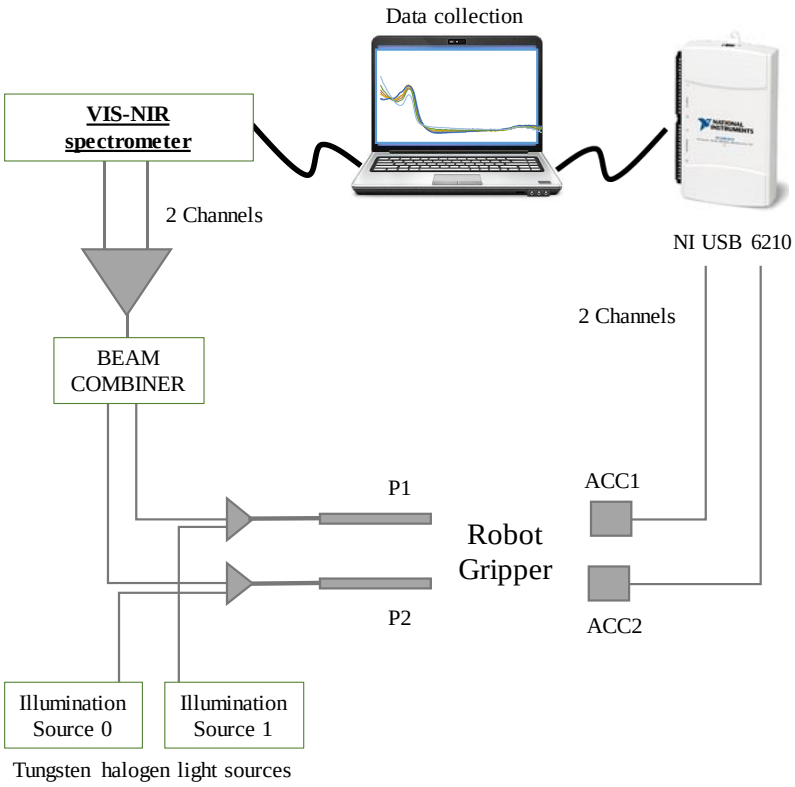

Figure 2. Diagram of the robot gripper, the sensors and the devices used to connect the sensors to the laptop.

Accelerometers *ACC1* and *ACC2* were joined to the rear side of the *FA1* and *FA2* respectively. They are intrinsic tactile sensors because they are not in direct contact to every manipulated mango. *P2* was attached to the *FA2* through a hole made in this finger. It was able to collect data as soon as both *FA1* and *FA2* were closed. Once *FA1* and *FA2* grasp a mango, *P1* approximates by means of the pneumatic cylinder action (C85E10-40, SMC, Japan). This probe was linked to the pneumatic cylinder rod by means of a ball joint. Ball joints allowed the probes to adapt to the shape of every different mango since they can rotate freely around

three rotation axes. Due to the mechanical configuration of the gripper, the sensors took measurements at different points over the surface of every mango (Figure 3).

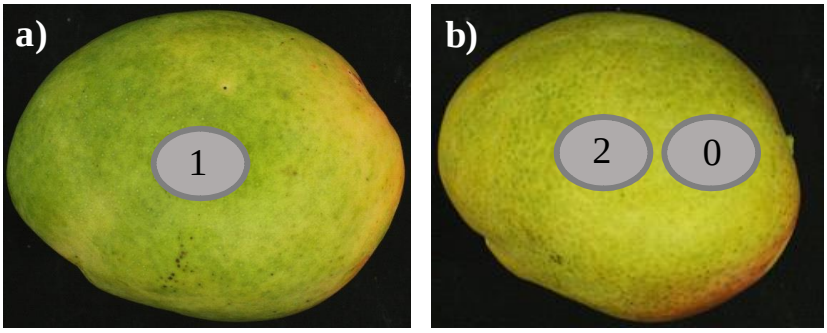

Figure 3. Non-destructive measurements in fruit by sensor fusion side view a) and b) (0: acquisition point of VIS-NIR spectrum with *P1*; 1: acquisition point of VIS-NIR spectrum with *P2* and the accelerometer *ACC2*; 2: acquisition point of the accelerometer *ACC1*.

2.3.1. VIS-NIR reflectance signals

Each reflectance probe, consisting of seven fibres with a diameter of 200 mm, delivered light to the sample through a bundle of six fibres, and collected the reflected light through the seventh one. The probe tip was designed to provide reflectance measurements at an angle of 45º so as to avoid specular reflectance from the surface of the fruit.

The spectra of mango samples were collected in reflectance mode using the multichannel spectrometer platform equipped with two detectors and a quartz beam splitter (BSC-DA, Avantes BV, The Netherlands). The first detector (AvaSpec-ULS2048 StarLine, Avantes BV, The Netherlands) included a 2048-pixel charge-coupled device (CCD) sensor (SONY ILX554, SONY Corp., Japan), 50 mm entrance slit and a 600 lines mm^{-1} diffraction grating covering the working visible and near-infrared (VNIR) range from 600 nm to 1100 nm with a spectral FWHM(full width at half maximum) resolution of 1.15nm. The spectral sampling interval was 0.255 nm. The second detector (AvaSpec-NIR256e1.7 NIRLine, Avantes BV, The Netherlands) was equipped with a 256 pixel non-cooled InGaAs (Indium Gallium Arsenide) sensor (Hamamatsu 92xx, Hamamatsu Photonics K.K., Japan), a 100 mm entrance slit and a 200 lines mm^{-1} diffraction grating covering

the working NIR range from 900 nm to 1750 nm and a spectral FWHM resolution of 12 nm. The spectral sampling interval was 3.535 nm. Two Y shaped fibre-optic reflectance probes (*P1* and *P2*) (FCR-7IR200-2-45-ME, Avantes BV, The Netherlands) were configured each with an illumination leg which connects the fibre-optic probe to stabilised 10Wtungsten halogen light sources (AvaLight-HALS, Avantes BV, The Netherlands). The light sources ensure a permanent light intensity over the whole measurement range. The other leg of the Y-fibre-optic probe was connected to a beam combiner (BSC-DA, Avantes BV, The Netherlands) which converted the two light beams into one light beam. Only this light beam was transmitted through another Y-shaped fibre optic probe to both detectors for simultaneous measurement.

The calibration was performed using a 99 % reflective white reference tile (WS-2, Avantes BV, The Netherlands) so that the maximum reflectance value over the range of wavelengths was around 90 % of saturation. The integration time was set to 240 ms for the VNIR detector and to 4200 ms for the NIR detector due the different features of both detectors. For both detectors, each spectrum was obtained as the average of five scans to reduce the thermal noise of the detector (Nicolaï *et al.*, 2007). The average reflectance measurements of each sample (S) were then converted into relative reflectance values (R) with respect to the white reference using dark reflectance values (D) and the reflectance values of the white reference (W), as shown in equation 3:

$$R = \frac{S-D}{W-D} \quad (3)$$

The dark spectrum was obtained by turning off the light source and completely covering the tip of the reflectance probe.

2.3.2. Accelerometer signals

The accelerometers used (ADXL278, Analog Devices, USA) have a measurement range of ±50 g. They are capable of sensing collisions and, motoring and control vibration. Only the deceleration signals of the axes normal to the fingers were collected. They were sampled during approximately 0.27 s at 30 kHz and low-pass filtered (Figure 4a), but only less than 0.1 s of signal was used for

analysing the tactile sensor responses. These signals were only processed between t_0 (0.0366 s) and t_1 (0.08 s) (Figure 4b) to capture the first contacts of the gripper fingers with every mango. Signals were rearranged using the maximum values as reference, for in this way maximum values will always be at 0.0125 s. Signals were also cut to collect 0.0315 s (Figure 4c) and were transformed by Fast Fourier Transform using LabVIEW 11.0 (National Instruments, USA), using the option measurement magnitude root main square with Hanning window, in order to obtain the frequency distribution of energy (Figure 4d).

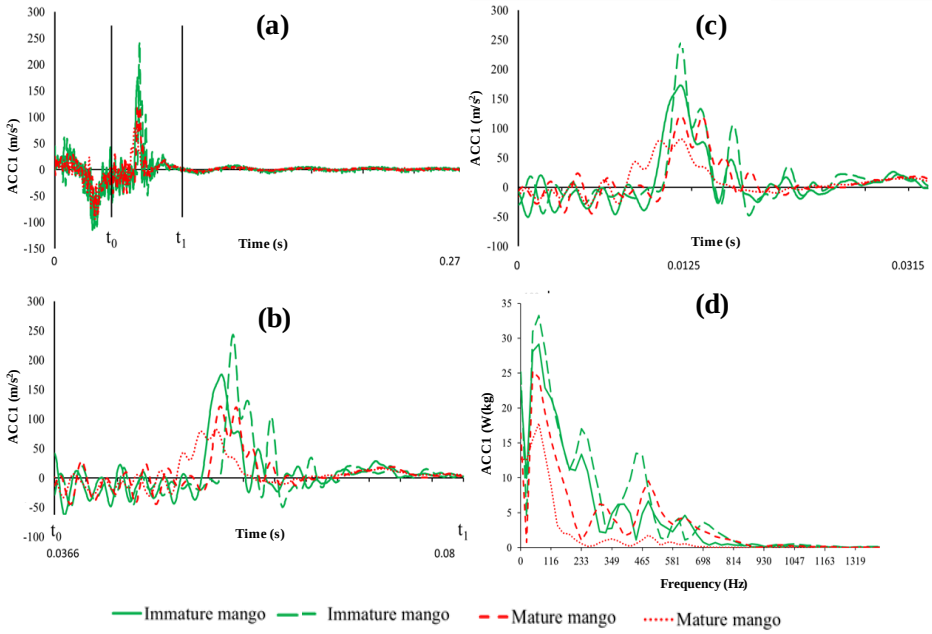

Figure 4. An example of the process done for processing deceleration signals as tactile sensors. (a) Original collected signals for decelerations of *FA1* for mangoes with different ripeness state, (b) cut signal between t_0 and t_1 and (c) signals reordered around the maximum values and (d) the spectra of the signals.

2.4. Robot gripper process and signal acquisition

A robot program controls every grasping and sensing operation of the gripper. Three electrovalves (SY3120, SMC, Japan) were used, one for the motion of *FA1*, one the motion of *FB1* and *FB2* and the last for moving the *P2*. Two

adjustable flowmeter control valves (AS2201F-01-04S, SMC, Japan) were used to adjust the speed of *FA1* and *P2*. A vacuum generator with blow function (VN-07-H-T3-PQ2-VQ2-RO1-B, Festo, Germany) provides the possibility of controlling the hardness of *FA1* by means of its internal valves 2 and 4. The data acquisition device used to collect the accelerometer signals starts to collect data when the robot sends the signal to close *FA1*.

When the gripper is at the approach position to grasp a mango, valve 1 is activated for closing *FA1*. After 0.3 s, valve 2 is activated for 0.05 s to change the pad of *FA1* to a softer state. During this time, valve 1 is deactivated to open *FA1*. Then, the signals of the valves 1 and 3 are activated to close *FA1*, *FB1* and *FB2* during 0.3 s and the pad of *FA1* changes to a harder state (valve 4 activated) and waits for 0.5 s. This process adapts the pad of *FA1* to every mango shape. The *P2* starts to collect data. The robot moves the gripper up. The pad of the *FA1* is in the hard state and starts an open/close loop (open during 0.05 s, close for 1 s). During this loop, the signals of *ACC1* and *ACC2* are collected. Then, valve 5 is activated, *P1* approaches the mango surface and starts to collect data. The whole process is shown in Figure 5.

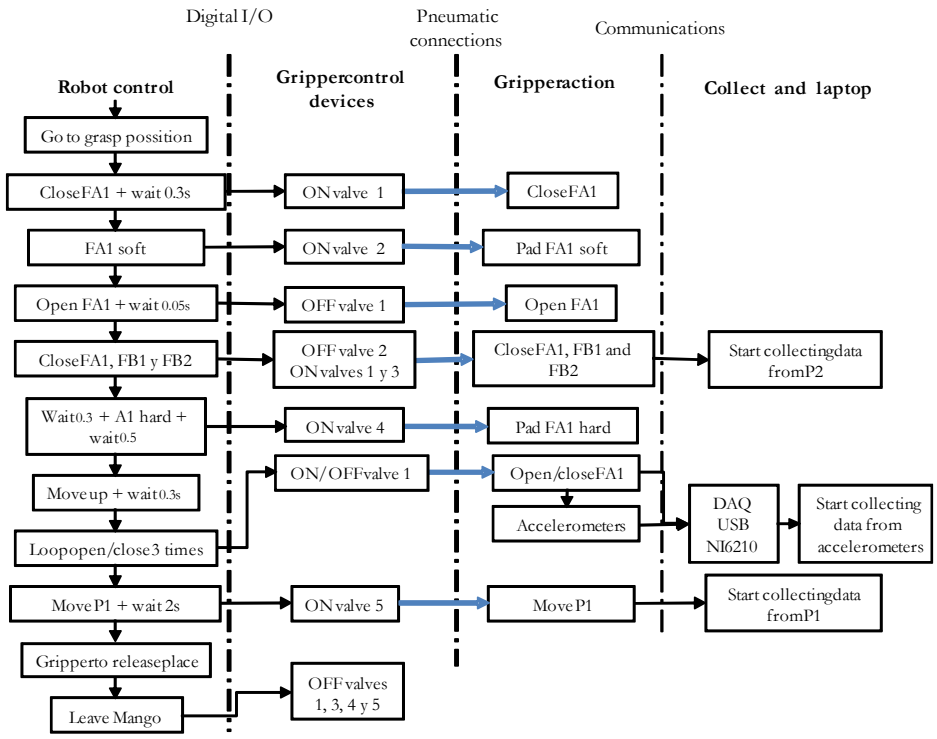

Figure 5. Diagram of the robot control operation the signals over gripper control devices, the gripper action and the collecting data of the sensors.

2.5. Signal pre-processing and statistical analysis

The raw spectra from the spectrometer were transformed to apparent absorbance (log(1/R)) values using The Unscrambler Version 10.2 software package (CAMO Software AS, Oslo, Norway) to obtain linear correlations of the NIR values with the concentration of the estimated constituents (Liu *et al.*, 2009; Shao *et al.*, 2007) and centred by subtracting their averages in order to ensure that all results will be interpretable in terms of variation around the mean.

Figure 6 shows raw VNIR and NIR spectra and its correction after the application of the pre-processing methods. Savitzky-Golay smoothing (with segment size 15) was applied to improve the signal-to-noise ratio in order to reduce the effects caused by the physiological variability of samples (Beghi *et al.*, 2017; Carr *et al.*, 2005). Due to the fresh fruit light scattering (Santos *et al.*, 2013), the light does not always travel the same distance into the sample before it is detected.

A longer light travelling path corresponds to a lower relative reflectance value, since more light is absorbed. This causes a parallel translation of the spectra. This kind of variation is not useful for the calibration models and needs to be eliminated by the EMSC technique (Bruun *et al.*, 2007; He *et al.*, 2007; Martens *et al.*, 2003). In addition to these pre-processing steps, the second derivate with Gap-Segment (2.3) gave the best results for the NIR spectra because it allowed the extraction of useful information (Rodriguez-Saona *et al.*, 2001). The different pre-treatments were applied in the sequence explained, specifying that the first two pre-treatments (smoothing and EMSC) were only applied to the VNIR spectra and those two with the third (second derivate) applied to the NIR spectra (Cortés *et al.*, 2016). Finally, the adjustment to the spectral intensities from each sensor *ACC1*, *ACC2*, *P1* and *P2* was range-normalised so the data from all samples were directly comparable to each other (Andrés & Bona, 2005; Blanco *et al.*, 2006).

The different sensor signals were combined through a 'low-level' fusion procedure (Roussel *et al.*, 2003a,b) by concatenating the pre-processed sensor signals e appending one to another e to create a single matrix with a total of 5516 variables, which was processed using The Unscrambler. Data were organised in a matrix where the rows represent the number of samples (#N = 275 samples) and the columns represent the variables (X-variables and Y-variables). The X-variables, or predictors, were the signals obtained by fusion of the data from the two fibre-optic probes of the spectrometer and the accelerometers. The Y-variable, or response, was the RPI of each sample. In order to correct the relative influences of the different instrumental responses on the model, a standardisation technique was used, where the weight of each X-variable was the standard deviation of the variable (Bouveresse *et al.*, 1996). Then, fifteen regression models for each combination of the spectra data from the different sensors were developed by partial least squares (PLS) to predict RPI. Samples were randomly separated into two groups, and 75% of the samples were used to develop the model that was validated by cross validation, while the remaining samples (25%) were used as the prediction set. The root mean square error of calibration (RMSEC), root mean squared error of cross validation (RMSECV), the root mean square error of prediction (RMSEP), the coefficient of determination for calibration (R_C^2), for

prediction (R_{P2}) and for cross validation (R_{CV}^2), and the required number of latent variables (LV) were used to judge the accuracy of the PLS model.

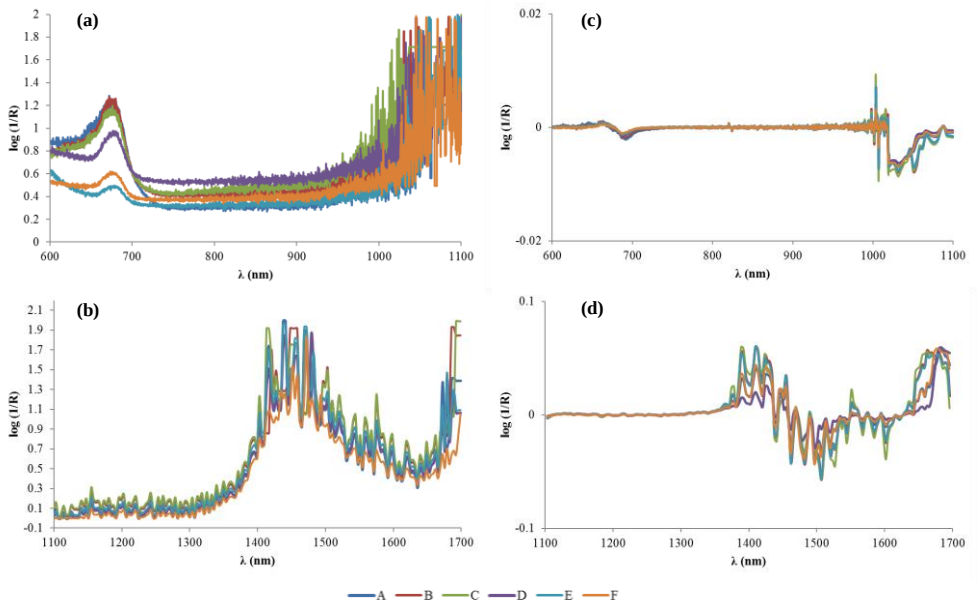

Figure 6. Averaged raw spectra (left) and averaged final spectra obtained with the pre-treatment and transformed signals (right) of the each set for (a,c) the VNIR region; and (b,d) the NIR region.

3. RESULTS AND DISCUSSION

3.1. Changes in mango quality during ripening

The changes observed in the physicochemical characteristics (F_{max}, TSS and TA) of mangoes during postharvest storage are shown in Table 1.

For all sets of mangoes there was a steady decrease in fruit firmness over time starting of around 137 N to fell to 28 N. These changes are due to significant changes in the composition and structure of cell walls and middle lamella due the solubilisation, de-esterification and de-polymerisation of the middle lamella (Singh *et al.*, 2013), and the enzymatic activity (Prasanna *et al.*, 2007; Yashoda *et al.*, 2007). A similar behaviour has been reported for other mango varieties such as 'Alphonso' (Yashoda *et al.*, 2005), 'Ataulfo' (Palafox-Carlos *et al.*, 2012), 'Keitt' (Ibarra-Garza *et al.*, 2015) or 'Osteen' (Cortés *et al.*, 2016). Similarly, the TA tends

to decrease due to the cell metabolisation of volatile organic acids and non-volatile constituents (Padda *et al.*, 2011) and in addition acids can be used as substrates for respiration when sugars have been consumed or participated in the synthesis of phenolic compounds, lipids and volatile aromas (Abu-Goukh *et al.*, 2010). In contrast, the TSS increased continuously during postharvest storage due to the conversion of starch to glucose and fructose, which are used as substrates during fruit respiration (Eskin *et al.*, 2013). Similar results have been observed by Quintana *et al.* (1984) who reported that TSS of mango increased gradually up to full ripeness.

RPI was calculated for every day of storage. Figure 7 shows the evolution of the RPI through median plots with 95 % confidence intervals during the storage. It can be observed that the values of the index clearly decreased during ripening. Initially, the RPI decline sharply when the fruits ripen to achieve their optimum organoleptic properties, and then, fruit reach the stage of over ripeness where the curve follows a constant trend because the product reaches a maximum content of TSS and minimum firmness and TA.

Table 1. Descriptive statistics for the quality parameters analysed in mango samples during the storage period.

		Set A	Set B	Set C	Set D	Set E	Set F
Mechanical properties	F_{max} (N)	137 ± 18^{a}	62 ± 16^{b}	45 ± 16^{c}	34 ± 11^{d}	35 ± 8^{d}	28 ± 8^{e}
Internal composition	TSS (%)	10.4 ± 0.9^{a}	$12\pm1^{b,c}$	$12\pm1^{c,d}$	12 ± 1^{d}	12 ± 1^{b}	$12\pm2^{b,c}$
	TA (%)	0.8 ± 0.2^{a}	0.62 ± 0.15^{b}	0.41 ± 0.08^{c}	0.30 ± 0.06^{d}	0.29 ± 0.06^{d}	0.19 ± 0.05^{e}

Values are mean ± SD.
a–e Different superscripts in the same row indicate significant difference among sets ($p < 0.05$).

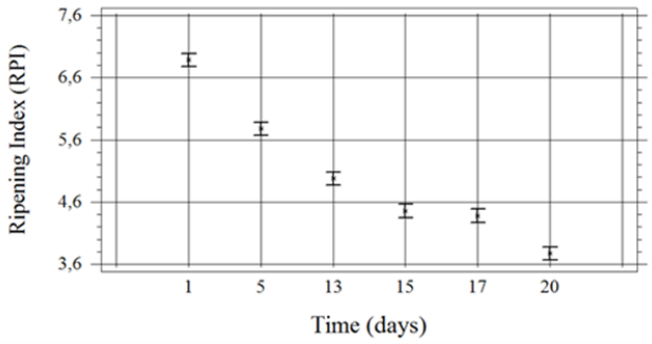

Figure 7. Evolution of the RPI during storage period of the mango samples.

3.2. Non-destructive prediction of mango ripening

The data were concatenated (accelerometers and VIS-NIR spectra) (Decruyenaere *et al.*, 2009; Roussel *et al.*, 2003a,b) to form a representative complex spectrum with a total of 5516 variables. Table 2 shows the results of the validation and prediction results of the PLS models built for the data obtained by every single sensor and for the data fusion performed among all possible combination of spectra data.

The best PLS model for prediction of RPI is presented in the Figure 8. Figure 9 shows the regression coefficients of the best developed model and the PRESS plot for identifying the optimum number of LVs. The results for this model were obtained using VIS-NIR fibre-optic probes and the two accelerometer signals. The calibration model for predicting RPI has an R^2_C = 0.945 and RMSEC = 0.235, and the validation of the calibration model has an R^2_{CV} = 0.804 and RMSECV = 0.447. The prediction model indicates a good prediction performance, with R^2_p = 0.832 and RMSEP = 0.520.

Table 2. Comparison of the prediction of mango ripening provided by different possible combination of sensor fusion to the two fibre-optic probes of VIS-NIR spectrometer and two accelerometers located at the fingers of the robot gripper.

		Calibration set				Prediction set	
Sensors	**#LV**	**R^2_C**	**RMSEC**	**R^2_{CV}**	**RMECV**	**R^2_P**	**RMSEP**
P2	1	0.769	0.506	0.742	0.537	0.732	0.663
P1	3	0.895	0.323	0.739	0.512	0.632	0.727
P2+ P1	3	0.933	0.268	0.782	0.487	0.802	0.554
ACC1	6	0.677	0.574	0.575	0.663	0.444	0.871
ACC2	4	0.611	0.626	0.48	0.727	0.300	1.020
ACC1 + ACC2	4	0.758	0.758	0.595	0.595	0.655	0.737
P2+ ACC1	2	0.854	0.373	0.77	0.471	0.778	0.613
P2+ ACC2	1	0.695	0.586	0.649	0.632	0.733	0.665
P1 + ACC1	4	0.940	0.251	0.753	0.513	0.662	0.698
P1 + ACC2	5	0.971	0.175	0.776	0.493	0.662	0.742
P2 + P1 + ACC1	4	0.973	0.166	0.786	0.467	0.797	0.550
P2 + P1 + ACC2	2	0.867	0.379	0.777	0.494	0.784	0.595
P2 + ACC1 + ACC2	2	0.813	0.460	0.705	0.580	0.813	0.567
P1 + ACC1 + ACC2	5	0.971	0.176	0.779	0.490	0.733	0.642
P2 + P1 + ACC1 + ACC2	3	0.945	0.235	0.804	0.447	**0.832**	0.520

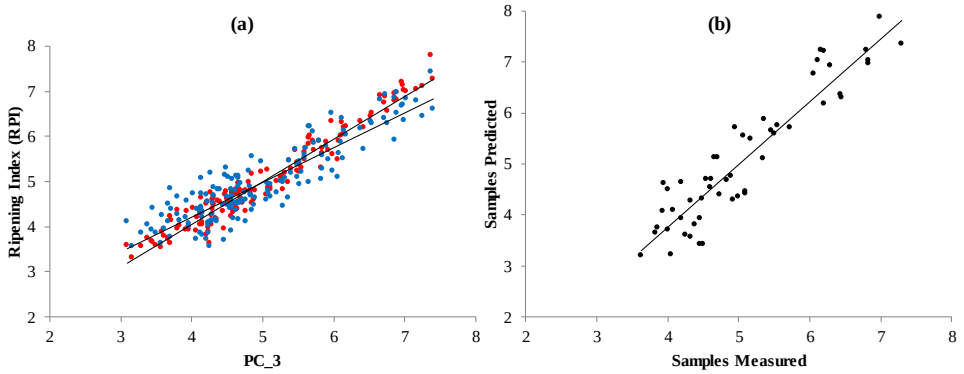

Figure 8. Performance of the PLS model (a) cross validation, respectively: calibration samples (blue) and validation samples (red), and (b) prediction of the RPI in mango cv. 'Tommy Atkins', built using the data from all the probes and accelerometers four sensors which resulted the best combination.

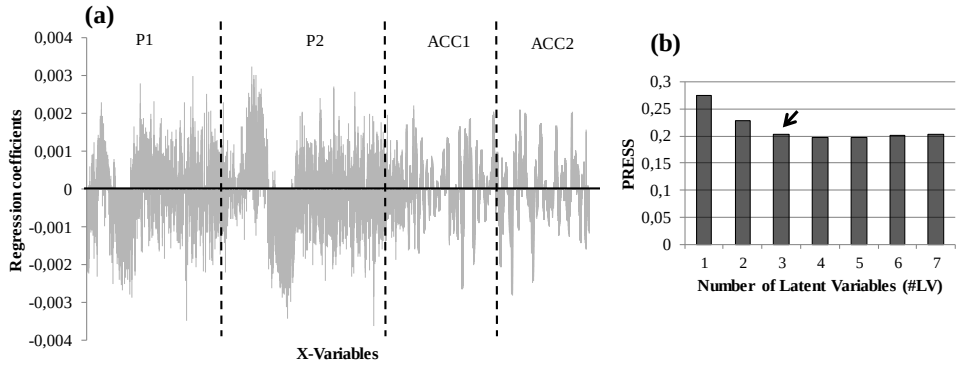

Figure 9. (a) Regression coefficients of three-components PLS model containing the fused individual matrices of the calibration set as X-variables and the RPI as the Y-variables. (b) The number of latent variables of the same model.

3.3. Integration of tactile sensing and reflectance data in the robot gripper

This novel gripper presents an important evolution from previous grippers for sensing and handling the firmness of aubergines and mangoes by using accelerometers as tactile sensors (Blanes, Ortiz, *et al.*, 2015; Blanes, Cortés, *et al.*, 2015). Unlike these previous grippers, which caused damage in some over-ripe mangoes due to the action of a suction cup needed for holding the fruits, this new

gripper incorporates four fingers and intrinsic sensors that avoid the need of a suction cup when holding the fruit for measurement and placing.

Besides, the combination of the two probes achieved better results than *P2* or *P1* alone, having a R^2_p of 0.802 compared to 0.732 and 0.632 respectively. In the same way, *ACC1* together with *ACC2* had better result than *ACC1* or *ACC2* alone with R^2_p of 0.655 compared to 0.444 and 0.300 respectively. It is important to remark that the composition of a fruit is not uniform and hence some parts of the mango may have different ripeness than others. Therefore, it is necessary to take simultaneous measurements at least for the three points studied to obtain reliable and robust results. Blanes *et al.* (2015b) developed gripper with three accelerometers to estimate the ripeness of mangoes cv. 'Osteen' achieving a R^2_p = 0.760 which is lower than the current robot gripper (R^2_p = 0.832). This highlights the important contribution of the integration of both tactile sensors and VNIR reflectance measurements in the robotic gripper to assess the quality of the mangoes during fruit handling.

A handicap of this system in the current version is the long time needed to process every mango. The incorporation of two spectrometer probes increases the processing time of every mango up to 9 s. However, experiments have been done in a first prototype for testing, where the algorithms, hardware and processes were not optimised for working at high speed. With improved integration of the hardware, optimising algorithms and parallelising some processes, the whole process could experience a dramatic reduction of the operation time. On the other hand, the combination of sensors of different nature provides the capability of obtaining simultaneously both mechanical and optical properties of the fruit. This innovative approach is highly interesting in the emerging competitive food sector where monitoring of product quality, reproducibility and traceability is decisive in manufacturing (Kondo, 2010).

4. CONCLUSIONS

A novel robot gripper equipped with sensors, i.e. with two accelerometers and two VIS-NIR reflectance probes, has been developed and tested for fruit handling. The design uses sensors that do not need direct contact, are intrinsic tactile sensors, and can take the measurements simultaneously during the mango

handling, which is an important advantage over the state of the art. The results show good prediction of the quality of the fruit, using a ripening index based on the information from VIS-NIR spectra and non-destructive impact measured during handling, achieving an R^2_p of 0.832 and RMSEP of 0.520. This innovative prototype integrates sensors of different nature, whose data information is combined to obtain better prediction. The fusion of different types of sensors like spectrometry (electromagnetic) and accelerometers (vibrational) achieved better results than using only the accelerometers, or similar results to using spectroscopy, but in this case, the measurements were made while the fruit was handled. In this way, results show the potential and advantages of performing simultaneous operations with sensors of different nature integrated on a robot gripper that can inspect and classify the mangoes by their ripeness during a pick and place robot process.

Acknowledgements

This work has been partially funded by the Instituto Nacional de Investigación y Tecnología Agraria y Alimentaria de España (INIA) and FEDER through research projects RTA2012-00062-C04-01, RTA2012-00062-C04-02, RTA2012-00062-C04-03, and by the Conselleria d' Educació, Investigació, Cultura i Esport, Generalitat Valenciana, through the project AICO/2015/122. V. Cortés thanks the Spanish MEC for the FPU grant (FPU13/04202).

5. REFERENCES

Abu-Goukh, A.A., Shattir, A.E. & Mahdi, F.M. (2010). Physico-chemical changes during growth and development of papaya fruit. II: Chemical changes. Agriculture and Biology Journal of North America, 2151-7517.

Blanes, C., Cortés, V., Ortiz, C., Mellado, M. & Talens, P. (2015b). Non-destructive assessment of mango firmness and ripeness using a robotic gripper. Food Bioprocess Technology, 8, 1914-1924.

Blanes, C., Mellado, M. & Beltrán, P. (2016). Tactile sensing with accelerometers in prehensile grippers for robots. Mechatronics, 33, 1-12.

Blanes, C., Ortiz, C., Mellado, M., & Beltrán, P. (2015a). Assessment of Eggplant Firmness with Accelerometers on a Pneumatic Robot Gripper. Computers and Electronics in Agriculture, 113, 44-50.

Bogue, R. (2009). The role of robots in the food industry: a review. Industrial Robot: An International Journal, 36 (6), 531-536.

Bouveresse, E., Hartmann, C., Last, I.R., Prebble, K.A. & Massart, L. (1996). Standardization of Near-Infrared Spectrometric Instruments. Analalytical Chemistry, 68, 982-990.

Cimander, C. & Mandenius, C. (2002). Online monitoring of a bioprocess based on a multi-analyser system and multivariate statistical process modelling. Journal of Chemical Technology and Biotechnology, 77 (19), 1157-1168.

Cimander, C., Carlsson, M. & Mandenius, C.F. (2002). Sensor fusion for on-line monitoring of yoghurt fermentation. Journal of Biotechnology, 99, 237-248.

Cortés, V., Ortiz, C., Aleixos, N., Blasco, J., Cubero, S. & Talens, P. (2016). A new internal quality index for mango and its prediction by external visible and near-infrared reflection spectroscopy. Postharvest Biol. Technol., 118, 148-158.

Eskin, N.A.M., Hoehn, E. & Shahidi, F. (2013). Fruits and vegetables. Eskin, N.A.M., Shahidi, F. (Eds.), Biochemistry of foods, 49-126.

Giovannoni, J.J. (2004). Genetic regulation of fruit development and ripening. Plant Cell, 16, 170-180.

Hernández, Y., Lobo, M.G. & González, M. (2006). Determination of vitamin C in tropical fruits: a comparative evaluation of methods. Food Chemistry, 96 (4), 654-664.

Huang, X., Xu, H., Wu, L., Dai, H., Yao, L. & Han, F. (2016). A data fusion detection method for fish freshness based on computer vision and near-infrared spectroscopy. Analytical Methods, 8, 2929-2935.

Ibarra-Garza, I.P., Ramos-Parra, P.A., Hernández-Brenes, C. & Jacobo-Velázquez, D.A. (2015). Effects of postharvest ripening on the nutraceutical and physicochemical properties of mango (*Mangifera indica L.* cv. Keitt). Postharvest Biology and Technology, 103, 45-54.

Jha, S.N., Chopra, S. & Kingsly, A.R.P. (2007). Modeling of color values for non-destructive evaluation of maturity of mango. Journal of Food Engineering, 78, 22-26.

Jha, S.N., Jaiswal, P., Narsaiah, K., Sharma, R., Bhardwaj, R., Gupta, M. & Kumar, R. (2013). Authentication of mango varieties using near infrared spectroscopy. Agricultural Research, 2 (3), 229-235.

Juriaanse, A.C. (1999). Changing pace in food science and technology: examples from dairy science show how descriptive knowledge can be transferred into predictive knowledge. Trends in Food Science & Technology, 10, 303-306.

Kienzle, S., Sruamsiri, P., Carle, R., Sirisakulwat, S., Spreer, W. & Neidhart, S. (2011). Harvest maturity specification for mango fruit (Mangiferaindica L. 'Chok Anan') in regard to long supply chains. Postharvest Biology and Technology, 61, 41-55.

Kondo, N. (2010). Automation on fruit and vegetables grading system and food traceability. Trends in Food Science & Technology, 21, 145-152.

Lee, M.H. & Nicholls, H.R. (1999). Tactile sensing for mechatronics – a state of the art survey. Mechatronics, 9, 1-31.

Liu, F., Jiang, Y. & He, Y. (2009). Variable selection in visible/near infrared spectra for linear and nonlinear calibrations: A case study to determine soluble solids content of beer. Analytica Chimica Acta, 635, 45-52.

Mercadante, A.Z. & Rodriguez-Amaya, D.B. (1998). Effects of ripening, cultivar differences, and processing on the carotenoid composition of mango. Journal of Agricultural and Food Chemistry, 46 (1), 128-130.

Munawar, A.A., Hörsten, D., Wegener, J. K., Pawelzik, E. & Mörlein, D. (2016). Rapid and non-destructive prediction of mango quality attributes using Fourier transform near infrared spectroscopy and chemometrics. Engineering in Agriculture, Environment and Food, 9, 208-215.

Nicolaï, B.M., Beullens, K., Bobelyn, E., Peirs, A., Saeys, W., Theron, I.K. & Lammertyn, J. (2007). Non-destructive measurement of fruit and vegetable quality by means of NIR spectroscopy: a review. Postharvest Biol. Technol., 46, 99-118.

Ornelas-Paz, J.D.J., Yahia, E.M. & Gardea-Bejar, A.A. (2008). Changes in external and internal color during postharvest ripening of 'Manila' and 'Ataulfo' mango fruit and relationship with carotenoid content determined by liquid chromatography–APcI+-time-of-flight mass spectrometry. Postharvest Biology and Technology, 50 (2), 145-152.

Padda, S.M., do Amarante, C.V.T., Garcia, R.M., Slaughter, D.C. & Mitcham, E.M. (2011). Methods to analyze physicochemical changes during mango ripening: a multivariate approach. Postharvest Biology and Technology, 62, 267-274.

Palafox-Carlos, H., Yahia, E., Islas-Osuna, M.A., Gutierrez-Martinez, P., Robles-Sánchez, M. & González-Aguilar, G.A. (2012). Effect of ripeness stage of mango fruit (Mangifera indica L., cv. Ataulfo) on physiological parameters and antioxidant activity. Science Horticultural, 135 (0), 7-13.

Prasanna, V., Prabha, T.N. & Tharanathan, R.N. (2007). Fruit ripening phenomena-an overview. Critical Reviews in Food Science Nutrition, 47, 1-19.

Quintana, E.G, Nanthachai, P., Hiranpradit, H., Mendoza, D.B. & Ketsa, S. (1984). Changes in mango during growth and maturation: Growth and development of mango. ASEAN Food Handling Bureau, 21-27.

Roussel, S., Bellon-Maurel, V., Roger, J.M. & Grenier, P. (2003). Fusion of aroma, FT-IR and UV sensor data bsed on the Bayesian inference. Application to the discrimination of white grape varieties. Chemometrics and Intelligent Laboratory Systems, 65 (2), 209-219.

Santos, J., Trujillo, L.A., Calero, N., Alfaro, M.C. & Muñoz, J. (2013). Physical characterization of a commercial suspoemulsion as a reference for the development of suspoemulsions. Chemical Engineering & Technology, 11, 1-9.

Schmilovitch, Z., Mizrach, A., Hoffman, A., Egozi, H. & Fuchs, Y. (2000). Determination of mango physiological indices by near-infrared spectrometry. Postharvest Biology and Technology, 19 (3), 245-252.

Shao, Y., He, Y., Gómez, A.H., Pereir, A.G., Qiu, Z. & Zhang, Y. (2007). Visible/near infrared spectrometric technique for nondestructive assessment of tomato 'Heatwave' (Lycopersicumesculentum) quality characteristics. Journal of Food Engineering, 81 (4), 672-678.

Singh, P.C., Singh, R.K., Smith, R.S. & Nelson, P.E. (1997). Evaluation of in-line sensors for selected properties measurements in continuous food processing. Food Control, 8, 45-50.

Singh, Z., Singh, R.K., Sane, V.A. & Nath, P. (2013). Mango–Postharvest biology and biotechnology. Crit. Rev. Plant Sci., 32 (4), 217-236.

Steinmetz, V., Roger, J. M., Moltó, E. & Blasco, J. (1999). On-line fusion of colour camera and spectrophotometer for sugar content prediction of apples. Journal of Agricultural Engineering Research, 73 (2), 207-216.

Tai, K., El-Sayed, A. R., Shahriari, M., Biglarbegian, M. & Mahmud, S. (2016). State of the art robotic grippers and applications. Robotics, 5 (2), 11.

Theanjumpol, P., Self, G., Rittiron, R., Pankasemsu, T. & Sardsud, V. (2013). Selecting variables for near infrared spectroscopy (NIRS) evaluation of mango fruit quality. Journal of Agricultural Science, 5 (7), 146-159.

Torres, R., Montes, E.J., Perez, O.A. & Andrade, R.D. (2013). Relación del color y del estado de madurez con las propiedades fisicoquímicas de frutas tropicales. Información Tecnológica, 24 (4), 51.

Ulloa, P.A., Guerra, R., Cavaco, A.M., Rosa da Costa, A.M., Figueira, A.C. & Brigas, A.F. (2013). Determination of the botanical origin of honey by sensor fusion of impedance e-tongue and optical spectroscopy. Computers and Electronics in Agriculture, 94, 1-11.

Vásquez-Caicedo, A.L., Sruamsiri, P., Carle, R. & Neidhart, S. (2005). Accumulation of all-trans-b-carotene and its 9-cis and 13-cis stereoisomers during postharvest ripening of nine Thai mango cultivars. Journal of Agricultural and Food Chemistry, 53, 4827-4835.

Vélez-Rivera, N., Blasco, J., Chanona-Pérez, J., Calderón-Domínguez, G., Perea-Flores, M.J., Arzate-Vázquez, I., Cubero, S. & Farrera-Rebollo, R. (2014b). Computer vision system applied to classification of 'Manila' mangoes during ripening process. Food Bioprocess Technology, 7, 1183-1194.

Vélez-Rivera, N., Gómez-Sanchis, J., Chanona-Pérez, J., Carrasco, J.J., Millán-Giraldo, M., Lorente, D., Cubero, S. & Blasco, J. (2014a). Early detection of mechanical damage in mango using NIR hyperspectral images and machine learning. Biosystems Engineering, 122, 91-98.

Wilson, M. (2010). Developments in robot applications for food manufacturing. Industrial Robot: An International Journal, 37 (6), 498-502.

Yashoda, H.M., Prabha, T.N. & mTharanathan, R.N. (2007). Mango ripening-role of carbohydrases in tissue softening. Food Chemistry, 102 (3), 691-698.

Yashoda, H.M., Prabha, T.N. & Tharanathan, R.N. (2005). Mango ripening-chemical and structural characterization of pectic and hemicellulosic polysaccharides. Carbohydrate Research, 340 (7), 1335-1342.

Zakaria, A., Shakaff, A.Y.M., Masnan, M.J., Saad, F.S.A., Adom, A.H., Ahmad, M.N. & Kamarudin, L.M. (2012). Improved maturity and ripeness classifications of magnifera indica cv. harumanis mangoes through sensor fusion of an electronic nose and acoustic sensor. Sensors, 12 (5), 6023-6048.

II.B. In-line Inspection

3.2.3. Chapter VII.

In-line application of visible and near infrared diffuse reflectance spectroscopy to identify apple varieties

Cortés, V.[1], Blasco, J.[2], Aleixos, N.[3], Cubero, S.[2] & Talens, P.[1]

[1]Departamento de Tecnología de Alimentos. Universitat Politècnica de València. Camino de Vera s/n, 46022, Valencia (Spain).

[2]Centro de Agroingeniería. Instituto Valenciano de Investigaciones Agrarias (IVIA). Ctra. CV-315, km. 10,7, 46113, Moncada, Valencia (Spain).

[3]Departamento de Ingeniería Gráfica, Universitat Politècnica de València. Camino de Vera s/n, 46022, Valencia (Spain).

Requested Patent

ABSTRACT

One of the most studied techniques for the non-destructive determination of the internal quality of fruits has been visible and near-infrared (VIS-NIR) reflectance spectroscopy. In the case of apples, it has been applied mostly for internal quality assessment and variety distinction. However, this technique has traditionally been used in laboratory setups for individual fruit inspection. This work evaluates a new non-destructive in-line VIS-NIR spectroscopy prototype to identify five apple varieties, with the advantage that it allows the spectra to be captured with the probe at the same distance from all the fruits regardless of their size. The prototype was tested using varieties with a similar appearance by acquiring the diffuse reflectance spectrum of the samples travelling at a speed of 1 fruit/s. Principal component analysis (PCA) was used to determine the variables that explain the most variance in the spectra. Seven principal components were then used to perform linear discriminant analysis (LDA) and quadratic discriminant analysis (QDA). QDA was found to be the best in-line classification method, achieving 98% and 85% success rates for red and yellow apple varieties, respectively. The results indicated that the in-line application of VIS-NIR spectroscopy that was developed is potentially feasible for the detection of apple varieties with an accuracy that is similar to or better than a laboratory system.

Keywords: apple, in-line, varietal discrimination, visible and near-infrared spectroscopy, non-destructive

1. INTRODUCTION

More than 7500 apple (*malus sp.*, *Rosaceae*) varieties are currently cultivated (Wu *et al.*, 2017) with significant differences in qualities, which makes this one of the most consumed fruits in the world (Ronald & Evans, 2016). Consumers have different tastes and preferences from one country or region to another. However, there are trends that are common to all of them, such as an increasing demand for higher quality, both external and internal. The external properties (presentation, appearance, uniformity, maturity, freshness, etc.) are the main reason governing the purchase decision of fruits, which is normally taken when the consumer sees the products exhibited on the shelves. The internal quality (flavour, aroma, texture, firmness, acidity, sugar content, absence of contaminants, etc.) (Wojdyło *et al.*, 2008) is linked to aspects that are generally not perceptible at first sight, although future purchasing decisions may depend on them. Indeed, because of the variety of consumers, it is difficult to establish a specific definition of quality, but generally a fruit has better quality when it is superior in one or several attributes that meet consumer expectations (Kader *et al.*, 1985). However, no matter how much effort is put into obtaining products with excellent quality, this consumer satisfaction will be defrauded when, either by mistake or by fraud, fruits, like apples, of similar appearance (external quality) but different internal quality are mixed in the market place (López, 2003).

Generally, several varieties of apples can be grown simultaneously in a single apple orchard, and they can be sold at the same time. Therefore, different apple varieties can easily be mixed during harvesting and marketing when they have a similar appearance. Proper identification of fruits has to be done by workers in a subjective and manual way because physical or chemical analytical methods for apple evaluation are expensive and time-consuming. This sorting results in high costs, tediousness and inconsistency associated with human beings (Ronald & Evans, 2016). Therefore, apple sellers need new electronic non-destructive techniques to distinguish apple varieties (Shang *et al.*, 2015). Several non-destructive techniques to discriminate among apple varieties have already been attempted. Visible and near-infrared (VIS-NIR) spectroscopy has been used by different researchers such as He *et al.* (2007), Wu *et al.* (2016), Luo *et al.* (2011), Wu *et al.* (2017) and Song *et al.* (2016). All of these studies only extract

information from the VIS-NIR spectra, or even only from the NIR spectra, of the apples for off-line discrimination among varieties; however, none of them develop in-line applications to classify apple varieties. Such an application is developed in this study through a preliminary in-line prototype. Other non-destructive techniques used to classify apple varieties have been dielectric properties, solid-state sensors (ISFET), digital image analysis or electronic nose. Shang *et al.* (2015) used 160 apples of three varieties in an attempt to discriminate them according to the dielectric spectra measured at laboratory scale. Alonso *et al.* (2003) analysed the ISFET by ions such as calcium, potassium and nitrates, both in apple juice and in in situ apple fruit. Regarding digital image analysis, Sabanci & Ünlersen (2016) and Ronald & Evans (2016) captured apple images and obtained a good classification using the measurement of different properties (colour and size). Finally, an electronic nose was developed by Marrazzo *et al.* (2005), who tested the feasibility of detecting the difference among volatile gases emitted from different intact apple varieties, but good results in terms of the classification of the three varieties was only obtained for day 1. Among these non-destructive methods, the most widely used is VIS-NIR spectroscopy, because it is extremely fast, chemical-free and suitable for in-line use (Wu *et al.*, 2017). The literature contains different studies on the applicability of in-line VIS-NIR spectroscopy. For example, Jie *et al.* (2014) developed an in-line prototype based on the VIS-NIR technology in the range of 687-920 nm for the prediction of the soluble solid content (SSC) of watermelon and achieved rpre of 0.70 and RMSEP of 0.33 ºBrix. Brunt *et al.* (2010) measured the chemical composition of potatoes by an automated semi-industrial system with in-line NIR reflectance. The system was only able to process 12 potato samples per hour, but the starch and the coagulating protein concentrations showed a good NIR prediction. Sun *et al.* (2016) determined the SSC and identified brown core pears simultaneously in-line by VIS-NIR transmittance spectroscopy. The spectra between 600-904 nm were recorded at a moving speed of five samples per second. The classification accuracy of brown core pears was 98.3% and the predictive precision of SSC was around 98%. Similarly, Shenderey *et al.* (2010) evaluated the ability of VIS-NIR mini-spectrometers (400-1000 nm) to detect mouldy core in 'Red Delicious' apples using an in-line development. The accuracy of the classification was higher than 92%

but, in this case, although the apples were in movement, both the probe and the apples were always at fixed positions during the measurements. Salguero-Chaparro *et al.* (2012) evaluated the effect of some parameters, such as focal distance and integration time, on the spectral repeatability for the analysis of intact olive fruits on a conveyor belt in the spectral range of 380-1690 nm using a diode array spectrometer. Regarding this last research, it should be pointed out that one of the major drawbacks hindering the incorporation of technology based on spectroscopy into automated in-line sorters is the large differences in size and shape that can be found from one fruit to another. Since the probe is located at a fixed point, the distance between the probe and the fruit will vary depending on the size of the fruit. However, it is important to ensure that the distance between the probe and the fruit is close enough to obtain a good spectrum, but not so near that it saturates the signal, and this distance must be constant for all objects. If the fruit is very close, the signal saturates even with very low integration times. This is because light practically does not penetrate inside the object and is only reflected on its surface towards the detector. Conversely, a distance of more than 13 mm (Salguero-Chaparro *et al.*, 2012) causes the detector to receive hardly any of the light reflected on the object. In addition, the optical configuration, the intensity of the light and the distance between the probe and the fruit are parameters that greatly influence the depth of penetration of light (Lammertyn *et al.*, 2000). Therefore, to avoid a negative influence on the measurements, it is very important to develop mechanisms to ensure that the distance between the fruit and the probe remains stable for any fruit in the inspection line, regardless of its size or shape. Since there is no previous research about the in-line application of VIS-NIR diffuse reflectance spectroscopy to classify apple varieties, the objectives of this work are (1) to develop a prototype system, using VIS-NIR reflectance spectroscopy, to be used for the in-line non-destructive measurement of apples, (2) to use an automated system that ensures that the distance between the probe and the fruit is the same regardless of the size of the fruit, and (3) to use the data obtained by the in-line system to differentiate apple varieties using chemometric methods.

2. MATERIALS AND METHODS

2.1. Apple samples

With the aim of carrying out the study using fruits with different internal and external properties, a total of 500 apples of five different varieties and origins were purchased from a local market (Figure 1). The set of fruits used in the experiments consisted of 100 pieces of each of the following varieties: Fuji (FU) from the region of Aquitaine (France), Red Delicious (RD) and Royal Gala (GA) from L'Alt Empordà (Spain), Golden Delicious (GD) from the Protected Geographical Indication of 'Alto Adige' (Italy) and Golden Delicious from the Protected Designation of Origin 'Pomme du Limousin' (France), known as Golden Rosé (GR). The reason for using Golden Delicious apples coming from two different origins was to know whether the system could also recognise fruits of the same variety but cultivated under different conditions and therefore with different properties.

The average diameter of each apple was measured by using a digital calliper in the equatorial and polar sections. The weight of each apple was measured using an electronic scale (Entris2202-1S, Sartorius Lab Instruments GmbH & Co. KG, Goettingen, Germany). The characteristic features of the fruits used in this study are summarised in Table 1.

Table 1. Characteristics of the five apple varieties studied.

Variety	Golden Delicious	Golden Delicious 'Rosé'	Fuji	Red Delicious	Royal Gala
Appearance	Green-yellow colour	Green-yellow colour with a coloured cheek	Red colour on a yellow background. Spherical shape	Dark red colour. Truncated cone shape	Red colour on a yellow background
Pulp	White colour, firm, sweet and not acidic	White colour	Cream sweet, juicy and crunchy	White colour, sweet and juicy	White colour, crunchy, sweet and slightly acidic
Eq. Diam. (mm) (min – max)	8.32 (7.60 – 8.80)	8.20 (7.70 - 8.90)	7.42 (6.60 – 8.40)	7.86 (7.00 – 8.70)	7.82 (7.30 – 8.30)
Polar Diam. (mm) (min – max)	8.02 (7.10-8.80)	8.47 (7.70-9.30)	8.16 (7.80-8.70)	7.85 (7.10-8.30)	7.48 (6.70-8.40)
Weight (g) (min – max)	257.81 (230.70-299.19)	273.83 (242.95-315.12)	263.96 (242.35-284.15)	237.10 (219.99-243.38)	228.76 (195.56-243.81)

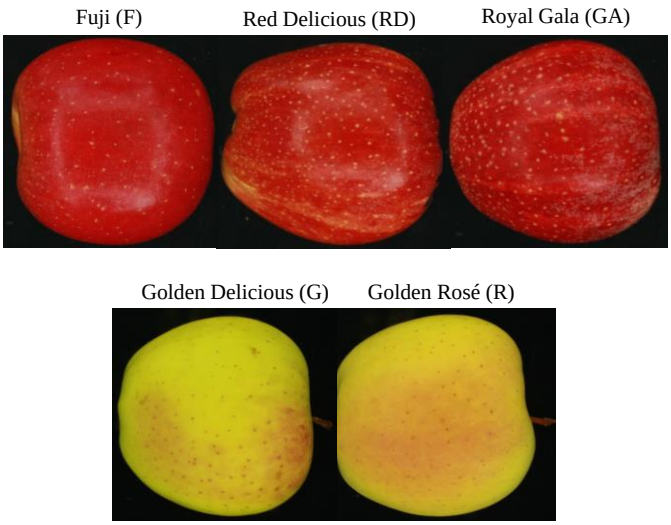

Figure 1. Visual appearance of the apple varieties used in this work.

2.2. VIS-NIR instrumentation

Diffuse reflectance of the apples was measured using a multichannel spectrometer platform (AvaSpecAS-5216 USB2-DT, Avantes BV, The Netherlands) equipped with two detectors. The first detector (AvaSpec-ULS2048 StarLine, Avantes BV, The Netherlands) included a 2048-pixel charge-coupled device (CCD) sensor (SONY ILX554, SONY Corp., Japan), 50 μm entrance slit and a 600-line mm-1 diffraction grating covering the visible and near-infrared range from 600 nm to 1100 nm (VNIR) with a spectral FWHM (full width at half maximum) resolution of 1.15 nm and a spectral sampling interval of 0.255 nm. The second detector (AvaSpec-NIR256-1.7 NIRLine, Avantes BV, The Netherlands) was equipped with a 256-pixel non-cooled InGaAs (Indium Gallium Arsenide) sensor (Hamamatsu 92xx, Hamamatsu Photonics K.K., Japan), 100 μm entrance slit and a 200-line mm-1 diffraction grating covering the near-infrared range from 900 nm to 1700 nm (NIR) with a spectral FWHM resolution of 12 nm and a spectral sampling interval of 3.535 nm.

The measurements were performed using a bi-directional fibre-optic reflectance probe (FCR-7IR200-2-45-ME, Avantes BV, The Netherlands). The probe is fitted with an illumination leg, composed of six 200 μm diameter fibres, which connects to a stabilised 10 W tungsten halogen light source (AvaLight-

HAL-S, Avantes B0V, The Netherlands) and the other leg of the fibre-optic probe, with a 200 µm diameter fibre, was connected to both detectors for simultaneous measurement using another Y-shaped fibre-optic probe (FCB-IR200-2-ME, Avantes BV, The Netherlands). The probe tip was designed to provide reflectance measurements at an angle of 45° so as to minimise specular reflectance from the surface of the fruit. To control the detectors and to acquire the spectra, a personal computer equipped with a commercial software package (AvaSoft version 7.2, Avantes, Inc.) was used.

A 99 % reflective white tile (WS-2, Avantes BV, The Netherlands) was used to calibrate the system so that the maximum reflectance value over each range of wavelengths was around 90 % of saturation (Lorente *et al.*, 2015).

2.3. VIS-NIR in-line system and spectra acquisitions

All the samples were equilibrated to room temperature (25 °C) before obtaining the spectral measurements. During the in-line test, the fruits were transported continuously using a conveyor belt composed of bi-conical rollers while they were being measured. Fruits were placed manually on the conveyor belt with the stem at the top to capture measurements of the equatorial part. To achieve a uniform distance between the probe and the fruits, a programmable electronic device (Raspberry Pi3, Raspberry Pi Foundation, United Kingdom) together with a small high-resolution IR camera (Raspberry Pi NIR Camera v2, Raspberry Pi Foundation, United Kingdom) were placed at a height of 25 cm above the conveyor belt and exactly perpendicular to the centre of the rollers. Illumination of the scene was achieved using two IR LED-based light sources synchronised with the camera module. A computer vision application captured an image of each fruit, detecting its exact location and estimating the diameter across the width of the rollers. The distance between the centre of the rollers and the end of the fruit on the measuring side are used to enable the probe to approach the fruit. Figure 2 shows all the parameters and components of the system.

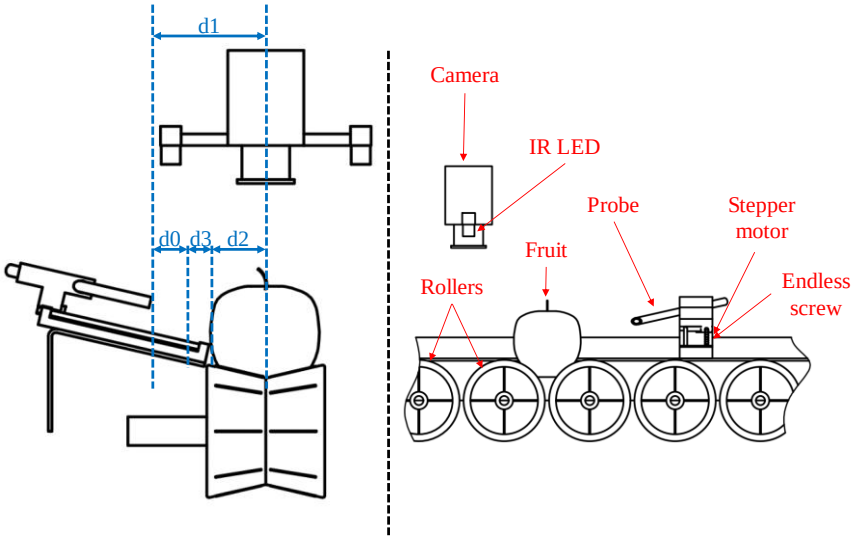

Figure 2. VIS-NIR in-line design composed by camera, illumination and lineal actuator with reflection probe.

To synchronise the acquisition of images and the movement of the probe with the advance of the apples, an optical encoder (WDG 40S-500-ABN-G05-K1, Wachendorff Elektronik, Germany) was coupled to the traction roller of the machine.

Using the distance between the fruit and the probe estimated by the image analysis system, and the position of the fruit on the conveyor belt estimated from the pulses given by the encoder, the electronic device activated a linear actuator composed of a stepper motor and an endless screw to bring the probe accurately towards the fruit. To calculate the displacement of the probe (d0), the distance between the centre of the rollers and the resting position of the probe (d1), the known distance between the centre of the rollers and the perimeter of the fruit on the measuring side given by the image analysis system (d2), and the distance between the probe and the fruit (d3) were used according to the distances shown in Figure 2 and Equation 1. All values were calculated in millimetres.

$$d0 = d1 - d2 - d3 \quad (1)$$

The process of bringing the probe closer to the fruit is shown in Figure 3. Different integration times were tested in preliminary tests at different distances between the fruits and the probe, with the aim of setting the minimum integration time that gives a good signal for the in-line application. Subsequently, the integration time was set to 150 ms for the VNIR detector and to 500 ms for the NIR detector. Each fruit was passed twice in the line to obtain two measurements of the diffuse reflectance spectrum. Due to the limitation of the integration time of the NIR detector, the speed of the conveyor belt had to be limited to 0.81 m/s.

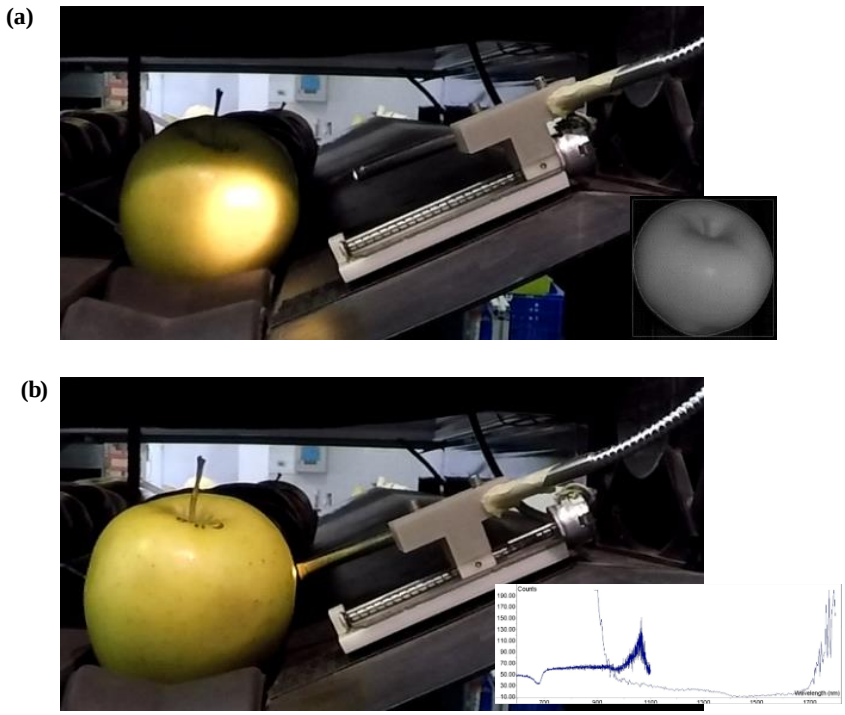

Figure 3. Lineal actuator with reflection probe in (a) resting position, and (b) measuring the fruit, a segmented image of the fruit (Figure 3a right) and VIS-NIR spectra obtained (Figure 3b right).

2.4. Data analysis

2.4.1. Chemometric analyses

The chemometric analyses of the collected spectra were performed using the Unscrambler V10.4 software package (CAMO ASA, Oslo, Norway). A matrix, where the rows represent the number of samples (N = 500 samples) and the columns represent the variables (X-variables and Y-variable), was produced with the spectral data. The spectral signals from the two detectors were the predictors, or X-variables. The categorical 'dummy' variable created by assigning different letters to the different apple varieties was the response, or the Y-variable.

The raw spectra were transformed to apparent absorbance (log (1/R)) values to linearise the correlation with the concentration of the constituents (Hernández *et al.*, 2006; Shao *et al.*, 2007; Liu *et al.*, 2009). To prevent a low signal-noise ratio occurring at the limits of the spectral sensitivity of the equipment used, only wavelengths ranging from 600 to 1700 nm were included in this study.

Because the high resolution captured in the VNIR range introduced increased noise in the signal (Cortés *et al.*, 2016), the VNIR spectra were pre-processed using a reduction factor of 10. Savitzky-Golay smoothing (the segment size is 3) was applied to reduce the effects caused by the physiological variability of samples (Carr *et al.*, 2005; Beghi *et al.*, 2017). Due to scattering effects, the light does not always travel the same distance inside the sample before it is collected by the probe (Santos *et al.*, 2013). A longer path travelled by the light results in a lower relative reflectance value, since more light is absorbed. This effect causes a parallel translation of the spectra that needs to be corrected to avoid a negative influence in the calibration models. A typical method to perform this correction, and the one used in this work, is the EMSC technique (He *et al.*, 2007; Martens *et al.*, 2003; Bruun *et al.*, 2007). Those two pre-treatments were considered the best results for the VNIR spectra, and those two pre-processing methods and the second derivate with Gap-Segment (2.3) were the best results for the NIR spectra (Cortés *et al.*, 2016).

After the pre-processing, principal component analysis (PCA) (Næs *et al.*, 2002) was applied to explore a possible clustering of the sample spectra that could be associated to the different apple varieties. This technique is a linear and unsupervised procedure that allows useful information to be extracted from the

data and to explore the data structure and the relationship between objects as well as the global correlation of the variables (Beebe *et al.*, 1998).

In addition, the linear discriminant analysis (LDA) and quadratic discriminant analysis (QDA) classification methods were applied on the spectra of the apples in order to classify the samples as belonging to one of the five varieties. The objective of these methods is to find models that allow the maximum separation among different classes in a set of objects. The difference between LDA and QDA is that LDA uses pooled covariance to assign an unknown sample to one of the pre-defined groups, while QDA uses the covariance of each of the groups instead of pooling them (Næs *et al.*, 2002). In both cases, the number of samples in the training set must be larger than the number of variables included in the model (Kozak & Scaman, 2008; Sádecká *et al.*, 2016), thus a reduction of the dimensionality is necessary. This was achieved by using the PCA scores as input data in the model instead of the raw variables, since the linear combinations of the original variables given by the PCA, called principal components (PCs), are uncorrelated (Rodríguez-Campos *et al.*, 2011).

To develop the discriminant model, a training set composed of 80% of the samples selected at random was used. The model was internally validated using full cross-validation (CV; leave-one-out method) (Casale *et al.*, 2008; Huang *et al.*, 2008). Predictions were carried out using the evaluation set composed of the remaining 20% of the samples (Soares *et al.*, 2013). The performance of the model was evaluated by accuracy, which is defined using the ratio of samples in the test set correctly assigned to their respective classes presented using confusion matrices.

3. RESULTS AND DISCUSSION

3.1. Features of VIS-NIR spectra

Preliminary tests were carried out on both red and yellow apples to determine the correct measuring distance between the probe and the fruit for each type of fruit. To do so, distances of 1, 5 and 10 mm were tested with the fruits travelling on the conveyor belt at the same speed (one fruit per second). The average spectra of yellow and red apples captured using different distances between the light source/detection probe and the fruit are shown in Figure 4. When

the probe was very close to the fruit (1 mm), it was observed that the signal saturated in some samples even with very low integration times. This is because practically no light penetrates inside the object and is only reflected on its surface towards the detector. Conversely, using a distance of 10 mm, the detector receives very little reflection, which is in accordance with Salguero-Chaparro *et al.*, (2012). Therefore, for this study, the diffuse reflectance spectrum of all fruits was acquired at 5 mm from the fruit, regardless of their size. In Equation 1, parameter d3 has a value of 5 mm.

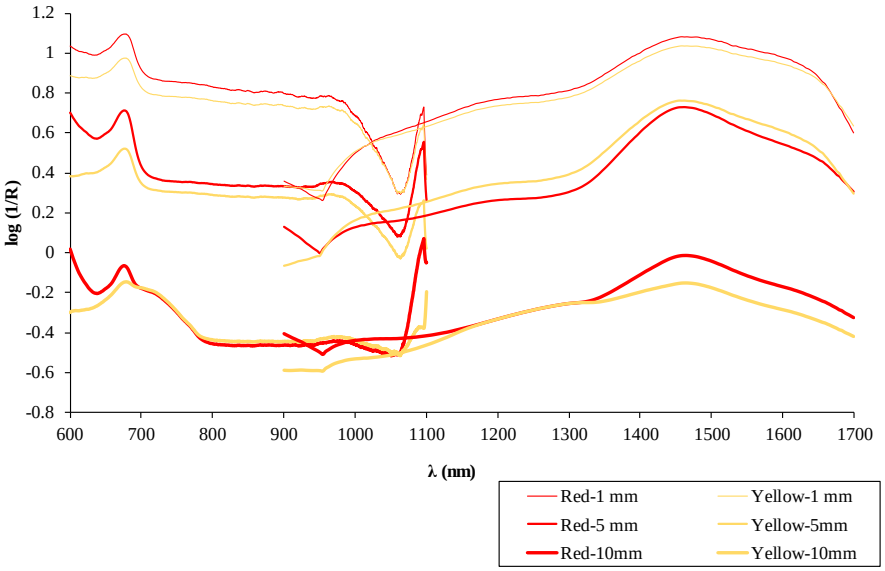

Figure 4. Average Log (1/R) of the 50 yellow and red apples at different testing distances.

Once the measurement distance had been determined, VIS-NIR spectra were measured for all apples. Figure 5 shows the raw spectra of all samples. The differences in colour among the apple varieties were detected in the VIS wavelength range (i.e. 600-700 nm). However, the acquired spectra exhibit similar profiles across the spectral range that was studied, and even overlapped heavily, especially the spectra between 730-1700 nm. According to Fernández-Ahumada *et al.* (2006), the use of the VIS and NIR wavelength range offers great expectations for NIR characterisation in some products such as potatoes. Because it was difficult

to discriminate the five kinds of apples just from the overlapping spectra, it was necessary to use feature extraction methods, such as PCA, LDA and QDA, to distinguish the apple varieties.

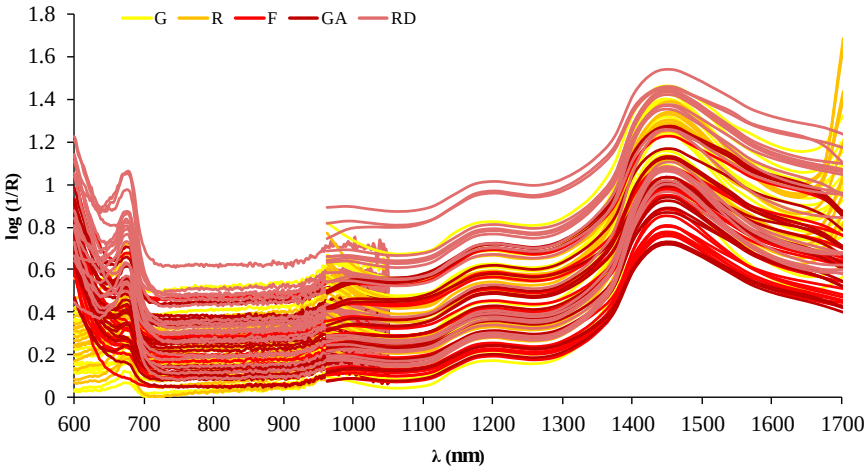

Figure 5. Raw VNIR and NIR spectra of five different varieties of apple.

3.2. Clustering analyses based on PCA

The PCA model, as previously mentioned, was first constructed in order to explore a possible clustering of the spectra of the samples that could be associated to the different apple varieties. Figure 6 shows the training spectra set plotted according to the values of the PCA scores. Each variety is shown with a different colour and shape for a better visualisation. As shown in this figure, red and yellow varieties can be separated easily due to the different spectral reflectance represented in the visible spectrum. However, colour and appearance are not always useful for discriminating apple varieties. There are some varieties that are very difficult to differentiate visually on the production line but show important compositional differences that are represented in the NIR spectrum, thereby affecting the taste and consequently their acceptance by the final consumers.

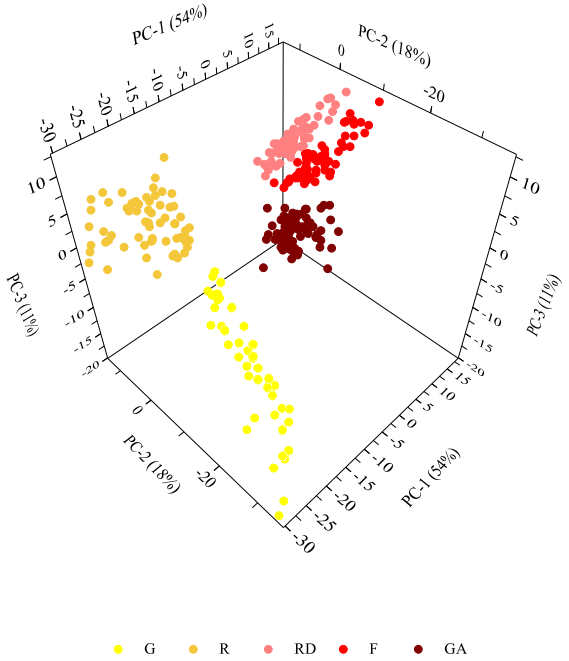

Figure 6. PCA analysis of apple varieties of the training samples.

Additionally, the PCA model was used to reduce the original variables for constructing the LDA and QDA models. The cumulated reliability of the seven PCs reaches 95.57% (Table 2). Hence the first seven PCs were adopted as the inputs in the LDA and QDA models.

Table 2. The contribution rates and accumulative contribution rates of the first seven PCs.

Number of principal components	PC1	PC2	PC3	PC4	PC5	PC6	PC7
Contribution rate (%)	53.54	17.69	10.85	6.53	3.56	1.89	1.52
Accumulative contribution rate (%)	53.54	71.23	82.07	88.60	92.16	94.05	95.57

3.3. Classification by LDA and QDA models

PCA can analyse the varieties of apples qualitatively, but it cannot discriminate these varieties quantitatively. In this study, LDA and QDA were used to build a quantitative analysis model to discriminate apple varieties, shown below.

Table 3 provides the confusion matrices that summarise the classification results using LDA and QDA techniques. From these matrices, it can be concluded that no red apple was classified as a yellow variety and vice versa. This expected correct classification is mainly due to the contribution of the visible spectrum mentioned previously. In general, QDA achieved better results than LDA for both types of samples, probably because LDA can only learn linear boundaries, while QDA can learn quadratic boundaries, LDA being a much less flexible classifier than QDA (James *et al.*, 2014). The results show that classification accuracy for LDA model was 82.5% and for the QDA model it was 85% for the same test set of yellow varieties that was used. Similarly, the red varieties obtained a classification accuracy for the LDA model of 75% and of 98.3% for the QDA model. The differences were observed mainly in the high classification accuracy achieved by the QDA model in red apples. However, it is important to note that the red apples were of different varieties, while the yellow ones both belonged to the same variety but different origins, thus demonstrating that this method can not only discriminate between varieties but also by the origin of the apple.

Table 3. LDA and QDA confusion matrices, both presented as as percentage of correctly classified samples in the test data set.

Method		**Classification accuracies (%)**					**Overall accuracy (%)**
		Golden	Golden Rosé	Fuji	Royal Gala	Red Delicious	
LDA	Golden	95	5	0	0	0	82.5
	Golden Rosé	30	70	0	0	0	
	Fuji	0	0	65	35	0	75.0
	Royal Gala	0	0	25	75	0	
	Red Delicious	0	0	5	10	85	
QDA	Golden	100	0	0	0	0	85.0
	Golden Rosé	30	70	0	0	0	
	Fuji	0	0	95	5	0	98.3
	Royal Gala	0	0	0	100	0	
	Red Delicious	0	0	0	0	100	

He *et al.* (2007) already used PCA and an artificial neural network (ANN) coupled with VIS-NIR (400-960 nm) to classify three red apple varieties ('Fuji' from China, 'Red Delicious' from USA and 'Copefrut Royal Gala' from USA). They used only 30 apples of each variety, obtaining an accuracy of 100% but using a static arrangement. Wu *et al.* (2016) applied four kinds of feature extraction methods, namely PCA, PCA+LDA, discriminant partial least squares (DPLS) and sorting discriminant analysis (SDA), on the NIR spectra (1000-2500 nm) of two varieties of apples with a red external colour ('Huaniu' and 'Fuji' from China). In their research, the SDA model was the best one with a classification accuracy of 96.67% for discriminating apple varieties. In these previous studies, He *et al.* (2007) and Wu *et al.* (2016) only classified red apple varieties on a laboratory scale using static measurements. In contrast, the new in-line detection prototype has been developed for spectral analysis while the fruit is transported by a conveyor belt in the processing line. The in-line system developed here allowed us to obtain as good or better results than previous studies involving laboratory systems. The speed of advance of the fruits when the spectra were measured was one fruit per second. This was the same speed as that used by Shenderey *et al.* (2010) in their experiments when they measured the spectra of apples in movement to detect those affected by mouldy core. In their work, the measuring device was placed on a rotating table that served as a laboratory device to test the spectrometry in moving fruits, thus demonstrating that it is possible to perform spectrometry on apples in-line. However, in this work, the practical implementation was performed in an industrial prototype with what was similar to a commercial conveyor belt and presents certain novel advantages such as ensuring the same measuring distance for all fruits.

4. CONCLUSIONS

A novel prototype for the in-line identification of apple varieties based on VIS-NIR spectroscopy has been developed and tested. One of the main disadvantages of the in-line system when fruits are travelling on a conveyor belt is that the diversity of fruit sizes causes the spectra to be taken at different distances, since the position of the probe is fixed. This has a negative effect on the robustness of the results obtained. This work proposes a new device that allows the

measurements to be captured at always the same distance from the fruit, thus ensuring that they are all taken in the same conditions. Two classification methods were used to determine the variety of the apples and, in the case of Golden Delicious, to detect fruits of different origins. QDA yielded better results than LDA reaching a 98% and 85% rate of success for red and yellow varieties, respectively. The proposed prototype may contribute to improve the control of production as a tool for detecting fraud in a non-destructive and highly accurate manner. However, in order to effectively transfer this system to industry, the speed of one fruit per second needs to be improved.

Acknowledgements

This work was partially funded by the Generalitat Valenciana through project AICO/2015/122 and by INIA and FEDER funds through project RTA2015-00078-00-00. Victoria Cortés López thanks the Spanish Ministry of Education, Culture and Sports for FPU grant (FPU13/04202).

5. REFERENCES

Alonso, J., Artigas, J. & Jimenez, C. (2003). Analysis and Identification of Several Apple Varieties Using ISFETs Sensors. Talanta, 59, 1245-1252.

Beebe, K.R., Pell, R.J. & Seasholtz, M.B. (1998). In: Chemometrics: a Practical Guide, New York, USA. John Wiley and Sons.

Beghi, R., Giovenzana, V., Brancadoro, L. & Guidetti, R. (2017). Rapid evaluation of grape phytosanitary status directly at the check point station entering the winery by using visible/near infrared spectroscopy. Journal of Food Engineering, 204, 46-54.

Brunt, K., Smits, B. & Holthuis, H. (2010). Design, construction, and testing of an automated NIR in-line analysis system for potatoes. Part II. Development and testin of the automated semi-industrial system with in-line NIR for the characterization of potatoes. Potato Research, 53, 41-60.

Bruun, S.W., Sondergaard, I. & Jacobsen, S. (2007). Analysis of protein structures and interactions in complex food by near-infrared spectroscopy. 1. Gluten powder. Journal of Agricultural and Food Chemistry, 55, 7234-7243.

Carr, G.L., Chubar, O. & Dumas, P. (2005). Spectrochemical Analysis Using Infrared Multichannel Detectors. In Bhargava, R., Levin, I.W. (Eds.), 1st ed. Wiley-Blackwell, Oxford, 56-84.

Casale, M., Casolino, C., Ferrari, G. & Forina, M. (2008). Near infrared spectroscopy and class modelling techniques for geographical authentication of Ligurian extra virgin olive oil. Journal of Near Infrared Spectroscopy, 16, 39-47.

Cortés, V., Ortiz, C., Aleixos, N., Blasco, J., Cubero, S. & Talens, P. (2016). A new internal quality index for mango and its prediction by external visible and near infrared reflection spectroscopy. Postharvest Biology and Technology, 118, 148-158.

Fernández-Ahumada, E., Garrido-Varo, A., Guerrero-Ginel, A.E., Wubbels, A., van der Sluis, C. & van der Meer, J.M. (2006). Understanding factors affecting near infrared analysis of potato constituents. Journal of Near Infrared Spectroscopy, 14, 27-35.

He, Y., Li, X. & Shao, Y. (2007). Fast discrimination of apple varieties using Vis/NIR spectroscopy. International Journal of Food Properties, 10 (1), 9-18.

Hernández, A., He, Y. & García, A. (2006). Non-destructive measurement of acidity, soluble solids and firmness of Satsuma mandarin using Vis/NIR-spectroscopy techniques. Journal of Food Engineering, 77, 313-319.

Huang, H., Yu, H., Xu, H. & Ying, Y. (2008). Near infrared spectroscopy for on/in-line monitoring of quality in foods and beverages: a review. Journal of Food Engineering, 87(3), 303-313.

James, G., Witten, D., Hastie, T. & Tibshirani, R. (2014). An Introduction to Statistical Learning: With Applications in R. New York: springer.

Jie, D., Xie, L., Rao, X. & Ying, Y. (2014). Using visible and near infrared diffuse transmittance technique to predict soluble solids content of watermelon in an on-line detection system. Postharvest Biology and Technology, 90, 1-6.

Kader, A.A., Kasmire, R.F., Mitchell, F.G., Reid, M.S., Sommer, N.F. & Thompson, J.F. (1985). Postharvest technology of horticultural crops. Cooperative Extension, University of California. Special Publication, 3311, 192.

Kozak, M. & Scaman, C. H. (2008). Unsupervised classification methods in food sciences: discussion and outlook. Journal of the Science of Food and Agriculture, 88, 1115-1127.

Lammertyn, J., De Baerdemaeker, J. & Nicolaï, B. (2000). Light penetration properties of NIR radiation in fruit with respect to non-destructive quality assessment. Postharvest Biology and Technology, 18(2), 121-132.

Liu, F., Jiang, Y. & He, Y. (2009). Variable selection in visible/near infrared spectra for linear and nonlinear calibrations: a case study to determine soluble solids content of beer. Anal. Chim. Acta 635, 45-52.

López, A.F. (2003). 'Manual para la preparación y venta de frutas y hortalizas, del campo al mercado'. PDF File: Boletín de servicios agrícolas de la FAO, 151. http://www.fao.org/tempref/docrep/fao/006/y4893S/y4893S00.pdf

Lorente, D., Escandell-Montero, P., Cubero, S., Gómez-Sanchis, J. & Blasco, J. (2015). Visible-NIR reflectance spectroscopy and manifold learning methods applied to the detection of fungal infections on citrus fruit. Journal of Food Engineering, 163, 17-21.

Luo, W., Huan, S., Fu, H., Wen, G., Cheng, H., Zhou, J., Wu, H., Shen, G. & Yu, R. (2011). Preliminary study on the application of near infrared spectroscopy and pattern recognition methods to classify different types of apples. Food Chemistry, 128, 555-561.

Marrazzo, W.N., Heinemann, P.H., Crassweller, R.E. & LeBlanc, E. (2005). Electronic Nose Chemical Sensor Feasibility Study for the Differentiation of Apple Cultivars. American Society of Agricultural Engineers, 48 (5), 1995-2002.

Martens, H., Nielsen, J.P. & Engelsen, S.B. (2003). Light scattering and light absorbance separated by extended multiplicative signal correction. Application to near-infrared transmission analysis of powder mixtures. Analytical Chemistry, 75, 394-404.

Næs, T., Isaksson, T., Fearn, T. & Davies, T. (2002). A user-friendly guide to multivariate calibration and classification. Chichester: NIR Publications.

Rodríguez-Campos, J., Escalona-Buendía, H.B., Orozco-Avila, I., Lugo-Cervantes, E. & Jaramillo-Flores, M.E. (2011). Dynamics of volatile and non-volatile compounds in cocoa (*Theobroma cacao L.*) during fermentation and drying processes using principal components analysis. Food Research International, 44, 250-258.

Ronald, M. & Evans, M. (2016). Classification of selected apple fruit varieties using Naive Bayes. Indian Journal of Computer Science and Engineering, 7(1), 13-19.

Sabanci, K. & Ünlersen, M.F. (2016). Different apple varieties classification using kNN and MLP algorithms. International Journal of Intelligent Systems and Applications in Engineering, 4, 166-169.

Sádecká, J., Jakubíková, M., Májek, P. & Kleinová, A. (2016). Classification of plum spirit drinks by synchronous fluorescence spectroscopy. Food Chemistry, 196, 783-790.

Salguero-Chaparro, L., Baeten, V., Abbas, O. & Peña-Rodríguez, F. (2012). On-line analysis of intact olive fruits by vis-NIR spectroscopy: optimisation of the acquisition parameters. Journal of Food Engineering, 112, 152-157.

Santos, P., Santos, F., Santos, J. & Bezerra, H. (2013). Application of extended multiplicative signal correction to short-wavelength near infrared spectra of moisture in marzipan. Journal of Data Analysis and Information Processing, 1, 30-34.

Shang, L., Guo, W. & Nelson, S.O. (2015). Apple variety identification based on dielectric spectra and chemometric methods. Food Anal. Methods, 8, 1042-1052.

Shao, Y., He, Y., Gómez, A.H., Pereir, A.G., Qiu, Z. & Zhang, Y. (2007). Visible/near infrared spectrometric technique for nondestructive assessment of tomato 'Heatwave' (Lycopersicumesculentum) quality characteristics. Journal of Food Engineering, 81 (4), 672-678.

Shenderey, C., Shmulevich, I., Alchanatis, V., Egozi, H., Hoffman, A., Ostrovsky, V., Lurie, S., Arie, R.B. & Schmilovitch, Z. (2010). NIRS detection of moldy core in apples. Food Bioprocess Technology, 3, 79-86.

Soares, S.F.C., Gomes, A.A., Galvão Filho, A.R., Araújo, M.C.U. & Galvão, R.K.H. (2013). The successive projections algorithm. Trends in Analytical Chemistry, 42, 84-98.

Song, W., Wang, H., Maguire, P. & Nibouche, O. (2016). Differentiation of organic and non-organic apples using near infrared reflectance spectroscopy - A pattern recognition approach. Sensors, 1-3.

Sun, X., Liu, Y., Li, Y., Wu, M. & Zhu, D. (2016). Simultaneous measurements of Brown core and soluble solids content in pear by on-line visible and near infrared spectroscopy. Postharvest Biology and Technology, 116, 80-87.

Wojdyło, A., Oszmiański, J. & Laskowski, P. (2008). Polyphenolic compounds and antioxidant activity of new and old apple varieties. Journal of Agricultural and Food Chemistry, 56(15), 6520-6530.

Wu, X., Wu, B., Sun, J. & Yang, N. (2017). Classification of Apple varieties using near infrared reflectance spectroscopy and fuzzy discriminant C-Means clustering model. Journal of Food Process Engineering, 40, 1-7.

Wu, X., Wu, B., Sun, J., Li, M. & Du, H. (2016). Discrimination of Apples Using Near Infrared Spectroscopy and Sorting Discriminant Analysis. International Journal of Food Properties, 19(5), 1016-1028.

4. GENERAL DISCUSSION

In the present PhD, different strategies were studied in order to evaluate the potential and the advantages of VIS-NIR spectroscopy as an analysis tool for the characterization and inspection of fruit quality both off-line in laboratory scale as in real time through simultaneous operations using different sensors in automation processes. This work arises in response to the current needs of the fruit sector, which demand non-destructive analysis of all production in terms of quality to minimize costs and satisfy final consumers.

Firstly, the viability of VIS-NIR spectroscopy was evaluated in static mode (off-line) in combination with the multivariate analysis techniques developing different experiments in order to characterise and inspect the fruit quality. The level and changes of astringency were predicted in intact and in the flesh of half cut persimmons cv. 'Rojo Brillante' harvested in L'Alcudia (Valencia, Spain) which were exposed to different treatments with 95% CO_2 at 20 ºC for a period of 0, 6, 12, 18 and 24 h to obtain samples with different levels of astringency. The prediction models (PLSR, SVM and LS-SVM) were created combined their VIS-NIR spectra and their soluble tannins content, obtaining the best performance in the models, which included SNV in the pre-processing, and using the six measurement points of the intact fruit. Other off-line experiment consisted in discriminate between two varieties of nectarine (cv. 'Big Top' and cv. 'Diamond Ray') grown in the same period and with similar appearance although different taste. Accurate classification models (LDA and PLS-DA) were obtained for the full spectral and with the most EWs, especially for the PLS-DA model. Similarly, the VIS-NIR reflectance spectroscopy were used to differentiate between two nectarine varieties (cv. 'Big Top' and cv. 'Magique') and to predict their internal quality by a new developed index (IQI). The prediction (PLS) and classifications (LDA and PLS-DA) models showed also good performance. Finally, the internal quality of intact mango cv. 'Osteen' was analysed based on the IQI and the ripening index (RPI). PLS models established the relationship between VIS-NIR spectra and indices which reached good performance in predicting the internal quality of the samples using the full spectra range and the most important wavelengths.

Secondly, an automation of the inspection processes was carried out through the development of new in-line prototypes. The first prototype consisted of a robotic gripper capable to measure the firmness of mangoes in a non-destructive mode during their manipulation. The developed PLS models obtained high

correlations between the information obtained from the accelerometers (non-destructive firmness) of the robotic grip and the physicochemical properties analysed (mechanical properties, flesh color, TSS, pH and TA) as well as the ripening index (RPI). Additionally, the same robotic gripper for mangoes was modified based on the integration of two VIS-NIR spectral probes and two accelerometers in the robotic gripper. This non-destructive tool combined the capability of obtaining mechanical and optical properties of the fruit simultaneously when the fruit is manipulated in the packinghouse during postharvest operations. Best prediction of RPI was achieved when combined the information of the two spectral probes and the signals of the two finger accelerometers. Finally, other in-line prototype was developed based on the integration of one spectral fibre-probe in a conveyor belt for spectral analysis while apples were transported in the processing line. The main advantage of this prototype was that it allowed the spectra to be captured with the VIS-NIR probe at the same distance from all the fruits regardless of their size something that does not happen with current commercial systems. LDA and QDA models achieved the best in-line classification of apple variety and, in the case of Golden Delicious, the best detection of apple origins.

In summary, it can be concluded that according with the quantitative and qualitative results of this off-line and in-line studies, external VIS-NIR reflection spectroscopy combined with chemometrics, demonstrated to be an excellent non-destructive technique capable of monitor the fruit quality for the post-harvest industry assuming a technological breakthrough compared to the present situation where the evaluation of the state of the fruits is mostly subjective and not accurate.

5. CONCLUSIONS

This point summarizes the main conclusions of this thesis and draws out their implications for fruit quality control. Seven main general conclusions can be drawn from the results of this work:

1. Visible and near-infrared spectroscopy is a rapid and non-destructive method for determining astringency in persimmon fruits. It results in a valid alternative to avoid costly and and tedious chemical analysis or the subjective evaluation of the tannin printing method. The best performance for intact fruits was obtained using PLSR on the full spectra of the six measurement points after pre-processing with SNV+1-Der, an R^2=0.904 and RPD=3.26 being achieved. Moreover, the best prediction results obtained with the EWs (41 bands) were obtained for the PLSR model using the six measurement points of the intact fruit in the NIR spectra and SNV+DOSC pre-processing (R^2=0.915; RPD=3.46).

2. Visible and near-infrared spectroscopy is an accurate classification tool for nectarine varieties with a very similar external and internal appearance but different tastes and organoleptic properties. PLS-DA model achieved better accuracy and less latent variables than LDA model, and specifically, good results with 100% classification accuracy were obtained using only the VNIR detector for the two models and eight selected wavelengths out of the 1838 available features. Therefore, PLS-DA and LDA resulted as robust models for discriminating varieties of nectarine with a satisfactory level of accuracy placing the visible and near-infrared spectroscopy as an accurate classification tool for nectarine varieties with a very similar appearance but different tastes that could be potentially used in an automated inspection system.

3. Visible and near-infrared spectroscopy is a technique capable of determining the internal quality of intact nectarines with significant reliability. The PLS analysis showed strong performance in predicting the internal quality of the samples, with an R^2_P and RMSEP of 0.909 and 0.235 for cv. ‘Big Top’, and 0.927 and 0.238 for ‘Magique’. Despite being two

varieties with a similar composition and grown in the same period, it was possible to separate the two with a perfect classification rate of 100 % using PLS-DA and 97.44 % using the model developed by LDA models. This represents an advance in the creation of tools for monitoring the quality of these fruits in postharvest compared to the present situation where the evaluation of the fruit quality is mostly carried out based on the subjective experience of trained workers.

4. External visible and near-infrared spectroscopy combined with chemometrics could be used for the non-destructive prediction of the internal quality of mango 'Osteen' using indices as the ripening index (RPI) and the internal quality index (IQI). The PLS analysis showed a strong performance in predicting RPI and IQI for the VIS, VIS-NIR and NIR detectors using the full spectral range (R^2_p=0.833-0.879, RMSEP=0.403-0.507 and RPD=2.341-2.826) and the most important wavelengths (R^2_p=0.815-0.896, RMSEP=0.403-0.537 and RPD=2.060-2.905). VIS-NIR spectroscopy has a great potential for its application to the evaluation of the quality of these fruits and therefore this technological achievement could even be integrated into fruit packing lines as part of the quality assurance system.

5. The physico-chemical analysis showed that the best parameters to assess the ripeness of cv. 'Osteen' mangoes were mechanical firmness, soluble solid content, and flesh luminosity. The prediction models, developed by PLS estimated correctly these parameters and also the RPI of the samples based on the information obtained from the robot gripper accelerometers. This research showed that it is possible to assess the firmness and ripeness of mango fruits using a non-destructive technique during robot handling operation with a robot gripper.

6. The integration of simultaneous tactile sensing using two accelerometers and two VIS-NIR reflectance probes in a robot gripper showed to have the potential to good estimate mango (cv. 'Osteen') quality through the RPI.

The intrinsic tactile sensors used do not need contact with the fruit and could take the measurements simultaneously during the mango handling, which is an important advantage over the current state of the technology for fruit quality assessment. PLS models were developed to predict the RPI, and the best model was created by combining the information from VIS-NIR spectra and non-destructive impact measured during handling, achieving an R^2_p of 0.832 and RMSEP of 0.520. This innovative prototype integrated sensors of different nature, whose data information was combined to obtain better prediction. The fusion of different types of sensors like spectrometry (electromagnetic) and accelerometers (vibrational) achieved better results than using only the accelerometers, or similar results to using spectroscopy, but in this case, the measurements were made while the fruit was handled. In this way, results show the potential and advantages of performing simultaneous operations with sensors of different nature integrated on a robot gripper that can inspect and classify the mangoes by their ripeness during a pick and place robot process.

7. A novel prototype for the in-line identification of apple varieties based on VIS-NIR spectroscopy has been developed and tested. The solution developed avoids one of the main disadvantages of the in-line system when fruits are travelling on a conveyor belt which is the errors in the measurements due the diversity of fruit sizes. Normally this diversity causes the spectra to be taken at different distances, since the position of the probe is fixed while in this contribution the probe always makes the measurement at the same distance of any fruit. Two classification methods were used to determine the variety of the apples and, in the case of cv. 'Golden Delicious', to detect fruits of different origins. QDA gave better results than LDA reaching a 98 % and 85 % of success for red and yellow varieties respectively. The proposed prototype may contribute to improve the control of the production as a tool for the detection of frauds non-destructively and highly-accurate and the patent of this systems is currently

being processed. However, in order to effectively transfer this system to the industry, the speed of one fruit per second needs to be improved.

6. FUTURE PERSPECTIVES

In the view of the results and conclusions of the present thesis, the following proposals for further work are expounded:

- Application of the proposed optical non-destructive measurements and analyses procedures to other climacteric fruits and varieties.

- Test the ability of the proposed indexes along a ripening treatment of non-climateric fruits and vegetables.

- Test the potential of classification and prediction proposed procedures to other postharvest origins.

- Adapt the proposed models for the fruit harvested at other different harvest times to ensure that can consistently reflect the quality of the harvested product.

- Implementation of and in-line prototype of conveyor belt using more probes to measurement at different points of the fruit obtaining more accurate quality information under real-time conditions.

- Improve in-line prototypes to reduce their analysis time adapting to a real industrial scale and offering the possibility to inspect the entire production.